Changing landscapes: Compositional and phenological shifts in New Zealand's natural grassland

Hua Xiaobin

华 晓宾

A thesis submitted for the degree of

Doctor of Philosophy

School of Geography, University of Otago

Dunedin, New Zealand

02 September 2019

Abstract:

Vegetation in a wide range of ecosystems across the globe is responding to recent anthropogenic climate change. There are two key ecological responses in plants associated with recent anthropogenic climate change: shifts in species' geographic distributions (range shifts) and shifts in the timing of key life cycle events (phenological shifts). These shifts can lead to temporal and spatial changes in vegetation composition and growth activity and hence ecosystem function. Understanding the patterns and processes of these shifts is crucial for the successful management of natural ecosystems under ongoing anthropogenic environmental change.

This thesis investigates recent spatiotemporal compositional and phenological shifts in New Zealand's natural grassland ecosystems and identifies potential topographical and climatic drivers of these shifts. Three grassland types in New Zealand are investigated (Alpine, Tall Tussock and Low Producing grasslands). They are characterised by high levels of indigenous endemic plant biodiversity and cover a wide elevation range. This thesis primarily utilises remote sensing information for quantifying growth dynamics and vegetation patterns in these grasslands over the last 16 years and across large spatial scales, i.e., the catchment of the river Clutha/Mata-Au River in South Island, New Zealand.

Shrub encroachment in grassland ecosystems is a globally observed example of compositional shifts in ecosystems associated with recent anthropogenic climate change. In New Zealand, where extensive area of current grassland habitats exist because of anthropogenic deforestation, shrub encroachment into grasslands has two distinct facets: firstly the invasion of non-native shrub species into native grasslands (i.e., exotic shrub invasion) and secondly the dispersal of native woody and shrub species into native grasslands (i.e., native shrub recovery). Propagule pressure is a measurement of species' seed source size in neighbourhood of a focal area, and it is a key determinant of the degree to which a location gets colonised by individuals from species present in the neighbourhood. The spatial patterns of potential native and exotic shrub propagule pressure on three grassland types in New Zealand were quantified with the assumption that proximity of higher shrub coverage indicates higher shrub propagule availability. Results show that Alpine grasslands are mostly surrounded by native shrublands, while Low producing grassland are most at risk from exotic shrub invasion from neighbouring areas. High native and exotic shrub propagule pressure does not generally coincide spatially, however, it occurs in very similar climates for Low Producing grassland but not

for Alpine and Tall Tussock grassland. The analysis of recent shrub encroachment over the last five years in a tussock grassland area in the central South Island showed a 0.35% $year^{-1}$ increase in shrub cover in grassland area located in immediate neighbourhood of shrub. Shrub encroachment speed was strongly correlated with shrub cover in the neighbourhood. Recent shrub encroachment into grasslands was most pronounced in areas with neighbouring shrub cover of greater than 40%.

A wide range of species and ecosystems worldwide have shown changes in the timing of life cycle events and growing seasons in a direction congruent with recent anthropogenic climate changes. In this study, temporal trends over the last 16 years in the start, peak and end dates of the growing season were analysed using remotely sensed data on the Normalised Difference Vegetation Index (NDVI) in New Zealand's three main grassland types. Overall, 90% of Alpine, 86% of Tall Tussock and 89% of Low Producing grassland areas showed an advancing start of the growing season over the last 16 years. In these areas start of the growing advanced by 7.2, 6.0 and 8.8 days per decade in Alpine, Tall Tussock and Low Producing grassland, respectively. Only small changes in timing of the end of the growing season were observed in the three grassland types. The length of growing season extended by 3.2, 5.2 and 7.1 days per decade in three grassland types.

Landscape topography (elevation and aspect) played an important role in particular in alpine grasslands: the start of the growing season was strongly correlated with elevation (later start with increasing elevation), while the end of the growing season was strongly correlated with aspect (later end of season on more south-facing slopes). The start of season was delayed by 7.5, 5.1 and 3.7 days/100 m elevation increase in Alpine, Tall Tussock and Low producing grassland, separately. The end of season was advanced by 1.7 (Alpine), 1.3 (Tall Tussock) and delayed by 0.3 (Low Producing) days/10-degree-south on the slopes in these three grassland types.

The results from this thesis show that recent shrub invasion into New Zealand grasslands is highest near shrub areas once a threshold of shrub cover in the neighbourhood is reached. Shrub encroachment was highest at lower elevations and on north-facing slopes. It also highlighted a measurable shift to an earlier start and extended length of the growing season in New Zealand's main grassland types over the last 16 years, but the magnitude of these shifts showed considerable geographic variation. Importantly, this study has shown a high degree of topographical control on the timing of the growing in New Zealand's grasslands with elevation and aspect acting differentially on start and end

of the growing season. This highlights the importance of landscape heterogeneity and microclimates for ecosystem responses to climate change. This study shows that remotely sensed data can be successfully used to elucidate ecosystem-level shifts in temporal dynamics and spatial patterns of vegetation growth in grassland ecosystems.

Table of Contents

List of Figures

List of Tables

Chapter 1 Introduction

Climate change influences the ecological shifts in the phenology and distribution of plant species worldwide (Parmesan and Yohe, 2003, Parmesan, 2006), and it is also evident in New Zealand. With concern regarding ecosystem conservation, it is necessary to tackle how the ecosystem responds to current climate change and further direct the efficient ecological management. To achieve this target, the long-term, large-scale data with a high temporal resolution is essential. The ground-based observations are usually costly and time consuming (Huang and Asner, 2009), and the deficiency of field observation may lead to the shortage of data about plants dynamic and phenology in New Zealand. Instead of field work, remote sensing is an efficient and adequate option to detect large-scale changes in land cover and phenology rapidly and economically (Bradley, 2014). Satellite imagery was widely used to detect plants' dispersal and phenology changes in several studies (Zhang *et al.*, 2004, Ganguly *et al.*, 2010, Kidane *et al.*, 2012, Weeks *et al.*, 2013a, Ali *et al.*, 2016, Yu *et al.*, 2017). This thesis investigated spatial patterns of recent compositional and phenological changes in New Zealand's grassland ecosystems through the use of temporally and spatially explicit remote sensing data.

1.1 Woody species expansion into non-woody ecosystems

Woody expansion or shrub encroachment, which refers to the woody species' invasion into the originally non-woody habitats, can change the ecological functions and replace native species fundamentally (Walker, 2000, Froude, 2011, Buitenwerf *et al.*, 2018). In the past century, shrub encroachment was evident globally coinciding with the anthropological climate change, and it became a focus of ecological and biogeographical researches (Archer *et al.*, 1995, Dullinger *et al.*, 2003, Briggs *et al.*, 2005, Naito and Cairns, 2011). Though the conversion of non-woody land cover to woody does not necessarily lead to functional degradation in the ecosystems (Eldridge *et al.*, 2011), shrub encroachment can decrease the coverage of the historically endemic species and alter the landscape dramatically (Knapp *et al.*, 2008, Van Auken, 2009). The drivers of shrub encroachment are likely to be current global warming, increased atmospheric CO_2 and anthropological disturbances (Komac *et al.*, 2013, Caracciolo *et al.*, 2016, Stevens *et al.*, 2017). However, the mechanism of wood expansion remains uncertain, because this phenomenon happens in diverse non-woody ecosystem types (savannas, subalpine, arctic grassland etc.) and under various abiotic circumstances. Instead of the well documented

shrub encroachments in the Northern Hemisphere, the record is relatively rare in the Southern Hemisphere.

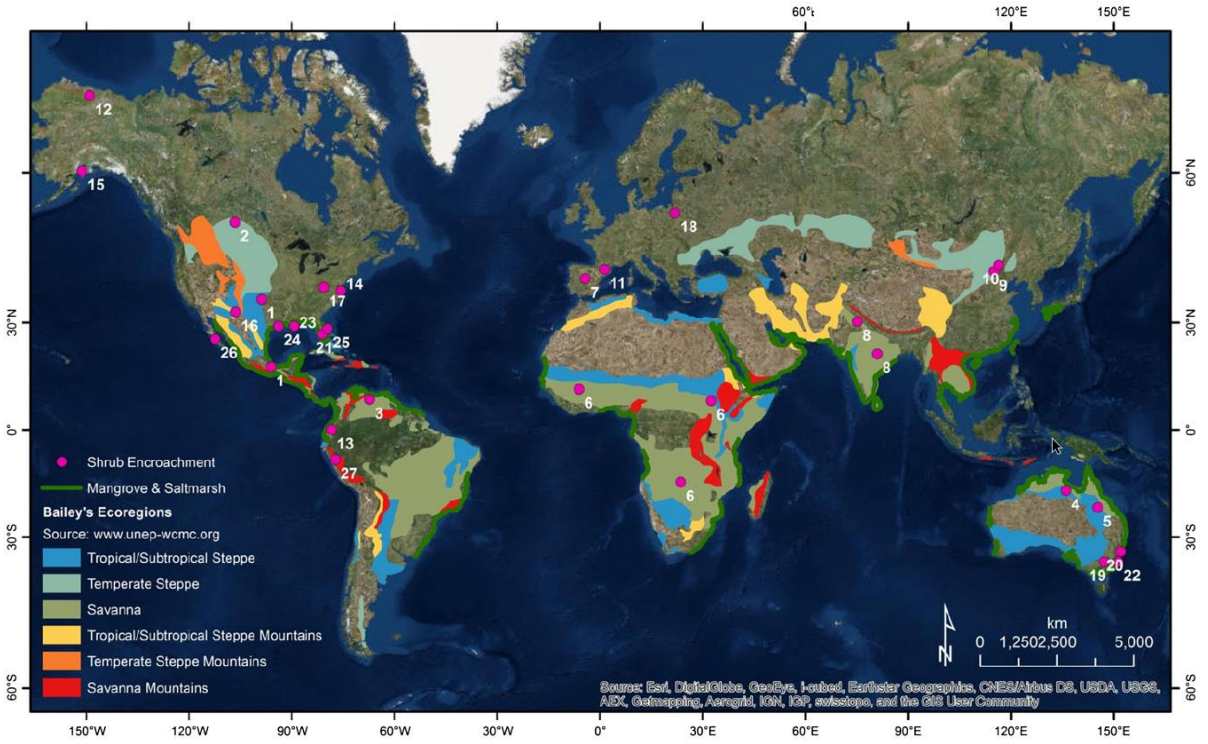

Figure 1.1 Shrub encroachment distribution in grassland globally.
Pink points are locations of documented shrub encroachment into grassland. Graph cited from the review of (Saintilan and Rogers, 2015), in which the land cover map is sourced from Bailey's Ecoregions map of the World (http://www.unep-wcmc.org/resources-and-data/baileys-ecoregions-of-the-world, accessed 26 August 2014).

In New Zealand, apart from wilding pines, there is little available evidence of the spatial extent and the amount of other woody species, i.e. shrubs, that have encroached into New Zealand's non-woody ecosystems. There are two types of shrub species expansion happening in New Zealand: Firstly, native shrub species are increasing (recovering) when grazing stops in grassland ecosystems, much of which in South Island was originally woody species occupied in prehumen era and these woody species were burnt during Polynesian colonisation (Mark, 1969, McGlone, 2001, McWethy *et al.*, 2009). On the other hand, exotic shrub plants are invading into grasslands. (McGlone, 2001)Several studies showed there was a possible tendency of shrub expansion into originally non-woody species dominated habitats in New Zealand: A study established in four protected natural areas in South Island revealed that the grazing removal benefitted the recovery of tussock grasslands and also aided shrub spread, which declined the biomass of tussock species and the biodiversity of this ecosystem (Grove *et al.*, 2002). Ground observations in Black Rock Scientific Reserve presented a dramatic gain of shrubs in snow tussock grassland

(Mark and Dickinson, 2003). Expansion of native shrub species were observed in Mackenzie Basin and Marlborough in former years (Meurk *et al.*, 2002, Rose and Frampton, 2007), and woody species became predominate at high altitude and exposed sites in indigenous grasslands (Ausseil *et al.*, 2011). A more recent work at Cass study site in Canterbury showed the prevalent trend of shrub invasion in the grassland (Young *et al.*, 2016). Above studies well recorded the transitions of shrub encroachment at the species scale, while the landscape scale investigation is still missing, which would be substantial at the concern of the overall indigenous non-woody species conservation in New Zealand.

1.2 Shifts in growth phenology

Phenology is defined as the study of the seasonal occurrences of flora and fauna (dates of flowering, migration, etc.) impacted by climate and the periodically changing form of organisms, especially when this affects their relationship with the environment (e.g. tree seedling, sapling and later mature) (Allaby, 2012). Sprouting and flowering of plants in spring, colour changes of leaves in autumn, bird migration and nesting, insect hatching, and animal hibernation are all examples of phenological events. In this thesis, I focus on the growth phenology of plants. Phenology stands as an important cue to trace the dynamics of plant species in the wild. It illustrates the duration of growth, which is a key feature of the ecological niche a plant species occupies. Plant species' seasonal activities, fitness to environment and sensitivity to climate change can be derived from phenological traits (Chuine, 2010). In some degree, the phenological characteristics decide the distribution of a specific species and the phenological shift is a good indicator of climate change.

In a global view, growth phenology of plant keeps changing due to either long-term historical climate shifts plus recently rapid fluctuations driven by human, or to the organisms' evolutions in order to gain adaptation to their living environments. In current century, plenty of evidence indicated that the phenology in many plant species had shifted related to climate change (Visser and Both, 2005, Buitenwerf *et al.*, 2015). It is generally agreed that the plant phenology has advanced and the growing period has lengthened in recent decades. For example, a recent meta-analysis of historical records showed that spring time has advanced globally by 2.3 days or 5.1 days per decade in different studies; a long-term observation in 21 European countries including 542 plant species found a evidential signal of earlier spring (leaf unfolding and flowering) and summer (fruit ripening) at a rate of 2.5 and 2.4 days per decade, respectively (Cleland *et al.*, 2007). A

study based on AVHRR (from the Advanced Very High Resolution Radiometer) satellite data combining field work investigations indicated a delayed autumn trend (3-4 days per decade) in European and North American temperate forests since 1982 (Jeong *et al.*, 2011, Richardson *et al.*, 2013).

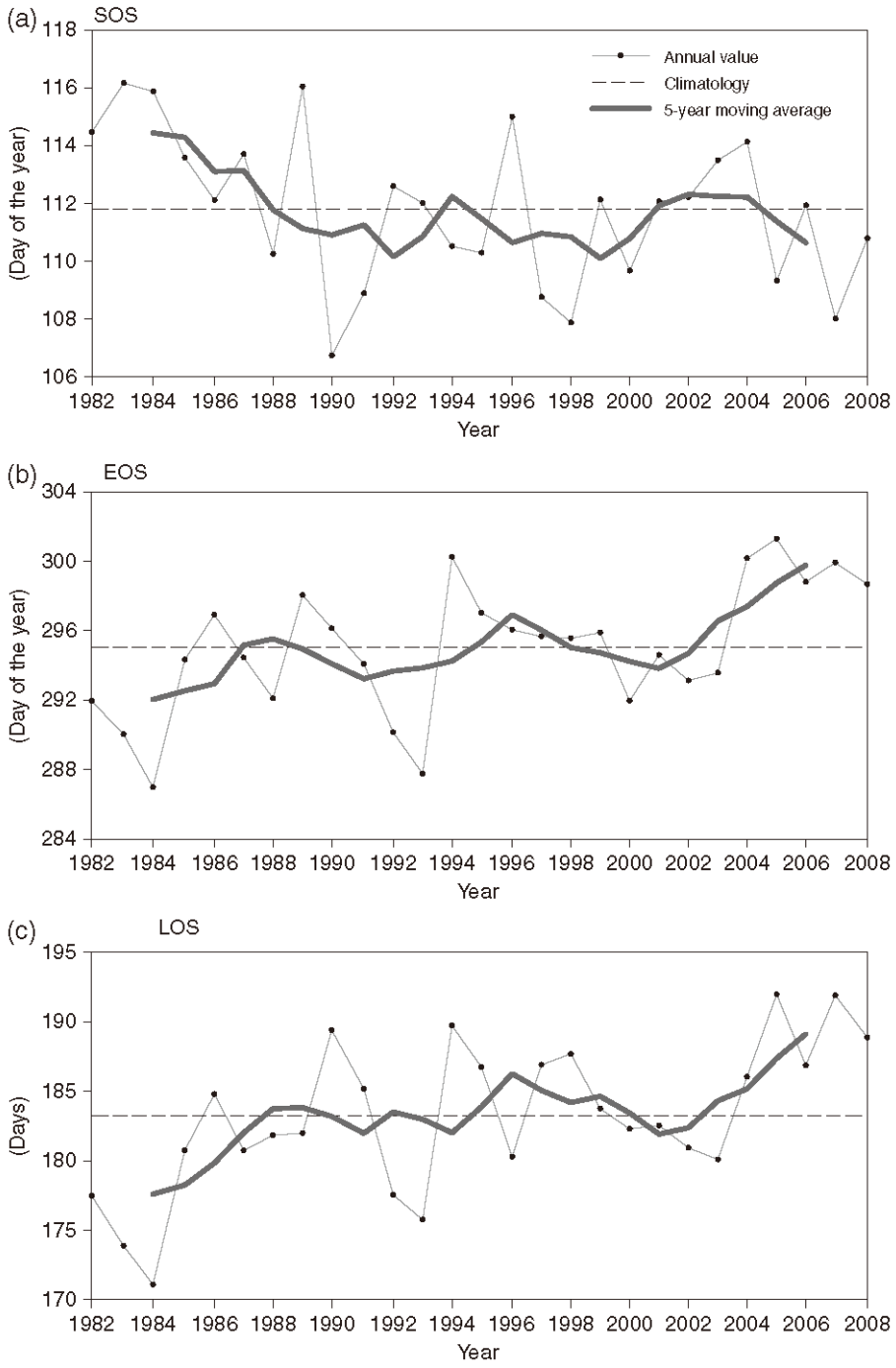

Figure 1.2 Inter-annual variations of phenology in the Northern Hemisphere for 1982–2008. Inter-annual variations of area-averaged start of season (SOS), end of season (EOS), and length of season (LOS) in temperate vegetation in the Northern Hemisphere for 1982–2008 (Jeong *et al.*, 2011).

However, the mechanism that how phenology shifts correlate with climate change is still uncertain. An experiment on coastal shrubs in the Mediterranean region showed a combined result of phenological events: delayed onset of autumn and advanced winter flowering (Llorens and Penuelas, 2005). In order to enhance the fundamental study and to improve cooperation in phenology research, numerous observational networks were constructed in Asia, North America and Europe (Betancourt *et al.*, 2005, Ide and Oguma, 2010, Dierenbach *et al.*, 2013).

In comparison to the vast amount of detailed phenological records in the Northern Hemisphere from Europe to Asia, the data in the Southern Hemisphere is sparse and discontinuous (McGlone and Walker, 2011). The earliest plant phenology data in New Zealand is the flowering schedule of nine species encompassing the period of 1893-1899. In last century, New Zealand Forest Service and Forest Research Institute (FRI) was formally found in 1949 aimed at the study of agriculture and forestry related phenological investigation (Schwartz, 2013). After then, the Department of Conservation (DOC) and Department of Land and Survey and Wildlife Service were launched with dedication to monitor all aspects of plant species including phenology(Mander *et al.*, 1998). The case studies which had been implemented to examine the flowering, seeding and breeding were listed in Schwartz & Mark's work (Schwartz, 2013).

In most of the records, the tendency of growth phenology shifts in New Zealand was not obvious. There were about 70% species (including plants and animals) who exhibited no apparently advanced or delayed phenological events in New Zealand (Schwartz, 2013). According to records till 2013, the main drivers of phenology shifts in New Zealand and Australia were air temperature, rainfall, sea-level change, radiation, snowmelt, ice, wind, etc. (Chambers *et al.*, 2013). Climate change may put more pressure on native plants than exotic species and make New Zealand even more vulnerable to invasion. For instance, lodgepole pines (*Pinus contorta*) spread above the treeline in plentiful locations, and had become a prior, immediate biodiversity hazard, as the invader is likely to evolve well to response to increasingly global warming (McGlone *et al.*, 2010). Although the specific geographic characteristics of New Zealand, such as oceanic weather, variable climate regime, steep topography, may minimise potential changes of plant phenology (McGlone and Walker, 2011), the sparse long-term biodiversity records remain insufficient to distinguish the tendency of phenological shifts.

1.3 Remote Sensing Applications for detecting ecological changes

In the ecological context, remote sensing normally refers to the technologies of recording electromagnetic energy emitted from objects or areas on the land surface, oceans or atmosphere. Remote sensing can facilitate scientists to identify and distinguish different geographic objects by their energy emission/reflectance properties, known as spectral signature. An increasing number of remote sensors become available for geographers and ecologists and the data types become abundant (Anderson, 2009). For ecological observation and mapping, which focus on the earth's surface and vegetation dynamics, the commonly used remote sensing data are digital formatted imagery captured by satellite or airborne sensors. Image data can be divided into two main types based on the sensors' physical bases: passive and active, for instance optical images and radar/lidar data (Wulder and Franklin, 2003). Remote sensing gives the opportunity to observe the changes in land use/land cover at a landscape scale and boosts the capabilities to monitor and forecast changes in climate/vegetation in a large region (Horning *et al.*, 2010). Homolová *et al.* (2013) illustrates the typical applications of remote sensing in ecological realm at different scales.

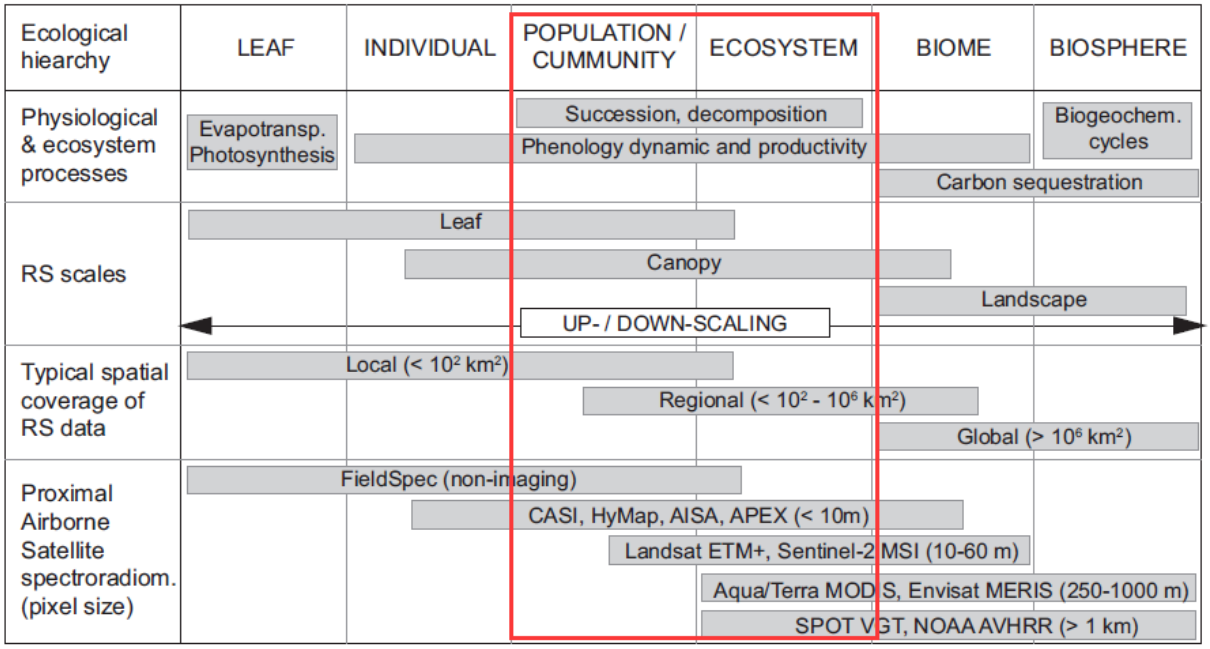

Figure 1.3 Link between ecological and remote sensing.
Spatial scales with examples of typical remote sensing spectro-radiometers. Graph modified from (Homolová *et al.*, 2013). In this thesis, remote sensing data were applied at the community and ecosystem scales.

As abundant satellite and airborne imagery has become available at various spectral, spatial, radiometric, and temporal resolutions, remote sensing data is getting sufficient to

additionally biological/ecological applications (Srivastava, 2014). Ecologists used remotely sensed data as a consistent long-term Earth observation data source at local to global scales (Wang *et al.*, 2010). In land use/land cover studies, remotely sensed time series data dramatically facilitated the monitoring of the biophysical processes on the Earth's terrestrial surface (Gomez *et al.*, 2016). Brockerhoff *et al.* (2008) re-examined the loss of indigenous vegetation coverage in New Zealand with new remote sensing data and field work samples. The result showed the overlooked potential losses of indigenous biodiversity, which was underestimated in the analysis of old land cover database. A research described a high accurate method for the mapping of New Zealand's forest nationally with Landsat TM and SPOT-5 imagery (Dymond *et al.*, 2012). The patterns of the conversion of New Zealand's indigenous grasslands in South Island were analysed with satellite imagery, showing the ongoing loss of grasslands (Weeks *et al.*, 2013b). In the land surface phenology (LSP) study, airborne and satellite datasets were used to derive metrics to describe the seasonality of vegetation. The ability to continuously capture phenology patterns across the landscape and retrospect the historical phenology in archived data enable remote sensing to be an advanced research tool(Reed *et al.*, 2009). Large scale Normalised Difference Vegetation Index (NDVI) data derived from satellite images can be used to establish algorithms for phenology change analysis nationally (White *et al.*, 2009). Song *et al.* (2011) used MODIS (Moderate-resolution Imaging Spectroradiometer) EVI (Enhanced Vegetation Index) products to analyse spatial pattern and differentiation of grassland phenology in the Northern Tibetan Plateau during the period of 2001 to 2010. A study analysed global phenology cycles over 2003 to 2008 with microwave remote sensing based Vegetation Optical Depth (VOD) retrieval method from AMSR-E and other ancillary data inputs(Jones *et al.*, 2011).

1.4 Grassland ecosystems

This thesis focuses on grassland ecosystems, which are dominated typically by herbaceous, non-woody species. Grassland ecosystems are often characterized by high levels of endemic biodiversity and a wide range of important ecosystem services worldwide (Global Biodiversity Outlook 4, 2014) and in New Zealand (Wardle, 1991, Mark *et al.*, 2013). To date (2002) there are 36,047 km^2 of indigenous grassland in New Zealand, among which there are 8,697 km^2 situated in high alpine regions (Mark and McLennan, 2005). These non-woody ecosystems are at risk from anthropological effects and climate change globally (Sala *et al.*, 2000, Rose *et al.*, 2004, Chazal and Rounsevell,

2009). The grassland ecosystems can be affected through two key processes: the functional changes through the expansion of woody species and the shifts in phenology. Plant species invasion has been and will continue being a serious threat to New Zealand's biosecurity (Giera and Bell, 2009). Recently, the woody plants were widespread and becoming predominant in New Zealand's indigenous grassland (Richardson and Rejmanek, 2011). Studies observed the invasions of woody species in New Zealand's tussock grasslands (Walker, 2000, Froude, 2011), nevertheless, the information of woody species' spatial expansion and quantity is still limited. On the other hand, current biology invasion study has concentrated increasing attention on understanding the role of phenology in shaping plant variations (Wolkovich and Cleland, 2014). There is mounting evidence that environmental conditions associated with recent climate change benefit woody species, and this has already led to increased woody biomass in grassland ecosystems in many parts of the world (Knapp *et al.*, 2008, Komac *et al.*, 2013, Ogden, 2015). Exotic species would exhibit adaptation priority to native species in phenology like earlier flowering following inter-annual variation in precipitation, soil moisture and temperature (Wolkovich *et al.*, 2013). However, the relationship of phenology and woody species expansion in New Zealand's grassland ecosystems is less known.

In many grassland studies, remote sensing plays a notable role in long-term vegetation dynamic monitoring and species mapping at landscape scale (Bradley and Mustard, 2006). High spatial resolution data mapping combined with field surveys are effective to grassland studies (Mohamed *et al.*, 2011, Olsson *et al.*, 2011). However, there is limited literature focusing on grassland ecosystems with remote sensing methods in New Zealand. Studies were done on land cover conversion in New Zealand's grassland with remote sensing (Weeks *et al.*, 2013a, Weeks *et al.*, 2013b). Long-term plant diversity and invasion dynamics in tussock grasslands have been investigated with transects data and GIS spatial-analysis tools, but remote sensing data and methods are not mentioned (Mark *et al.*, 2011, Day and Buckley, 2013).

1.5 Thesis outline

This thesis applied the satellite imagery time series to fill the knowledge gap of grassland dynamics at large scale. The aim of this thesis is to better understand the vulnerability of the New Zealand's indigenous grassland ecosystems to current climate changes. The compositional and phenological shifts in the threatened endemic species during the past decade were investigated. Specifically, I focus on shrub expansion and growth phenology

in the indigenous grassland, to tackle how the natural ecosystems adjusted their ecological behaviours to the environmental variations. There are six chapters conducted in this thesis:

Chapter 1 provides a general introduction to the key concepts underpinning this thesis;

Chapter 2, "Woody propagule pressure on New Zealand's indigenous grasslands – patterns in geographic and environmental climatic space", presents an analysis of the spatial patterns of native and exotic shrub propagule pressure in New Zealand's grassland ecosystems;

Chapter 3, "Recent shrub encroachment in a tussock grassland landscape in New Zealand's South Island", detected how much the shrub encroached into a tussock grassland site, which is supposed to be under high woody propagule pressure according to the result from Chapter 2;

Chapter 4, "Spatial pattern and temporal dynamics in growing phenology in New Zealand's indigenous grassland", discusses the spatial heterogeneity and the shifts of growing phenology in New Zealand's three types of indigenous grassland;

Chapter 5, "Topographical effects on the timing of growing season in New Zealand's natural grasslands", refers to the elevation and aspect effects on the shifts of growth phenology in New Zealand's indigenous grassland;

Chapter 6 is an overall conclusion summarising and synthesizing the main findings of this research.

Chapter 2 Woody propagule pressure on New Zealand's indigenous grasslands – patterns in geographic and environmental climatic space

(This chapter has been published (Hua and Ohlemüller, 2018), see Appendix VII)

Abstract

Indigenous grassland ecosystems worldwide are increasingly subject to encroachment from shrub species. A key factor determining encroachment patterns is the availability of shrub propagules in the areas surrounding the grasslands. This study investigates the geographic distribution (geographic space) and the climatic conditions (environmental space) of the potential areas from which native and exotic shrub propagule pressures can come from for New Zealand's main grassland types. Results show Alpine grassland and Tall Tussock grassland are mostly under pressure from native shrubs, while Low Producing grasslands have more exotic shrub pressure in the neighbourhood. In geographic space, there is little spatial overlap of regions with high native and exotic shrub propagule pressure for all three grassland types. In climatic space, grassland areas with high native and exotic propagule pressure are located in different climatic conditions for Alpine grasslands but in more similar climates for Tall Tussock and Low Producing grasslands. The results show climatic patterns can provide useful and additional information to analyse the spatial patterns of woody propagule pressure in grassland ecosystems. This allows for the identification of the spatial distribution and also of the environmental conditions of areas with high pressure from native and exotic shrub expansion.

Key words

Woody encroachment, Climate change, Grassland, Shrubs, Land cover, Climate niche

2.1 Introduction

Woody plant encroachment, the increase of woody species into originally grass-dominated ecosystems, is a global phenomenon (Knapp *et al.*, 2008, Reisinger *et al.*, 2013). In recent decades, grassland and other non-woody ecosystems worldwide have experienced the woody expansion caused by both native and exotic species (Briggs *et al.*, 2007, Srinivasan, 2012). Evidence suggests that recent anthropogenic environmental change, such as fire disturbance, pasture, land cover change, etc., favours woody plant growth, giving woody species a competitive advantage (Archer *et al.*, 1995, Briggs *et al.*,

2005, Zavaleta and Kettley, 2006). The displacement of grass species by woody plants can alter the ecosystem functions, reduce grassland productivity, decrease the number of native grassland species and lead to degradation cultural and ecological values of indigenous grasslands (Komac *et al.*, 2013, Ogden, 2015). Therefore, it is important to understand where the woody encroachment is most likely to occur in terms of (i) geographic space that is the geographic/spatial distribution of grassland areas most likely to be invaded and (ii) environmental space that is the environmental (climatic) conditions of these areas.

Propagule pressure is a measure of the number of individuals from one or more species released into a region(Lockwood *et al.*, 2005). Two key factors determine the degree to which an indigenous grassland is prone to both native and exotic woody species invasions: environmental suitability for woody species in the grassland area and the proximity of woody species, the latter is the availability of woody propagules in the neighbourhood of the grasslands. Propagule pressure from surrounding landscapes at different scales is recognised as one of the main driving forces of woody encroachment (Briggs *et al.*, 2005, He *et al.*, 2015). Propagule pressure is an instinctive factor in biological invasion. Its intensity, generally decreased by spatial distance from invaders' habitats, has been shown to be a predictor of the degree how an ecosystem is vulnerable to species invasion (Rouget and Richardson, 2003, Colunga-Garcia *et al.*, 2010). However, the magnitude of propagule pressure is often difficult to calculate, because it is not only sensitive to spatial scales but also deeply related to land cover factors and environmental gradients (Milbau *et al.*, 2009). Study shows spatial scales and neighbourhood size chosen can affect the result when evaluating the intensity of propagule pressure (Thomas and Moloney, 2015). Thus, hierarchical approach across several spatial scales are used to obtain different levels of propagule pressure at local, landscape and regional scales (Thomas and Moloney, 2013). Such analyses are an effective tool to integrate different factors of invasibility and to infer levels of woody invasion threat at a range of spatial scales (Kidane *et al.*, 2012, He, 2014, Caracciolo *et al.*, 2016). The patterns of shrub propagule pressure across regions and environmental conditions are useful to measure to which degree non-woody communities are at the risk of invasion from woody species (Pauchard *et al.*, 2009, Faulkner *et al.*, 2014)..

The indigenous grassland ecosystems in New Zealand are facing threat from woody species competition. New Zealand's non-woody indigenous ecosystems are comprised of two main vegetation types: grasslands below the treeline and alpine grass/herb-field

above treeline. Many of New Zealand's non-forest ecosystems are usually recognized obtaining high level of biodiversity and offering a wide range of ecosystem services (Wardle, 1991, Mark *et al.*, 2013). There was original ca. 82,400 km^2 of indigenous grassland pre-human in this land, however currently less than half (44%) left till (Mark and McLennan, 2005). Between 2001 and 2008,, there were 321 km^2 of indigenous grasslands converted to other non-indigenous types, due to economic motivated land cover conversion (Weeks *et al.*, 2013b). Some indigenous grass-dominated ecosystems are often not free of woody species. They would have significant woody components at least in parts of their range in pre-human times in many cases (Walker *et al.*, 2009). Besides, Polynesian fires turned large parts of New Zealand's woody ecosystems into open, grass dominated ecosystems and repeated fires facilitated tussock grasslands to establish and dominate in areas where scrub and forests used to dominate (McGlone, 2001, McWethy *et al.*, 2010). Long-term monitoring at selected New Zealand sites suggested there were complex spatial patterns and interactions of native and exotic woody and non-woody species in indigenous grassland areas (Bellingham, 1998, Walker, 2000, Rose *et al.*, 2004, Walker *et al.*, 2009). There is currently limited information available on the spatial distribution and relative prevalence of native versus exotic woody shrub species and where they are located in relation to New Zealand's indigenous grasslands. This study fills this gap and facilitates future research in this field.

Aiming to provide a multi-scale spatial analysis of potential propagule pressure from native and exotic shrub species on New Zealand's indigenous grasslands, this study analysed the spatial patterns of the proximity of New Zealand's indigenous grasslands to native and exotic shrublands at different spatial scales. The following three questions were addressed:

1) Which grassland areas have the highest potential woody propagule pressure and where are they located?

2) Do grassland areas with high native and high exotic propagule pressure coincide spatially and do they occur in similar climatic conditions?

3) How does the scale of analysis (local, landscape and regional) change the assessment of the spatial distribution of potential woody propagule pressure on grasslands?

2.2 Methods

2.2.1 Approach overview

The overall aim of this study is to quantify the prevalence of native and exotic shrub cover in the neighbourhood of the three main indigenous grassland types. The principal assumption is that grassland grid cells with a larger area of shrub land cover in their neighbourhood are exposed to higher potential shrub propagule pressure. I did not include any micro-topographical or species trait information that might affect actual dispersal of the propagules. Based on recent published land cover data of New Zealand (including Rakiura–Stewart Island), analysis was conducted at the grid cell level on a 1×1-km grid. For each grid cell I quantified the area of shrub land cover in neighbourhood at three different spatial scales (neighbourhood sizes). Each grassland pixel is assigned with the number of how many native/exotic shrub cells in the neighbourhood. Then the grassland cells are ranked from high to low above zero. The zero cells, which have no shrub neighbourhood in a certain radius, are excluded in ranking. Therefore, the grassland pixels on the top of ranking are anticipated to be under high shrub propagule pressure. I obtained the top ranked grassland by threshold (e.g. top 5% cells) to map the spatial patterns of high shrub propagule pressure in grassland ecosystems. Then these highly-pressured habitats are compared in niche overlap analysis (Figure 2.1).

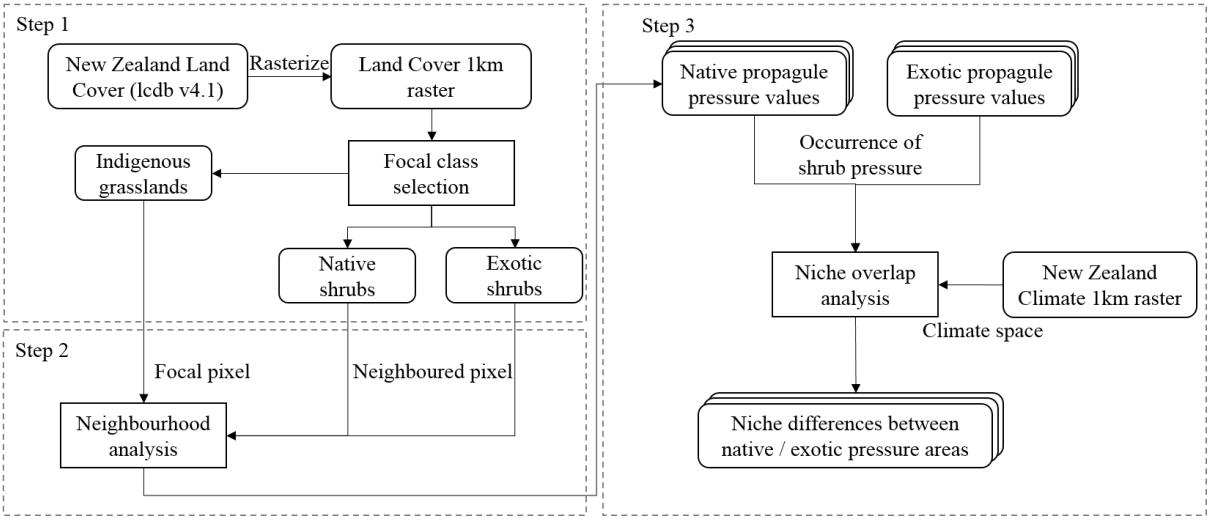

Figure 2.1 Method of potential propagule pressure estimation
Step1. Rasterization: convert vector-formatted land cover data to 1×1 km grid cells in ArcGIS 10.1. Step2. Neighbourhood: use indigenous grassland as focal pixels and calculate the number of shrubs pixels in neighbourhood at different spatial scales. Rank the grassland pixels by neighboured shrub pixel numbers. High number means high possible propagule pressure. Step3. Niche overlap: map the distribution of grassland under high native and exotic shrub propagule pressure in geography, then use niche overlap analysis to calculate the similarity of climate conditions in which the grassland under different shrub propagule pressure situate.

2.2.2 Land cover data collection and process

This study based on the New Zealand Land Cover Database (LCDB-v4.1, 2015). It is a regularly updated data for the whole New Zealand national domain. I used the most recent information (2012/2013) as the land cover map. LCDB's information was derived from satellite imagery by manual drawing and automatic detection approach, which confirms its reliable accuracy (Dymond *et al.*, 2017). Even though this dataset has limitation in ecological change detection (Weeks *et al.*, 2013b, Dymond *et al.*, 2017), I considered it as adequate for propagule pressure analyses at different spatial scales as I did not utilise any between-year change data.

The vector formatted LCDB data was rasterized to 1×1-km grid raster in module "Polygon to Raster" with "cell-centre" assignment option in ArcGIS 10.1. Three land cover classes were considered as indigenous grasslands: (i) Alpine grassland, (ii) Tall Tussock grassland and (iii) Low Producing grassland. The latter land cover class can contain significant parts of exotic elements in parts of its range (Cieraad *et al.*, 2015). For native shrub ecosystems, I used the land cover classes: (i) manuka and/or kanuka, (ii) subalpine shrubland and (iii) matagouri or grey scrub. For exotic shrubs, I used the classes: (i) gorse and/or broom and (ii) mixed exotic shrubland (Figure 2.2). For detailed description of these classes, see Appendix I.

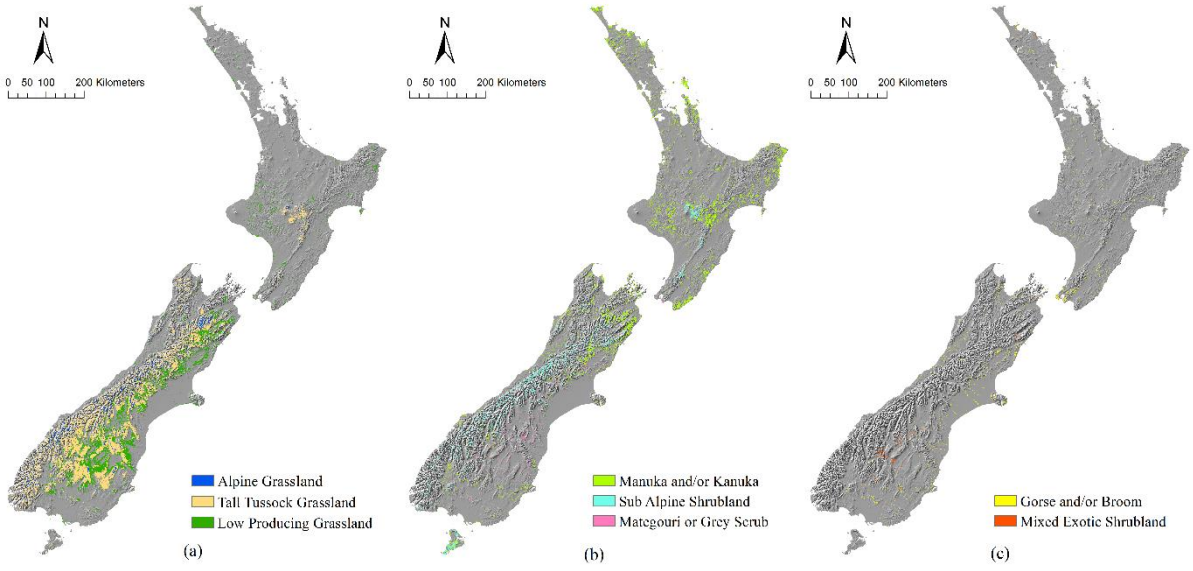

Figure 2.2 Grassland and shrub classes.
(a) Indigenous grassland: Alpine grassland, Tall Tussock Grassland, Low Producing Grassland. (b) Native Shrubs: Manuka and/or Kanuka, Sub Alpine Shrubland, Matagouri or Grey Scrub. (c) Exotic Shrubs: Gorse and/or Broom, Mixed Exotic Shrubland.

2.2.3 Neighbourhood analysis

I conducted a spatial neighbourhood analysis for each grassland grid cell in order to quantify how many (native and exotic) shrub grid cells are located in the neighbourhood within a distance of 1 km (local), 5 km (landscape) and 25 km (regional). The neighbourhood calculation was operated in the tool "Focal statistics" in ArcGIS 10.1. Grassland cells are set as focal cells and shrub cells are set to neighbouring cells. For each focal cell, a rectangular neighbourhood was built to calculate the number of shrub pixels within the rectangle area. In ArcGIS, the neighbourhood were configured as rectangle with side length of 3,000m, 11,000m and 51,000m, which are two times of radius plus the focal cell side length (e.g. at 5 km scale, the neighbourhood side length = radius size 5,000m × 2 + cell size 1,000m = 11,000m). I calculated for each grassland grid cell the proportion of grid cells in its neighbourhood that are shrubland, leading to each grassland grid cell having a value between 0.0 (no shrub grid cell in neighbourhood = no propagule pressure) and 1.0 (all neighbouring cells are shrub = high propagule pressure). This was done for native and exotic shrubs and for the three neighbourhood sizes (Figure 2.3).

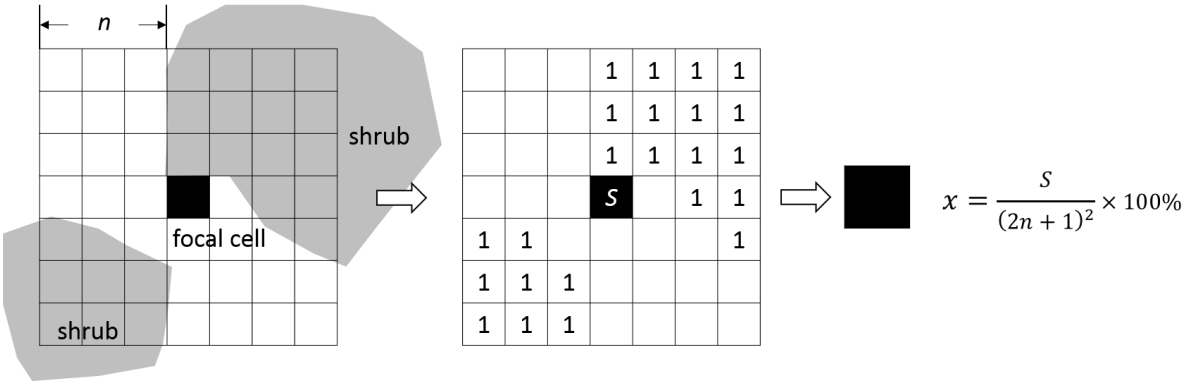

Figure 2.3 Shrub in neighbourhood calculation
The black cell in centre represents a focal grassland grid cell. "n" is the scale of neighbourhood radius. "S" is the count of shrub cells in the neighbourhood. "x" is the proportion of shrub in neighbourhood, which is used to quantify the intensity of potential shrub propagule pressure.

I ranked all grid cells within each grassland type from highest to lowest propagule pressure resulting in all grassland grid cells with at least one shrub land cover within their neighbourhood being categorised in one of five groups: top 5, 25, 50, 75 and 100%; any grassland grid cell with no shrub grid cell in its neighbourhood was not part of the ranking. I considered the top 25% of grid cells as 'high pressure' and the top 5% as 'very high pressure' locations. At last I mapped each grassland grid cell for each neighbourhood size whether the grid cell was part of the high propagule pressure group for native shrubs, exotic shrubs or both.

2.2.4 Niche Overlap Assessment

In order to characterise the climatic conditions in which the grassland ecosystems with high shrubland surrounded occur, six variables relevant for shrub species growth were selected from WorldClim (Hijmans *et al.*, 2005). These variables are mean annual temperature (bio1), temperature seasonality (bio4), lowest temperature of the coldest month (bio6), annual precipitation (bio12), precipitation seasonality (bio15) and precipitation of driest quarter (bio17). These data represent the 1950–2000 average and were used to characterise the climatic conditions (climatic niches) of the different grassland ecosystems.

I conducted a principle component analysis (PCA) based on the six climatic factors for all the grassland types, which allowed us to show the position of each ecosystem in a 2-D climate space of the two first PCA axes. My aim was to quantify if hotspots of native and exotic propagule pressure occurred in the same climatic conditions. To achieve the goal, I calculated the niche overlap of the native and the exotic hotspot area in climate space for a given grassland type and neighbourhood size using the niche overlap index Schoener's D. It is a commonly used ecological metric to quantify the overlap in environmental conditions of two species or populations based on spatial occurrence records (Warren *et al.*, 2008). I applied this index to calculate the overlap in climatic conditions between grassland areas under high native and high exotic propagule pressure. The index was calculated using the package 'ecospat' in the statistical software R (version 3.3.3, 2017-03-06) (Broennimann *et al.*, 2012). The Schoener's D ranges from 0 to 1 (Rodder and Engler, 2011) and in this study indicates that for any given grassland type, native and exotic high-propagule pressure grassland areas occur in different (D = 0) or in similar (D = 1) climates.

2.3. Results

2.3.1 Spatial patterns of woody propagule pressure

The three grassland types in this study cover a total of 15.55% of the New Zealand land area with Alpine grassland having the smallest (0.8%) and Tall Tussock Grassland having the largest extent (8.7%, Table 2.1). The majority of indigenous grassland cover is located in the South Island (Figure 2.4). The spatial distribution of grasslands exposed to native and/or exotic shrub propagule pressure diverse at different scales.

At the local scale (1 km neighbourhood), all grassland types are mostly exposed to native rather than exotic propagule pressure (Table 2.1, Figure 2.4). More than one-third of the area in each grassland type has at least some native shrubs within a 1 km neighbourhood. In contrast, only 0.5% of Alpine grassland, 2.4% of Tall Tussock grassland and 11.2% of Low Producing grasslands have at least some exotic shrubland nearby. The largest spatial overlap of areas under native and exotic pressure at this local level is for low producing grassland, with 3.3% of grid cells being located in areas where at least some native and exotic shrubs are within 1 km.

Table 2.1 Shrub propagule pressure affected grassland pixels

Grass types	Propagule Pressure		Scales					
	Intensity	Sources	Local (1km)		Landscape (5km)		Regional (25km)	
			Pixels	%	Pixels	%	Pixels	%
Alpine Grassland, 0.85% of NZ	Top 5%	Native	108	4.80	121	5.38	113	5.03
		Exotic	12	0.53	19	0.85	82	3.65
		Both	1	0.04	5	0.22	7	0.31
	Top 25%	Native	367	16.33	592	26.33	564	25.09
		Exotic	12	0.53	114	5.07	414	18.42
		Both	1	0.04	52	2.31	147	6.54
	All	Native	952	42.35	2189	97.38	2248	100.0
		Exotic	12	0.53	202	8.99	1632	72.60
		Both	6	0.27	193	8.59	1632	72.60
Tall Tussock Grassland, 8.71% of NZ	Top 5%	Native	539	2.29	1126	4.78	1188	5.04
		Exotic	31	0.13	278	1.18	1042	4.42
		Both	0	<0.01	0	<0.01	12	0.05
	Top 25%	Native	3410	14.48	5530	23.48	5900	25.05
		Exotic	556	2.36	1796	7.63	5286	22.44
		Both	47	0.20	233	0.99	795	3.38
	All	Native	8245	35.00	20770	88.18	23551	99.99
		Exotic	556	2.36	5311	22.55	20372	86.49
		Both	137	0.58	4534	19.25	20372	86.49
Low Producing Grassland, 5.99% of NZ	Top 5%	Native	422	2.62	720	4.48	813	5.05
		Exotic	107	0.67	466	2.90	803	4.99
		Both	1	0.01	2	0.01	48	0.30
	Top 25%	Native	2221	13.81	3654	22.72	4022	25.01
		Exotic	1805	11.22	2975	18.50	3986	24.78
		Both	215	1.34	623	3.87	1105	6.87
	All	Native	5315	33.05	14391	89.47	16072	99.93
		Exotic	1805	11.22	8878	55.20	15944	99.13
		Both	536	3.33	7987	49.66	15932	99.05

Note: Percentages indicate the percent area of grassland that is classified as having very high (top 5%), high (top 25%) and any (all) woody propagule pressure. 'Top 5%' indicates the 5% of grassland grid cells with the highest proportion of woody land cover in their neighbourhood; 'all' indicates all grassland grid cells with at least one shrub grid cell within their neighbourhood. In Alpine grassland for example, 108 pixels are under high 'native' shrub propagule pressure at the

threshold of top 5%, and 4.8% is the proportion of the 108 pixels in all 2,248 pixels in that land cover class.

At the landscape scale (5 km neighbourhood), almost all grid cells of all grassland types have at least some native shrubland in their neighbourhood. Alpine has 97.4% of grid cells, Tall Tussock has 88.2% and Low Producing grassland has 89.5%. Similar with the local neighbourhood, these values are much smaller for exotic shrubs, with 9%, 22.6% and 55.2% for the three grassland types. At this spatial scale, however, one fifth of Tall Tussock and half of Low Producing are exposed to both native and exotic shrub species propagule pressure in their neighbourhood (Table 2.1). These native and exotic spatial locations are mostly located on the eastern foothills of the Southern Alps in the northern half of the South Island (Figure 2.4).

At the regional scale (25 km neighbourhood), basically all grassland areas have at least some native shrub habitats within their neighbourhood (>99.9% of grassland cells, Table 2.1) while more than 73%, 86% and 99% of Alpine, Tall Tussock and Low Producing grassland areas have at least some exotic shrubland in the neighbourhood. Focusing on the top 25% quartile of grid cells with the highest proportions of neighbouring shrub cover, Alpine and Low Producing grasslands have over 6% of their area under combined pressure of native and exotic species, and the value for Tall Tussock grassland is 3.38%. Most of these areas are located in the northern half of the South Island (Figure 2.4).

At all three spatial scales, the three grassland types are all exposed to more native shrubs propagule pressure than exotic shrubs, especially at local scale (1km neighbourhood). Alpine grassland is mainly under native shrub propagule pressure, while Low Producing grassland is supposed to be under the highest propagule pressure from exotic shrubs among the three grassland types.

In geography, most of the native shrub neighbouring grasslands are located in north part of South Island and centre of North Island. The hotspots of high native pressure are Waihopai Valley in Marlborough, the mountains in West Coast and Mt Ruapehu in North Island. The exotic shrub propagule pressure often threatens the grassland at lowlands in southern part of South Island, which are close to residential regions and farmlands, including large areas of central Otago and Canterbury Region. The grasslands under pressures from both shrub types situate in northeast of South Island, along the boundary of Canterbury and Marlborough Regions (Figure 2.4). Neighbourhood size plays a remarkable role in distribution of the shrub pressures.

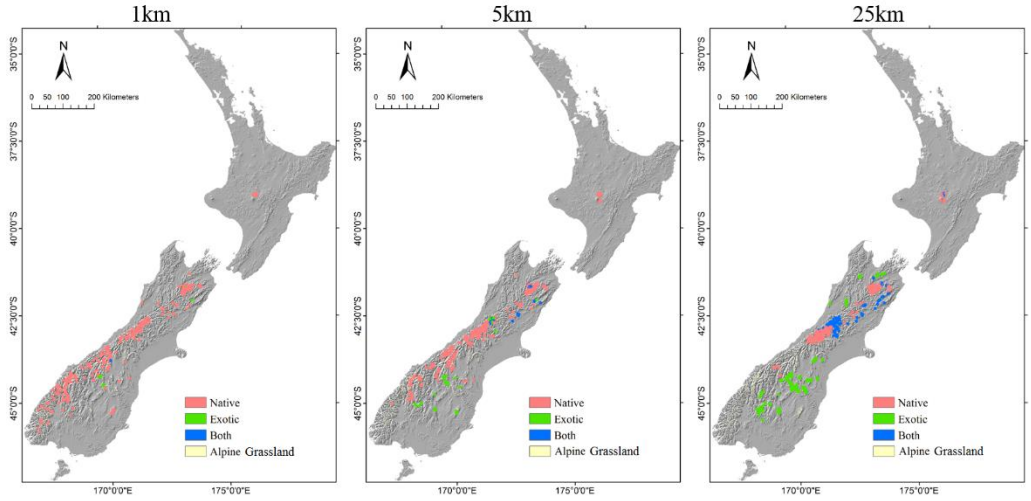

a) Alpine Grass land

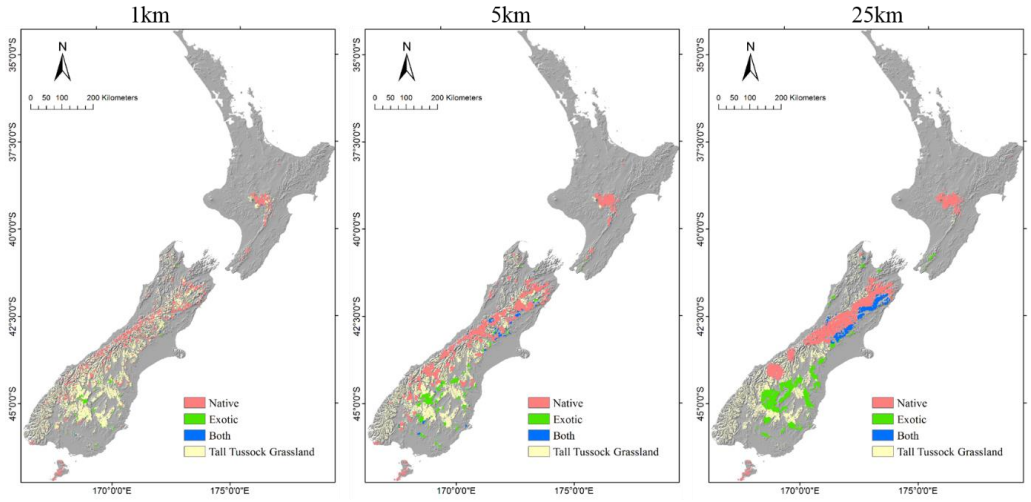

b) Tall Tussock Grassland

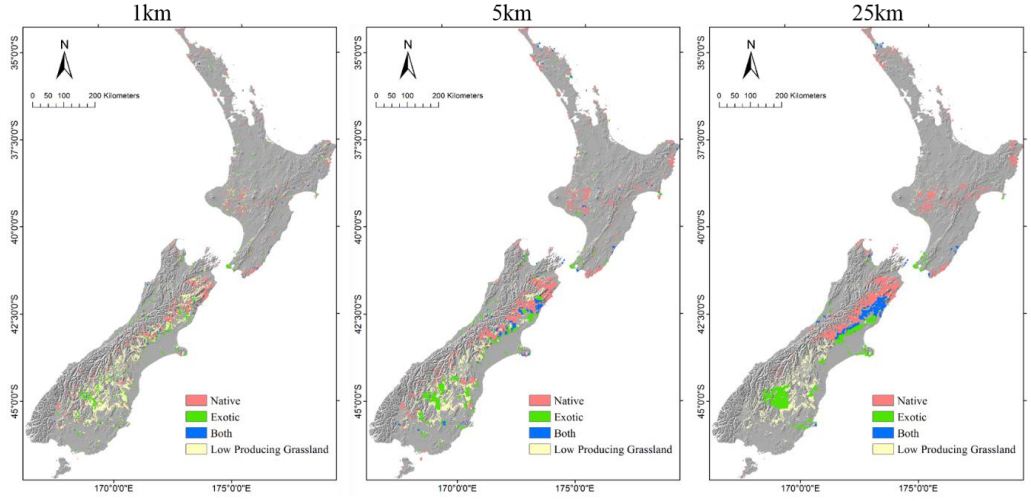

c) Low Producing Grassland

Figure 2.4 Spatial distribution of potential shrub propagule pressure in indigenous grasslands Spatial distribution of high shrub propagule pressure (upper 25%) in indigenous grasslands in New Zealand. The light Red areas are grasslands under high native shrubs' pressure only, while the green areas colours are under high exotic pressure only and. Blue areas regions named "Both" are pixels are under both high native and exotic shrubs' pressures. Light yellow coloured lands are the rest of grassland pixels which are not included in the top 25% threshold of highest propagule pressure.

2.3.2 Climatic patterns of woody propagule pressure

The three grassland types investigated here occupy distinct climatic niche space (Figure 2.5), which is a reflection of their geographic distribution. As expected, Alpine grassland occupy cooler and moderately wet parts of the climate space available in New Zealand (Figure 2.5a). Tall Tussock grasslands occur in drier and cooler areas (Figure 2.5b) while Low Producing grasslands are found in warmer and very dry areas (Figure 2.5c). Climatic preferences between any of the grassland and any of the shrubland types are most similar for Low Producing grassland and native matagouri/grey scrub (D = 0.72; Table 2.2). Of all grassland types, Low Producing grasslands have the highest and alpine grasslands the lowest similarity in climatic conditions with exotic shrublands (Table 2.2).

Table 2.2 Climatic niche overlap between three grassland and five shrubland types

	Alpine grassland	Tall Tussock grassland	Low Producing grassland
Native shrubland			
Manuka and/or kanuka	0.03	0.07	0.27
Subalpine shrubland	0.33	0.47	0.16
Matagouri or grey scrub	0.12	0.28	0.72
Exotic shrubland			
Gorse and/or broom	0.01	0.04	0.27
Mixed exotic shrubland	0.08	0.18	0.37

Climatic niche (Schoener's D) values range from 0 to 1 with higher values indicating more similar climatic conditions within which the two ecosystems occur.

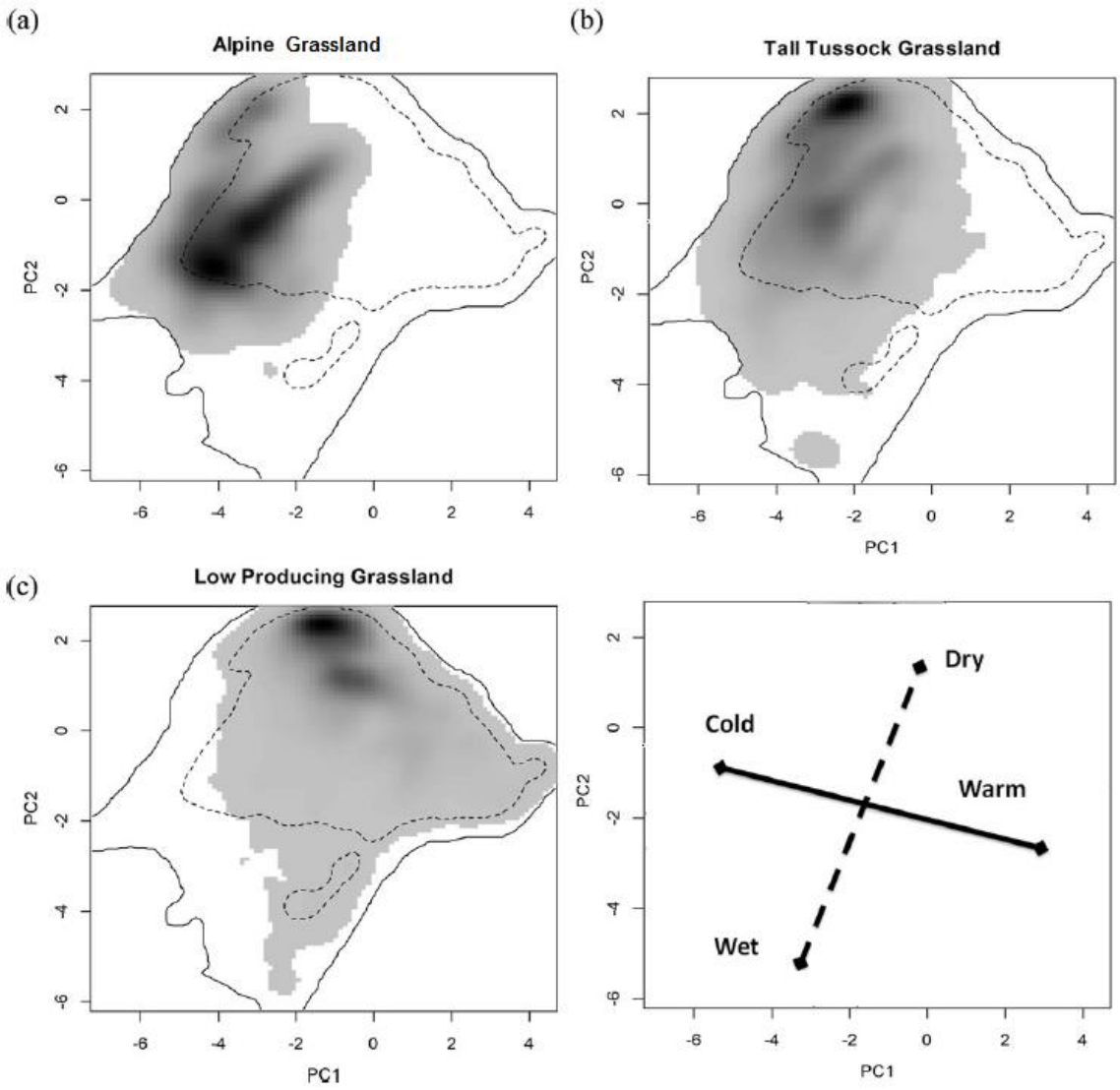

Figure 2.5 Climate conditions in three grassland types
Climate conditions of the three indigenous grassland types (a–c) investigated in this study. Grey areas show the space occupied by each grassland type in 2-D climate space made up of the first two axes of a principal component analysis (PCA) of six climate variables (see Methods section). PCA axis 1 represents a cold to warm gradient, axis 2 a wet to dry gradient (see inset). The solid outline illustrates the overall climate space available in New Zealand, and the dotted line is the 50% quantile region. Darker grey tones indicate more grid cells in that part of the climate space.

The degree of similarity of climate conditions in which a grassland area exposed to the combined native and exotic shrub propagule pressure depends on the level of propagule pressure and the neighbourhood size applied (Table 2.1). When considering all grassland grid cells with at least one native and/or one exotic grid cell in the neighbourhood, climatic niche overlap between grassland areas under native pressure and the areas under exotic pressure was low for alpine and Tall Tussock grassland (D = 0.11, 0.28), and highest for Low Producing grasslands (D = 0.63) at the local scale (”Local 1km”, Table 2.3). This indicates that in the immediate surroundings of grassland areas native and exotic

shrubs occupy much more similar climates in the vicinity of low producing grasslands than in alpine grasslands. This pattern is constant for higher propagule pressure intensities, for example when considering the top 5% of grassland grid cells with the largest areas of native and exotic shrubland in the neighbourhood (Table 2.3).

At larger spatial scales (landscape and regional), overlap between native and exotic climate niches increases, but the relative order of grassland types remains: for alpine grasslands, areas with high combined native and exotic shrub pressure occur in more different climate conditions than for Tall Tussock grasslands and low producing grasslands. Overall, these niche overlap values (Schoener's D values) indicate that native and exotic shrub propagules have less specific climate preferences near low producing grassland than near the other two grasslands.

Table 2.3 Climate niche overlap (Schoener's D) between grassland areas affected by native and exotic shrubs at different levels of propagule pressure intensity

Grassland types	Pressure intensity (Top %)	Local (1km)	Landscape (5km)	Regional (25km)
Alpine Grassland	Top 5%	0.06	0.68	0.01
	Top 25%	0.07	0.13	0.09
	Top 50%	0.11	0.22	0.25
	Top 75%	0.11	0.46	0.54
	All	0.11	0.55	0.88
Tall Tussock Grassland	Top 5%	0.02	0.03	0.01
	Top 25%	0.22	0.25	0.09
	Top 50%	0.28	0.35	0.29
	Top 75%	0.28	0.54	0.57
	All	0.28	0.60	0.92
Low Producing Grassland	Top 5%	0.42	0.27	0.07
	Top 25%	0.51	0.37	0.27
	Top 50%	0.63	0.63	0.49
	Top 75%	0.63	0.77	0.74
	All	0.63	0.83	0.98

'Top 5%' indicates the 5% of grassland grid cells with the highest proportion of shrubland cover in their neighbourhood; 'all' indicates all grassland grid cells with at least one shrub grid cell within a given neighbourhood size. Local, landscape and regional scales indicate three neighbourhood sizes within which the area of woody land cover was quantified (see 2.2 Methods section).

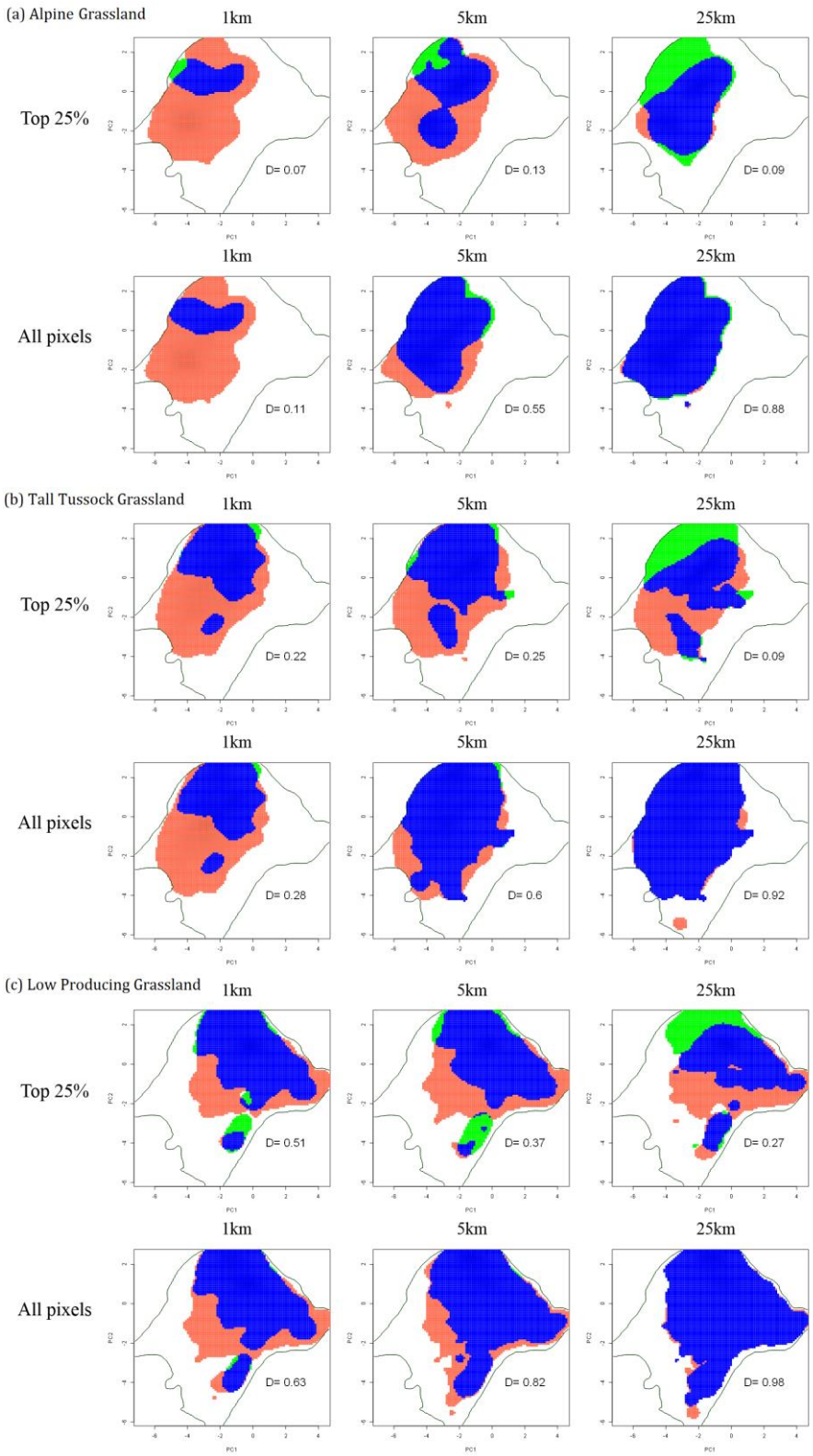

Figure 2.6 Climatic niche overlaps of grassland under native or exotic shrub propagule pressures High pressure pixels (top 25%) and all affected pixels (top 100%) were plotted at three neighbourhood scales. The red colour represents native shrub pressured regions, the green colour stands for exotic pressure, and blue area is the overlapped region. The x- and y-axes are the first two axes of a principal component analysis of six climate variables – areas close together in the diagram have similar climate conditions. Line indicates overall climate conditions available in New Zealand

Climatic niche overlap shows when considering all the grassland pixels with at least one shrub pixel in the neighbourhood, the grassland areas under native and exotic shrub pressures have more climatic niche overlap at the wider spatial scale (Figure 2.6). However, the relatively high (top 25%) native and exotic shrub propagule pressure in the vicinity of grasslands occupy more similar climates at landscape scale than the other two scales. For alpine grassland, the top 25% of pixels with most native and exotic shrubs in neighbourhood have the highest similarity of climate preference at landscape scale (5 km, D=0.13). The same trend can also be seen for top 25% of Tall Tussock grassland cells, that the climatic niche overlap is higher at 5 km scale (D=0.25) than the other two scales (D=0.22 at 1 km, D=0.09 at 25 km). Nevertheless, for low producing grassland the highest value appears at local scale (1 km, D=0.51) but not at landscape scale (5 km, D=0.37). This indicates the scale effect is various for different grassland types. The graphical representation of climate niche overlap also illustrates the grasslands surrounded by exotic shrubland locate in the regions colder and drier than the habitats occupied by grasslands with native shrubs in neighbourhood.

2.4. Discussion

2.4.1 Quantifying shrub propagule pressure in indigenous grassland types

The results suggest that alpine grass/herbfield are the grassland type most exposed to native shrub propagule pressure while low-producing grasslands are most exposed to exotic propagule pressure (Table 2.1). Shrubs' ecological characteristics, such as seed dispersal types, were not considered in this study. The proximity to shrubs is the only factor to measure the "potential" shrub propagule pressure on specific grassland. As the shrub land cover types (Appendix I) used here are identified as communities rather than species, and the scales of proximity are large in spatial, I reckon my neighbourhood analysis method gave an appropriate similarity of ranges shrubs' propagules can reach. This is, at the most general level, a reflection of the spatial distribution of these grassland types in relation to native and exotic shrublands (Figure 2.1).

The changes from grassland types to shrub lands recorded in LCDB dataset (LCDB-v4.1, 2015) would be a good reference to test the results. According to the "change pivot table" included in the LCDB v4.1 files, there are no conversions between Alpine Grass / Herbfield and shrub lands during the periods of 1996-2001, 2001-2008 and 2008-2012. For Tall Tussock grassland, there are 1,274, 464 and 52 ha transferred to shrubland during these three time periods. However, the major change in Tall Tussock grassland was associated

with the rising of artificial land cover types for pasture and forestry: 9,011, 5,309 and 1,911 ha of Tall Tussock grassland had changed to exotic forest during the three time periods (LCDB-v4.1, 2015). Large area of Tall Tussock grassland also had been converted to high producing grassland: 5,527 and 4,139 ha of Tall Tussock grassland changed to this land cover during 2001-2008 and 2008-2012. During 2008-2012, there were 2,708 ha of Tall Tussock grassland changed to low producing grassland. The decreasing trend possibly indicates a change in awareness and appreciation of New Zealand's native grassland ecosystems (Mark and McLennan, 2005, Mark *et al.*, 2009). Most change from Tall Tussock grassland to other land cover types detectable with the LCDB land cover methodology was due to agricultural activities rather than invasion of (native or exotic) species. Local on-the-ground or high-resolution airborne multi-year surveys are needed to reliably detect shrub species invasions into grasslands.

For Alpine grassland, there are no changes detected in LCDB v4.1, but the results show that they are under high-propagule pressure from native shrubs (Table 2.1). Montane and alpine regions, where climate conditions are harsh to most species, are not 'immune' to woody invasion as long as the woody species can reach the places (Tecco *et al.*, 2016). My analysis was based only on spatial patterns of certain land cover types. Even though there might be large areas of shrubland near an area of grassland, the shrub propagules might not be able to reach the grassland area because of topography, wind direction etc. and this will be particularly relevant in alpine environments.

For Low Producing grassland, besides the huge area converted to high producing grassland (14,061 ha) and exotic forest (46,722 ha), there were 3,535 ha of low producing grassland changed to shrubland during 1996-2001. The area changed to shrubland in 2001-2008 and 2008-2012 are -1,882 and -11,958 ha, which means low producing grassland expanded during these years. Grasslands classified as low-producing grasslands are the most anthropogenically modified grassland types that are also in closest proximity to agricultural activity (Walker *et al.*, 2009, Cieraad *et al.*, 2015). The conversions in this grassland type might be deeply affected by human's activities rather than natural process. Further work is needed to distinguish the natural changes in low producing grassland and to estimate the shrub threat to indigenous grass species.

There are uncertainties and accuracy issues associated with the LCDB dataset in specific indigenous grassland areas (Brockerhoff *et al.*, 2008), small changes may not be recorded correctly (Dymond *et al.*, 2017). Some transitions from grasslands to shrubland might

have really happened but they were not obvious enough to be captured by the remote sensing methodology applied in the current LCDB datasets. More accurate observation would be helpful to verify the propagule pressure results.

2.4.2 Spatial coincidence of high native and exotic propagule pressure

Of the three grassland types, low-producing grassland had the highest propensity to be located in areas where high native and exotic propagule pressure coincide (Table 2.1). At the landscape and regional scale, 50% and 99% of low producing grasslands have at least some native and exotic shrublands in their neighbourhood. Alpine grass/herbfield is the least likely to be located in areas with high pressure from natives and exotics with only 9 and 73% of its area being located in areas that have at least some shrubland in the neighbourhood at the landscape and regional scale (Table 2.1).

Woody native shrubs such as manuka (*Leptospermum scoparium*), kanuka (*Kunzea* spp.), monoao (*Dracophyllum subulatum*), inaka (*Dracophyllum longifolium*) are a typical and natural feature in New Zealand's native grasslands, as for instance in red tussock (*Chionochloa rubra ssp. rubra*) communities in Rangipo and Mangaohane areas in central North Island (Rogers and Leathwick, 1994). In a study near Porters Pass, South Island (Bellingham, 1998), native and exotic shrub invasions into alpine grassland were already observed over 20 years ago. The native shrub, matagouri (*Discaria toumatou*), was often observed in habitats where tussock species decreased. The exotic Scotch broom (*Cytisus seoparius*) was seldom seen among the gaps between tussock and matagouri communities, but the exotic shrub was predicted to surpass the biomass of matagouri (Bellingham, 1998). In recent years, expansion of several native woody species continue to be observed in tussock-dominated areas at high elevation, (species from the genera *Brachyglottis*, *Coprosma* and *Dracophyllum*), with manuka and kanuka being more prominent in lower altitude grassland sites (Ausseil *et al.*, 2011). Several exotic shrub invasions into indigenous grasslands have been observed and documented in recent research, for instance Scotch heather (*Calluna vulgaris*) had invaded North Island's volcanic plateau, Spanish heath (*Erica lusitanica*) has spread into tall tussock grasslands in Otago and gorse (*Ulex europeaus*) and broom (*Cytisus scoparius*) extended into low altitude grass habitats (Mark *et al.*, 2013). The latter areas coincide with the high exotic pressure areas in the South Island (Figure 2.4).

The results indicate that even at the local scale (i.e. 1 km distance around a grassland grid cell) there are usually both native and exotic shrubland present near grassland areas and

the proportion of grassland grid cells for which this is the case increases with neighbourhood size (Table 2.1). The spatial distribution of grassland areas that are under high native and exotic pressure is spatially more scattered at the local scale than at the regional scale (Figure 2.4). A general pattern emerges at larger spatial scales: alpine and eastern foothill areas in the upper South Island seem to be the areas mostly prone to both native and exotic propagule pressure acting on any grassland area (Figure 2.4). There are substantial amount areas dominated by mixed types of shrubs in LCDB dataset. Plenty of native shrubs including *Leptospermum*, *Coprosma*, *Ozothamnus*, *Melicytus* were found as dominant species among riparian, valley and rocky regions in Marlborough and Canterbury Plains (Mark and McLennan, 2005). This literature agrees to the mapping of potential shrub propagule pressure in this study. The results might be a good indicator for shrub encroachment in New Zealand.

2.4.3 The preference of climate conditions for native/exotic shrub propagules

Local climatic factors can affect the establishment and dispersal of the expanding shrubs based on species' traits, but the dominant drivers in shrub encroachment are often propagule pressure and human activities(Briggs *et al.*, 2005). Global climate change and increase of CO_2 in the atmosphere should favour woody shrub growth (Saintilan and Rogers, 2015) but the degree to which this happens will depend on the system and species in question (Van Auken, 2009). Woody plant encroachment is also likely to alter interactions between species and climate, CO_2 enrichment, fire disturbance and grazing management (Naito and Cairns, 2011). Often, climatic preference and introduction history of an invasive species can explain a large proportion of the variation in the spatial distribution of alien species (Feng *et al.*, 2016), and the traits and growth form of a species can play substantial roles in the invasion process(Giorgis *et al.*, 2016). Research indicates the environmental factors would not be a resistance when the propagule pressure is high enough (Berg *et al.*, 2016a). Biological invasion is more likely a consequence of species' natural expansion to fulfil their environmental niche rather than the direct result of climate change (Hulme, 2017). However, given the importance of propagule pressure in determining shrub encroachment rates into grasslands(Dullinger *et al.*, 2003), I only consider my analysis as a first step towards a better understanding of national-wide threats to New Zealand's grassland.

I showed where (Figure 2.4) and in which climate conditions (Figure 2.6) the highest potential for high propagule pressure from native and exotic (and both combined) species

exists. At the local scale, low producing grasslands with high-propagule pressure (top 25%) occur in areas with climatic conditions suited for native and exotic woody species (high niche overlap, D = 0.51, Table 2.3, Figure 2.6). For alpine grasslands in contrast, niche overlap at the local scale is low (D = 0.07) indicating that alpine grassland areas with native and exotic shrubs in their immediate neighbourhood occur in climatically dissimilar conditions. This might have implications for management strategies for native versus exotic shrub invasions into alpine grasslands under changing climate conditions. Understanding which shrub species will actually invade a grassland ecosystem at what rate and in which regions of New Zealand requires more local understanding of the environment and the species involved.

2.5. Conclusion

This study highlights the high degree of spatial variability in shrub propagule pressure among the three main types of indigenous grasslands in New Zealand. In particular at the local scale that is in the immediate neighbourhood of grassland areas there is large variation in the spatial distribution of highest propagule pressure areas between grassland types. Over 40% of Alpine grassland areas have native shrubs in its immediate neighbourhood (1 km), while 35% of Tall Tussock and 33% of Low Producing grassland are immediate neighboured with native shrubs. Alpine grassland is most at risk from native shrub invasion. Less than 1% of Alpine grassland and 2.4% of Tall Tussock grassland have exotic shrubs within their 1km neighbourhood, however the number for Low Producing grassland is 11%. Low Producing grassland is facing the most threat from exotic shrub expansion.

In geographic space, high native and high exotic propagule pressure does not coincide spatially at the local scale for any of the grassland types. However, in environmental space, high native and high exotic pressure areas occur in very similar climates for Low Producing grassland but not so for Alpine and Tall Tussock grasslands. The spatial scale of investigation greatly affects where grassland areas with highest potential pressure from native, exotic and combined shrub invasion are considered to be (Figure 2.4). In the central South island, Tall Tussock grasslands have only small areas of exotic shrub land in their immediate neighbourhood but considerably larger areas at the landscape and regional scale. It is therefore important to understand species-specific dispersal processes and local landscape topography for more accurate predictions of actual shrub invasion risk. Using this information on the spatial distribution and the climatic conditions of

native versus exotic shrub propagule pressure in grassland areas is a first step towards a predictive model of potential future shrub encroachment patterns and rates in New Zealand's grasslands ecosystems.

Chapter 3 Recent shrub encroachment in a tussock grassland landscape in New Zealand's South Island

Abstract

Shrub encroachment into grassland ecosystems has been observed and documented in many parts of the world in recent years. New Zealand's grasslands are characterised by high levels of endemic plant biodiversity but analyses of recent shrub invasions into these grasslands are limited. In order to fill this knowledge gap, SPOT 6/7 multispectral satellite imagery with a four-year interval were used to monitor the recent dynamics of shrub/grass land cover in an area of tussock grassland near Arrowtown, South Island. The spatial distribution of shrubland and grassland was obtained and the conversion rate of shrub and grass between 2013 and 2017 was calculated. Neighbourhood shrub cover and topography as possible drivers of spatial variations in conversion rates were analysed. Results show the shrubland extended by 31.60 ha in the study area during the four-year study period at a rate of 0.35% year^{-1}. The retreat rate of grassland is 0.43% year^{-1}. The shrub expansion rate is strongly correlated with the shrub cover density in neighbourhood but interestingly recent shrub encroachment in grassland areas was only observed in grassland areas with a neighbourhood shrub cover of greater than c. 40% and smaller than 90%. Shrub expansion was mostly observed in low elevations below the natural treeline (< 900 m) and more on the north- and northeast-facing slopes.

Key words

Shrub encroachment, Grassland, Remote sensing, Topography, Aspect, Elevation

3.1 Introduction

Shrub encroachment or woody expansion, the phenomenon that shrub species extend to the originally grass-dominated habitats, is evident worldwide and became a research focus in ecology and biogeography (Briggs *et al.*, 2005, Naito and Cairns, 2011, Buitenwerf *et al.*, 2018). The conversion from grass to shrub in these ecosystems can reduce the coverage of native species and ultimately altered the ecosystem function at landscape scale (Knapp *et al.*, 2008, Van Auken, 2009). In New Zealand, the woody invasion has been a long-term issue with the concern of endemic species conservation (Bellingham, 1998, Walker, 2000, Froude, 2011). Several studies show the potential trend of woody invasion into New Zealand's indigenous non-woody ecosystems (Mark and Dickinson, 2003, Rose and Frampton, 2007, Ropars *et al.*, 2018). A study conducted in South Island showed the

grazing removal can facilitate shrub dispersal, which reduced the area of tussock grassland and decreased biodiversity of this ecosystem (Grove *et al.*, 2002). Besides shrub species invasion, the process of native shrub re-development is also happening. An investigation observed expansion of native shrubs to grassland in Mackenzie Basin (Meurk *et al.*, 2002) and woody species became predominate in originally indigenous grasslands at high elevation and exposed sites (Ausseil *et al.*, 2011). In more recent study at Cass, Canterbury, a prevalent trend of shrub expansion into grassland was detected (Young *et al.*, 2016).

Above studies well recorded the transitions from grass to shrub at species scope, however the information of woody encroachment at landscape scale are still missing. Landscape scale information is substantial in estimating the spatial extent and the amount of woody encroachment. Furthermore, due to the high heterogeneity of the abiotic conditions in the grassland ecosystems, the mechanism of shrub expansion is still uncertain. More evidence of the spatial pattern and quantity of shrubs in New Zealand would be investigated to discover the drivers of shrub encroachment.

Remote sensing has been commonly used to detect the changes in land use/land cover at landscape scale. In the past 40 years, remote sensing techniques have developed rapidly and widely applied in terrestrial biodiversity investigations (McPhearson and Wallace, 2008). It highly improved the capability of monitoring and predicting ecological changes in large area (Horning *et al.*, 2010). With multispectral images, vegetation indices can be calculated to discriminate species' types and health status. The lower cost and less time-consuming than ground observation make remotely sensed vegetation indices time-series to be an efficient and economic tool in studying plant dynamic (Huang and Asner, 2009). In species invasion research, remote sensing also plays a substantial role, especially in vegetation dynamic monitoring and land cover mapping (Bradley and Mustard, 2006). Space borne vegetation indices have good accuracy in species mapping and infestation prediction (Clinton *et al.*, 2010). High spatial resolution imagery combined with traditional field survey is proven to be efficient in grassland studies (Mohamed *et al.*, 2011, Olsson *et al.*, 2011). For example, the SPOT image time series was used to investigate the bush encroachment in savanna rangeland in South Africa (Munyati *et al.*, 2011). A 20-year time series of Landsat-5 Thematic Mapper (TM) was applied to identify woody encroachment in montane grassland in Spain (Gartzia *et al.*, 2014). SPOT-5 imagery was used in modelling shrub encroachment in alpine treeline ecosystems in Switzerland to locate the prior areas for habitat management (Braunisch *et al.*, 2016). Landsat time series

and Lidar data were combined to assess the changes in shrub and grassland near alpine and high-latitude treeline ecotones in Canada (Bolton *et al.*, 2018).

Though numerous studies conducted in Northern Hemisphere, there is limited literature about shrub encroachment research using remote sensing in Southern Hemisphere. For instance, Landsat imagery was obtained to extract the patterns of prickly acacia (*Acacia nilotica*) invasion in the Mitchell grass plains of North Queensland In Australia (Lawes and Wallace, 2008). The loss of indigenous land cover in New Zealand was re-examined and updated by new remote sensing data with field work samples (Brockerhoff *et al.*, 2008). In recent work, four remote sensing methods were compared in detecting land cover changes in New Zealand's grasslands (Weeks *et al.*, 2013a). The SPOT-4 VEGETATION imagery was used in tracking New Zealand's indigenous grassland changes and a 3% (70,200 ha) reduction was found between 1990 and 2008 (Weeks *et al.*, 2013b). As high quality remote sensing data source become more available for New Zealand, the shrub expansion in New Zealand's grassland ecosystems can be mapped and quantified at landscape scale.

In this study, SPOT 6/7 satellite imagery captured on two dates (2013 and 2017) was used to distinguish the shrub and grass land covers. The potential shrub propagule pressure map from Chapter 2 was used as an indicator of the possible zones at risk of shrub expansion. A region in the tussock grassland in South Island was selected as the study site based on the shrub propagule pressure map. The changes between shrub and grass land covers were analysed to address the following question:

1) Does shrub encroachment happen in the areas which are anticipated to be under high potential shrub propagule pressure?

2) In what spatial pattern and at what speed are the shrubs extending into grassland?

3) Are the shrub coverage in neighbourhood and topographical factors (elevation and aspect) correlated to shrub expansion?

3.2 Methods

3.2.1 Study Area

I chose a tussock grassland site near Arrowtown, South Island as the study area, where is anticipated under high potential shrub propagule pressure (Figure 3.1). This region includes a large area of tussock grassland in the centre and east, and a shrubland in the northwest. The land cover types were determined from LCDB v4.1 (LCDB-v4.1, 2015).

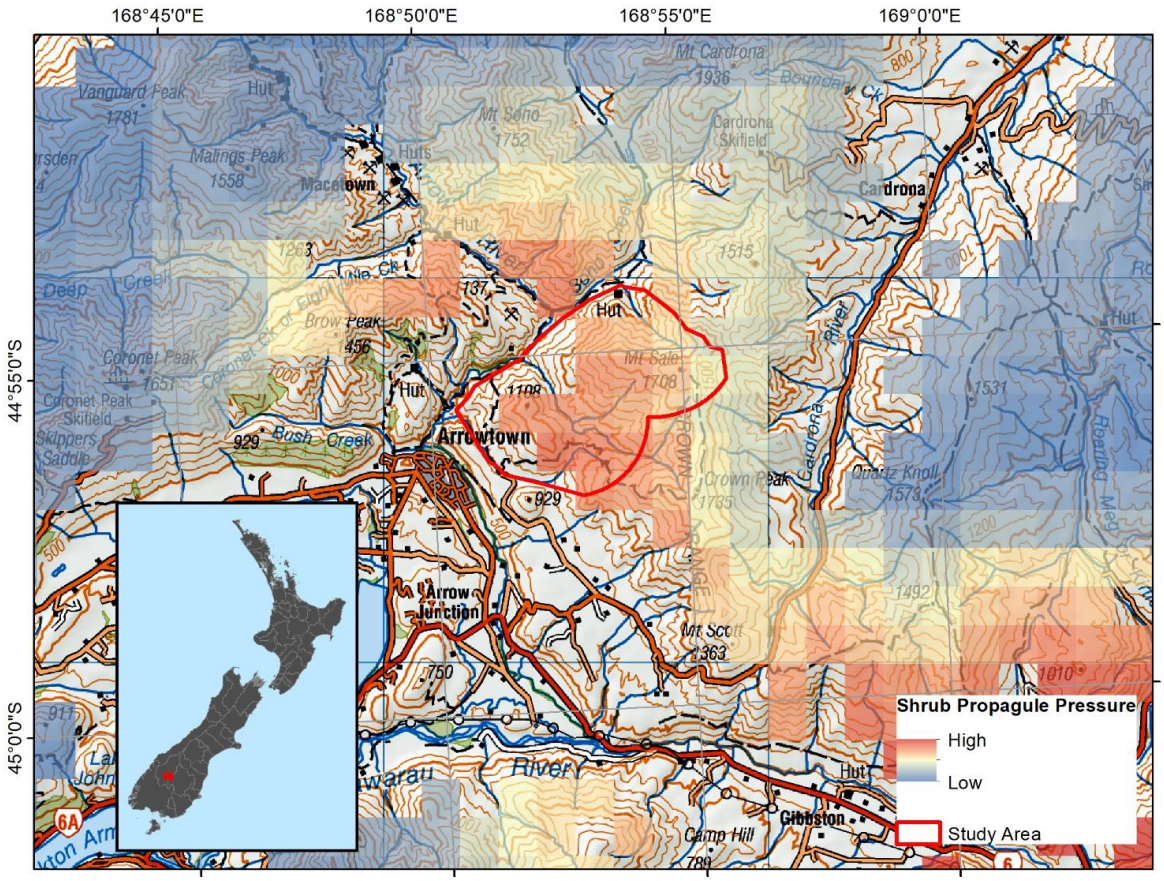

Figure 3.1 Study area of shrub encroachment near Arrowtown, New Zealand
The study area locates at the boundary of shrubland and grassland, and the grassland is under high potential shrub propagule pressure. The degree of shrub propagule pressure in grassland was derived and re-drawn based on Figure 2.4 b at 1km scale (see Chapter 2). The redder areas indicate the grassland which have higher shrub proportion in the immediate neighbourhood.

3.2.2 Data and processing

SPOT 6/7 Panchromatic (1.5 m) and multispectral (6 m) products were used. The exact capture times are 21-01-2013 and 18-11-2017. There is a four-year interval between the two scenes. As no ground control points are available in this study, I used the RPC (Rational Polynomial Coefficients) model to do geometric rectification. The SPOT 6/7 data was orthorectified in ENVI 5.3 by the module "RPC Orthorectification Workflow". The DEM input in this module is NZSoSDEM 15m (Columbus *et al.*, 2011). The output pixel size was set to 6.00 meters for multispectral and 1.50 meters for panchromatic. Image Resampling used "cubic convolution" method. Other parameters in ENVI 5.3 software were set as default. After orthorectification, the multispectral bands were pan-sharpened to 1.5 m resolution by "Gram-Schmidt Pan Sharping" module in ENVI 5.3. The sensor option was set to "spot-6" and the resampling method was "Cubic Convolution". Visual

inspection found the processed images of two times can be co-registered with each other with an acceptable accuracy (1-3 pixels) (Figure 3.2).

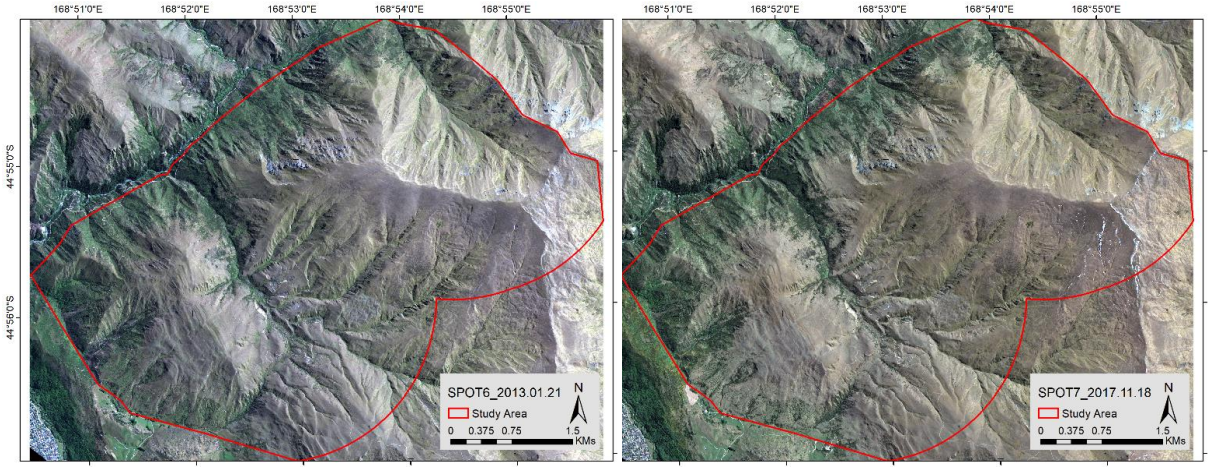

Figure 3.2 Two times of SPOT 6/7 images for the study area
SPOT 6/7 images captured in 2013 and 2017 were orthorectified and pan-sharpened. They are displayed in true colour combination (RGB). The red line circled regions is the study area.

The original digital number (DN) needs to be transferred to reflectance before vegetation indices calculation in ENVI 5.3. I used the "QUick Atmospheric Correction (QUAC)" module to reduce the atmospheric effects and convert the DN images to reflectance images. QUAC in ENVI 5.3 does not offer a specific algorithm for SPOT 6/7 sensor, so I selected the "generic" option, which suits the general land area data processing.

3.2.3 Shrub/grassland separation

After preliminary trials, three vegetation indices were chosen as the candidates for shrub/grass separation. The widely used Normalized Difference Vegetation Index (NDVI) was selected, which is a good index to measure the activity of green vegetation and applicable in a wide range of conditions (Rouse Jr *et al.*, 1974, Pettorelli *et al.*, 2005). It ranges from -1 to 1, and the vegetation is usually above 0.

$$NDVI = \frac{(NIR - Red)}{(NIR + Red)} \tag{3.1}$$

In (3.1), "NIR" and "Red" stands for the reflectance in the near infrared band and in red band, respectively.

Another candidate is Green Atmospherically Resistant Index (GARI). This index is sensitive to chlorophyll signals in vegetation, similar as NDVI. But GARI is expected to be less sensitive to atmospheric effects (Gitelson *et al.*, 1996). It ranges from -1 to 1. Vegetation usually shows high positive values.

$$GARI = \frac{NIR - [Green - \gamma(Blue - Red)]}{NIR + [Green - \gamma(Blue - Red)]} \tag{3.2}$$

In (3.2), "NIR", "Red", "Green" and "Blue" stand for the reflectance in the near infrared, red, green and blue bands, respectively. The γ is a constant depending on the aerosol condition. In ENVI 5.3 I used the recommended value of 1.7 (Gitelson *et al.*, 1996, Gitelson *et al.*, 2002).

The third index I tested is Green Leaf Index (GLI). This index was originally designed for RGB cameras to detect crop coverage (Louhaichi *et al.*, 2001), while it performs also well to distinguish shrub and grass in preliminary trials. GLI ranges from -1 to 1. Positive values usually represent vegetation, while negative values indicate non-plant regions. Since GLI misses near infrared information, so the vegetation signal is not expected to be strong by design.

$$GLI = \frac{(Green - Red) + (Green - Blue)}{2 \times Green + Red + Blue} \tag{3.3}$$

These three vegetation indices were calculated by the "Spectral Indices" module in ENVI 5.3 (Figure 3.3).

(a) NDVI

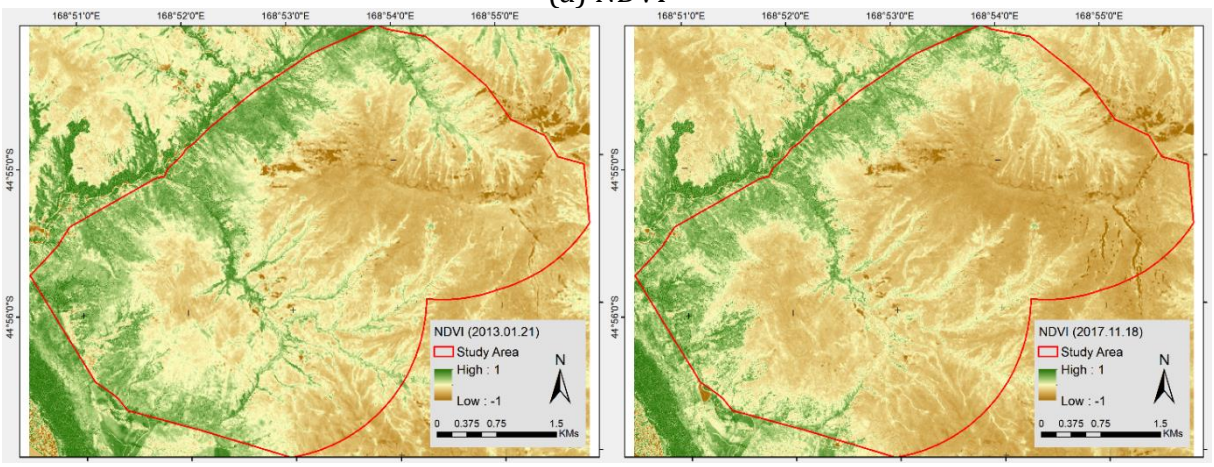

(b)GARI

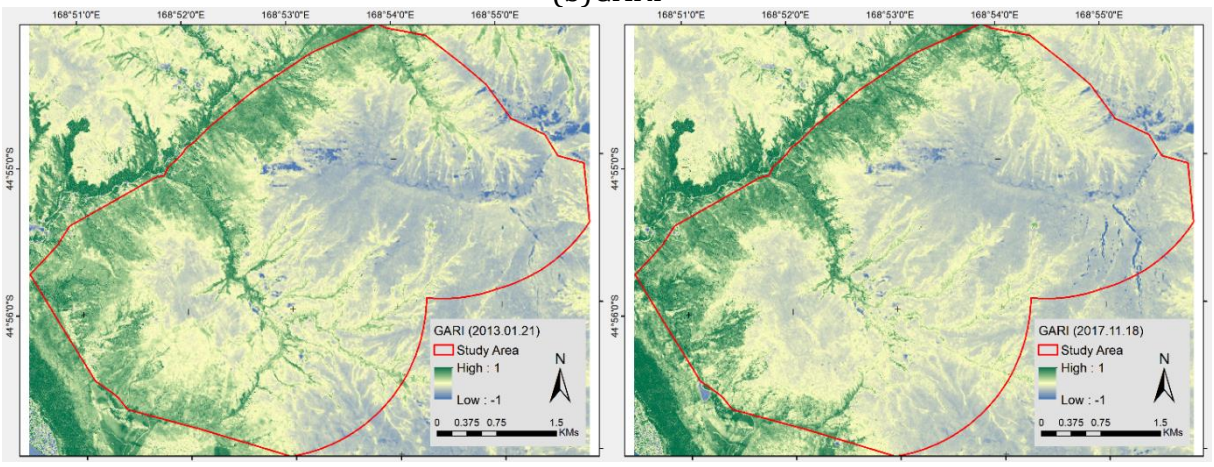

(c)GLI

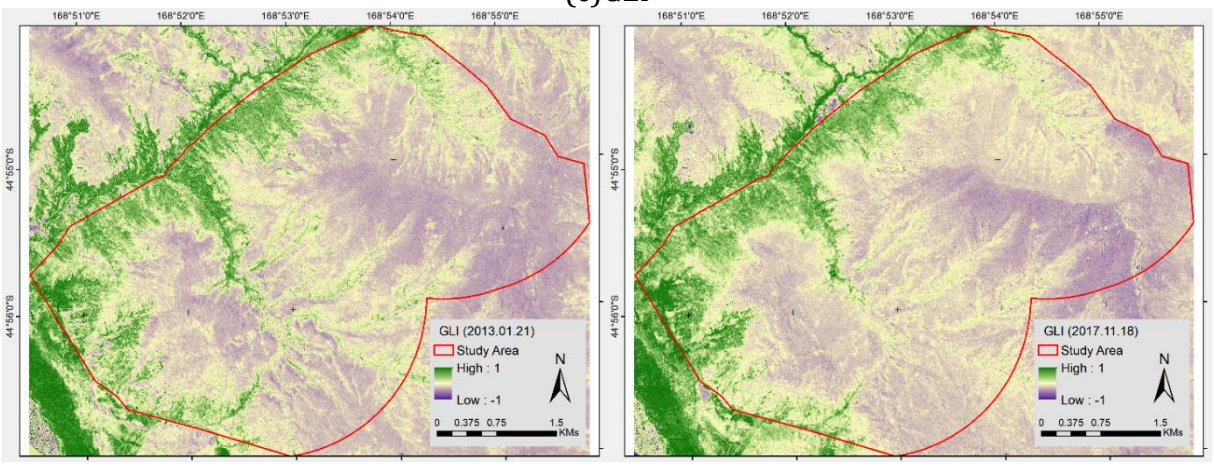

Figure 3.3 Vegetation indices calculated from SPOT data
NDVI (a), GARI(b) and GLI (c) all range from -1 to 1. For all indices, higher values mean the denser and more active of the vegetation.

In order to obtain the representative signals of shrub/grass in vegetation indices, training samples were chosen manually in ArcGIS 10.1. The regions in which the shrubland and grassland have not changed between the two times were circled by polygons (Figure 3.4a). Near the training polygons, I draw other polygons covering the same land cover types as the validation samples. I used the module "Create Random Points" in ArcGIS 10.1 to create

200 points inside each land cover type as sample points. The samples for changed land covers between the four years were picked manually through visual interpretation. In total 100 “Grassland to Shrub” and 100 “Shrub to Grassland” points were picked as validation samples for changing detection (Figure 3.4b).

The signals of shrubland and grassland were extracted from three vegetation indices based on the training points (Figure 3.5). The distinct separation of shrub/grass signals makes them possible to distinguish the two land cover types by a threshold on indices. For instance in NDVI signals in 2013 (Figure 3.5a), the shrubs present a Gaussian distribution with mean at 0.85, while the grassland points exhibit the similar shape but with a lower mean at 0.65. There is only 8% of overlap between the two types based on NDVI in 2013. In 2017, the separating capability of NDVI is even better, that there is less than 0.1% overlap of NDVI between shrubland and grassland. I noticed there was an overall decrease in the NDVI signals for the two types in 2017 than in 2013. The reduction on NDVI in both land covers simultaneously might be due to seasonal effects, because the two-time images were captured in different seasons (late spring in 2017, mid-summer in 2013). Similar signal distinctions and seasonal shifts were also observed in GARI (Figure 3.5b) and GLI (Figure 3.5c).

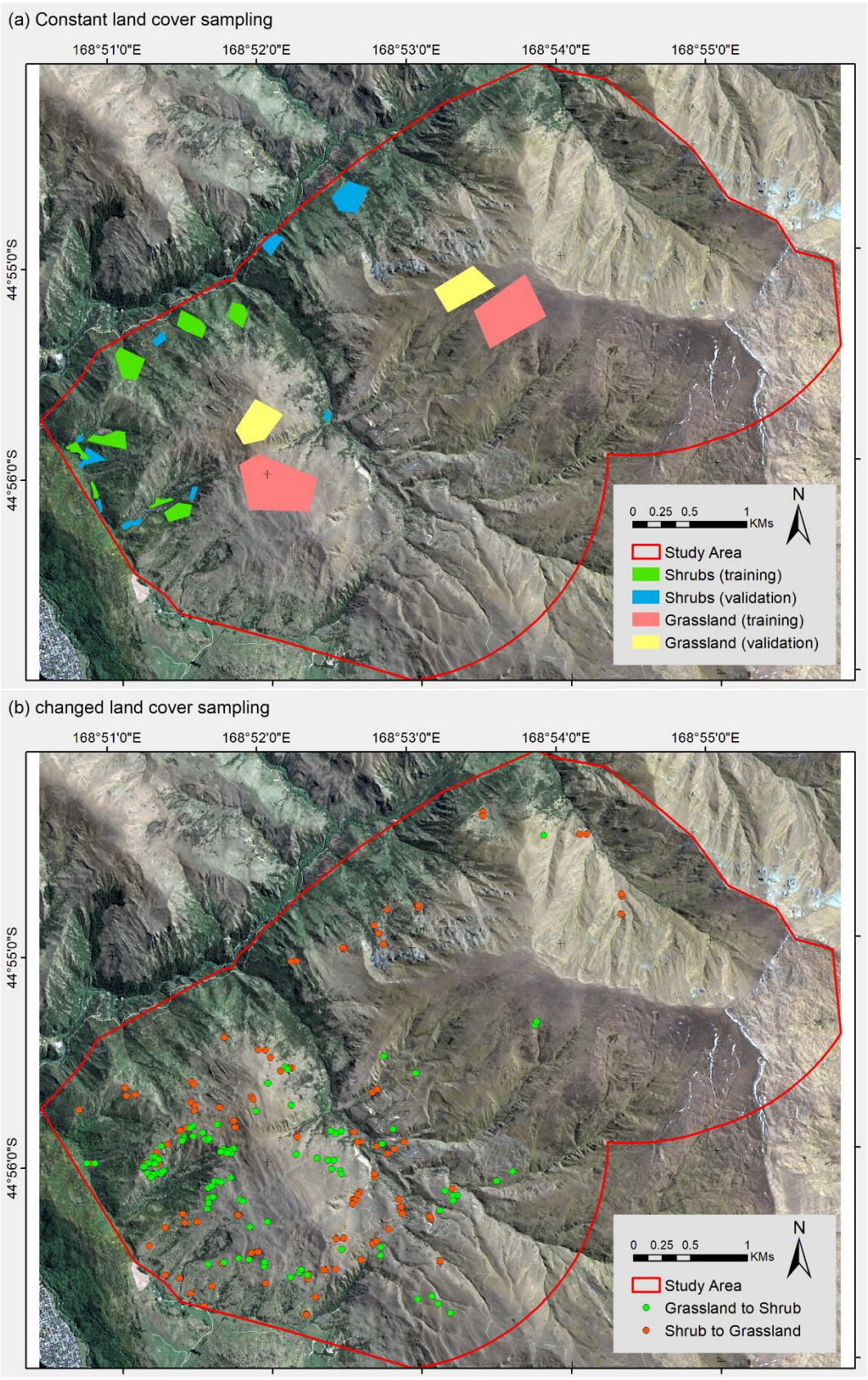

Figure 3.4 Training and validation samples for shrub/grass classification
The (a) constant shrubs/grassland polygons and (b) shrubs/grassland transition points are picked through visual interpretation. In (a), there are 200 points created in polygons of each type as training and validation data. In (b), the 100 points for each type are used as validation data.

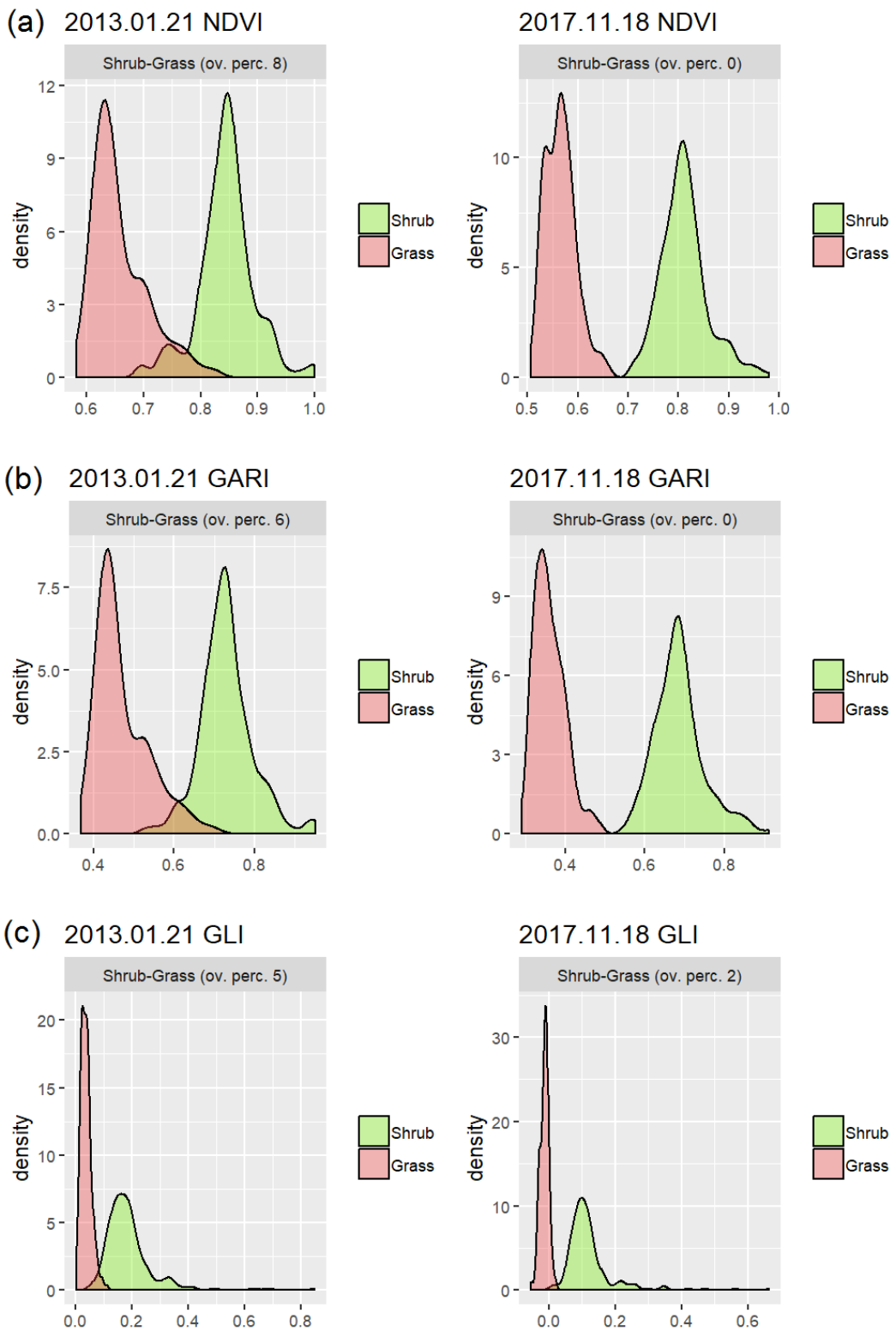

Figure 3.5 The distributions of shrub/grass signals in vegetation indices
The graphs show the distribution of shrub/grass signals on NDVI (a), GARI (b) and GLI (c). Shrub signals are in green and grass signals are in red. Grassland has lower signals than shrubland in all vegetation indices. The signals of two types are all lower in 2017 than in 2013 due to seasonal effects.

For the good separation of the two land cover types on vegetation indices, I used a simple criterion to classify shrub and grassland. Firstly, I used the intersect point of the signal densities of the two types as the threshold to separate the overlapped region (Figure 3.6). Secondly, I used the 1% percentile of grassland signals and 99% percentile of shrub signals as the lower and higher thresholds, beyond which pixels will be classified as others. So, there will be three categories in the classification result: Shrub, Grass and Others. Due to the seasonal effects (Figure 3.5), the separation thresholds cannot be the same for different images captured on different dates. I calculated the thresholds every time for each scene of image and for each vegetation index.

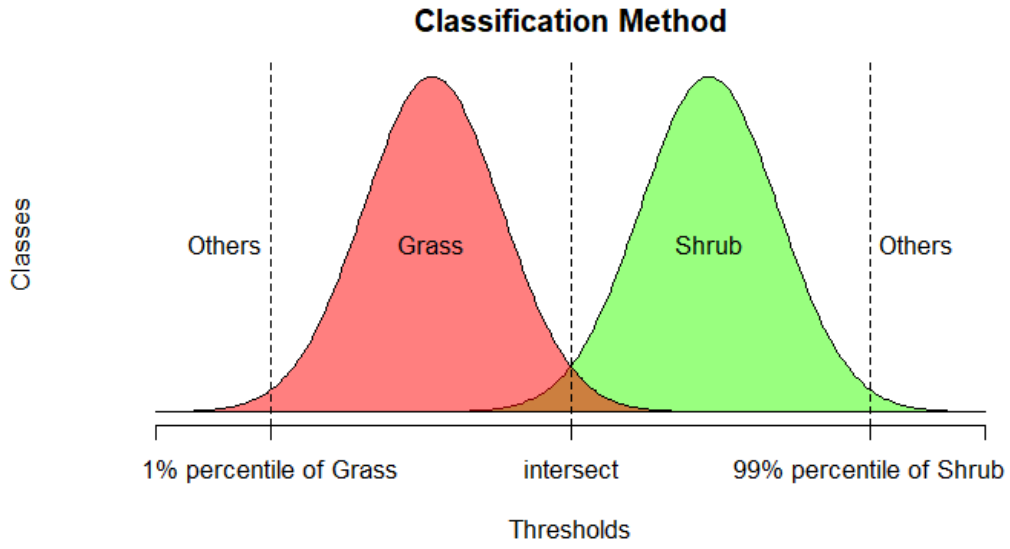

Figure 3.6 Shrub/Grass Classification method
The intersect point of the two signal distributions is used to separate shrubland and grassland in their overlapped region. The 1% percentile of grassland and the 99% percentile of shrub are the thresholds to distinguish shrub/grass from other land cover types. These thresholds need to be calculated every time when change the input image.

3.2.4 Land cover change analysis

Because the two scenes of SPOT 6/7 data cannot be matched with each other by pixel (1-3 pixels error), I built a grid mask to analyse the shrub/grass coverage changes, in order to reduce the effect of mismatch. I used the "Fishnet" tool in ArcGIS 10.1 to generate a net mask with nearly 100,000 of 15×15m grid cells covering the whole study area. Each grid cell includes 10×10 SPOT image pixels (1.5 m resolution). The classified land covers (Shrub, Grassland or Others) of the 100 pixels were counted and the proportions of shrub/grass were assigned to each grid cell. By comparing the shrub/grass coverage (proportion) in 2013 and 2017 for each grid cell, I can quantify the changes of shrubland and grassland during the four years (Figure 3.7).

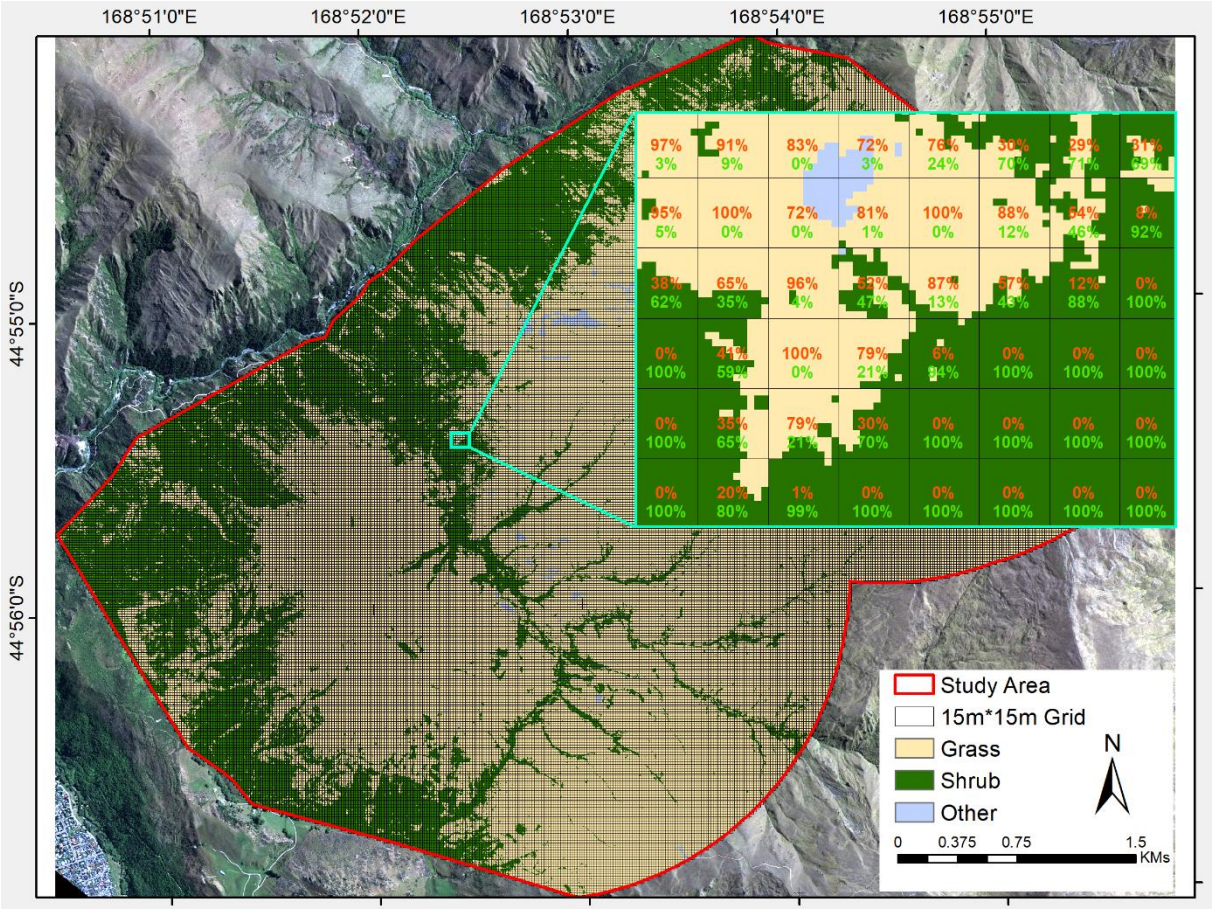

Figure 3.7 15×15m grid cell mask for shrub/grass proportion calculation
The 15×15m square gird cells were used to calculate land cover type proportion in each year. For example, each 1.5×1.5 m SPOT pixel is classified to one of three types: Grassland (yellow), Shrub (green) and Other (light blue). The inset shows how the proportions of shrub (number in green) and grassland (number in red) were calculated and assigned to each 15×15m grid cell.

To investigate how the shrub/grass coverage in neighbourhood affect the changes of shrub/grass proportion in 15×15 m grid cells, I built a 150×150 m neighbourhood for each grid cell. The percentage of shrub/grass in neighbourhood was calculated on the same way in Figure 3.7 by "Focal Statistics" module in ArcGIS 10.1. I used the 2013 classification, which is the initial condition in this study, as the input. So the shrubland/grassland changes in each grid cell can be connected with the coverage of shrubs/grass in its neighbourhood.

In order to analyse the correlation between shrub encroachment and topography, I extracted the elevation and aspect values from the NZSoSDEM dataset (Columbus *et al.*, 2011) for each 15×15 m grid cell. The relationship between shrub expansion rate and topography can be analysed.

3.3 Results

3.3.1 Classification of land covers

The classification results from the three candidate vegetation indices showed the similar spatial distribution of shrubland and grassland in 2013 and 2017 (Figure 3.8). Focusing on the NDVI classification (Figure 3.8a), the gaps in the shrubland in the northwest of the study area were getting denser, indicating an increasing trend of shrub coverage during 2013-2017. While the sparse shrubs in the central gullies surrounded by the grassland had decreased or moved northward. The GARI result exhibits nearly identical situation as NDVI result shows, however GARI suggests higher original shrub coverage in 2013 (Figure 3.8b). The GLI presents a more scattered distribution of shrubland in 2013. More pixels in the central and northern gullies were classified as shrubs in GLI (Figure 3.8c). As expected, the classification derived by three indices in 2017 are more consistent with each other than the result in 2013, due to the better separation of the shrub/grass signals in 2017 than in 2013 (Figure 3.5). This means the indices derived from SPOT 6/7 in spring time (November 2017) are more effective in distinguishing shrubland and grassland in the study area.

In order to find out whether combining the three vegetation indices can increase the accuracy of classification, I calculated the three-index agreed classification (Figure 3.8d). The pixels are classified to a certain type only when the type was agreed by all the three indices. The pixels which are not agreed by all three indices are classified to a new type named “Uncertain”. The result shows most of the “Uncertain” types occurred at the edges of shrubland and grassland, where the signals of shrub/grass are more likely to be overlapped. There are more “uncertain” pixels in 2013 than in 2017, due to shrub and grass exhibit more similar signals in summer time (January 2013).

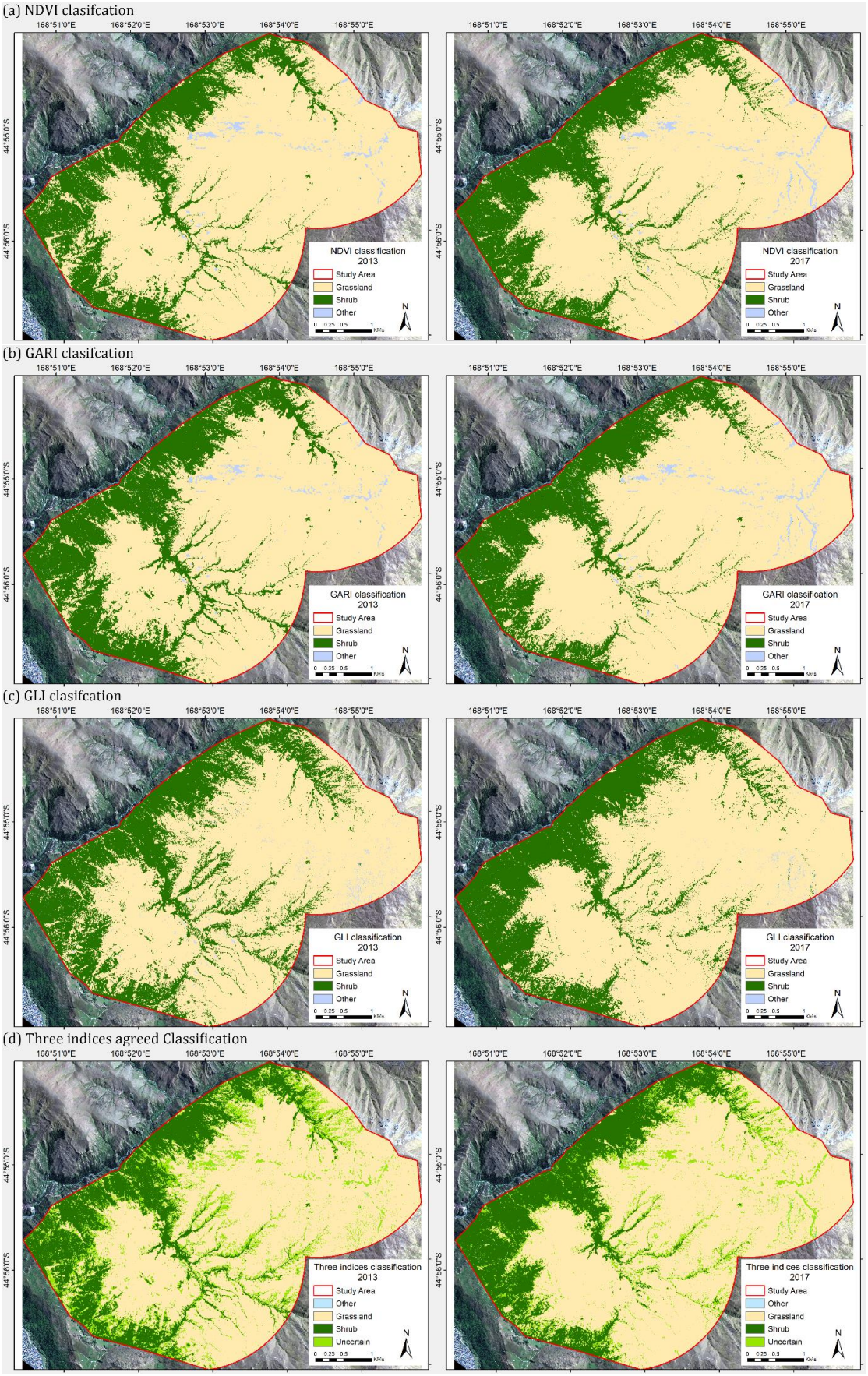

Figure 3.8 Classifications of three vegetation indices and their combined result
In NDVI(a), GARI(b) and GLI(c) classifications, dark green represents the shrubland, yellow stands for the grassland, and other land are in light blue. In (d), land cover is decided by the type all three indices agree to. If a pixel is not agreed by all three indices, it is classified to "Uncertain".

Confusion matrices show NDVI exhibits the highest overall accuracy of 81.83% (Table 3.1a). GARI is 80.17 % and GLI is only 74.67% (Table 3.1b, c). The three indices agreed classification has the lowest overall accuracy of 71.00% (Table 3.1d). The classification method performed well in separating constant shrubland and grassland in all indices. The producer accuracy shows approximate 90% of constant shrubs were correctly classified, and the accuracy close to 100% for constant grassland. However, the conversion between shrub and grass have lower classification accuracy. For NDVI and GARI, the producer accuracy show that only half of the changed points were correctly detected. For GLI and Three-agreed result, the producer accuracy is even low to nearly 20% and 40% in distinguishing grass to shrub (GS) and shrub to grass (SG) changes. The changes (GS and SG) are mostly wrongly recognized as no change types (SS and GG), which leads to the relatively higher user accuracy than producer accuracy in all results. For example, NDVI has 74% and 96% user accuracy for GS and SG types, which is much higher than the corresponded producer accuracy (64% and 53%). The difference between producer and user accuracy indicates my classification method might lose part of information in shrubland/grassland conversion. However, the detected changes of shrub/grass coverage in the classification show a high accuracy. My classification might underestimate the extent and quantity of shrub expansion, but can detect it correctly.

I finally chose NDVI classification as the final result and used it in following analysis of shrub encroachment. That is because when considering the capability in correctly detecting shrubland/grassland changes and the balance of all aspects of accuracy (producer, user and overall), NDVI gives the most reliable information among all the classification results.

Table 3.1 Confusion matrices of classification based on three vegetation indices and their agreed result

(a) NDVI

	SS.ref	GG.ref	GS.ref	SG.ref	Total	**User**
SS	176	0	4	30	210	**83.81%**
GG	1	198	32	16	247	**80.16%**
GS	22	0	64	1	87	**73.56%**
SG	0	2	0	53	55	**96.36%**
OT	1	0	0	0	1	
Sum	200	200	100	100	600	**Overall**
Producer	**88.00%**	**99.00%**	**64.00%**	**53.00%**		**81.83%**

(b) GARI

	SS.ref	GG.ref	GS.ref	SG.ref	Total	**User**
SS	183	0	7	27	217	**84.33%**
GG	1	197	47	15	260	**75.77%**
GS	14	0	44	1	59	**74.58%**
SG	0	2	2	57	61	**93.44%**
OT	2	1	0	0	3	
Sum	200	200	100	100	600	**Overall**
Producer	**91.50%**	**98.50%**	**44.00%**	**57.00%**		**80.17%**

(c) GLI

	SS.ref	GG.ref	GS.ref	SG.ref	Total	**User**
SS	186	0	2	35	223	**83.41%**
GG	1	195	61	20	277	**70.40%**
GS	10	0	24	2	36	**66.67%**
SG	3	5	4	43	55	**78.18%**
OT	0	0	9	0	9	
Sum	200	200	100	100	600	**Overall**
Producer	**93.00%**	**97.50%**	**24.00%**	**43.00%**		**74.67%**

(d) Three agreed

	SS.ref	GG.ref	GS.ref	SG.ref	Total	**User**
SS	173	0	1	25	199	**86.93%**
GG	0	193	30	15	238	**81.09%**
GS	7	0	20	0	27	**74.07%**
SG	0	1	0	40	41	**97.56%**
UC	20	6	49	20	95	
Sum	200	200	100	100	600	**Overall**
Producer	**86.50%**	**96.50%**	**20.00%**	**40.00%**		**71.00%**

Note: SS—constant shrubland, GG—constant grassland, GS—grass to shrub, SG—shrub to grass, OT—others, UC—uncertain. The abbreviations with the suffix ".ref" mean the validation samples.

3.3.2 Status of shrub/grass transformation

The changes of shrub coverage during 2013-2017 are calculated for each 15×15 m grid cell based on NDVI classification (Figure 3.9). The green colours indicate the expansion of shrubs, while the purple colours show the shrub retreat. An increasing trend of shrub coverage has been observed in most regions inside and close to large area of shrub-dominated habitats. High increase of shrub coverage occurred in the west and north of the study area, where the ground is surrounded by large pieces of shrubland. Minor increase of shrubland can also be found on the south-facing slopes of gullies in the centre and northeast of the study area (Figure 3.9). On the other hand, high value of shrub decrease often happened at the edge of large areas of grassland and shrubland. Shrub retreat also appeared in the regions near the farmland in south. Some reduction of shrubs are also seen on the north-facing slopes in the gullies at centre of the study area.

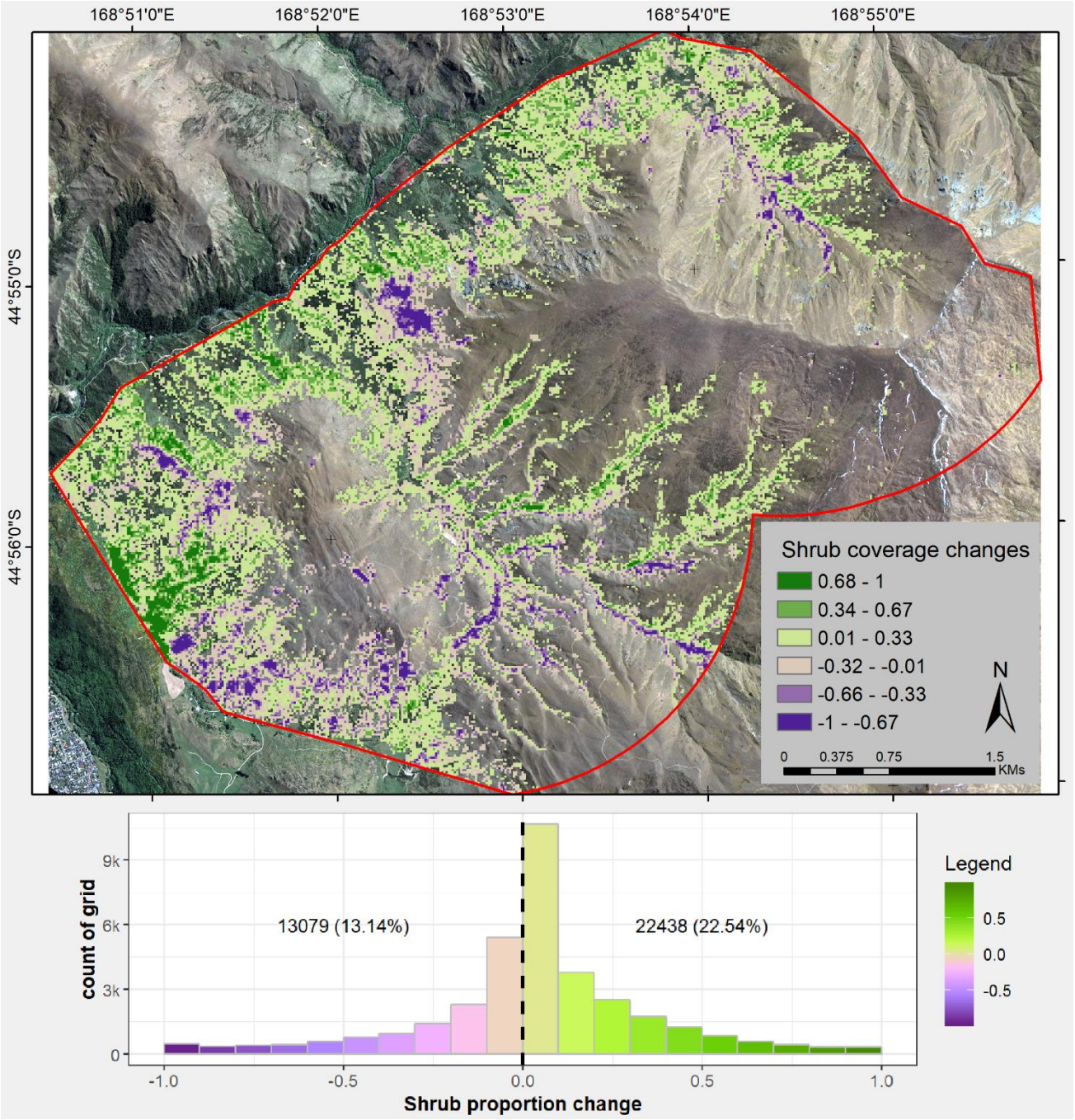

Figure 3.9 Shrub cover change during 2013-2017 based on NDVI classification
The change in proportion of shrub cover is calculated for each 15×15 m square grid cell. The change value ranges from -1 to 1, in which 0.5, for instance, means the shrub cover increased by 50% in a grid cell, while -0.5 means decreased by 50%. The positive changes are in green and the negative changes are in purple. The grid cells with no change of shrub cover are not displayed. The histogram under the map illustrates the distribution of grid cells with different levels of shrub cover changes. The numbers above the bars are the counts of grid cells showing decrease (left) or increase (right) of shrub cover. The percentages are their proportions of all grid cells in the study area. The change maps based on GARI and GLI can be seen in Appendix II.

There are 103.23 ha of extended shrubland during the time of 2013-2017, while 71.63 ha of shrubs converted to grassland or other types (Table 3.2). The net increase of shrub is 31.60 ha in total, which takes 1.41% of the 2239.34 ha study area. The gain/loss areas of

grassland are nearly equal to the loss/gain of shrubland. The gain and loss areas of shrubland are 4.61% and 3.20% respectively, which indicates the transition of shrub and grass occurred in over 7% of the study area, though the net change is less than 2%. For the coverage change in 15×15 m grid cells, I found 22.54% of the grid cells showed an increasing trend of shrub coverage, and 13.14% showed a decreasing trend. The numbers in grassland are 14.50% of grid cells had grassland cover increased, and 24.50% showed a decrease of grassland cover. The shrub/grass cover changes happened in over 35% of the study area. The percentage of changed grid cells (count) is much higher than the percentage of changed areas (ha), indicating the fact that the shrub species are spreading gradually in a wide range of land. The average rate of shrub increase is 0.35% $year^{-1}$, and the decrease rate of grassland cover is -0.43% $year^{-1}$.

Table 3.2 Quantity of shrubland / grassland changes

Area of change (ha)			**Percentage**	
	Shrubland	Grassland	Shrubland	Grassland
Gain	103.23	76.81	4.61%	3.43%
Loss	-71.63	-115.41	-3.20%	-5.15%
Net	31.60	-38.60	1.41%	-1.72%
				Total area: 2239.34
Count of 15×15 m square with change			**Percentage**	
Increase	22438	14427	22.54%	14.50%
Decrease	13079	24388	13.14%	24.50%
Sum	35517	38815	35.69%	39.00%
				Total count of grids: 99526
Change rate ($year^{-1}$)	0.35%	-0.43%		

Note: the numbers in the sub-table of "Count of 15×15 m square with change" are the count of 15×15 m square grid cells with positive ("Increase") or negative ("Decrease") change in shrubland or grassland coverage.

3.3.3 Neighbourhood effect on shrubland/grassland transitions

A remarkable increase of the shrub proportion in 15×15 m grid cells has been observed in the grid cells with 40%-90% shrub cover in 150×150 m neighbourhood (Figure 3.10). This result indicates the shrub expansion happens when the neighbouring shrub coverage reaches a certain range. The shrub proportion keeps steady or even slightly declines when shrub coverage in neighbourhood is lower than 40%. However, when shrub coverage in neighbourhood exceeds 40%, shrub species start to expand quickly. The median shrub proportion in grid cells increased by 0.14 with 45% shrub coverage in neighbourhood. The increasing rate keeps growing as the shrub coverage in neighbourhood rises. A peak

value was reached when a grid cell has 60% shrubs in neighbourhood, where the median shrub proportion in grid cells grows by a maximum of 0.23. Shrub expansion rate decreased gradually when the neighbouring shrub coverage is higher than 60%. Expansion rate finally drops down to zero at 90% shrub coverage in neighbourhood, as the shrub proportion in grid cell is going to be full (Figure 3.10a). Because the dominant land cover type is grassland in the study area, large number of the grid cells have no shrubs in their neighbourhood (Figure 3.10b). Obviously, the shrub encroachment mostly happens at the boundary of shrubland and grassland.

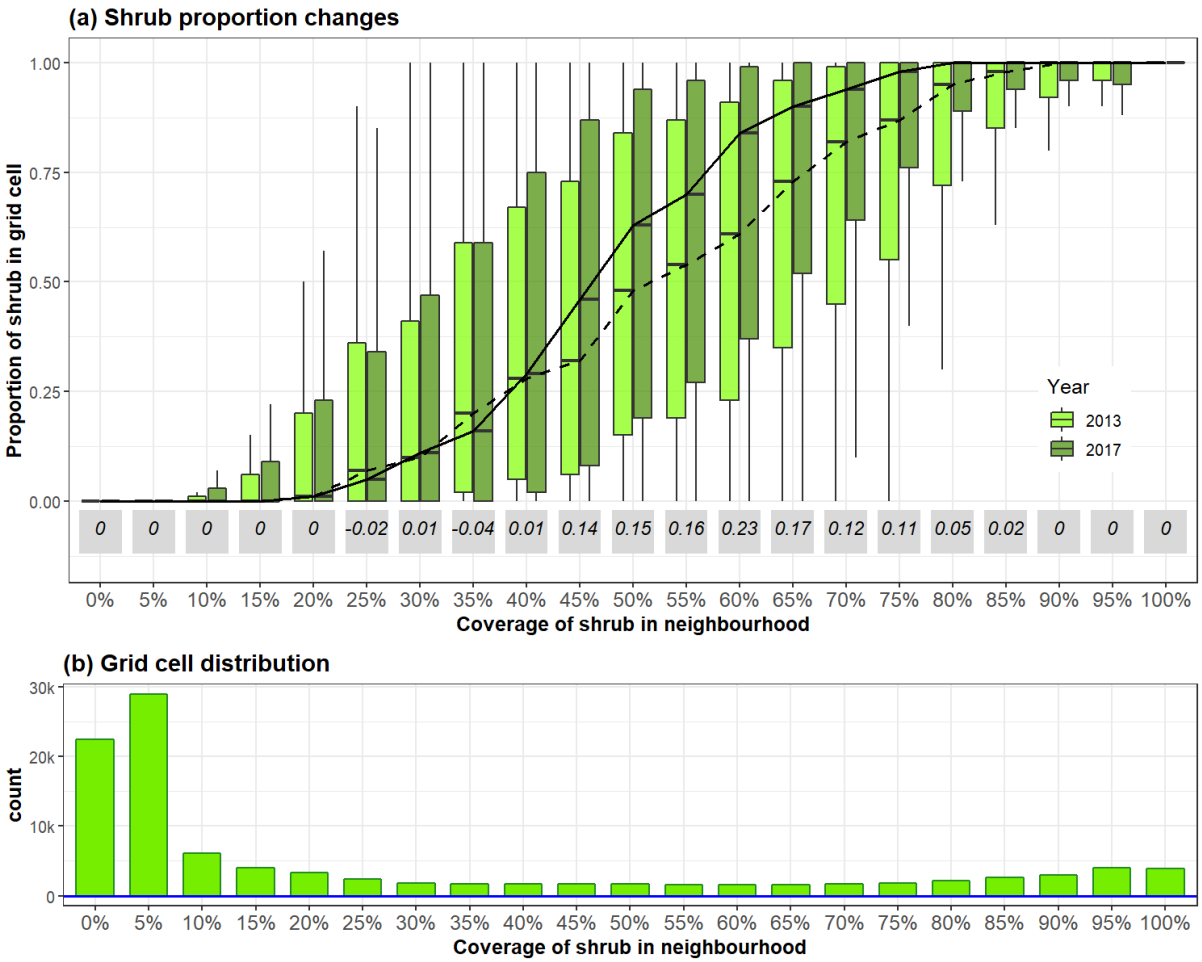

Figure 3.10 Shrub proportion changes with different levels of shrub coverage in neighbourhood (a) shows the shrub proportions in 15×15 m square grid cells in year 2013 and 2017. The top and bottom of the boxes indicate the upper and lower quartiles (75th and 25th percentiles). The distance between upper and lower quartiles names inter-quartile range (IQR). The segment inside the boxes shows the median. The vertical lines outside the box represent the whiskers, which are defined as the larger (smaller) value of upper quartile + 1.5 × IQR and maximum (lower quartile - 1.5 × IQR and minimum). The dotted and solid curves represent the changes of shrub proportion median in grid cells in 2013 and 2017. The shaded number under each box is the change of shrub proportion medians between 2013 and 2017. (b) shows the count of grid cells in each level of shrub coverage in neighbourhood.

An opposite trend in the changes of grass proportion in grid cells with different levels of grass coverage in neighbourhood was found (Figure 3.11). Grass proportion in 15×15 m square grid cells decreased during the time 2013-2017 when the neighbouring grassland at the range of 20-65%. Grassland was roughly constant when the grass coverage in neighbourhood is higher than 65%. When the neighbouring grass coverage drops lower than the threshold of 65%, grassland proportion in focal grid cells will reduce dramatically. The highest drop (-0.23) of grass proportion are in grid cells with 45% grass coverage in neighbourhood. The areas with neighbouring grass coverage lower than 15% would stop decreasing of grass proportion, for their grass proportions are already close to zero (Figure 3.11a). A large quantity of grid cells with full (100%) grass coverage in neighbourhood are very stable during the study time period (Figure 3.11b). There is a gap between the thresholds of grassland decrease (65%) and shrubland expansion (40%), showing shrub expansion and grass retreat seemed not happen simultaneously.

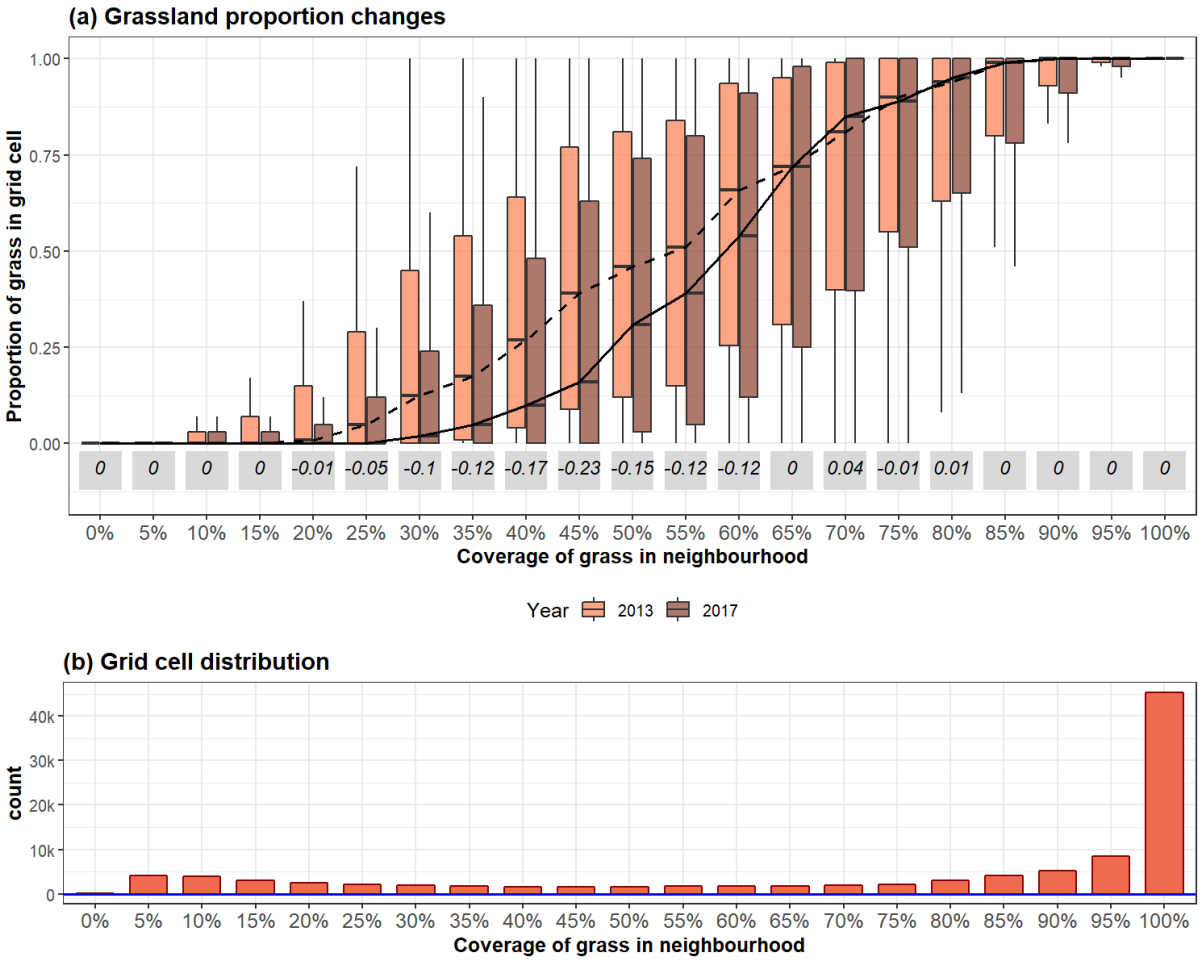

Figure 3.11 Grass proportion changes in grid cells with levels of grass cover in neighbourhood (a) shows the grass proportions in 15×15 m square grid cells in year 2013 and 2017. The symbols have the same meaning introduced in Figure 3.10. (b) shows the count of grid cells in each level of grass coverage in neighbourhood.

3.3.4 Correlation between shrubland/grassland changes and topography

The correlation of shrub/grass changes with elevation shows the shifts from grassland to shrubland mainly happened at low elevation (Figure 3.12). A noticeable shrub expansion has been observed at 500-800 m elevation, where the shrub proportion changes are mostly above zero. The peak rise of shrub proportion appears at 600 m altitude with 0.16 growth in median. Above 900 m elevation, the shrubland and grassland become stable, with the median proportion changes close to zero. Minor increase in shrub proportion can be seen at 1150-1550 m, and the number of changed grid cells is small (no more than 2.7% of all cells, Figure 3.12c). The pattern of changes in grassland roughly mirrored the changes in shrubland, instead a decrease trend in both shrub and grass proportions can be seen above 1600 m elevation. The number of changed grid cells (Figure 3.12c) indicates approximate 58% of changes happened under 900 m elevation. The most active regions are at the range of 801-900 m with over 22% of all changes occurred there (the bins of 850m and 900m, Figure 3.12c).

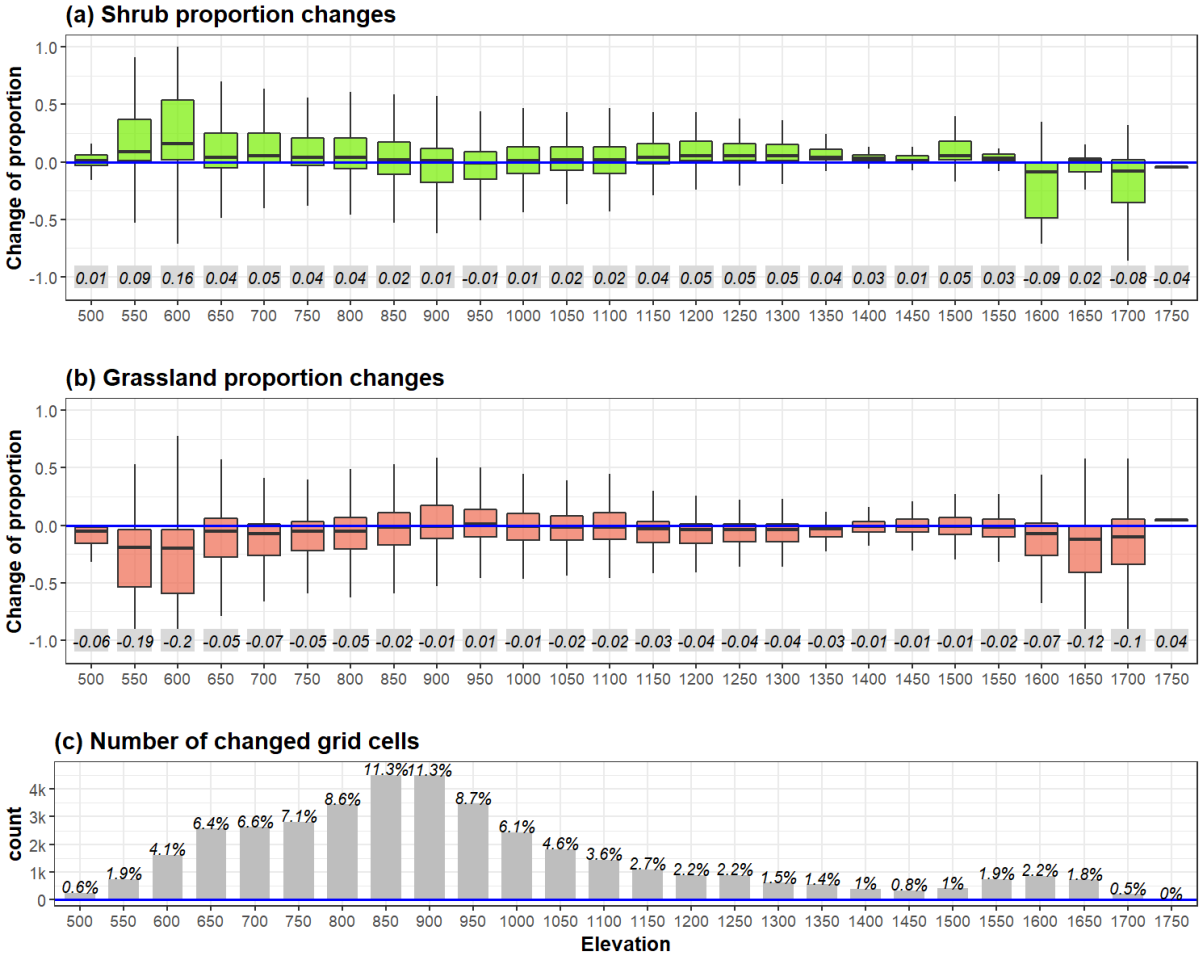

Figure 3.12 Shrub/grass proportion changes on elevations

In (a) and (b), the top and bottom of the boxes indicate the upper and lower quartiles (75th and 25th percentiles), and their distance is inter-quartile range (IQR). The segment inside the boxes show the median. The vertical lines outside the boxes represent the whiskers, which are defined as the larger (smaller) value of upper quartile + 1.5 × IQR and maximum (lower quartile - 1.5 × IQR and minimum). The shaded numbers under the boxes are the numbers of median changes between 2013 and 2017. (c) shows the count of grid cells on different elevations. The grid cells with no change are not included.

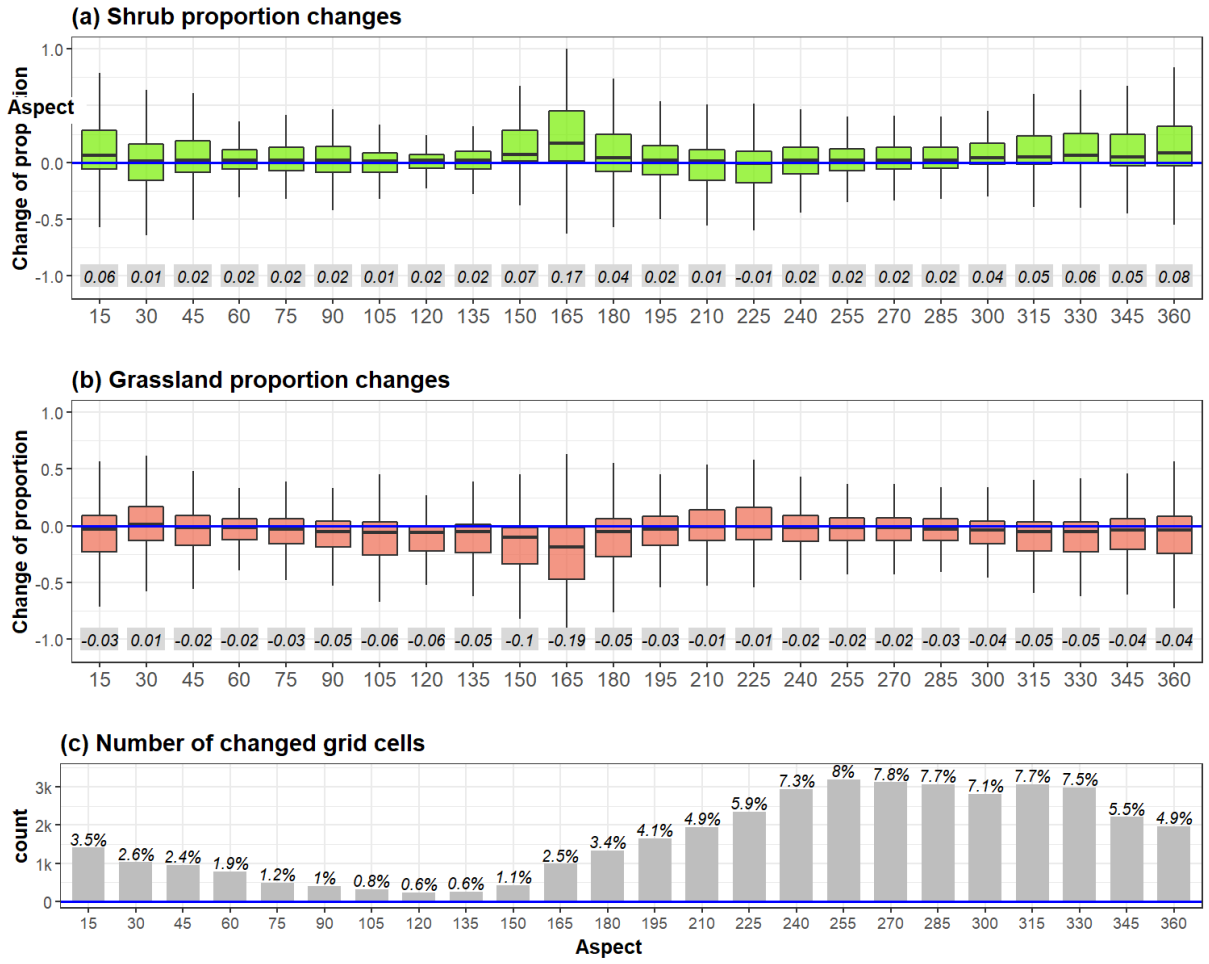

Figure 3.13 Shrub/grass proportion changes on aspects
In (a) and (b), the symbols have the same meaning as in Figure 3.12. (c) shows the count of grid cells on aspects. The no-change grid cells are excluded.

There is a weak trend indicating that shrub expansion usually happens on the north- and south-facing slopes, but less on the east- or west-facing hills (Figure 3.13a). A considerable increase of shrub proportion was observed on the south-facing slopes (150-195 degree) with a high rise of 0.17 (17% of shrub proportion) at 165 degree. Another region showing large increase of shrubs is on the north-facing hills (330-360 and 0-15 degree on aspect), with a high growth of 0.08 at 360 degree. The changes in grassland proportion roughly mirrored the distribution of shrub changes, showing the decrease of grassland mostly happened on north- and (Figure 3.13b). The number of changed grid

cells on aspect showed that even though the increase of shrub was high in number on the south-facing lands, they only take 11.1% of all the changed grid cells (150-195 degree, Figure 13.3c). In contrast, there are 21.4% of shrub increase occurred on the north-facing hills (330-360 and 0-15 degree, Figure 13.3c). Many minor changed grid cells are found on the west-facing slopes (210-300 degree), but less can be seen on the east-facing slopes (45-150 degree).

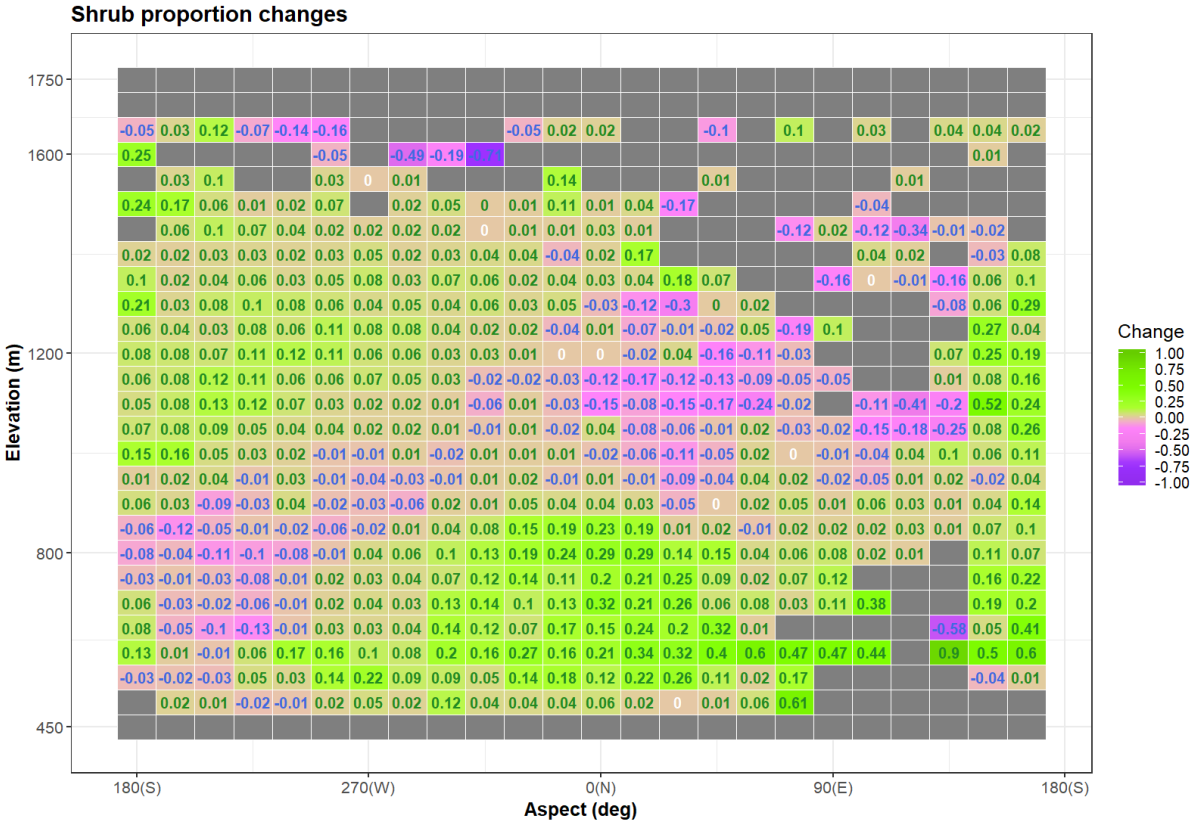

Figure 3.14 Shrub proportion changes on the coordinate of elevation and aspect
The green colours indicate the regions with shrub encroachment, while the purple colours represent the reduction of shrubs. The numbers in the grids are the values of shrub proportion change, which ranges from -1.0 (100% loss) to 1.0 (100% gain). The empty grids (dark) mean no data in the range of elevation and aspect. Notice that the north-facing slopes (0 degree, sunny slopes) is put in the middle of aspect axis.

The interaction correlation between shrub proportion changes and topography shows both elevation and aspect are substantial factors in modifying the pattern of shrub expansion (Figure 3.14). Same as the former analysis, most of the shrub increase was found under 850 m elevation. On these low elevations, most rise of shrubs occurred on the north-facing hills, with a small amount of increase found on the south-facing lands. However, some deductions in shrubs happened on southwest slopes at the same elevation. Above 900 m elevation the situation has reversed, that more shrub expansion can be seen on the south and southwest hills, but high decrease appears on the north and northeast

slopes. When elevation gets higher than 1,400 m, the grid cells distribute scattered and the pattern of increase/decrease in shrubs turns to be irregular. In all, the shrub/grass transition is more frequent on the north-facing slopes. Shrub encroachment mostly happens at elevation lower than 850 m, while grassland increase occurred on higher elevation. Small area of shrub increase can be seen on south-facing hills at all elevations.

3.4 Discussion

3.4.1 Seasonal effects on classification accuracy

When using the classification method in this study, the seasonal effect on the signals of shrubland and grassland should be taken into account. The classification method using a single vegetation index band can be adequate in this study based on the fact that the two focal land cover types (shrub and grass) exhibit distinct signals in the certain vegetation index. Furthermore, the study area was manually circled on land cover reference map, in order to avoid other land covers which may have similar signals of shrub/grass.

Aiming to find out whether shrubland and grassland can be distinguished by only one vegetation index (NDVI) band, a monthly Sentinel 2 NDVI time series captured in 2017 was used in preliminary trials. The training samples of shrub/grass are the same points in Methods (Figure 3.4). The result shows shrub and grass have distinctive signals on NDVI in spring and summer time, whereas these two land covers cannot be separated in autumn and winter time (Figure 3.15). This means NDVI is sufficient to separate shrub and grass in the study area during summer months. By the way, due to the temporal limit for historical achieve of Sentinel 2 (starts from June 2015), I cannot collect Sentinel 2 images with longer time interval than 2 years. Thus, SPOT 6/7, which has longer time series available and higher spatial resolution, was preferred as my final data source selection in this study.

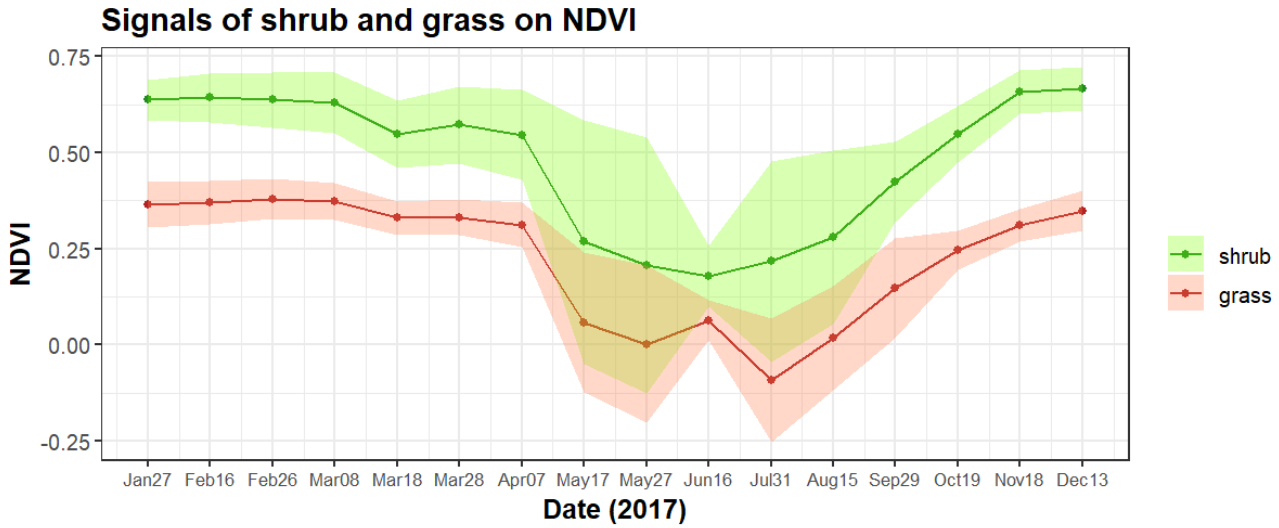

Figure 3.15 Signals of shrub and grass on monthly NDVI in 2017
NDVI time series was derived from Sentinel 2 MSIL1C dataset by SNAP 6.0 software. The line and points represent the mean value of NDVI. The shade around the line indicates the range of standard deviation.

Secondly, the gorse habitat, a component of shrubs in this study, shows higher sensitivity to seasonal changes in SPOT 6/7 NDVI signals. The validation samples show that several points in constant shrubland type are wrongly classified as grassland in 2013, but not in 2017 (Figure 3.16). These points clustered in a certain area, which was verified to be gorse habitats through aerial imagery and fieldwork photos (Figure 3.16). The gorse habitats and other shrubland with no gorse are re-examined with grassland samples in NDVI (Figure 3.17). Result shows gorse exhibited a different signal with other shrub species in summer (January 2013), but exhibited the same signal in late spring (November 2017). It explains the false classification in shrubs in 2013, namely that gorse had NDVI signals overlapped with grassland, in particular more in January compared to November. As a component of shrub species, the seasonal variance in the signals of gorse (perhaps due to flowering) reduced the accuracy of classification. The sensing time of SPOT 6/7 data should be carefully considered before applying the method of this study.

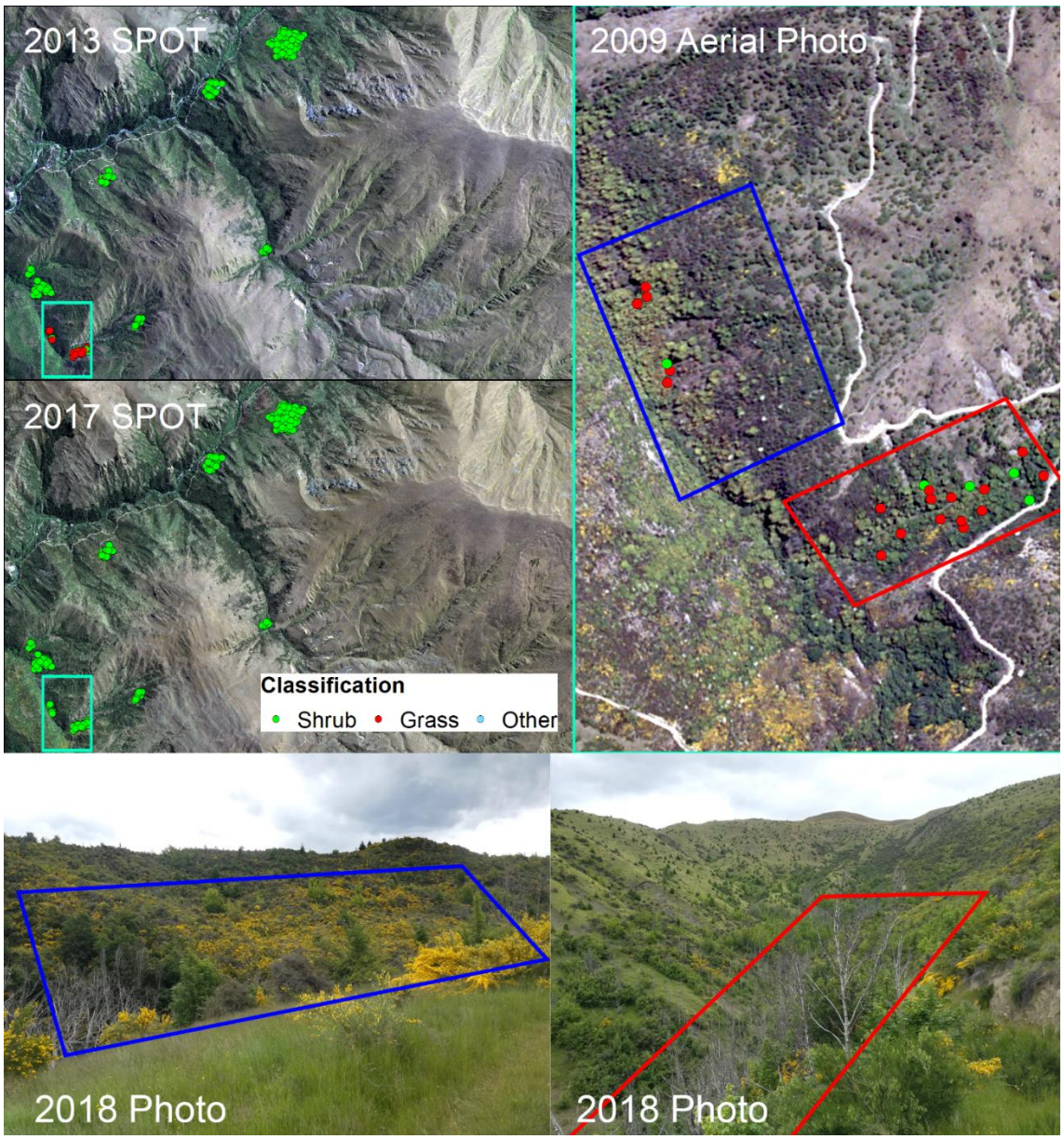

Figure 3.16 Classification validation of the constant shrubland
In "SPOT 2013" and "SPOT 2017", the constant shrubland validation points are expected to be classified as "Shrub" (green). The red points are the positions where are wrongly classified as "Grass" in my classification. The "2009 Aerial Photo" on the top right represents the rectangle region in "SPOT 2013" and "SPOT 2017" images on the top left. The red and blue polygons in the aerial photo correspond to the regions in the field work photos at bottom.

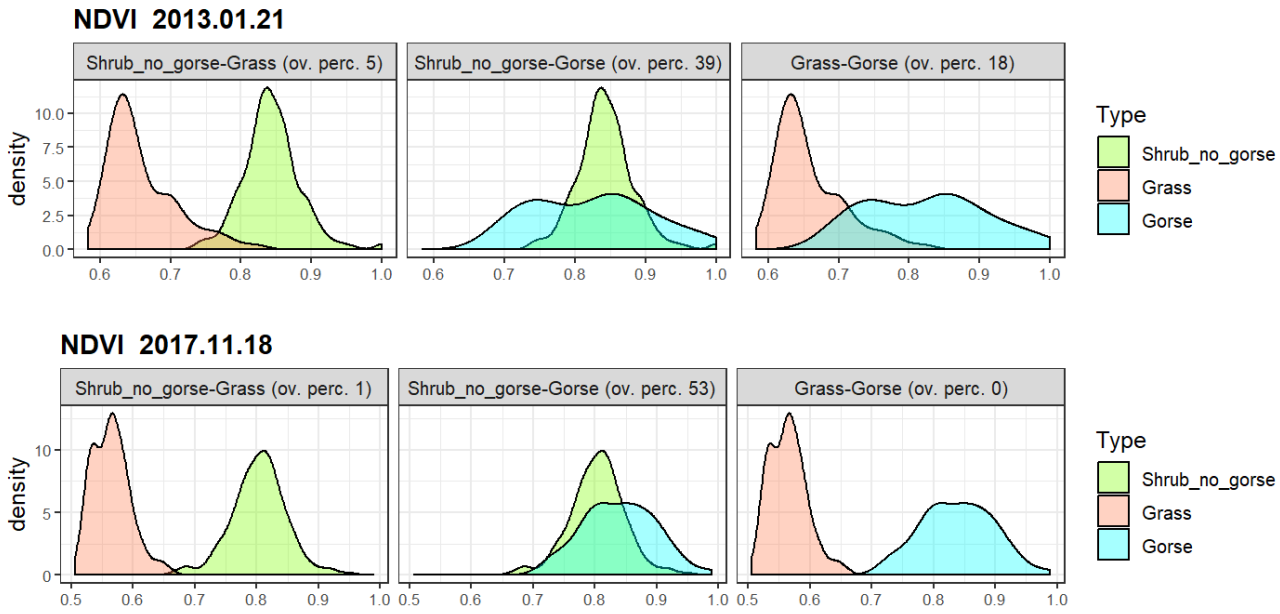

Figure 3.17 The signals of gores/shrub (without gorse)/grassland on NDVI
The shrub training points are divided to two parts: gorse, other shrubs without gorse component. The signals show that gorse has more overlap with grass type in January 2013, but shows similar signals as other shrubs in November 2017.

3.4.2 Further assessment of classification accuracy

In order to improve the classification accuracy, I produced the three-index agreed classification map (see Section 3.2.3), with the expectation that the multiple-index combination would increase the certainty of classification and reduce the wrongly classified shrub/grass transitions. However, the confusion matrices (Table 3.1) indicate this mixture only slightly increased the user accuracy (about 1%) in detecting shrub/grass changes, but dramatically dropped the producer accuracy (4%-44%). As change detection is the priority in this study, I chose the NDVI classification as the final result, due to its best producer accuracy among all the methods with the similar user accuracy.

After further assessment of NDVI classification result, I found my classification method may underestimate the shrubland/grassland conversion. Most of the "Grass to Shrub" validation points are correctly classified as grass in 2013 (96 of 100), however one third of these points (32 of 100) are wrongly classified in 2017, which is the reason for the decrease of producer accuracy in "Grass to Shrub" detection (Figure 3.18). These fail-to-observed shrub expansion points mostly locate in regions surrounded by large area of grassland, and these new emerged shrub points exhibit lower NDVI than large area of

shrubland, so they are failed to be separated from grassland. In contrast, the shrub expansion happened at the shrub/grass edges is more likely to be correctly identified.

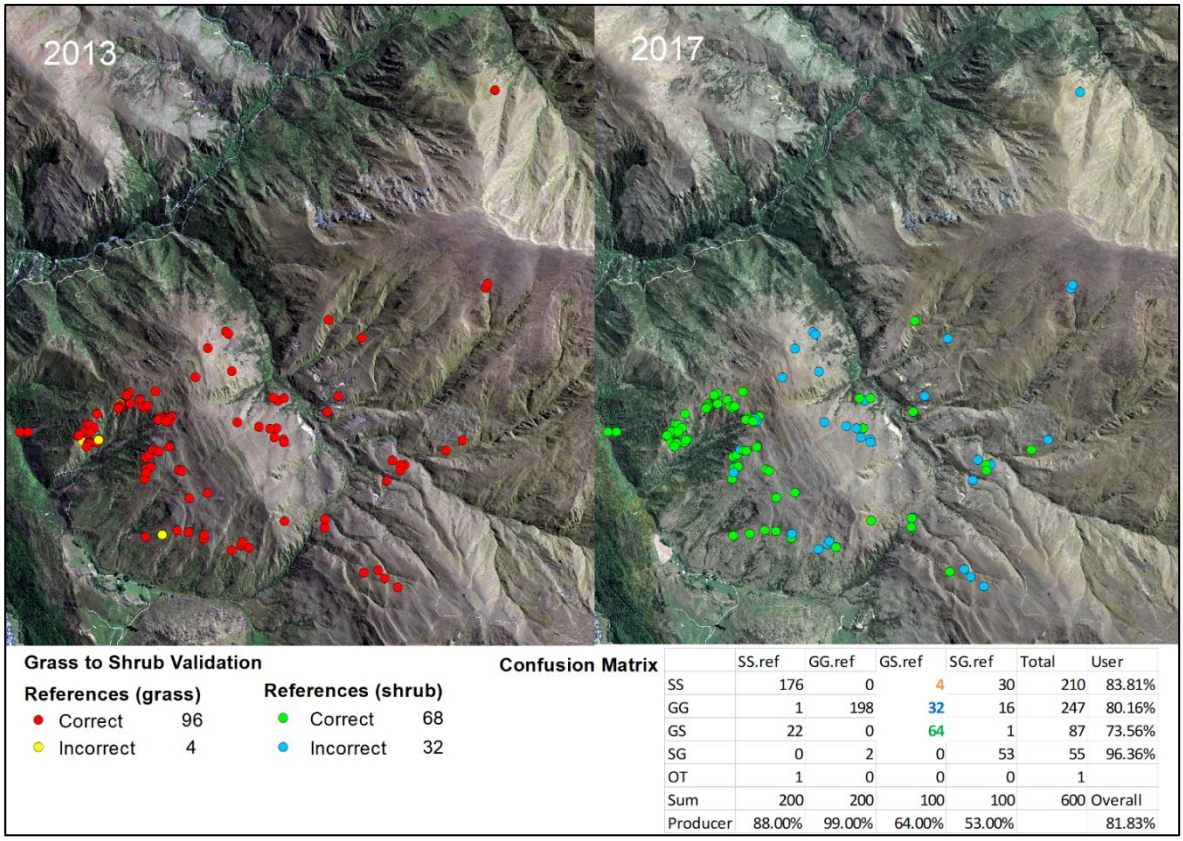

	SS.ref	GG.ref	GS.ref	SG.ref	Total	User
SS	176	0	4	30	210	83.81%
GG	1	198	32	16	247	80.16%
GS	22	0	64	1	87	73.56%
SG	0	2	0	53	55	96.36%
OT	1	0	0	0	1	
Sum	200	200	100	100	600	Overall
Producer	88.00%	99.00%	64.00%	53.00%		81.83%

Figure 3.18 Classification accuracy assessment for "Grass to Shrub" type
For "Grass to Shrub" validation points, the expected classification would be grass in 2013 and shrub in 2017. For 2013, the red points are the correctly classified locations, while the yellow points are incorrect classified. For 2017, the green colours are right classified and the blue are wrongly classified. In Confusion matrix, the numbers in yellow and blue are corresponding to the wrongly classified points in maps, and the number in green is the right classified.

For the "Shrub to Grass" type, there are 17 (of 100) shrub points wrongly classified as grass in 2013, most of which are found inside large area of grassland (Figure 3.19). On the other hand, 31 (of 100) grassland points are wrongly classified to shrub type in 2017, all of which locate in regions where shrub species just begin to retreat. In brief, my classification method performs excellent in distinguishing pure shrubland/grassland, and it is sufficient to detect the shrub/grass transitions at the boundary of large pieces of shrubland/grassland. Nonetheless, scattered shrub invasion or shrub retreat with minor NDVI changes might not be detected correctly by my method. The NDVI classification is adequate to monitor shrub encroachment in the study area, but the result might underestimate the amount of change.

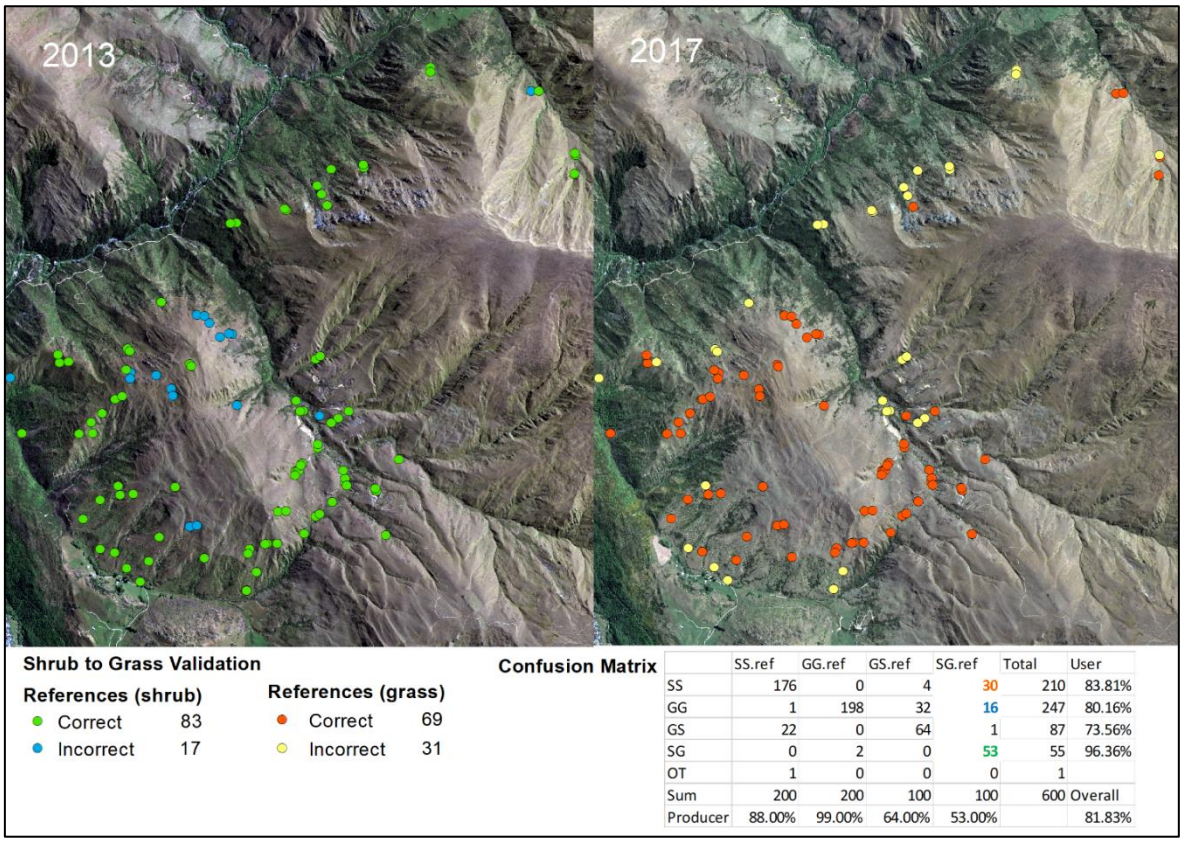

	SS.ref	GG.ref	GS.ref	SG.ref	Total	User
SS	176	0	4	30	210	83.81%
GG	1	198	32	16	247	80.16%
GS	22	0	64	1	87	73.56%
SG	0	2	0	53	55	96.36%
OT	1	0	0	0	1	
Sum	200	200	100	100	600	Overall
Producer	88.00%	99.00%	64.00%	53.00%		81.83%

Figure 3.19 Classification accuracy assessment for "Shrub to Grass" type

For "Shrub to Grass" validation points, the expected classification would be shrub in 2013 and grass in 2017. For 2013, the green points are correctly classified points, while the blue are wrongly classified locations. For 2017, the red colours are correct and the yellow are incorrect. In Confusion matrix, the yellow and blue numbers correspond to the wrongly classified points, and the green number is the right classified points.

3.4.3 Shrub encroachment in New Zealand

A gradual expansion trend of shrubs in New Zealand's tussock grassland was found in this study. Other research also observed this tendency in different grassland ecosystems in New Zealand. An investigation in the indigenous short-tussock grasslands showed this ecosystem was being invaded by exotic trees and shrubs, especially in lowland environments within rain shadow region of Central Otago (Walker *et al.*, 2004). A study on New Zealand's natural habitats described recent trends in indigenous grasslands that shrub species such as *Brachyglottis, Coprosma, Dracophyllum, Carydium,* etc. are predominant at high altitude and exposed sites, where used to be grassland (Ausseil *et al.*, 2011). Native shrubs such as manuka (*Leptospermum scoparium*) and kanuka (*Kunzea* spp.) commonly established among lower grasslands, and numerous woody species also appeared in tussock-dominated landscapes (Ausseil *et al.*, 2011). Recent work at Cass, Canterbury illustrated the quick increase of shrubland: native woody species (especially *Corokia cotoneaster, Coprosma propinqua, Discaria toumatou, Ozothamnus leptophyllus,*

Leptospermum scoparium) are currently invading into grasslands and this process appears to be ongoing as woody plants had been becoming prevalent in grassland in the past 10-20 years (Young *et al.*, 2016). Permanent cameras in Mt Aspiring National Park recorded some increase of shrub cover to treeline in the upper Waipara and Arawhata Valleys, Te Naihi Valley and Matukituki Valley, as while as shrubs (mostly *Dracophyllum longifolium*) have been obvious along the crest of Maungatua Scenic Reserve. On the mid-upper slopes of Rock & Pillar Range, there has been some gains of shrubs, mostly Hebe (*Veronica odora*) (Email contact with Prof. Alan Mark, 23 Nov 2016). In my study area, the main invading shrubs are wilding pines (*Pinus sylvestris*, etc.) and native shrubs (*Coprosma dumosa*, *Ozothamnus leptophyllus,* etc.). These shrubs are extending along slopes between large shrubland and grassland, between which is a mixed habitat of scattered shrubs and grass species with high greenness (Appendix III).

The shrub encroachment speed calculated in this study (0.35% year^{-1}) is moderate when comparing to the results from other research. A study in savanna ecosystem in Southern Hemisphere shows the woody encroachment rate ranges in 0.1-0.7 % year^{-1}, and Australia has the lowest speed of 0.1% year^{-1} (Stevens *et al.*, 2017). The research in southern Africa found a wide range of woody cover increase at −0.131 to 1.275% year^{-1} (O'Connor *et al.*, 2014). A study in the Lampasas Cut Plain, USA discovered a large re-distribution of woody cover across landscape, with a low expansion rate at 0.1-0.3% year^{-1} (Berg *et al.*, 2016b). A recent study established in eastern Otago, New Zealand indicated a dramatic expansion rate of woody cover at 0.83% year^{-1} (29% increase in 35 years) (Ropars *et al.*, 2018).

It should be noticed that the grass cover loss rate in this study is -0.43% year^{-1}, which is faster than the shrub expansion rate. This indicates shrub encroachment might be a reflection of grass retreat, but not the cause of it. This idea was also described in American grasslands (Van Auken, 2009). In New Zealand, shrub replacement of grassland is only one reason for grassland retreat. Other drivers include topdressing (fertilizing), over grazing, wild fire and dry weather, etc. (Espie and Barratt, 2006, McGlone *et al.*, 2014). Further research on how to separate the effects of all the drivers for grassland retreat is still needed.

3.4.4 Correlated factors with shrub encroachment

The rate of shrub cover expansion appears correlated with the proximity of other shrub habitats. The results show the increase of shrub proportion is positively related with the shrub coverage in neighbourhood when neighbouring shrub coverage reaches the

threshold of 40%. High original shrub coverage facilitates the further expansion of shrubs, and this correlation was also observed in other studies (Brandt *et al.*, 2013, Gartzia *et al.*, 2014). A negative relation between shrub increase and initial shrub coverage was found in a study in eastern Otago (Ropars *et al.*, 2018). Its results are consistent with my observation, that shrub expansion rate can be decreased when the neighbouring shrub coverage exceeded a certain value, so that no more habitats can be further occupied. For the grassland, high proportion of neighbouring grass coverage can keep the grassland stable. If the surrounded grass coverage dropped down a threshold (65%), grassland will begin to retreat. The shrub/grass coverage in neighbourhood has a non-linear relation with shrub/grass transitions. There are certain points where the relation between shrub/grass transition speed and their coverage in neighbourhood will reverse.

In topographic factors, elevation is a substantial indicator for the activity of shrub/grass transformation. In the study area, most of the shrub coverage increase happened under treeline (900 m), with the peak rate at 600 m elevation where shrub proportion exhibited the fastest growth. Similar situation was also observed in eastern Otago, that most shrub changes occurred in low-altitude gullies (< 500 m) and shrub expansion began to get slow when elevation higher than 650 m (Ropars *et al.*, 2018). Secondly, the analysis on aspect effects in this study showed there was a slight tendency that most shrub expansion found on sunny facing slopes at low elevation. This distribution of shrub expansion on aspect was also verified in the eastern Otago study (Ropars *et al.*, 2018). The locations on north- and east-facing slopes at low elevation are the hotspots of shrub encroachment. In all, except the neighbourhood effect, topographic factors also modify the spatial pattern of shrub/grass transition.

3.5 Conclusion

SPOT 6/7 vegetation indices with high spatial resolution (1.5 m) can separate shrubland and grassland in the study area. The simple and efficient method used in this study can monitor shrub encroachment in New Zealand's tussock grassland at a reasonable accuracy. During the time period 2013-2017, shrubland increased by 31.60 ha and 38.60 ha of grassland had lost in the study area (2239.34 ha in total). The expansion rate of shrub cover was 0.35% $year^{-1}$ on average, while the decreasing rate of grassland cover was 0.43% $year^{-1}$. Shrub encroachment rate is strongly correlated with the shrub coverage in neighbourhood. When the neighbouring shrub cover exceeded a threshold of 40%, shrub species began to extend into the habitats where used to be grassland. While

the grass species started to retreat when the surrounded grass coverage gets lower than 65%. Shrub expansion mostly occurred at low elevation below the natural treeline (< 900 m) and on north- and northeast-facing slopes.

Chapter 4 Spatial pattern and temporal dynamics in growth phenology in New Zealand's indigenous grasslands

Abstract

Shifts in the timing of life cycle events (phenology) are a key response of species and ecosystems to recent anthropogenic climate change. However, observations of phenological shifts in New Zealand are rare and only anecdotal. The aim of this study is to investigate temporal dynamics of growing season phenology in New Zealand's indigenous grassland over the last 16 years, and to identify potential climatic drivers of these dynamics. The MODIS Normalised Difference Vegetation Index (NDVI) time series of 2001-2016 was used to extract five phenological indices in three main grassland types in Clutha/Mata-Au River catchment, New Zealand. The correlations between growing phenological indices and eight climate factors were investigated. Over 86% of the indigenous grasslands areas showed an advancing start of the growing season, and over 63% showed an extending period of growing season. The results show the start of the growing advanced by 7.2, 6.0 and 8.8 days per decade in Alpine, Tall Tussock and Low Producing grassland, respectively. Minor change in the end of season was found in all three grassland types. The length of growing season extended by 3.2 (Alpine), 5.2 (Tall Tussock) and 7.1 (Low Producing) days per decade. An earlier trend in season peak and overall increasing NDVI in three grassland types indicate a tendency of higher biophysical activities in these ecosystems over recent years. Growing season start and length are closely correlated with atmospheric pressure and precipitation, while the season end is also sensitive to air temperature and solar radiation.

Key words

MODIS, NDVI, Growth phenology, Indigenous grassland, New Zealand

4.1 Introduction

Shift in phenology, changes in the timing of biological life cycle events, is a key biotic response to recent anthropogenic climate change. The seasonal patterns in the life-cycle events of organisms on our Earth can help us better understand the relationship between climate change and natural ecosystems, and further assist management of our natural environments (Morisette *et al.*, 2009). There is evidence from a wide range of organisms and regions that shifts in phenological events have occurred responding to anthropogenic

climate change (Visser and Both, 2005, Korner and Basler, 2010). Plants tend to tune their seasonality adapting to the oscillations in abiotic circumstances (Cleland *et al.*, 2007). A long-term observation in 21 European countries investigated 542 plant species shows a remarkable signal of earlier spring events (leaf unfolding, flowering, etc.) and summer events (fruit ripening, etc.) at a rate of 2.5 days /decade correlating to temperature (Menzel *et al.*, 2006). An advancing trend of first flowering was observed in 385 British plant species by 4.5 days /decade on average in 1990s (Fitter and Fitter, 2002). A number of studies observed or predicted advanced flowering and leafing, earlier bud burst, delayed senescence and extended growing season in various species globally (Elzinga *et al.*, 2007, Miller-Rushing and Primack, 2008, Linkosalo *et al.*, 2009, Jeong *et al.*, 2011, Vitasse *et al.*, 2011, Sun *et al.*, 2015). At landscape scale, phenological shifts are the sign of plant adaptation to changing environments, and also the reflection of species distribution variance. Though the shifts and trends of plant phenology in the past century were well documented, the long-term, large scale observations are still far from complete, especially in Southern Hemisphere (Schwartz, 2013).

As an important element in natural ecosystems worldwide, grassland makes up c. 40% of the global natural vegetation cover (Blair *et al.*, 2014). They are often found in alpine areas above tree-line, making them particularly vulnerable to recent climate change. There is evidence of current changes in growth phenology in grassland (Cleland *et al.*, 2006, Jentsch *et al.*, 2009, Zhang *et al.*, 2018). An earlier winter-spring onset and longer growing season according to simulated rising of CO_2 was found in phenology shifts modelling of European grasslands (Chang *et al.*, 2017). A study in the grassland in Inner Mongolia, China shows the growing season start and end perform different correlations with environmental factors and specific grassland species have different sensitivities to environment (Ren *et al.*, 2018). Shifts of growth phenology play a substantial role in explaining the biophysical and compositional changes in grassland ecosystems.

In New Zealand, grassland ecosystems cover c. 49% of the land area, in which 40% are exotic grassland till 2012. New Zealand's indigenous grasslands are comprised of two main vegetation parts: grasslands below the treeline and alpine grassland above treeline. According to the land cover data(LCDB-v4.1, 2015), three main indigenous grassland types are investigated in this study. The Alpine grassland corresponds to the habitats above treeline, and the Low producing grassland represents the part under treeline. The Tall Tussock grassland type, covering c. 9% of New Zealand's territory, occupies large range of elevation below and above treeline. It is a good representative showing the

transition of grassland ecosystems above and below treeline in New Zealand. Several studies had been conducted on the spatial distribution and compositional conversions in New Zealand's indigenous grasslands (Day and Buckley, 2013, Mark *et al.*, 2013, Weeks *et al.*, 2013b, Dymond *et al.*, 2017), however the evidence of how climate change impacts on the behaviours of grassland species is still rare.

Long-term field observations are important and widely used in phenology studies (Menzel *et al.*, 2006, Chen *et al.*, 2015, Wright *et al.*, 2015), however, the ground based observation is expensive, limited to local scale and usually requires organisation at national level. Remote sensing is a powerful tool for long-term landscape phenology observation. The application of remote sensing has dramatically developed over the past 20 years in the field of land surface phenology (LSP) study. The ability to continuously capture phenology patterns at landscape scale and retrospect the historical phenology in archived data enables remote sensing to be an advanced research tool (Reed *et al.*, 2009). Vegetation index (VI) generated from Moderate-resolution Imaging Spectroradiometer (MODIS) was introduced to monitor phenology dynamics at national scale and used in northeast United States (Zhang *et al.*, 2003). A study in Swiss Alps verified the capability of Normalized Difference Vegetation Index (NDVI) time series to track vegetation dynamics in alpine grasslands at large scale (Fontana *et al.*, 2008). A study in Qinghai-Tibetan Plateau with SPOT VGT time series successfully found the phenological signals in alpine grassland were closely related to heat and water supply (Ding *et al.*, 2013). More recent studies show remote sensing imagery are adequate and less expensive in monitoring phenological variance in grassland ecosystems (Leong and Roderick, 2015, Xin *et al.*, 2015, Zhu and Meng, 2015, Yu *et al.*, 2017).

In this study, I focus on the phenological shifts in New Zealand's indigenous grassland during 2001-2016, in order to find out the difference in phenological shifts in alpine and non-alpine grasslands and how the shifts of phenology responds to the changes in climatic factors. The near-daily MODIS imagery time series was used to monitor the growing phenology in grassland. MODIS has proven to be a promising tool to track alpine vegetation growth phenology in studies (Zhang *et al.*, 2003, Fontana *et al.*, 2008, Ganguly *et al.*, 2010). I investigated five indices of growing season in three main grassland types in South Island, New Zealand, to address the following questions:

1) Is there a trend for the timing of growth season in New Zealand's indigenous grasslands during the study time period (2001-2016)?

2) How does the spatial distribution of phenology trend exhibit in these indigenous grasslands?

3) How does the variability in the timing of growth correlate to climate factors through the 16 years?

4.2 Methods

4.2.1 Study Area

The study area is the domain of Clutha/Mata-Au River catchment in South Island, New Zealand. The Clutha/Mata-Au is the largest catchment (20,800 km^2) in New Zealand (Murray, 1975), which locates in the south half of the South Island. Three main grassland types, Alpine grassland, Tall Tussock grassland and Low Producing grassland are investigated, which are defined from the New Zealand Land Cover Database (LCDB-v4.1, 2015) (see Chapter 2 and Appendix I). There are two-thirds (36.1%) of land area in this catchment above 900m elevation (treeline for South Island), which is defined as the alpine ecosystems (Wardle, 2008). Over 6,400 km^2 Tall Tussock grassland and 3,800 km^2 Low Producing grassland situate in Clutha catchment (Figure 4.1).

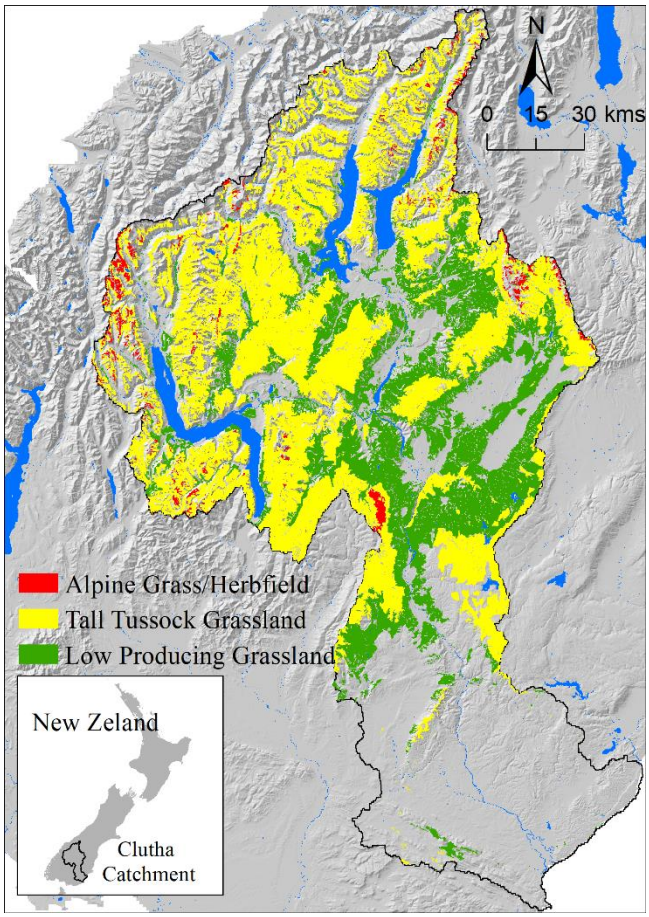

Figure 4.1 Grassland types in Clutha/Mata-Au river catchment, New Zealand

4.2.2 NDVI and climate data

Remotely sensed data was used to calculate indices of growth phenology and topographical factors. I used the Normalized Difference Vegetation Index (NDVI) derived from a near-daily MODIS dataset to calculate growth phenological indices (Figure 4.2). A 5-day maximum value composite was created from the near-daily NDVI time series to eliminate the noise due to high cloud/snow coverage in the raw data (Fontana *et al.*, 2008). The exact area of three grassland types were extracted from LCDB-v4.1(LCDB-v4.1, 2015, Dymond *et al.*, 2017). The LCDB data is in vector format. I converted it to a raster format in ArcGIS 10.1 using the MODIS NDVI pixels (250m) as reference, so that the rasterized land cover data can match the NDVI time series by pixel.

Climate data was obtained from the Virtual Climate Station Network (VCSN) (NIWA Data: https://data.niwa.co.nz). VCSN is a grid dataset at 0.05 degree latitude & longitude resolution covering the whole New Zealand land domain. Each point of this VCSN grid provides daily climatic values, which are calculated by interpolating method from the actual climate monitoring stations. The climate data for the time period from 01-07-2000 to 30-06-2016 was used to coincide with the dates of NDVI time series.

4.2.3 Phenology indices calculation

Five phenological indices were calculated for each pixel for each year (Table 4.1):

Table 4.1 Definitions of five growing phenological indices

No	Index	Content	Abbreviation
1	Start of season	The beginning of growth season, described by Julian day of year.	SOS
2	End of season	The end of growth season, described by Julian day of year.	EOS
3	Length of season	The length of growth season, which is the time period between start and end of season, described by days.	LOS
4	Peak of season	The peak of growth season, described by Julian day of year.	POS
5	Peak day NDVI	The fitted NDVI value on the day of the Peak of season	P-NDVI

I used the TIMESAT software (Jonsson and Eklundh, 2002) to calculate the five phenological indices based on the 5-day max value composite of NDVI time series. Several tools were developed and used to extract phenological signals from MODIS dataset (Jonsson and Eklundh, 2002, Ganguly *et al.*, 2010, Udelhoven, 2011, Rodrigues *et al.*, 2013, Geng *et al.*, 2016, Xu *et al.*, 2017, Testa *et al.*, 2018). In this study I chose the tool TIMESAT 3.3 (http://web.nateko.lu.se/timesat/timesat.asp?cat=0, visited on July 4 , 2018) on the Matlab R2013b platform (Jonsson and Eklundh, 2004). TIMESAT became my final option

over other similar tools (package 'phenex' in R platform, PhenoSat, TimeStats, etc.) because it is specific in calculating growth cycle seasonality from NDVI dataset performs more robust in processing data when comparing to other tools.

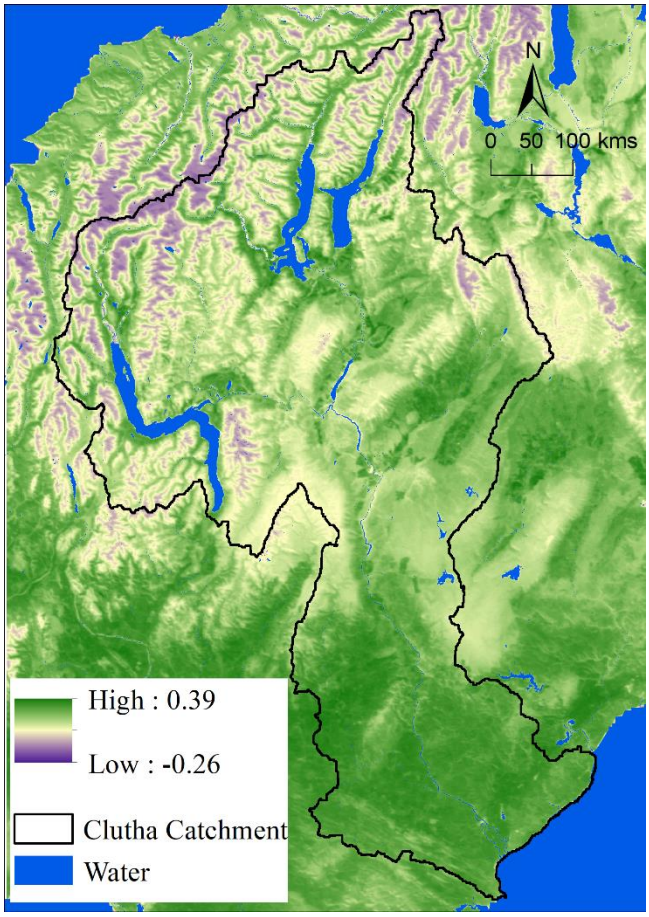

Figure 4.2 The 16-year average NDVI in Clutha catchment

There are three options of smooth function in TIMESAT, namely Savitzky-Golay, Asymmetric Gaussian and Double Logistic. The Savitzky-Golay method is "over-sensitive" to intro-annual changes in NDVI time series (Fontana *et al.*, 2008, Tan *et al.*, 2011), that large number of pixels in my data failed to be fitted by Savitzky-Golay function. The Asymmetric Gaussian and the Double Logistic functions gave the similar phenology indices estimation, however the Double Logistic method had more failed-fitted pixels than the Asymmetric Gaussian method. Other studies also demonstrated the Asymmetric Gaussian is more reliable when applying to mountainous environment (Beck *et al.*, 2006, Tan *et al.*, 2011, Li *et al.*, 2017). Thus, I finally chose the Asymmetric Gaussian function for phenology indices calculation.

Preliminary trials show the entire growing season mostly happens from 1st July to 30th June of next year in Southern Hemisphere. For convenience, I used the modified day of year (mDOY, 1st July is the first day of year and next 30th June is the last day of year) to

describe season start, end and peak (Figure 4.3). In detail, peak of season (POS) is defined as the day with highest NDVI in each year. The difference of NDVI value between the peak NDVI and the base level (the mean of the two lowest NDVI before and after POS in each year) is named as the "seasonal amplitude" for each year. In TIMESAT software, I set the seasonal amplitude for start / end of season both at 0.5 (50%) threshold. That means, start of season (SOS) is defined as the day on which NDVI grows by 50% of seasonal amplitude from the left lowest NDVI in each year. Similar, end of season (EOS) is the day on which NDVI drops by 50% of seasonal amplitude after peak of season in each year (inset in Figure 4.3). The count of days between SOS and EOS is length of season (LOS). The setting of TIMESAT software in this study can be seen in Appendix IV. Other parameters (Spike and Adaptation) in TIMESAT, which can tune the result of the regression model, were set to suit this study (spike = 2.0, adaptation = 3.0, Number of envelope = 3) through a trial-and-error method.

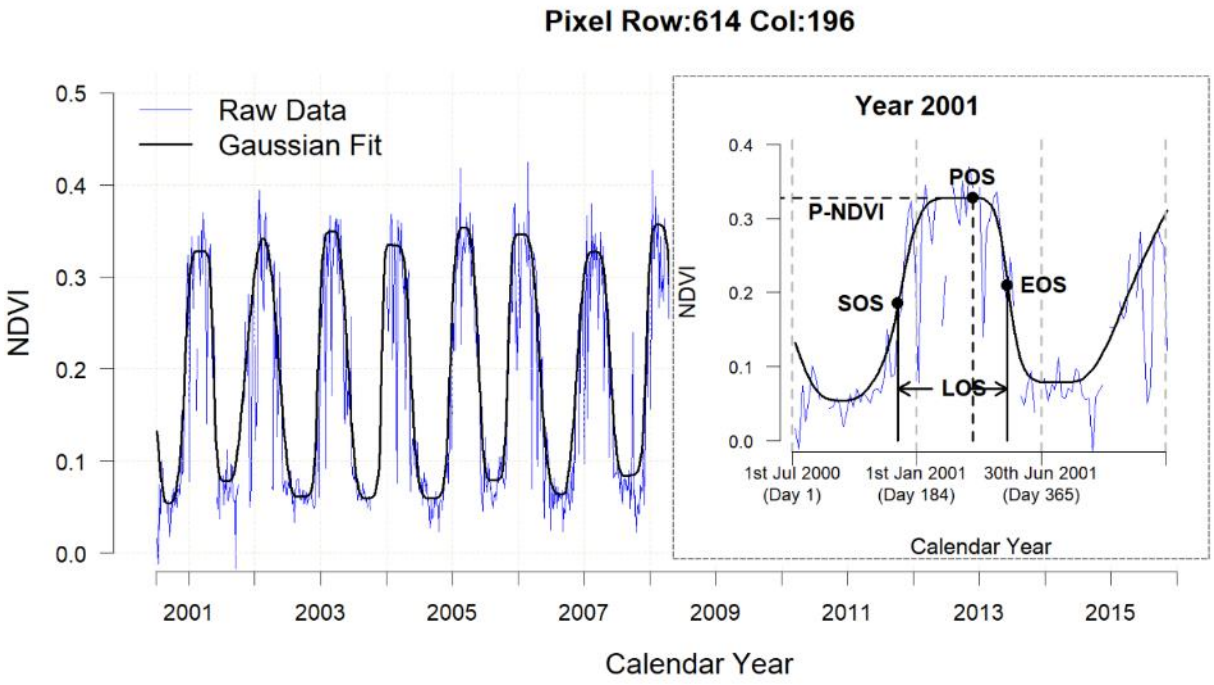

Figure 4.3 Calculation of five phenological indices

Taking one pixel (row: 614, column: 196) from the 16-year NDVI time series for example: The blue line is the raw NDVI data. The black curve is the Asymmetric Gaussian function fitted values. Growing phenological indices were derived from the fitted values. Inset shows how the five phenological indices were calculated. SOS = Start of season, EOS = end of season, LOS = length of season, POS = peak of season, P-NDVI = peak day NDVI. The phenology year in this study starts from 1st July and ends on 30th June in next year, and I use the modified day of year (mDOY) to describe the phenological indices.

4.2.4 Tendency and climate correlation analysis

The tendency of five phenological indices in the three grassland types during the 16 years was analysed by each MODIS NDVI pixel. A linear regression model (ordinary least squares, OLS) was used to describe the 16-year inter-annual variations for each growth phenology index for each pixel. The estimated slope and p value calculated from ANOVA test were used to quantify the trend of phenological indices. Positive OLS slope means later season start/end/peak or longer season length, while negative slope means the opposite. The p value indicates whether the trend of changes is significant in statistics (significant if $p<0.05$).

In order to calculate the relationship between growth phenology and climate, MODIS NDVI time series (250m) was resampled to 0.05 degree longitude & latitude resolution to match the VCSN climate grid (0.05 Deg.). There are 11 climatic factors provided by VCSN, namely Earth temperature 10cm at 9am (ETmp), mean sea level pressure (MSLP), potential evapotranspiration (PET), rainfall (Rain), relative humidity (RH), soil moisture (SoilM), solar radiation (Rad), maximum and minimum temperatures (Tmax, Tmin), vapour pressure (VP) and wind speed (Wind). An auto-correlation test within the 11 climate factors was used to remove dependent variables. Result shows PET, SoilM and VP can be excluded due to high correlation to other factors (Appendix V), so I chose 8 climatic variables to investigate (Figure 4.4).

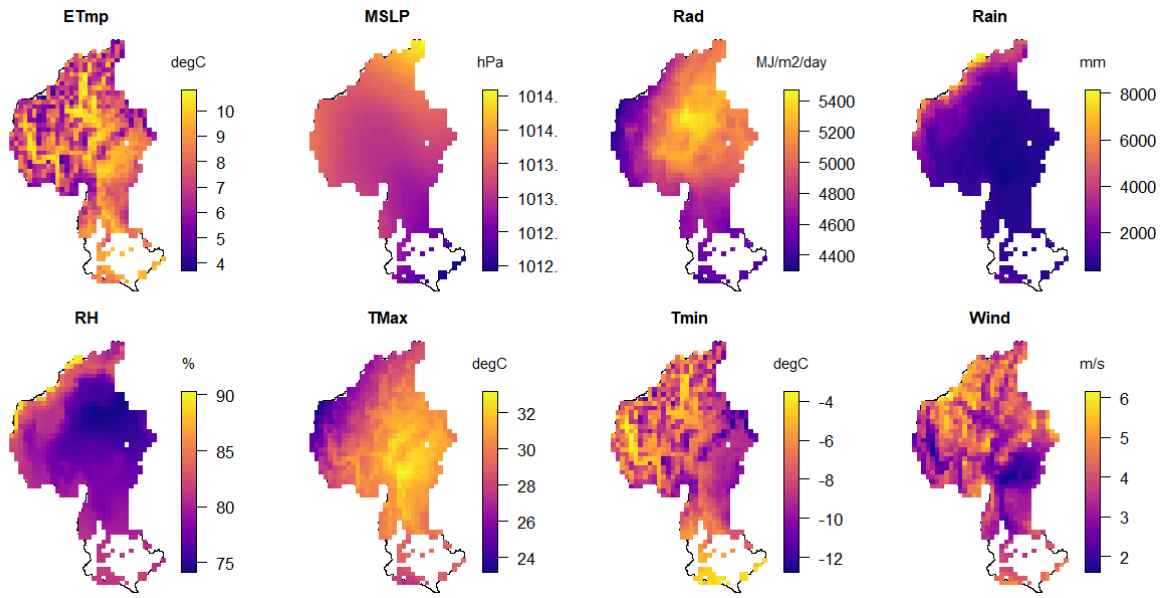

Figure 4.4 16-year average of climatic factors in study area

Abbreviations: ETmp: 10cm earth temperature; MSLP: mean sea level pressure; Rad: solar radiation; Rain: rainfall; RH: relative humidity; Tmax, Tmin: maximum and minimum temperatures; Wind: wind speed.

The relationships between growth phenology indices and climate variables were calculated by Pearson Correlation Coefficient (PCC) method. The Pearson "product moment correlation coefficient" is a commonly used index to describe the linear relationship between variables. PCC ranges from -1 to 1, indicating negative to positive covariance of two variables. The correlation was calculated for all pairs of phenological index and climatic factor in each grassland type. The originally daily VCSN climate data was transformed to seasonal and annual average values. In detail, the winter and spring (June to November) average is related to Start of season, spring and summer (September to February) average is for Peak of season, summer and autumn (December to May) is for End of season, the annual average is for Length of season and Peak NDVI. Pearson Correlation was calculated for each VCSN pixel (0.05 Deg.). The standardised correlation and significant test were conducted in R 3.5.3 with "stats" package(Team, 2013).

4.3 Result

4.3.1 Spatial distribution of growth phenology in New Zealand's indigenous grassland

During the 16 years, the start of season (SOS) in Alpine grassland occurs in late spring on average (149.9 mDOY), with approximate one month (31.96 days) variance (Table 4.2). The season start in Tall Tussock grassland happens one-month earlier than in Alpine grassland on average (119.4 mDOY). The Low Producing grassland has growing season start normally in early spring (93.4 mDOY) with less variations (24.76 days). The growth season start in New Zealand's grassland can appear from winter till early summer in different grassland types. In geography, the early season start appears mostly in low elevations in the centre and east of Clutha catchment, also in sporadic areas near lakes (Figure 4.5a). The high mountains in the north and west of the study area have 1-2 months later of start of season than in lowlands. On the summit of hills growth season only can begin in early summer.

The end of season (EOS) occurred in mid-autumn in both Alpine and Tall Tussock grassland (313.6, 314.1 mDOY), while Low Producing grassland finish growing season about one month earlier (275.3 mDOY) (Table 4.2). Except the Low Producing grassland in the east low elevations having season end in late summer, most of the three grassland types have growing season stopped in mid-autumn. There is an obvious altitudinal differentiation in season end in montane regions that higher elevation stops growth period later (Figure 4.5c).

The Tall Tussock grassland have the longest growth season (LOS, 194.7 days) on average, and the shortest growth season is in Alpine grassland with 163.7 days on average (Table 4.2). Low Producing grassland have a shorter season length than Tall Tussock grassland. The spatial pattern of length of season presents a high geographical diversity (Figure 4.5d). In mountains in the north and west of study area, the growth season length declines as elevation rises. Most high ranges show a season length lower than 100 days, while the low mountains can have growth season up to 220 days. Conversely, in the lowlands at the centre and east of Clutha catchment, grassland at lower elevation tends to have shorter growth season. Especially in the Low Producing type in the east of study area, the grassland only have 131-160 days of growing season.

Low Producing grassland reach their growing season peak (POS) in mid-summer (182.7 mDOY), following the Tall Tussock grassland reach the growth peak one month later (219.7 mDOY) and half-month later Alpine grassland have the season peak (233.8 mDOY) (Table 4.2). The season peak in three grassland types show a high spatial consistency, that in mountainous areas season peak appears in the last 2 months of summer, and the higher elevation shows the later of season peak (Figure 4.5b). The regions in the eastern lowlands reach the growth peak in late spring. On average, all grassland types reach their growth peak in summer months.

The mean peak NDVI increases from 0.33 (Alpine) to 0.47 (Tall Tussock) and to 0.59 (Low Producing) in three grassland types, indicating lower habitats have higher vegetation activities (Table 4.2). The peak NDVI in grassland shows a spatial pattern mainly covariant with elevation. The high montane regions exhibit low peak NDVI close to 0.1. The highest peak NDVI appears in the grassland near water bodies such as Lake Wakatipu, Lake Wanaka, Lake Hawea and Clutha/Mata-Au River. The eastern flat lands without natural water supply also show high peak NDVI perhaps due to artificial irrigation (Figure 4.5e).

Table 4.2 Summary of five phenological indices for three grassland types

Phenological Index	Alpine		Tall Tussock		Low Producing	
	Mean	SD.	Mean	SD.	Mean	SD.
Start (mDOY)	149.9	31.96	119.4	28.10	93.4	24.76
End (mDOY)	313.6	23.75	314.1	21.34	275.3	45.86
Length (days)	163.7	39.82	194.7	32.49	181.9	40.47
Peak (mDOY)	233.8	20.27	219.7	19.92	182.7	31.90
Peak NDVI	0.33	0.109	0.47	0.078	0.59	0.088

The 16-year (2001-2016) average value and standard deviation of each phenological index was calculated from all pixels for each grassland type.

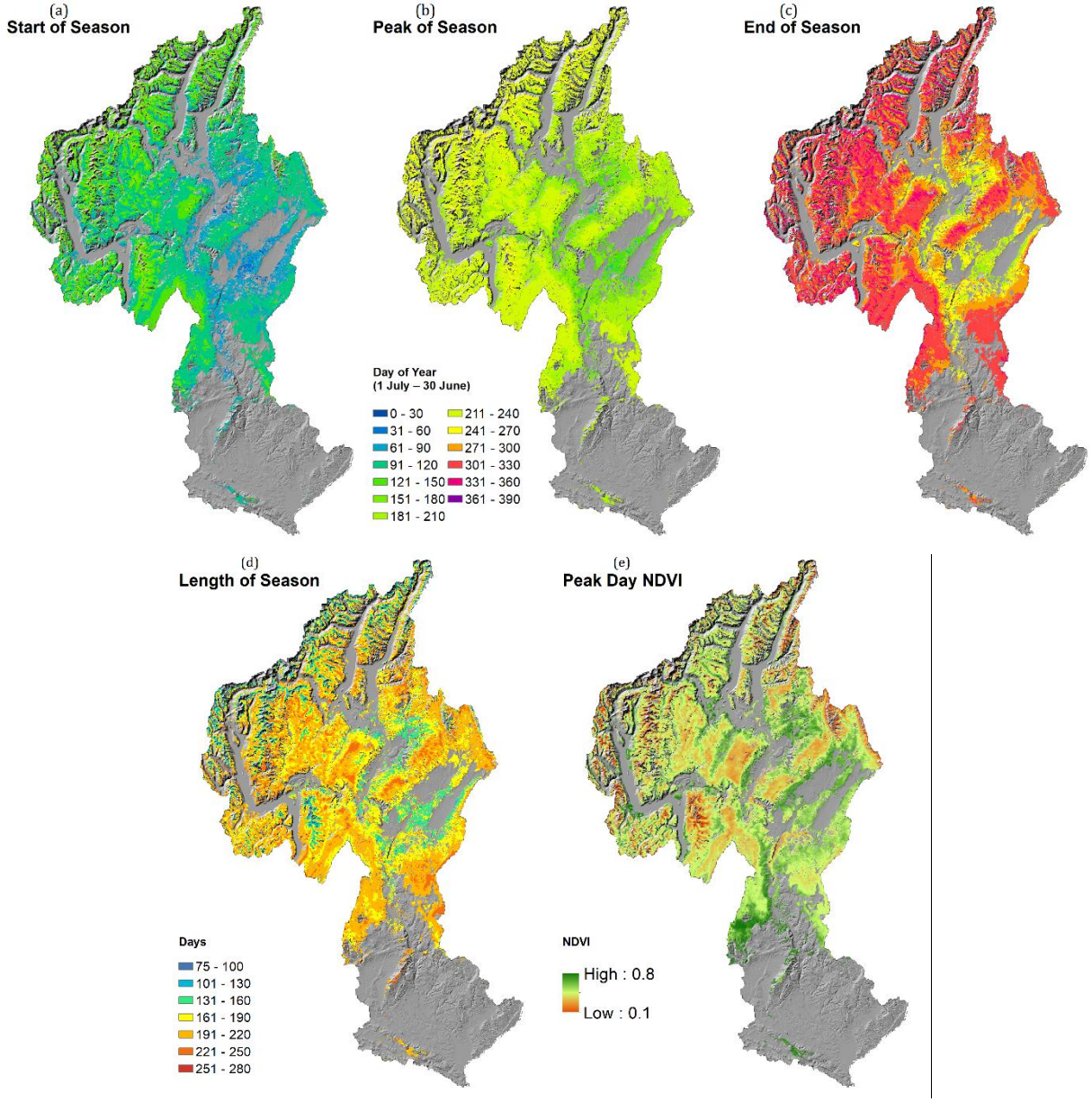

Figure 4.5 The 16-year average of five growth phenology indices

Start (a), End (c), Peak (b), Length (d) of season and season peak NDVI (e)for the time period 2001-2016 in all three grassland types. Start, End and Peak of season are described by modified day of year (mDOY, from 1st July to 30th June in next year) and sharing the same colour scale with monthly interval.

4.3.2 Trend of growth timing in New Zealand's indigenous grassland

Negative median trends of start of season was observed in all three grassland types, with changes of -0.72, -0.60 and -0.88 days/year for Alpine, Tall Tussock and Low Producing grassland respectively (Table 4.3). It indicates an overall earlier tendency in start of growing season in New Zealand's indigenous grasslands. The most negative trend of start of season (Min) shows higher absolute value that the most positive trend (Max) in each grassland type, indicating more advancing trends of season start in grasslands.

The median trends of season end are close to zero in Tall Tussock and Low Producing grasslands (-0.04 days/year), showing the end of season was less changed in these two grassland types during the 16 years. Instead, the median trend of season end in Alpine grassland exhibits a remarkable earlier tendency (-0.45 days/year) (Table 4.3).

Consequently, a positive median trend in length of season was detected in all three grassland types, with 0.32 (Alpine), 0.52 (Tall Tussock) and 0.71 (Low Producing) days longer /year (Table 4.3). The extending trend in season length is obviously due to earlier season start and less changed season end.

Table 4.3 Trends of five phenological indices during 2001-2016

phenology index	Alpine			Tall Tussock			Low Producing		
	Med	Max	Min	Med	Max	Min	Med	Max	Min
Start	-0.72	2.43	-5.73	-0.60	5.80	-6.83	-0.88	10.82	-11.99
End	-0.45	5.27	-4.60	-0.04	5.76	-6.48	-0.04	12.07	-9.03
Length	0.32	9.76	-3.99	0.52	9.14	-6.05	0.71	12.65	-10.69
Peak	-0.63	1.98	-3.05	-0.32	4.11	-4.41	-0.66	10.26	-9.00
Peak NDVI	0.05	0.82	-1.24	0.02	1.61	-1.49	-0.04	2.54	-1.90

The median (Med) and extremes (Max, Min) of trend slopes through the 16 years were calculated by linear model for each grassland type. For Start, End, Length and Peak of season, the unit is days /year; for Peak NDVI, the unit is 0.01NDVI /year.

The peak of season presented a notable earlier trend in grasslands, with median value of -0.63, -0.32 and -0.66 days /year in Alpine, Tall Tussock and Low Producing grassland individually. The relative small differences between extreme trend slopes (Max, Min) of season peak in Alpine and Tall Tussock grasslands illustrated a unified shift in season peak in these two types.

The peak day NDVI shows an increasing median trend in both Alpine and Tall Tussock grasslands (0.05^{-2}, 0.02^{-2} NDVI/year), however a declining trend was observed in Low Producing grassland (-0.04^{-2} NDVI/year), showing the species in higher elevation are becoming more active during the 16 years (Table 4.3).

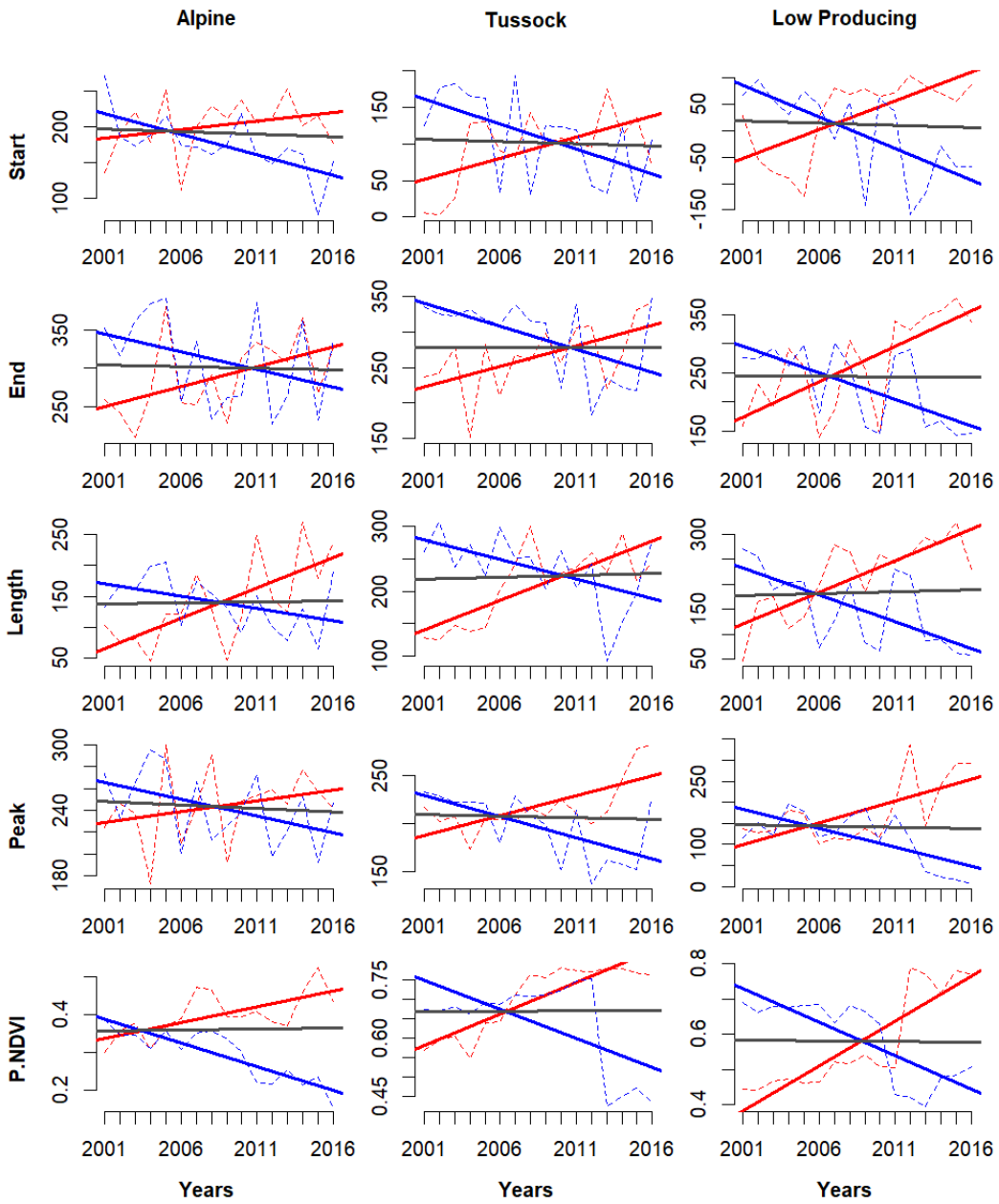

Figure 4.6 Trends of five phenological indices for three grassland types during 2001-2016
The extremes and median of trends in five phenology indices were drawn for three grassland types. The red/blue solid lines are the most positive/negative tendency during the 16 years, and the dotted red/blue line is raw data. The grey line represents the median trend slopes in each scenario.

In geography, an advancing tendency in the start of season was observed in the whole Clutha catchment with large area showing statistically significant trend (Figure 4.7a). The significant earlier trend of start of season usually occurred in the valley landscapes close to water bodies. The Low Producing grassland in the southeast flat land without large water body in neighbourhood also showed significant earlier trend in start of season. Only small areas of delaying trend in start of season was found in the south lowlands, most of which were insignificant in statistics.

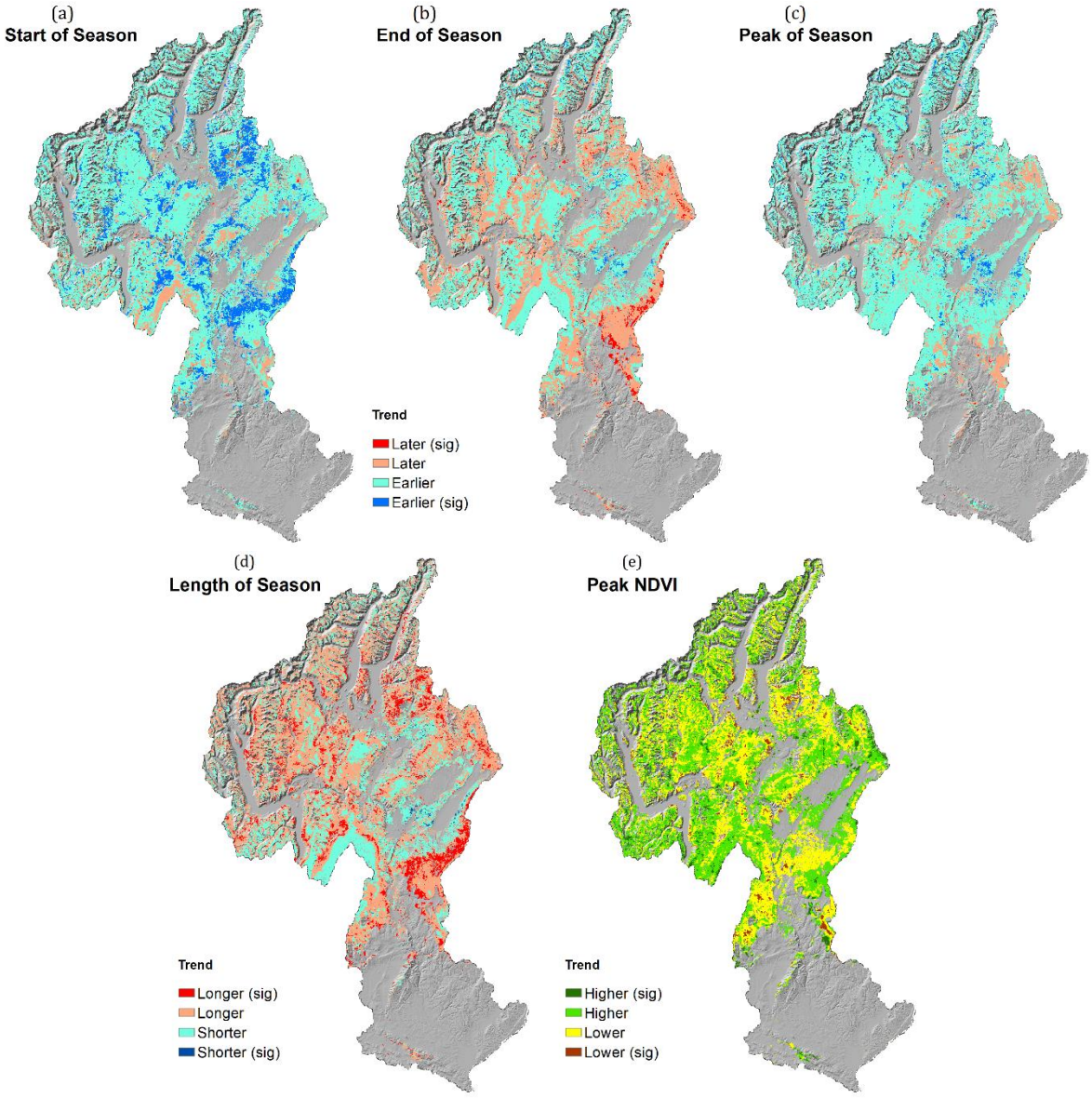

Figure 4.7 The tendency distribution of five growth phenological indices
For Start (a), End (b), Peak (c) and Length (d) of season, the red colours represent the areas showing positive trend (later Start, End and Peak of season, or longer Length of season). The dark red colours are the regions with significant positive trend ($p<0.05$). The blue colours are the pixels with negative trend (earlier Start, End and Peak of season, or shorter Length of season). Dark blue means significant negative trend in phenology. For Peak NDVI (e), the green regions have increasing trend in peak day NDVI and dark green indicates significant. While the yellow areas show a decreasing trend in peak day NDVI and brown means significant.

No significant changing trend of the end of season was observed in all the grasslands during the 16 years (Figure 4.7b). Grasslands on the montane regions are more likely had earlier end of season, while the areas in gullies tended to have later end of season. Small area of significant earlier trend in end of season was detected in central and northern mountains. The Low Producing grassland in low elevation in the east also showed an earlier trend of end of season. Most significant later trend of end of season was observed in the Tall Tussock grassland on the southeast mountains.

Nearly 90% of the grasslands showed an earlier trend in peak of season (Figure 4.7c). The significant earlier trend of peak of season was mostly found in Alpine grassland in high elevation, as well as in Low Producing grassland at low elevation. A small number of grassland pixels showed a weak later trend of peak of season in low elevations in Clutha catchment. There is hardly significant earlier or later trend of peak of season found in Tall Tussock grassland.

There is a longer trend of length of season in the northern mountains of Clutha catchment, including Alpine and Tall Tussock grassland types (Figure 4.7d). The significant longer trend of length of season typically appeared in valleys beside water bodies and in lowlands. Large area of Low Producing grassland in the southeast ridges showed a significant extending trend of length of season. While an insignificant shortening trend of length of season was observed mostly in the central and southern low elevation regions. Considerable Low Producing grassland in the eastern lowlands of the Clutha catchment showed a shortening growing season.

There is no regular spatial pattern of the changing trend of peak NDVI in the indigenous grasslands of Clutha catchment (Figure 4.7e). Large areas of grassland in the central mountains showed a decreasing trend in peak day NDVI. This tendency was also found in the flat lands in the south. An increasing trend of P-NDVI was widely observed in the east lowlands and ridges with high significance. Considerable grassland pixels in the western mountains near Queenstown city showed high variations in P-NDVI.

In quantity, over 85% area in each grassland type exhibit an earlier (negative) trend of start of season (Figure 4.8). However, the proportions of significant earlier trend are small in Alpine (7.56%) and Tall tussock (8.73%) grasslands. A high percentage of significant advancing trend (27.90%) in start of season in Low Producing grassland was detected, with about 2 days earlier /year.

An earlier trend of the end of season had been observed in 73.50% area of Alpine grassland in the study area with 3.44% significance (Figure 4.8). Nevertheless, only half of the area in Tall Tussock grassland (52.19%) and Low Producing grassland (51.51%) showed an advancing trend of end of season with less than 3% significance. The shift of end of season in three grassland types was weak during the 16 years.

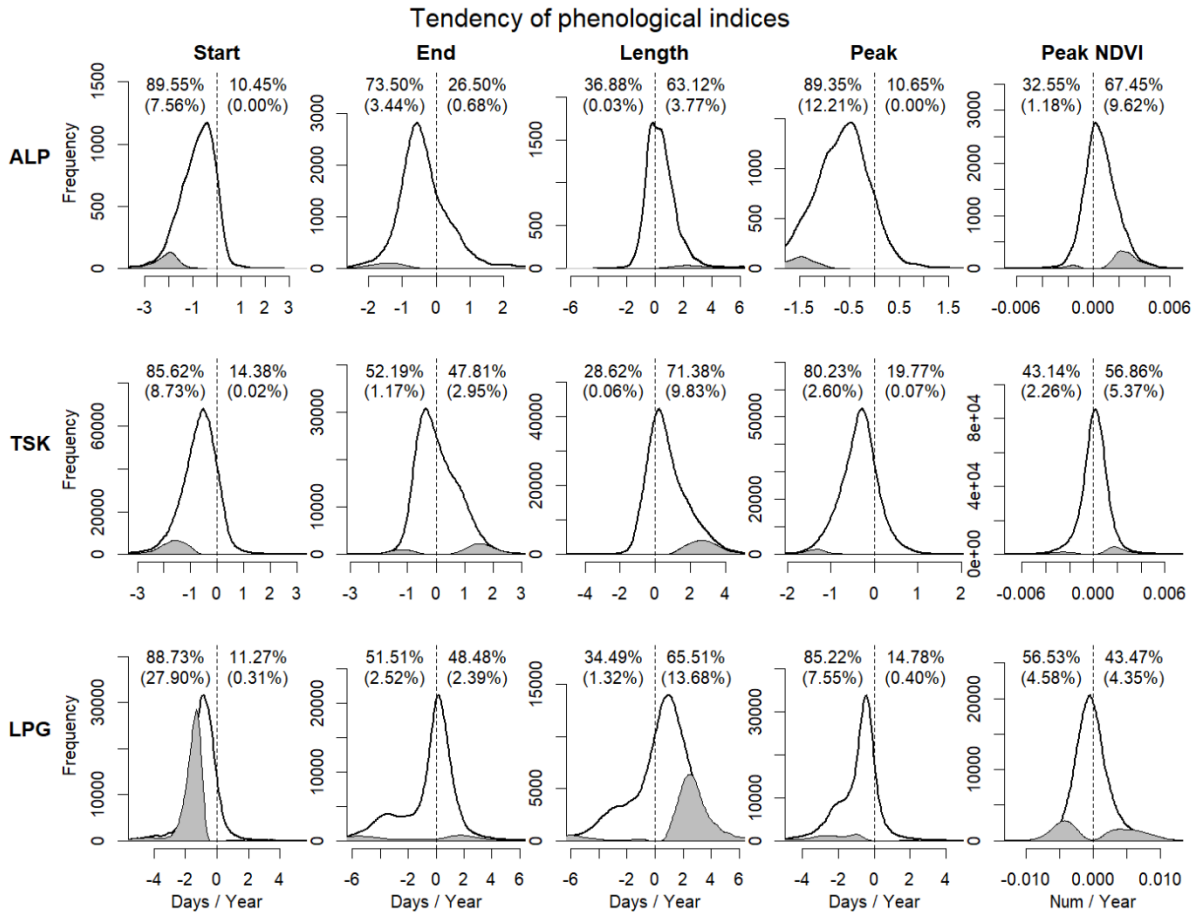

Figure 4.8 The distribution of the trend of each growth phenological index in each grassland type ALP: alpine grassland; TSK: tall tussock grassland; LPG: low producing grassland. The dotted vertical line in each panel separates the positive and negative trends. The shadowed the region indicates the significant ($p<0.05$) trend slopes. The proportion values in each panel show the percentage of positive/negative trends among all pixels and the values in round brackets are the portions in significance.

Over 60% of the areas in three grassland types exhibited an extending trend of length of growing season during 2001-2016 (Figure 4.8). The longer trend of length of season is relatively weak in Alpine grassland (63.12%) with only 3.77% of area showing strong longer trend. Tall Tussock grassland had a high proportion (71.38%) of area showing an increasing length of season during the 16 years. Low Producing grassland had the highest proportion of area (13.68%) with significant extending trend in length of season among the three grassland types.

The peak of growing season showed a prevailing earlier trend in over 80% of areas in three grasslands (Figure 4.8). Close to 90% of Alpine grassland presented an advancing peak of season during the study period with high significant percentage (12.21%). The trend is relatively weaker in Tall Tussock grassland, however, there was still over 80% of

area showing an earlier trend in peak of season. The earlier trend of peak of season was also observed in 85.22% of Low Producing grassland.

The trends of peak day NDVI (P-NDVI) showed different patterns in three grasslands. In Alpine grassland, over 65% of area tended to have higher NDVI value on season peak day and 9.62% of area showed significance. Only half of Tall Tussock grassland (56.86%) presented a positive trend in P-NDVI with low significant proportion (5.37%). In Low Producing grassland, over half of the area (56.53%) showed a negative trend in P-NDVI. The overall shift of P-NDVI was very weak in three grassland types.

4.3.3 Correlations between the growth phenology and climate factors

Start of season was strongly correlated to atmospheric pressure (MSLP) and rainfall (Rain) in large areas in three grassland types (Figure 4.9). A significant negative correlation between start of season and MSLP was observed in 78 % of Alpine grassland and 64 % of Tall Tussock grasslands, as well as in mountainous areas of Low Producing grassland (25 %) (Figure 4.9, Table 4.4). As the atmospheric pressure is mainly controlled by elevation, this negative relation indicates start of season was delayed as elevation grows (MSLP declines) in grasslands. Over 20% of areas in three grassland types showed a strong positive correlation between start of season and precipitation. In the west and north ridges (21%) of Alpine grassland the start of season would be delayed by 0.14 days if annual precipitation increased by 1mm (Table 4.4). The start of season also showed a significant positive relation with rainfall in 26% of Tall Tussock grassland and 23% of Low Producing grassland with 0.16 days delay /1mm rainfall increase annually.

The end of season was correlated to temperature (ETmp), radiation (Rad) and rainfall (Rain) in different grassland types. A significant positive correlation of end of season and temperature was found in 16% of Alpine grassland near Lake Wanaka and in 19% of Tall Tussock grassland in the east of the study area (Figure 4.9), showing 8.15 and 12.23 days delay in end of season /Celsius degree higher (Table 4.4). End of season was positively related to solar radiation in the north ridges of Alpine grassland (29%) and of Tall Tussock grassland (16%). In these regions the end of season tended to be delayed by 0.04-0.05 days if radiation increases 1 MJ/m^2/year. A strong positive correlation between end of season and precipitation was only observed in the 32% of Low Producing grassland in the eastern part of the study area (Figure 4.9), exhibiting 0.46 days delay in end of season /1mm annual precipitation grows. In addition, end of season presented a strong positive

correlation with annual minimum temperature (Tmin) in 17.77% of Alpine grassland in the western mountains.

The length of growth season is sensitive to atmospheric pressure (MSLP) in three grassland types. A significant positive relation between length of season and MSLP was found in 11% of Alpine grassland, 13% of Tall Tussock grassland and 16% of Low Producing grassland (Table 4.4). Particular in 15% of Low Producing grassland, length of season showed a positive relation with precipitation with 0.18 days longer the growing season as rainfall increases by 1mm annually. A positive correlation was also found between length of season and wind speed (Wind) in 12% of Tall Tussock grassland and 11% of Low Producing grassland in the northeast of the study area (Figure 4.9).

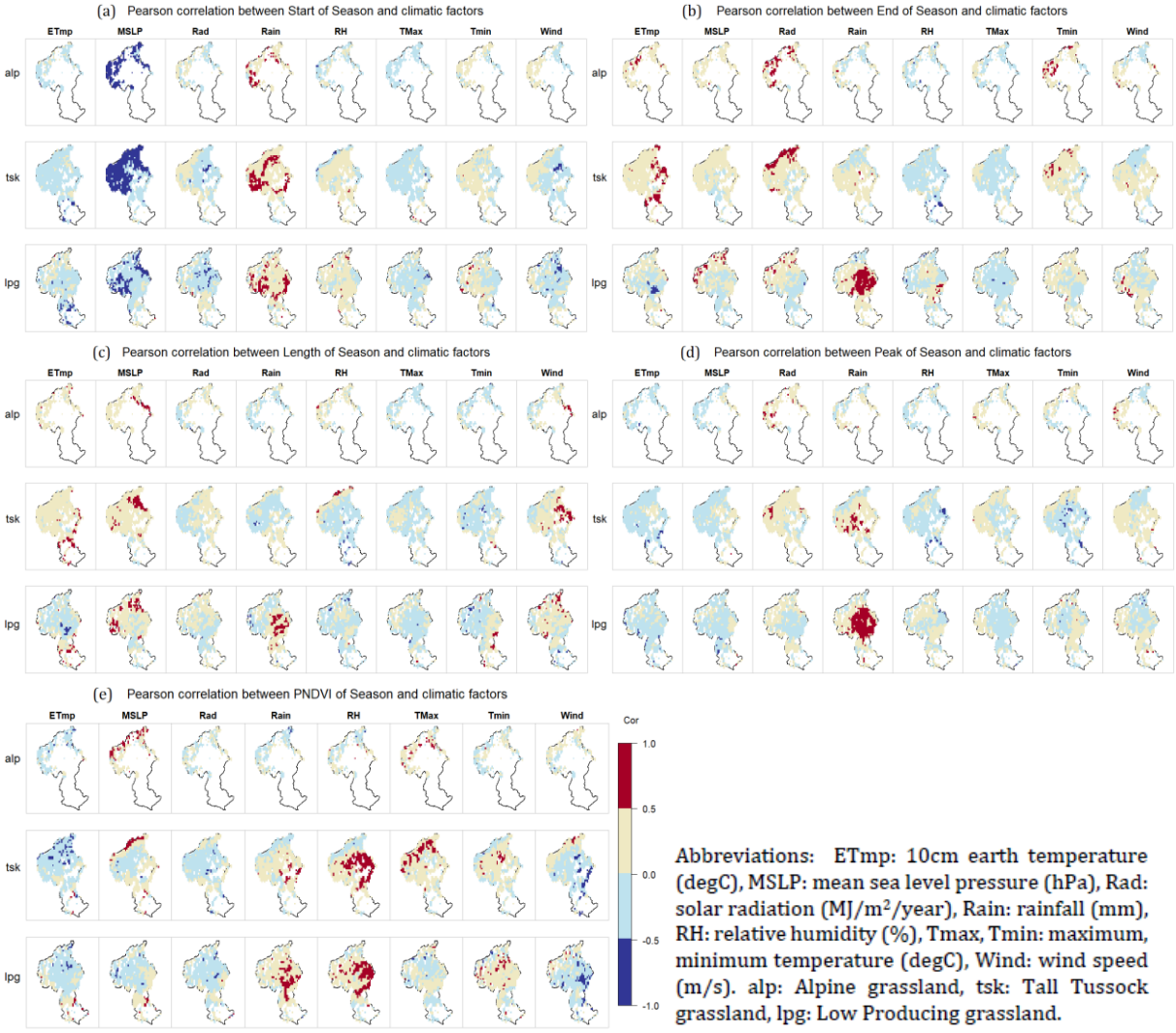

Figure 4.9 Pearson correlation coefficient between growth phenology indices and climate factors Five phenological indices were analysed with eight climatic factors (a-e). The red and blue colours represent the positive and negative correlations between variables. ANOVA test shows the correlation is significant ($p<0.05$) when PCC is higher than 0.5 (dark red) or lower than -0.5 (dark blue).

Table 4.4 The response of growth phenological indices to climate factors

Abbreviations: ETmp: 10cm earth temperature (degC), MSLP: mean sea level pressure (hPa), Rad: solar radiation (MJ/m^2/year), Rain: rainfall (mm), RH: relative humidity (%), Tmax, Tmin: maximum, minimum temperature (degC), Wind: wind speed (m/s). alp: Alpine grassland, tsk: Tall Tussock grassland, lpg: Low Producing grassland.

Index	Type	ETmp	MSLP	Rad	Rain	RH	TMax	Tmin	Wind
Start (mDOY)	alp	-17.65	-3.35	-0.43	0.14	-4.71	-4.46	5.82	4.02
		1%	78%	1%	21%	2%	2%	1%	1%
	tsk	-23.58	-3.05	-0.09	0.16	0.91	4.62	7.50	-13.20
		3%	64%	4%	26%	3%	1%	1%	4%
	lpg	-17.49	-2.25	-0.06	0.16	4.95	-3.09	4.32	-16.04
		8%	25%	9%	23%	4%	3%	5%	8%
End (mDOY)	alp	8.15	1.80	0.05	0.10	-3.80	-6.20	3.97	25.10
		16%	2%	29%	2%	2%	1%	18%	4%
	tsk	12.23	NA	0.04	0.35	-4.25	-2.56	2.83	28.79
		19%	0%	16%	2%	4%	<1%	7%	2%
	lpg	-33.43	1.76	0.01	0.46	8.17	-3.39	4.86	13.27
		6%	7%	4%	32%	4%	2%	1%	4%
Length (days)	alp	19.54	10.14	0.02	-0.04	5.23	-2.99	-8.53	21.94
		5%	11%	1%	1%	2%	1%	2%	5%
	tsk	36.42	10.65	0.04	-0.05	-1.50	-3.07	-7.58	37.36
		9%	13%	1%	2%	7%	<1%	4%	12%
	lpg	-5.35	11.44	-0.02	0.18	-3.11	1.64	-0.09	24.06
		10%	16%	3%	15%	2%	1%	6%	11%
Peak (mDOY)	alp	-10.34	-2.10	0.07	0.13	-2.61	4.38	-0.30	18.48
		1%	1%	13%	4%	2%	2%	2%	4%
	tsk	-12.67	3.68	0.05	0.15	-2.31	1.26	-6.43	25.42
		3%	<1%	5%	11%	5%	<1%	6%	1%
	lpg	-10.87	-1.25	0.02	0.28	0.04	-2.54	-1.34	-1.87
		3%	3%	1%	40%	2%	1%	3%	3%
P-NDVI	alp	-1.32E-02	1.15E-02	2.23E-05	5.37E-06	-6.68E-04	3.58E-03	-4.12E-04	-1.81E-03
		6%	26%	1%	5%	6%	16%	3%	2%
	tsk	-1.01E-02	5.66E-03	-5.60E-05	1.87E-04	8.72E-03	2.94E-03	9.56E-03	-5.32E-02
		14%	9%	3%	7%	30%	17%	7%	12%
	lpg	-1.32E-02	-4.38E-03	-4.54E-05	2.23E-04	1.22E-02	-4.63E-03	1.22E-02	-6.78E-02
		9%	6%	5%	19%	28%	4%	11%	16%

The relationship was quantified by linear regression model (OLS function: phenological index = a + b × climate factor) for each phenological index & climatic factor pair in each grassland type. Only the pixels with significant Pearson Correlation Coefficients (Figure 4.9) were fitted by model. The numbers in black are the estimated slopes (b values). The percentage in grey under the slopes are the proportions of the significant pixels of all grassland pixels in each type. The proportions higher than 10% were highlighted.

The peak of season was sensitive to solar radiation (Rad) and rainfall (Rain) in different grassland types. Peak of season was strongly correlated to radiation in 13% of Alpine grassland with 0.07 days later as radiation rises by 1 MJ/m^2/year (Table 4.4). Later peak of season was significantly related to higher precipitation in 11% of Tall Tussock grassland and in over 40% of Low Producing grassland, in which every mm precipitation increase correlated to 0.15 and 0.18 days later of the peak of season in these two grassland types.

The peak day NDVI (P-NDVI) was correlated to several climatic factors in different grassland types. P-NDVI was strongly related to relative humidity (RH) in over 30% of Tall Tussock grassland and 28% of Low Producing grassland, in which higher humidity correlated to higher P-NDVI (Table 4.4). In Alpine grassland, P-NDVI had a positive correlation with atmospheric pressure (MSLP) in 26% of this grassland. In Low Producing grassland, P-NDVI showed an increasing trend as radiation grows in 19% of this grassland. P-NDVI also tended to increase if annual maximum temperature (Tmax) was higher in over 16% of Alpine and Tall Tussock grasslands. Wind speed (Wind) had a negative correlation with P-NDVI in 12% of Tall Tussock grassland and 16% of Low Producing grassland.

4.4 Discussion

4.4.1 Current growth phenology shifts in grassland worldwide and in New Zealand

Evident growth phenology shifts have been observed in grassland ecosystems globally. A long-term observation on Tibetan Plateau showed an advanced spring leafing in alpine grassland due to climate warming (Zhou *et al.*, 2014). A three-year experiment in Minnesota, USA showed that the spring green-up time was sensitive to warming climate, but the senescence was not substantially affected by warm temperature (Whittington *et al.*, 2015). The extending length of growing season was found in Icelandic subarctic grassland, impacted by the warming environment (Leblans *et al.*, 2017). In Southern Hemisphere, the advanced spring events were discovered by a study with most data collected from Australia and New Zealand (Chambers *et al.*, 2013). More studies (Ma and Zhou, 2012, Chang *et al.*, 2017, Cui *et al.*, 2017) also demonstrated the trend of earlier start of season, unstable end of season and extended growing season in grassland ecosystems, which are also observed in this study.

A recent study in Australian Alps showed the grassland habitats exhibited earlier start of season, later end of season and longer growing season length during 2000-2014

(Thompson and Paull, 2017). I compared the results of this study with the results: The start of growing season in Australian Alps was 96 mDOY at 1400-1599 m elevation and 125 mDOY at 1800-1999 m on average. In this study the grassland in New Zealand exhibited later start of season at the similar elevation, with 149 mDOY in Alpine grassland (1300-1900 m) and 119 mDOY in the Tall Tussock grassland (800-1600 m) on average. The end of growing season in Australian Alps was 320-335 mDOY at 1400-1999 m elevation, while the value was 310-315 mDOY at similar elevation in New Zealand. In consequence the growing season in New Zealand's grassland (160-200 days) was about 40 days shorter than in Australian grassland (200-240 days). The comparison shows New Zealand's indigenous grasslands have later start of season, earlier end of season and shorter growing season than the grasslands in Australia.

The trend of growing phenology observed in this study was compared to the results from other studies. In the study period (2001-2016) the start of season had a trend of 6.0-8.8 days earlier /decade in three grassland types. The end of season showed nearly no trend in Tall Tussock and Low Producing types, but a trend of 4.5 days earlier/decade in Alpine grassland. The growing season length was extended by 3.2, 5.2 and 7.1 days/decade in Alpine, Tall Tussock and Low Producing grassland, respectively. A study in Qinghai-Tibetan Plateau discovered 6.0 days earlier /decade of start of season, 2.0 days later /decade of end of season and 8.0 days longer /decade of growing season in alpine grassland ecosystem (Ding *et al.*, 2013). The study in Australian Alps reported the start of season was 9-10 days earlier /decade, end of season showed 0-18 days later /decade and length of season got 11-29 days longer /decade during 2000-2014 (Thompson and Paull, 2017). A recent study in grasslands in China (Yu *et al.*, 2017) observed 2.8 days earlier of start of season /decade, 2.8 days later of end of season /decade and 6.6 days longer growing season /decade. The results indicate the growth phenology in New Zealand's grassland ecosystems was relatively stable in recent years at global scale.

4.4.2 The responses of growing phenology indices to climate change

Some studies claimed the increased temperature would be an important driver for earlier start of growing season and further extended the growing season time (Ma and Zhou, 2012, Xia and Wan, 2012). Precipitation and drought are also substantial factors in affecting the start of season in grassland ecosystems (Xia and Wan, 2012, Cui *et al.*, 2017). In contrast, my results indicated the start of growing season was correlated mainly to atmospheric pressure (elevation) and precipitation, but temperature plays a less

important role (Figure 4.9 and Table 4.4). The air temperature increased significantly in the east and south of Clutha catchment (Figure 4.10). These warming regions matched the distribution of advanced start of season in the east, but not in other regions (Figure 4.7a). The precipitation in Clutha catchment was stable during the past 16 years, except a dramatic increase in the northwest ridges. The locations with decreasing precipitation (Figure 4.10) matched the distribution of earlier start of season (Figure 4.7a). The atmospheric pressure (MSLP) presented a positive trend in all Clutha catchment during the study period, which was consistent with the pattern of advanced start of season. Therefore, the start of growing season in New Zealand's indigenous grasslands was strongly correlated with MSLP (which is generally decided by elevation) and modified by precipitation and temperature.

My results showed the end of season in Alpine and Tall Tussock grassland types were sensitive to temperature and solar radiation, and in Low producing grassland it was strongly correlated with precipitation. End of season in any grassland type was not sensitive to MSLP changes, which indicates the end of season was not correlated to elevation. A recent study also showed that the end of season in specific grassland types was strongly correlated with temperature or related to precipitation (Ren *et al.*, 2018), and the end of season in Australian grasslands was not sensitive to elevation changes (Thompson and Paull, 2017). In addition, I found some pixels presenting significant earlier trend in end of season in Low Producing grassland in centre and east of Clutha catchment (Figure 4.7b). As the earlier end of season occurred near the irrigation regions (Figure 4.11), the anthropologic management would be the reason for the advanced end of season.

The spatial distribution of the tendencies of the growing season length in New Zealand's grasslands (Figure 4.7d) was not consistent with any single climate factor, suggesting the season length was correlated with multiple climatic elements. In general, the growing season length tends to prolong in most area of the three grassland types, except the Tall Tussock grassland in south and the Low Producing grassland in east of Clutha catchment. Length of season was strongly correlated with atmospheric pressure and precipitation, and it was also sensitive to wind speed in small area of Tall Tussock grassland. This indicates the length of season in New Zealand's grasslands was more likely correlated with the climate factors which affecting start of season rather than end of season.

According to my results, the peak of season was mainly related to rainfall, especially in Low Producing grassland. This phenomenon was observed in another study, showing that plentiful precipitation would be a substantial factor in delaying the growing peak in grassland ecosystems (Cleland *et al.*, 2006). The same study found the increasing temperature can lead to the earlier peak of season in grassland species. This negative relationship was also detected in this study. On the other hand, the earlier trend of peak of season was predominant during the 16 years in Clutha catchment (Figure 4.7c, 4.8), nevertheless the temperature and precipitation had not increased during the same time. Thus the shift of peak of season could be affected by other environmental elements not included in this study.

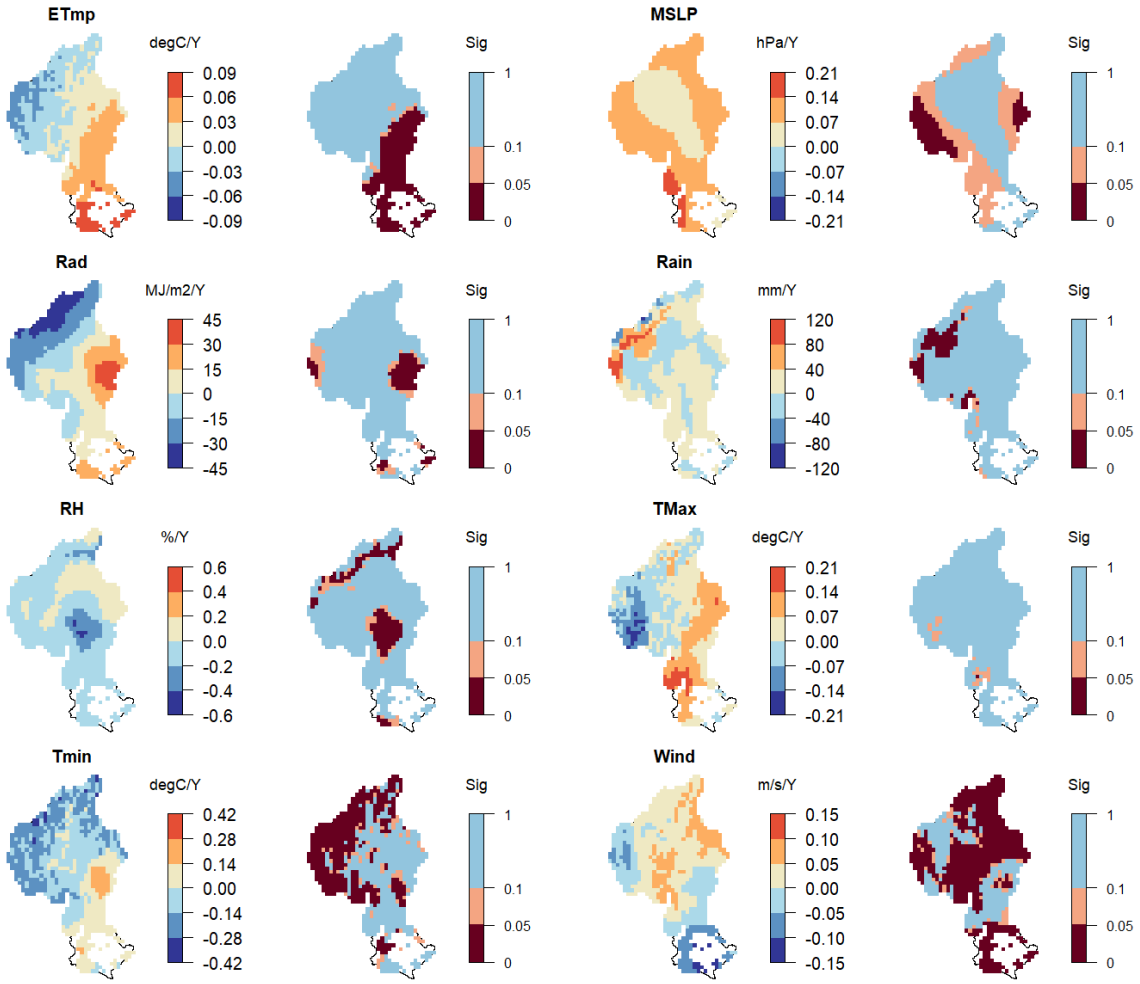

Figure 4.10 The changing trend of eight climate factors during 2001-2016
The trend (estimated slope) and significance (p-value) of climate factor changes during 2001-2016 were calculated in OLS linear model for each pixel. For each climate factor, the left panel shows the trend of how the climate factor changed annually, and the right panel shows the significance of the changing trend. Abbreviations: ETmp: 10cm earth temperature (degC /year), MSLP: mean sea level pressure (hPa/year), Rad: solar radiation (MJ/m2/year), Rain: rainfall (mm/year), RH: relative humidity (%/year), Tmax, Tmin: maximum, minimum temperature (degC/year), Wind: wind speed (m/s/year).

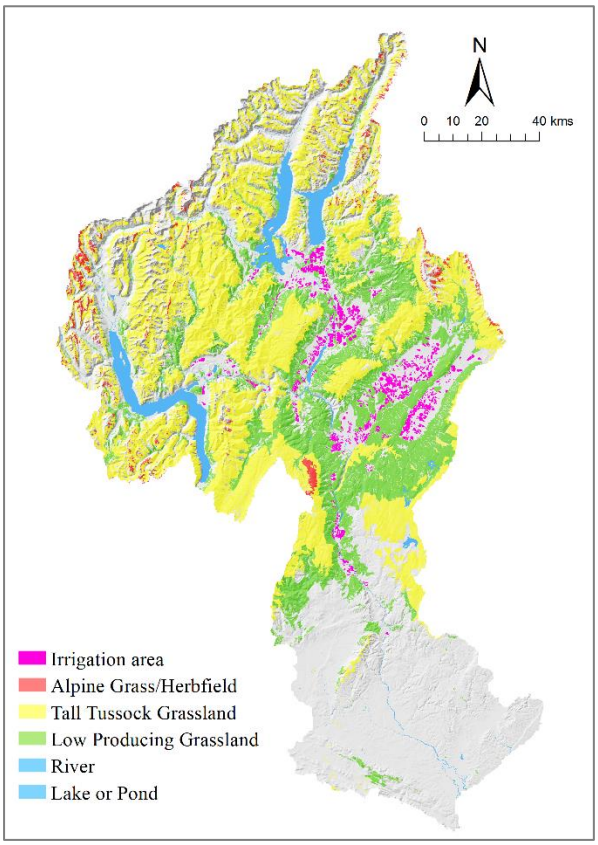

Figure 4.11 The irrigation regions in Clutha catchment
The data was obtained from Ministry for the Environment, New Zealand (https://www.mfe.govt.nz/fresh-water/freshwater-guidance-and-guidelines/irrigated-land-new-zealand).

4.4.3 Limitations in data

This study aims to focus on the phenological shifts in New Zealand's indigenous grassland ecosystems, however, there is no information of grass species discussed in this study. At landscape scale, I dealt with a large range of grassland species in each grassland type. The definitions of the three grassland types in land cover data (LCDB v4.1, see Appendix I) show that Alpine grassland (Alpine Grass/Herbfield) is comprised of herbaceous cushion, mat, turf, rosette plants and lichens with plenty of component of abiotic elements such as stones, bare lands. The Alpine type should be recognised as the habitats with low herbaceous coverage above treeline, where various taxa occur in different regions though they are classified to the same group in land cover data. There are two main sub types of Tall Tussock grassland based on definition: the indigenous snow tussock which generally happens in alpine / montane regions in South Island, and the red tussock which is usually found in lower elevations in both North Island and South Island. Due to the relatively high indigenous proportion in Tall Tussock grassland, this type is a decent representative of New Zealand's indigenous ecosystem. The Low Producing grassland, whose name

indicates it is more like a functional but not an ecological category, includes complicated components of both native and exotic species. Though some pastoral lands containing exotic species are also classified as Low Producing grassland, the indigenous short tussock in South Island is a substantial element in this type.

Remote sensing methodologies enable us to derive the growth phenology dynamics at landscape scale, which is hardly impossible to be finished by field observations. However, the ground validation is important in remote sensing studies. In this study, the five phenological indices were derived from MODIS NDVI time series without ground truthing data. In order to extract reliable seasonal signals, curve regression and raw data modification were used to eliminate noisy and erroneous grid cells. There were originally 4,837, 102,448 and 61,102 pixels in Alpine, Tall Tussock and Low Producing grassland respectively. There are 406, 2,172 and 4,639 pixels were excluded as erroneous pixels, due to failed fitness in TIMESAT software. The proportion of cleaned pixels is less than 10% in each grassland type. The rest grassland pixels can be efficient to describe the situations in these grassland ecosystems. Research showed field measurements validated the sufficiency of MODIS data in deriving accurate growth phenology in grassland (Fontana *et al.*, 2008, Ganguly *et al.*, 2010, Geng *et al.*, 2016). Thus, the phenological indices calculated in this study can be reliable even though lack of ground validation.

4.5 Conclusion

Five growth phenological indices in New Zealand's indigenous grasslands were derived from a MODIS NDVI time series for the time period 2001-2016. The start of growing season showed 7.2, 6.0 and 8.8 days earlier /decade in over 86% of Alpine, Tall Tussock and Low Producing grassland, respectively. The end of season presented 4.5 days earlier /decade in Alpine grassland, but showed less changes in Tall Tussock and Low Producing grassland. The length of growing season extended by 3.2 (Alpine), 5.2 (Tall tussock) and 7.1 (Low Producing) days /decade in most of these indigenous grasslands. The growing peak advanced by 6.3, 3.2 and 6.6 days /decade in three grassland types. There was a slight increasing trend of peak NDVI in Alpine and Tall Tussock grassland, while a weak decline trend of peak NDVI in Low Producing grassland. The earlier start of growing season and the less changed end of season lead to the extended growing season in all the indigenous grasslands.

The growing phenological indices were more sensitive to atmospheric pressure and precipitation than to temperature. Start of season was strongly correlated with

atmospheric pressure, and precipitation was another high-related climate factor with start of season in three grassland types. Higher precipitation delayed the end of season and peak of season in Low Producing grassland, but not in other two types. The length of season mainly responded to the changes in atmospheric pressure and rainfall in New Zealand's indigenous grasslands.

Chapter 5 Topographical effects on the timing of growing season in New Zealand's natural grasslands

Abstract

Alpine ecosystems are vulnerable to the impacts of recent anthropogenic climate change in many parts of the world. The phenology of alpine plant species is very sensitive to changes in the environment. Alpine environments are typically characterised by high topographic heterogeneity leading to a wide range of microhabitats and high microclimatic variation over small spatial scales. In order to quantify the topographical effects on the timing of plant growth in New Zealand's alpine ecosystems, a 16-year MODIS NDVI time series was used in Clutha River catchment, South Island, New Zealand. Results show that, particularly in alpine grasslands, the start of the growing season is strongly correlated with elevation, whereas the end of the growing season is strongly correlated with aspect. The start of season was delayed by 7.5, 5.1 and 3.7 days /100 m elevation increase in Alpine, Tall Tussock and Low Producing grassland, respectively. The end of season advanced by 1.7 and 1.3 days /10-degree-south on the slopes in Alpine and Tall Tussock grassland, while delayed by 0.3 days /10-degree-south in Low Producing grassland. In alpine grasslands investigated here, the start of the growing season was strongly correlated with elevation (later start with increasing elevation), while the end of the growing season was strongly correlated with aspect (later end of season on cooler, south-facing shaded slopes). This topographical effect is more pronounced above 1,300 m than at lower elevation. Elevation can explain most of the changes in the timing of growing season in non-alpine ecosystems, while both aspect and elevation are important explaining factors in alpine ecosystems. Aspect and elevation independently affect the timing of growing season in New Zealand's natural grasslands.

Key words

MODIS, NDVI, Topography, Phenology, Alpine grassland.

5.1 Introduction

Montane landscapes are characterised by high environmental heterogeneity over small spatial extent, leading to high biodiversity and high ecological significance (Dufour *et al.*, 2006, Opedal *et al.*, 2015). Mountain and alpine ecosystems are expected to be highly

vulnerable to the impacts of recent anthropogenic climate change in many parts of the world (Gottfried *et al.*, 2012, Rogora *et al.*, 2018). It is important to understand the response of vegetation to climate/ topography changes in mountain areas. Because of the rapid variation of topography within a small horizontal region, mountains usually exhibit high climatic heterogeneity, which offers a great opportunity to study the effects of microclimatic variation on alpine vegetation.

Research showed that topographical differences are considerable gradients affecting the growing season in alpine habitats. For example, regional difference in slope and aspect affects timing and duration of snow cover (Tennant *et al.*, 2017, Redpath *et al.*, 2018), which in turn affects timing of growth and other ecological processes in alpine vegetation. European larch (*Larix decidua*) in the Swiss Alps showed delayed needle appearance and stem growth with increasing elevation (Moser *et al.*, 2010). A shorter growing season length was found in a Colorado montane forest as elevation increased or in the north-facing (shaded) sites (Barnard *et al.*, 2017). In the Australian Alps, the start of growth season in alpine species in the recent years (2000-2014) was found to be sensitive to elevation change(Thompson and Paull, 2017). Alpine species can shift their biological timing to adapt the dramatic topographical variances in montane environment.

Climate change has two key effects on vegetation: range shifting and changes in phenology. An upward trend of plant species range shifts has been observed in many alpine or montane areas across the world and these shifts are in a direction that is congruent with the direction expected under global warming conditions (Chen *et al.*, 2011, Telwala *et al.*, 2013). Mountainous species have moved upwards over the last 100 year in response to upwards shift of analogous climate condition (Lenoir *et al.*, 2008, Scherrer and Korner, 2010). As a result, upwards shifting of alpine species may lead to these species running out of room when mountaintops are reached. However, the high topographical heterogeneity in montane landscapes might offer another option for these species: Instead of moving uphill, a sideways move to a different aspect might be possible in order to find analogous climate conditions as the climate changes (Spasojevic *et al.*, 2013, You *et al.*, 2018). A study in shaded alpine ecosystems at high elevation (1,370–1,800m elevation) in New Zealand shows the microclimate factors can shape the distribution of alpine plants which adapt to unique environmental drivers (Bickford *et al.*, 2011). Is moving up the same as moving around the mountain for alpine vegetation? To

answer this question, a good approach is to tackle the relationships between topography and plant phenology in mountain zones.

In this study, I focused on the alpine regions in New Zealand's South Island. Three main grassland types in Clutha River catchment (see Chapter 4, Section 4.2) were investigated to show how the topographic effect changes between alpine and non-alpine regions. The Alpine grassland is recognised as alpine species, while Low producing grassland is treated as non-alpine. Tall tussock grassland, which situates across wide range of elevation, is considered as the mixture of alpine and non-alpine types, where the transition at the ecotone can be investigated.

The research on alpine plants' phenology in New Zealand is comparatively rare (Mark and Dawson, 2012), partly because in situ long-term monitoring and recording of alpine species is time consuming and expensive. A 16-year MODIS NDVI time series was used in this study for growth phenology observation. I analysed the single and interaction effects of topographical factors (aspect and elevation) on the timing of growth in three types of grassland in Clutha catchment, South Island, New Zealand, to address the following questions:

1) To what degree do topographical factors (aspect and elevation) affect the timing of growth in New Zealand's alpine grasslands?

2) Are there any differences in the effects of aspect/elevation on growth phenology between alpine and non-alpine grassland ecosystems?

5.2 Methods

5.2.1 Study Area

The research area is the Clutha/Mata-Au River catchment in South Island, New Zealand, which has been referred in former chapter (Chapter 4, Section 4.1). Three main types of New Zealand's indigenous grassland, namely "Alpine Grassland", "Tall Tussock Grassland" and "Low Producing Grassland", were investigated. They are defined in the New Zealand Land Cover Database (LCDB-v4.1, 2015) (Chapter 2, Section 2.2). Alpine grassland has an average elevation of 1,574m, and 80% of this alpine ecosystem situates in the range of 1,302m-1,857m elevation. There are 6,400km^2 Tall Tussock Grassland in the northern and central parts of Clutha catchment, with the mean elevation at 1,200m. Over 80% of Tall Tussock grassland locate on the 807m - 1,600m elevation. Over half of this type

appears above the natural treeline (900m), which was defined as alpine region in South Island (Wardle, 2008). There are 3,800 km^2 Low Producing grassland in my study area with a mean elevation at 640m. Over 80% of this grassland can be found on the 338-929m elevation. This type is recognised as non-alpine regions in this study (Figure 5.1a).

5.2.2 Growth phenology and topography data

Moderate-resolution Imaging Spectroradiometer (MODIS), proven to be a promising tool to track growth phenology of alpine vegetation (Zhang *et al.*, 2003, Fontana *et al.*, 2008, Ganguly *et al.*, 2010), was used to obtain the long-term growth phenology signals. Five growth phenology indices in the three types of grassland were calculated in Chapter 4 and were reused in this study. The Normalized Difference Vegetation Index (NDVI) was derived from the near-daily MODIS dataset at 250m resolution to calculate the timing of growth season with TIMESAT software (see Section 4.2.3). Five phenological indices are Start of season (SOS, mDOY), End of season (EOS, mDOY), Length of season (LOS, Days), Peak of season (POS, mDOY) and Peak day NDVI (P-NDVI). Here I used the Modified Julian Day (mDOY) to describe phenological time point for Southern Hemisphere (mDOY was described in Chapter 2, section 2.3.).

The NZSoSDEM 15m digital elevation model (Columbus *et al.*, 2011) (Figure 5.1b) was used to extract topographic factors (aspect and elevation). This 15m DEM dataset was resampled to 250m resolution by "Mean" in ArcGIS 10.1, using the 250m NDVI as reference. I converted the original aspect to be a new variable named "southness", and used it as a variable only in linear regression modelling. To produce southness, I transformed the aspect value 181-360 into 179- 0, and kept the original aspect 0-180 unchanged. Thus, southness indicates the degree of north-facing (sunny slopes) or south-facing (shaded slopes), ranging from 0 (N) to 180 (S).

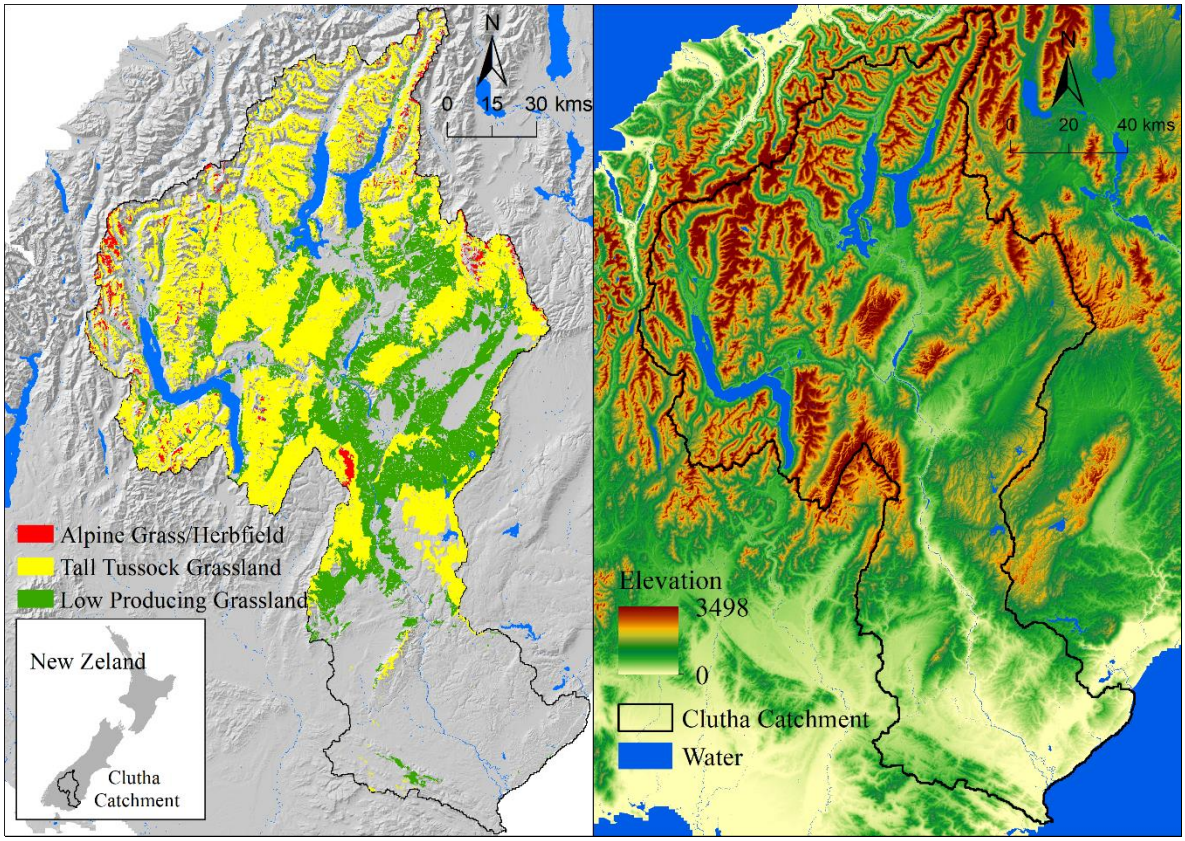

(a) (b)

Figure 5.1 The study area is the Clutha/Mata-Au river catchment
(a) Three grassland types in study area. (b) The NZSoSDEM dataset for study area.

5.2.3 Topographical effect analysis

The relationship between the five phenological indices (SOS, EOS, LOS, POS and P-NDVI) and the two topographic factors, Southness and Elevation, were analysed using linear regression analysis. Spatial autocorrelation, which generally exists in spatial samples, can compromise the statistical assumption of independence. The generalised least squares (OLS) model will be invalid if the samples are spatially auto-correlated. Therefore, I applied a Simultaneous Auto-Regressive (SAR) model (Dormann *et al.*, 2007) to exclude spatial autocorrelation effects in the parameter estimation of the relationship between phenology and topography. Three specifications of SAR model were used in this study.

The SAR-lag model:

$$Y = \rho WY + X\beta + u \quad (5.1)$$

The SAR-error model:

$$Y = X\beta + \lambda W\varepsilon + u \quad (5.2)$$

The SAR-sac/sarar model:

$$Y = \rho W1Y + X\beta + \lambda W2\varepsilon + u \quad (5.3)$$

where Y represents the vector of response variable (phenological indices), X is the matrix of predictor variables (southness and/or elevation), β is the coefficient of linear regression model, W is the spatial weights matrix, ρ is the autoregressive coefficient for spatial lagged dependent variable Y, λ is the autoregressive coefficient for spatial weighted error term, ε is a spatially dependent error term, u is a non-spatial error term. In SAR-lag model, the λ assumes to be 0, while in SAR-error model the ρ assumes to be 0. In SAR-sac/sarar model, ρ and λ are all non-zero. In formula (5.3) the W for spatial lagged item and spatial error item could be different. I set it to the same in this study.

The inverse distance weighting technique was used to generate the spatial weights matrix (W) in SAR model. All the alpine grassland pixels were considered as spatial points. A focal point's spatial proximity to other samples was described by the weights negatively associated with distance between points (Fortin, 2005). A fixed distance-based weights matrix was calculated for each pair of variables (phenology vs topography) for each year. The distance threshold was determined through a semi-variogram test (Hession and Moore, 2011). Semi-variograms demonstrate the association between the OLS model residuals and neighbourhood distances, which indicates within what distance the residuals are spatially auto-correlated. Spherical semi-variogram model were established to fit the OLS residuals, then the parameter "Range" in the model was used as the distance threshold to build the weights matrix.

The SAR model specification selection is based on Lagrange Multiplier (LM) test and followed the strategy discussed in (Elhorst, 2014). When a linear model and specific spatial weight matrix are confirmed, the spatially lagged dependence and error dependence were tested first by LMlag and LMerr statistics. If LMlag is significant ($p<0.05$) but not LMerr, the SAR-lag model is chosen, while in the opposite situation the SAR-error model is selected. If both LMlag and LMerr are significant, the robust LM tests (RLMlag, RLMerr) will be applied. Similarly, if RLMlag is much more significant than RLMerr (the statistic of RLMlag is bigger than ten times of RLMerr), the SAR-lag model is selected, and the opposite indicates SAR-error is appropriate model. When both RLMlag and RLMerr are significant and the statistics values are close, the SAR-sac/sarar model is selected.

In order to compare how good the single topographical variable and variable combinations can explain the changes in growth timing, the widely used Akaike information criterion (AIC) was calculated to assess the effectiveness of variant functions in SAR model (Maggini *et al.*, 2006, Kissling and Carl, 2008). The intercept function was used as null model, and four functions of southness and/or elevation were tested for all the five phenological indices for each year from 2001 to 2016. SAR model regression, semi-variogram, AIC calculation and Lagrange Multiplier tests were all operated with the package "spdep" in R v3.5.3.

5.3 Results

5.3.1 The relationship between aspect and phenology

The start of the growing season generally happened later on northeast- and east-facing slopes than on other aspects in three grassland types (Figure 5.2a). In Alpine grassland, the start of growing showed isotropic dispersal on aspect circle with a range of 144.3-153.7 mDOY. The growing season began later than average (149.9 mDOY) on the north- and east-facing slopes (153.2-153.7 mDOY) (Table 5.1). In Tall tussock grassland, the start of season was latest on northeast-facing hills, with about 13 days later than the earliest on southwest-facing slopes (113.6 mDOY). In Low Producing grassland, the east-facing locations had the latest start of season (100.1 mDOY), which is 6.7 days later than average in this grassland type.

The end of the growing season showed a later tendency on the north- and northeast-facing slopes in Alpine and Tall Tussock types, but on southeast-facing slopes in Low Producing grassland (Figure 5.2b). In Alpine type, the end of season happened later than average on north-facing hills, and the latest dates appeared in northeast (327.4 mDOY). Alpine grassland on northeast slopes (NE) can have approximate 30 days later to cease growth season than on the opposite direction (SW). In Tall Tussock grassland, the end of season exhibited the identical pattern as in Alpine grassland. The northeast-facing hills showed the latest end of growing (324.0 mDOY) on average, which is 22.4 days later than the earliest in southwest-facing lands, and 10 days later than the mean in this type. In contrast, Low Producing grassland showed a southeast-delay trend in the end of season. Low Producing grassland had later end of growing in south-facing locations (277.7 mDOY) than in north-facing (269.3 mDOY), which is opposite to the trend in other two grasslands.

The length of growing season exhibited a longer trend in north-facing slopes in both Alpine and Tall Tussock grasslands, however showed a shorter trend in Low Producing type (Figure 5.2c). The Alpine grassland had about a 20-day longer growing season on north-facing side (sunny) than on south-facing side (shaded). Similar pattern of length of season was also found in Tall Tussock grassland, but the north-facing sites only had 10 days longer of growing season that the south-facing places. Nevertheless, Low Producing grassland showed a reverse pattern of length of season, that the south-facing lands can have 12 days longer of growing season than in the north-facing areas.

The peak of season exhibited the identical patterns as end of season in three grassland types that later peak days appeared on the northeast-facing slopes in Alpine and Tall Tussock grasslands and in the east-facing slopes in Low Producing grassland (Figure 5.2d). In Alpine grassland, there was a 22.3-day difference between the latest peak of season in northeast-facing lands (243.7 mDOY) and the earliest in southwest-facing sites (221.4 mDOY). Similar distribution of growing peak day can be seen in Tall Tussock grassland with 19.5 days difference between the latest in northeast and earliest in southwest. In Low Producing grassland, the peak of season showed a late-to-early trend from east- to west-facing lands and there was a 10-day difference between the latest and earliest growing peaks.

The tendency of higher peak day NDVI (P-NDVI) in the east-facing slopes can be found in three grassland types (Figure 5.2e). In Alpine grassland, the high P-NDVI appeared in the east half of the aspect circle, with highest value at 0.357 in east direction. Unlike the sparkle shape in Alpine grassland, Tall Tussock grassland showed a compact shape in the aspect circle, that all high P-NDVI gathered on the east side. Nonetheless, the absolute difference is only 0.024 between the maximum (0.487 in east) and minimum (0.463 in west) in Tall Tussock grassland. In Low Producing grassland, the high P-NDVI appeared in the southeast-facing areas, with 0.029 higher than in the northwest-facing lands.

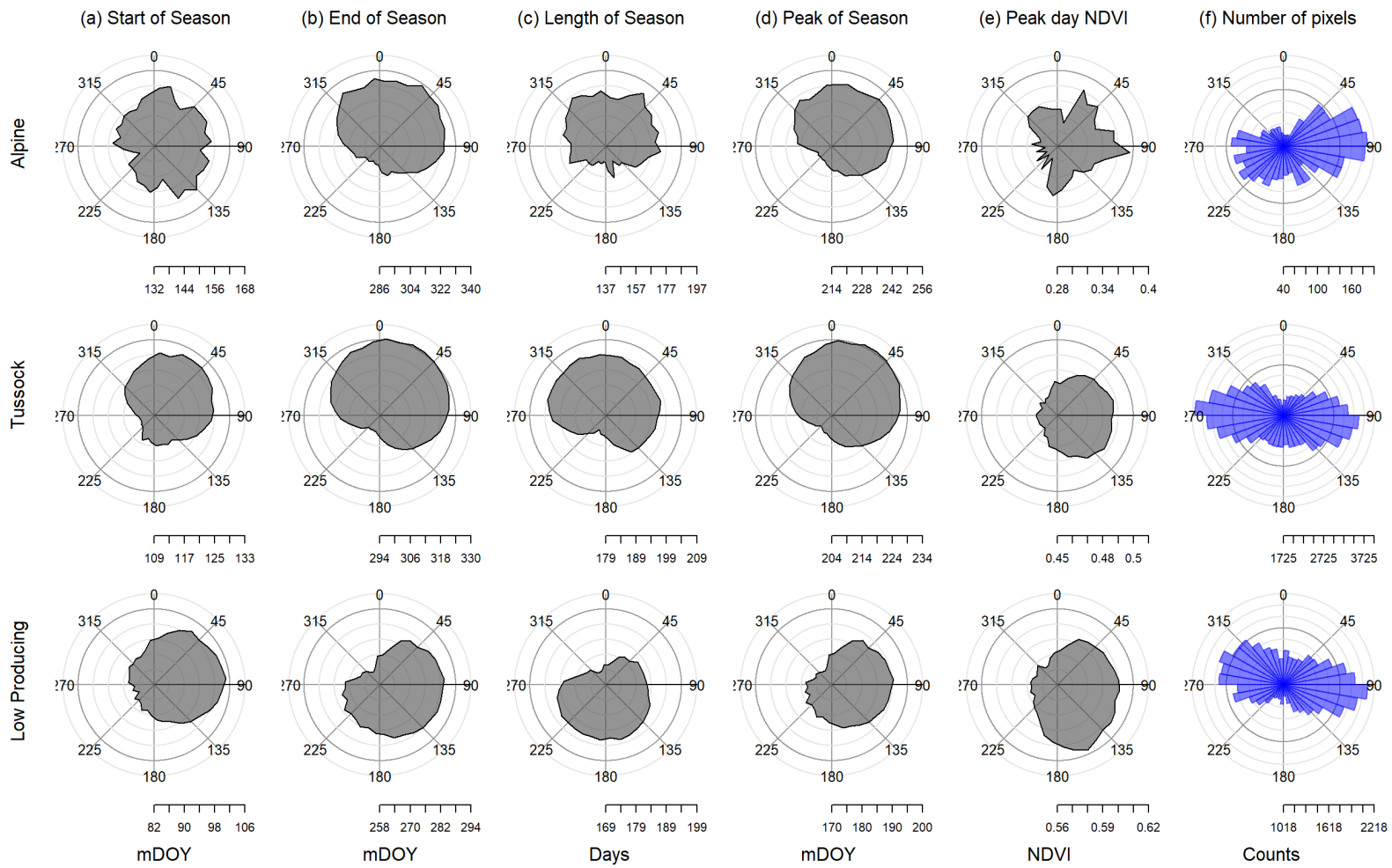

Figure 5.2 The relationship between aspect and 16-year average of growth phenological indices

Five phenological indices are plotted in aspect circles (a-e). In each aspect circle, 0 degree represents North direction, and 90 for East, 180 for South and 270 for West. The shade in each panel illustrates the distribution of 16-year average of each phenological index in each grassland type. (f) shows the counts of pixels in different directions.

Table 5.1 The 16-year average of five phenological indices on different aspects

Phenological index	Grassland type	Aspect (Deg.) and Direction								
		225 SW	270 W	315 NW	0(360) N	45 NE	90 E	135 SE	180 S	Mean of all
Start of season	Alpine	144.3	144.3	148.3	153.7	153.2	153.2	153.3	148.9	149.9
	Tall Tussock	113.6	113.8	119.3	124.4	126.5	124.0	118.8	116.4	119.4
	Low Producing	87.9	88.1	89.9	93.9	99.2	100.1	95.6	90.6	93.4
End of season	Alpine	297.5	306.1	319.6	324.6	327.4	323.7	309.5	299.6	313.6
	Tall Tussock	301.6	310.4	318.4	323.3	324.0	320.5	312.5	303.0	314.1
	Low Producing	274.5	270.9	265.4	269.3	279.9	282.8	281.8	277.7	275.3
Length of season	Alpine	153.2	161.8	171.3	170.9	174.2	170.5	156.1	150.7	163.7
	Tall Tussock	188.0	196.6	199.1	198.9	197.5	196.5	193.7	186.6	194.7
	Low Producing	186.5	182.8	175.4	175.4	180.8	182.7	186.2	187.0	181.9
Peak of season	Alpine	221.4	226.5	236.6	241.8	243.7	241.5	232.9	224.9	233.8
	Tall Tussock	209.7	215.0	222.1	227.6	229.2	225.6	218.4	211.9	219.7
	Low Producing	179.7	177.8	175.7	179.8	188.0	189.7	187.2	182.9	182.7
Peak day NDVI	Alpine	0.305	0.305	0.329	0.326	0.346	0.357	0.327	0.333	0.331
	Tall Tussock	0.464	0.463	0.463	0.472	0.483	0.487	0.485	0.473	0.474
	Low Producing	0.581	0.578	0.575	0.583	0.596	0.600	0.604	0.599	0.589

Note: The number of aspect represents the central degree of each band. Each band includes a 45-degree range around the central aspect number. For instance, North (N) means the range of 337.5-360 and 0-22.5 degree.

5.3.2 The relationship between elevation and phenology

The start of growing season in three grassland types all showed a delaying trend as elevation increases. In Alpine grassland, the changing rate of start of season was steady along elevation, at 8.5 days later per 100m higher (Figure 5.3a). The average start date of growing season in Alpine grassland ranged from 118.6 to 182.8 mDOY from low to high elevation (Table 5.2). In Tall Tussock grassland, the start of season delayed at average rate of 5.2 days per 100m higher the altitude, while the delaying rate varied in different elevations. A faster delaying rate above 1,200 m and a lower delaying rate in low elevation were found in Tall Tussock grassland (Figure 5.3a). In Low Producing grassland, the delaying rate of start of season was 3.7 days per 100m uphill on the elevation from 300 m to 1,200 m. When higher than 1,200 m the changing rate increased to 8.2 days later per 100m higher in this type. For all three grassland types, the start of growing season was more sensitive to altitudinal change above 1,300 m elevation.

The end of season in three grassland types was less sensitive to elevation variance, especially in Alpine grassland (Figure 5.3b). There was a weak delaying trend in the end of season in Alpine grassland under 1,300 m elevation, above which the end of season keeps stable at 310-320 mDOY with less change (Table 5.2). The end of season in Tall Tussock grassland above 1,300 m showed nearly no change, below this elevation a 4.9-day delay per 100 m upward was observed. In Low Producing grassland, the same inflection can also be seen at 1,300 m, above which the end of season kept steady around 320 mDOY, while under 1,300 m the end of season exhibited 5.8 days later per 100 m uphill.

The length of season was sensitive to altitudinal change in high elevations above 1,300 m, too (Figure 5.3c). The length of growing season in Alpine grassland under 1,400 m had no correlation with altitudinal change, that growing period oscillated around 190 days in these alpine habitats. A negative relation can be seen from 1,400 m to 1,900 m elevation, that the length of growth season decreased by 10.0 days per 100m uphill. Above 1,900 m the season length became stable again (Figure 5.3c). In Tall Tussock grassland, 1,400 m elevation is also an inflection. Above 1,400 m, the growing season length showed 9.4 days shorter per 100m uphill, while under this elevation it was roughly constant at 200 days. Low Producing grassland also showed a decline trend in the length of season above 1,400 m with 11.8 days shorter per 100m higher. A gradual increasing trend in the length of

season was found from 300 m to 1,300 m, at a rate of 3.5 days longer per 100m uphill. In three grassland types, the growing period showed a weak relationship with elevation at low elevation, but a strong negative correlation above 1,300 -1,400 m.

The peak of season has a negative correlation with elevation in all three grassland types (Figure 5.3d). In Alpine grassland, the season peak delays about 4.4 days per 100m higher in the elevation of 1,200 - 2,100 m. In Tall Tussock grassland, the season peak delays quicker (13.3 days per 100m uphill) in low elevation (400 -700 m) but slower above 700 m (3.5 days later per 100m higher). In Low producing grassland, the growth peak delayed by 5.3 days per 100m uphill on average.

The Peak NDVI value was negatively correlated with elevation in all grassland types (Figure 5.3e). In Alpine type, the decreasing rate of peak NDVI was -0.04/100m uphill. The rate in Tall Tussock grassland was -0.03/100m uphill. Low Producing grassland had an average rate of -0.02/100m higher the elevation. Unstable fluctuation of P-NDVI happened in low elevations in Tall Tussock and Low Producing types.

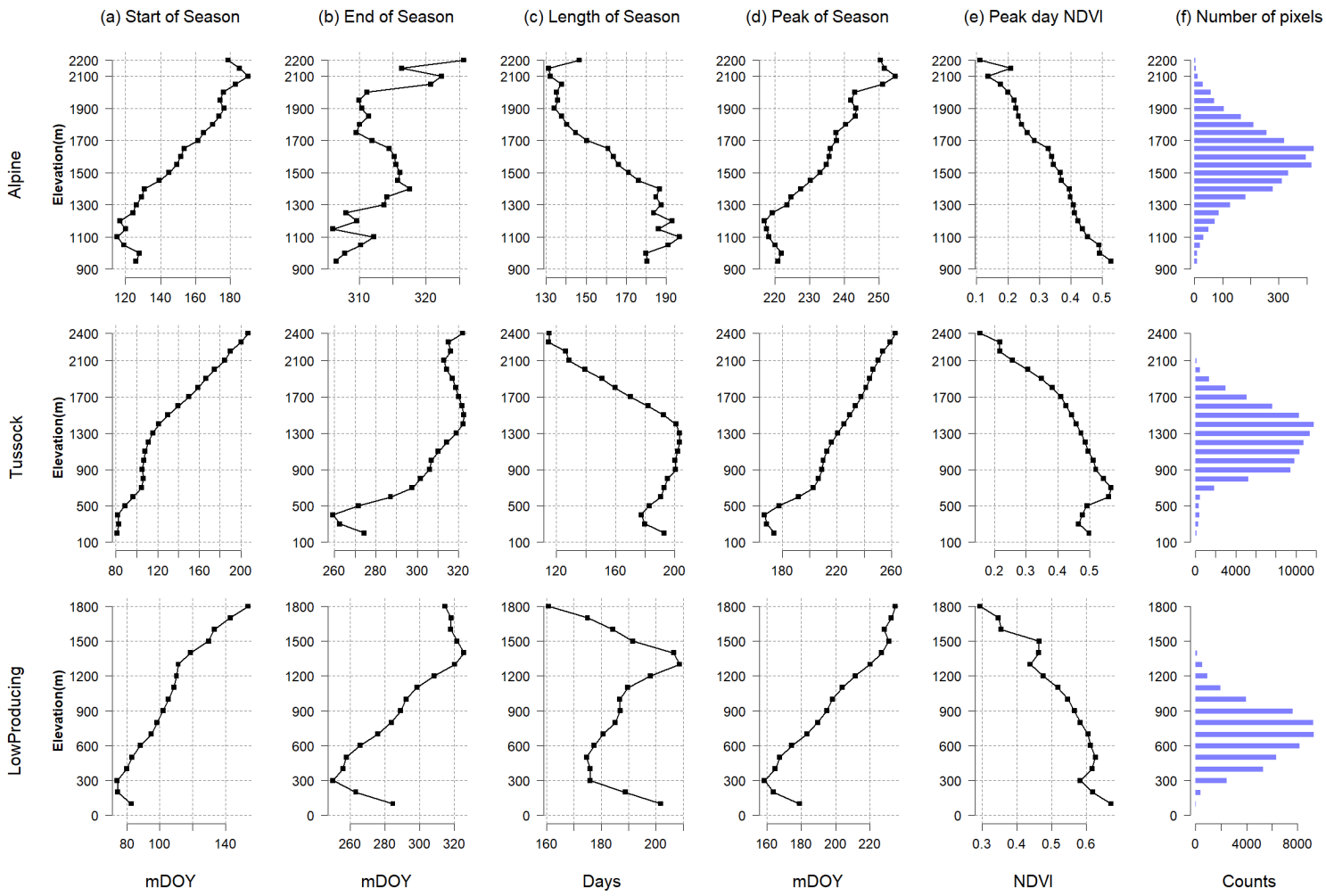

Figure 5.3 The relationship between 16-year average growth phenology and elevation

The line in each panel represents the distribution of each phenological index along elevation (y axis) for each grassland type. (f) shows the counts of grassland pixels in elevation bands.

Table 5.2 The 16-year average of five phenological indices on elevations

Phenological index	Grassland type	Elevation (m)								
		0-300	301-600	601-900	901-1200	1201-1500	1501-1800	1801-2100	2101-2400	Mean of all
Start of season	Alpine	——	——	——	118.6	135.4	156.7	175.7	182.8	149.9
	Tussock	82.3	89.5	105.5	108.6	121.9	146.6	169.2	191.5	119.4
	Low Producing	74.3	84.3	98.3	106.9	113.4	138.2	——	——	93.4
End of season	Alpine	——	——	——	308.9	315.3	313.3	311.8	319.8	313.6
	Tussock	265.6	273.8	303.7	310.6	321.2	320.6	316.2	316.4	314.1
	Low Producing	252.5	260.4	282.4	296.2	321.2	317.7	——	——	275.3
Length of season	Alpine	——	——	——	190.4	179.9	156.6	136.1	137.0	163.7
	Tussock	183.3	184.3	198.2	202.1	199.3	174.0	147.0	124.8	194.7
	Low Producing	178.1	176.2	184.1	189.2	207.7	179.4	——	——	181.9
Peak of season	Alpine	——	——	——	218.1	228.3	236.6	243.8	251.1	233.8
	Tussock	170.0	179.8	207.5	212.9	224.9	236.3	244.9	254.5	219.7
	Low Producing	159.8	169.8	189.0	201.8	221.8	230.3	——	——	182.7
Peak day NDVI	Alpine	——	——	——	0.446	0.384	0.309	0.219	0.173	0.331
	Tussock	0.474	0.514	0.533	0.497	0.458	0.412	0.333	0.215	0.474
	Low Producing	0.590	0.619	0.586	0.530	0.444	0.349	——	——	0.589

Units: Start of season (mDOY), End of season (mDOY), Length of season (days), Peak of season (mDOY), Peak day NDVI (unitless).

5.3.3 Inter-annual relationships between topography and phenology

The linear relationships derived from SAR models were summarized to quantify the effects of topography on the five phenological indices in three grassland types for each year separately (Figure 5.4, 5.5). The SAR regression estimations for each year and each grassland type can be seen in Appendix VI.

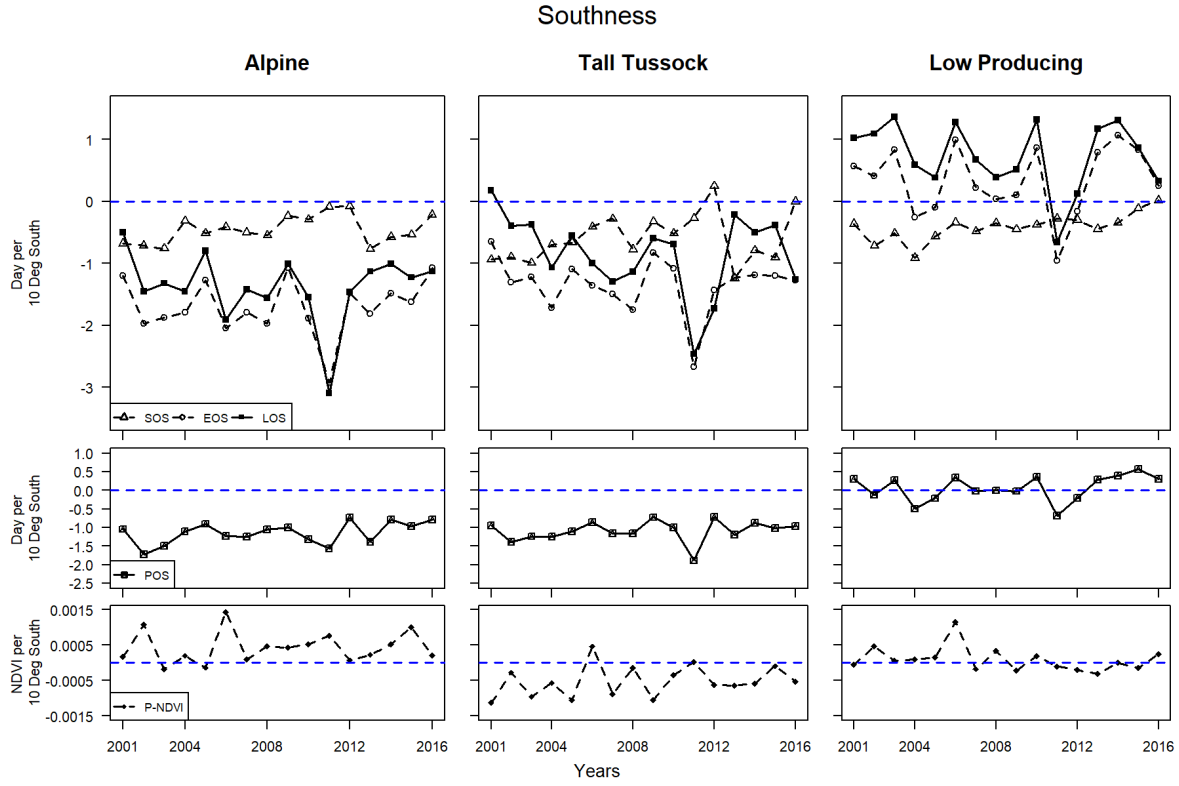

Figure 5.4 The relationship between five phenological indices and southness (aspect)
For each year, SAR regression model was built of the relationship between each phenological index and southness for each grassland type. The slopes of the fitted regression models are shown on the y axes. The lines represent the changes of correlation between phenology and southness through the 16 years. The zero dotted line in each graph indicates whether the relationship is positive (>0) or negative (<0). In each grassland column, the (a) shows the Start (SOS), End (EOS) and Length (LOS) of season together. The (b) shows the Peak of season (POS), and the (c) shows the P-NDVI.

The start of the growing season (SOS) showed a weak negative relationship with southness (aspect) in three grassland types. In Alpine grassland, the start of season exhibited a weak delaying trend with less than 1.0 days /10-degree-south change (Figure 5.4a), indicating season start advanced slightly on more shaded slopes. The analogous situation was also found in Tall Tussock and Low Producing grassland with different patterns of inter-annual oscillation.

Instead, the end of season (EOS) showed a strong negative correlation with southness in Alpine and Tall Tussock grassland, but not in Low Producing type (Figure 5.4a). In most years, the end of season occurred 1-2 days earlier per 10-degree-south in Alpine grassland, particular in year 2011 with 2.92 days earlier per 10-degree-south. Tall Tussock grassland showed the identical relation between the end of season and southness as in Alpine type, however the response of the end of season was less sensitive. A reversed relation had been observed in Low Producing grassland, that the end of season in this type showed a weak positive correlation with southness.

A negative relation between the length of growing season (LOS) and southness was found in Alpine and Tall Tussock grasslands, and a positive correlation was detected in Low Producing grassland. The inter-annual relationship of growing season length and southness was mainly corresponding to the relation of end of season and southness (Figure 5.4a), due to the strong negative correlation of end of season with southness and weak relation between the start of season and southness. The quantities of the relationship were 1.4 days shorter of the growing season per 10-degree-south on average in Alpine grassland, and 0.84 days shorter per 10-degree-south in Tall Tussock type, while 0.74 days longer the growing season per 10-degree-south in Low Producing grassland.

The response of peak of season (POS) to southness in Alpine and Tall Tussock grassland showed an advancing trend in more south-facing areas, however no obvious relationship was found in Low Producing grassland (Figure 5.4b). On average, the species reach growth peak 1.1 days earlier /10-degree-south in both Alpine and Tall Tussock grasslands. In Low Producing grassland, the line of growing peak fluctuated around zero, indicating it was inert to aspect change.

A very weak relationship between southness and peak day NDVI (PNDVI) had been observed in three grassland types, that no more than ±0.001 per 10-degree-south changes in NDVI was detected during the 16 years. In Alpine grassland, the average correlation was +0.0004 NDVI per 10-degree-south. In Tall Tussock grassland, the mean value is -0.0005 per 10-degree-south. There was hardly a relationship between P-NDVI and southness in Low Producing grassland (Figure 5.4c).

Phenological indices were more sensitive to elevation change, except the end of season (Figure 5.5). The start of season (SOS) in Alpine grassland exhibited a high correlation

with elevation that 5.5-10.3 days delay per 100m upward. In Tall Tussock grassland, a weaker delaying trend of start of season as elevation increases was found (3.8-6.3 days later per 100 m uphill). The start of season had the weakest relation with elevation in Low Producing grassland with 1.3-4.7 days delay per 100 m higher. The start of season positively responded to elevation changes in three grassland types (Figure 5.5a).

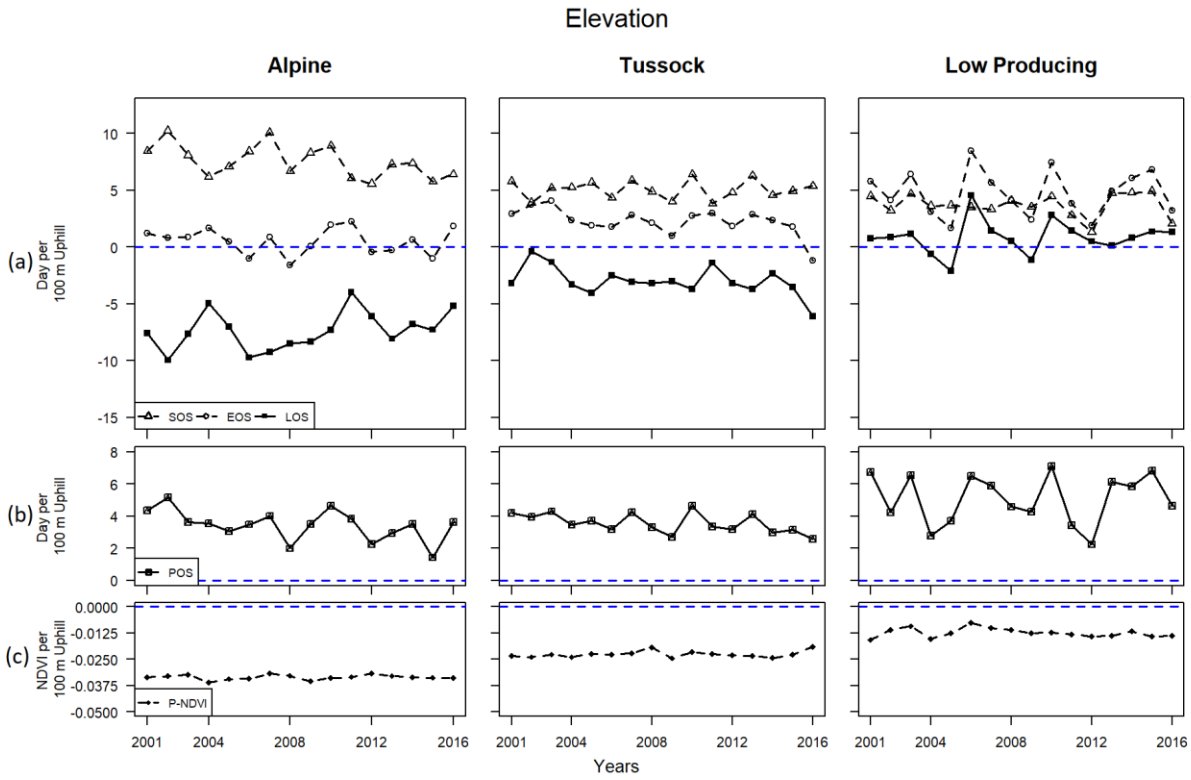

Figure 5.5 The relationship between the five phenological indices and elevation
For each year, SAR regression model was built of the relationship between each phenological index and elevation for each grassland type. The lines represent the changes of correlation between phenology and elevation through the 16 years. The zero dotted line in each graph indicates whether the relationship is positive (>0) or negative (<0). In each grassland column, the (a) shows the Start (SOS), End (EOS) and Length (LOS) of season together. The (b) shows the Peak of season (POS), and the (c) shows the P-NDVI.

The end of season (EOS) showed a weak positive relation with elevation (Figure 5.5a). In Alpine grassland, there was only 0.5 days delay in end of season per 100m higher on average, and positive and negative responses were observed. A more noticeable positive correlation can be seen in Tall Tussock grassland, showing that 1.0-4.0 days delay of end of season per 100 m uphill. The end of season in Low Producing grassland was more sensitive to elevation, exhibiting a 4.7-day delay per 100 m higher on average.

The length of growing season showed a negative relationship with elevation in high elevation, but an insignificant relation in low elevation. In Alpine grassland, the length of

season (LOS) mirrored the response of start of season to elevation (Figure 5.5a) but on a negative way, with 4.0-10.0 days shorter of growing period per 100 m uphill. The growing season length shortened by 3.0 days per 100 m higher in Tall Tussock grassland. But there was hardly relationship between season length and elevation in Low Producing grassland.

The season peak (POS) showed a delaying tendency as elevation upward in three grassland types (Figure 5.5b). The peak of season in Alpine grassland was expected to be 3.4 days later per 100 m uphill on average of the 16 years. The growth peak in Tall Tussock grassland delayed by 3.6 days per 100m higher, and peak of season showed the same inter-annual pattern of start of season in this type. Stronger response of growth peak to elevation was found in Low Producing grassland with 5.1 days delay per 100m higher on average.

The constant decline trend of peak NDVI (P-NDVI) as altitude rises can be seen in three grassland types (Figure 5.5c). The lower the elevation, the weaker of the negative relation between P-NDVI and elevation. On average, 0.03 P-NDVI reduction was found per 100 m higher in Alpine grassland. The value came down to 0.02 P-NDVI reduction per 100 m uphill in Tall tussock grassland. The rate was even weaker in Low Producing type at 0.01 P-NDVI decrease per 100 m uphill on average. The correlation between P-NDVI and elevation had nearly no inter-annual variance through the 16 years.

5.3.4 Interaction effects of topography on timing of growth seasons

The contours of start of season are generally parallel with elevation in three grassland types (Figure 5.6). In the habitats under 1,400 m, including all the Low Producing grassland, half of the Tall tussock grassland and the bottom of Alpine grassland, the contours were roughly horizontal along aspect axis, but with a concave at 90 degree (east direction). This indicates the start of season is mainly correlated with elevation, the east-facing slopes on the same elevation had start of growing season later than the west-facing slopes. The tilt in contours disappeared above 1,400 m in Tall Tussock and Alpine types, where the season start was hardly correlated with aspect (Figure 5.6a).

Conversely, the end of season showed a quite different contour shape in three grassland types (Figure 5.6b). For the alpine species, namely all the Alpine grassland and the Tall Tussock type above 900m treeline, there was an “anticyclone” in the north direction at 1,400-1,500m elevation, where the end of season occurred later on north-facing slopes

at the same elevation. In the middle elevations, including the Tall Tussock grassland under 900m and the Low Producing grassland above 500m, the end of season changed only along elevation without directional variance. A depression circle in northwest appeared under 500m elevation in Low Producing grassland, indicating the northwest slopes ceased growing season earlier than other regions.

The contours of peak of season were various in three grassland types (Figure 5.6c). In Alpine grassland the season peak was strongly correlated to both aspect and elevation. In general, the peak of season in Alpine grassland exhibited a delaying trend as elevation increases. On the other hand, all the east-facing slopes reached season peak later than west-facing locations on the same altitude. The situation was simple in Tall Tussock grassland that the peak of season was mainly delayed on higher elevation in all aspects. The same correlation can also be found in Low Producing grassland above 500m. The Low Producing type below 500m showed a directional variance that the west slopes reach the growth summit earlier than the eastern regions (Figure 5.6c).

The length of season mainly became shorter as elevation rises, while the changing rate differed with aspect (Figure 5.6d). The north-facing slopes in Alpine grassland had the longest season length among all aspects above 1,200 m elevation. When under 1,200 m the west slopes showed the longest growing season in Alpine type. In Tall Tussock grassland above 1,200 m the season length decreased with elevation increase, while the growing season was a little longer on north-facing slopes. Under 1,200 m in Tall Tussock grassland the north-facing habitats tend to have the shorter season length. In Low Producing grassland there was a concave at 400 m elevation, above which the north-facing and higher elevation exhibited longer growing season, and the opposite tendency appeared below 400m.

Generally the peak NDVI (P-NDVI) decreased as elevation rises in three grassland types (Figure 5.6e). P-NDVI was strongly correlated with elevation in both alpine and non-alpine ecosystems. Above 1,000 m elevation, the P-NDVI steadily declined uphill at the same rate in all aspects. The Tall Tussock grassland under 1,000 m was expected to have a higher P-NDVI on south-facing slopes, and the same in Low Producing grassland under 800 m.

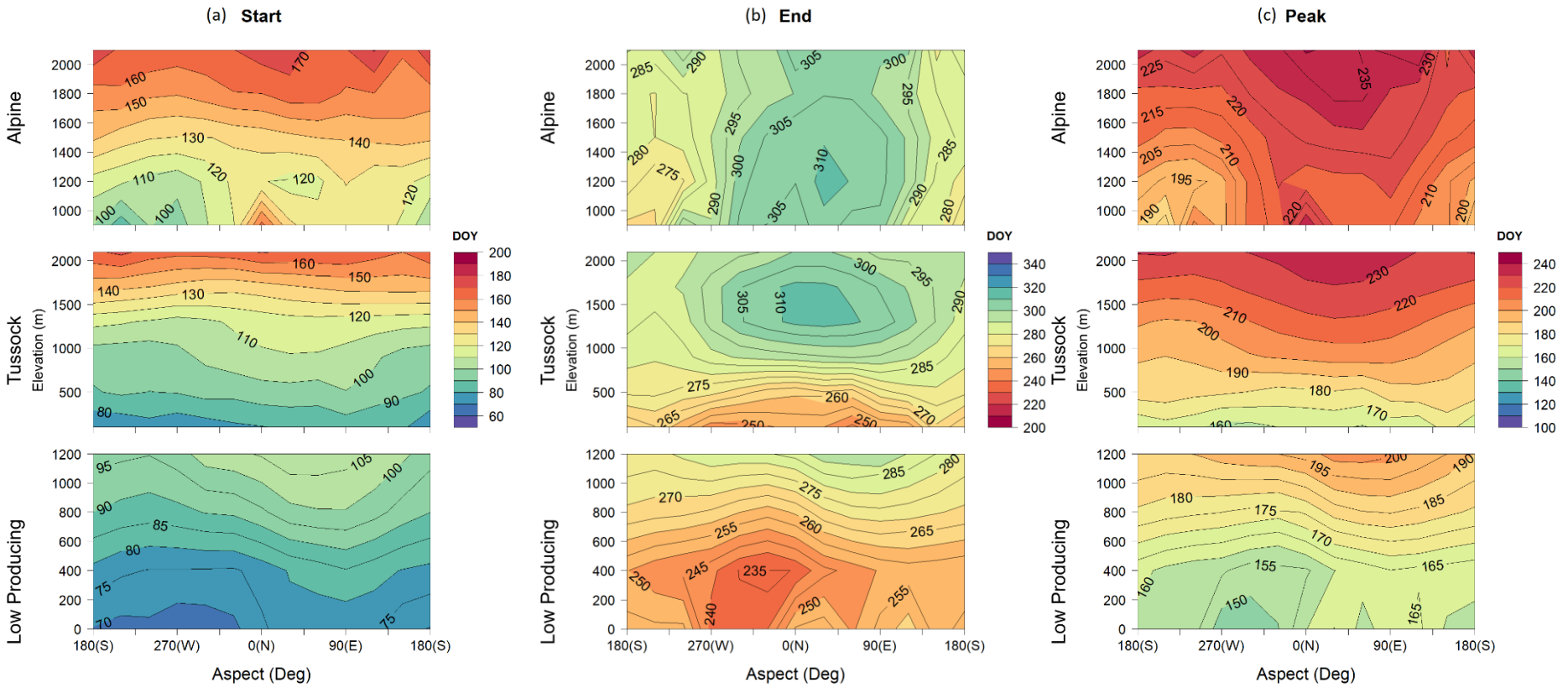
(a) Start
(b) End
(c) Peak
Alpine
Tussock
Low Producing
Elevation (m)
DOY
Aspect (Deg)
180(S)
270(W)
0(N)
90(E)
180(S)

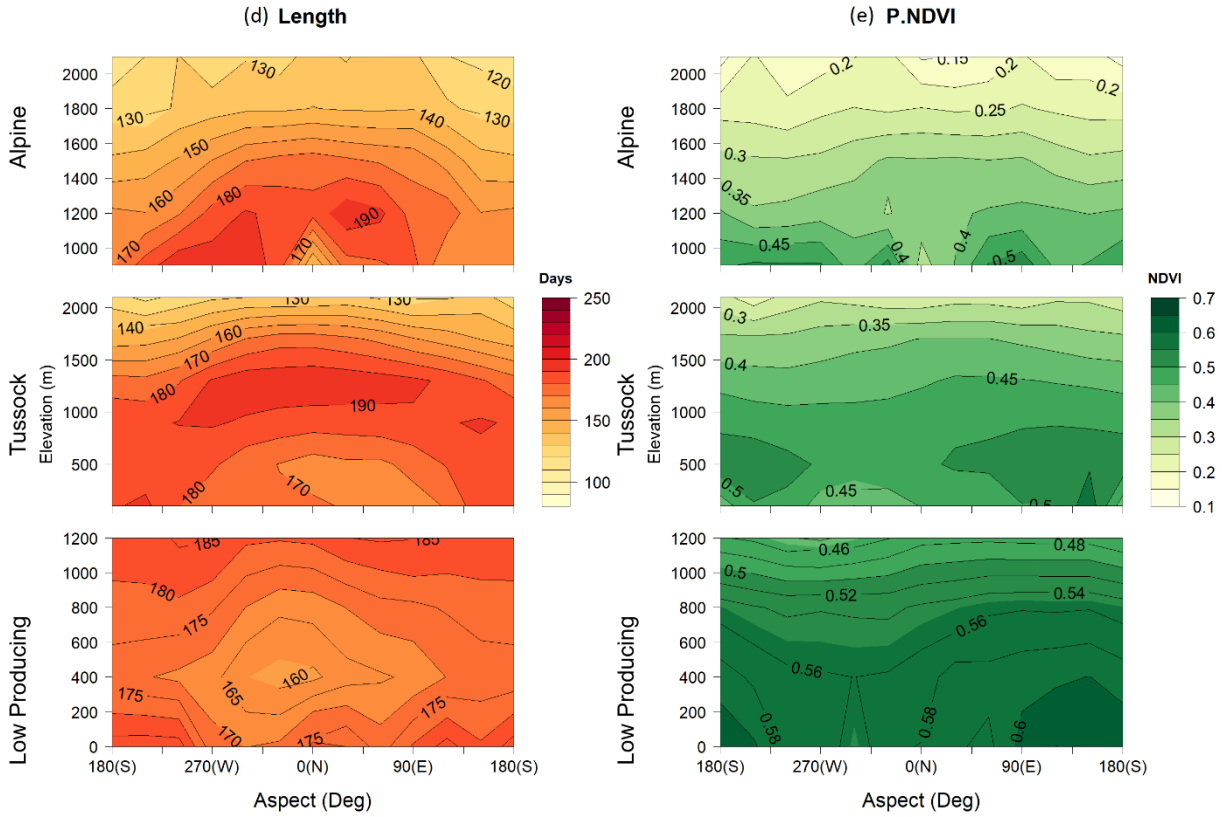

Figure 5.6 The contours of phenological indices in the aspect -elevation coordinate
Particularly on the aspect axis the 0 (North) was put in the centre, in order to facilitate the comparison between East- (right) and West- (left) facing habitats. (a-e) represent the means of Start, End, Peak, Length of season and P-NDVI, respectively.

In order to quantify the capacity of topographic factors in explaining the changes in the timing of growth season, I used the Akaike information criterion (AIC) to compare the fitness of different functions in SAR model. The intercept function (~1) was used as null hypothesis. Four functions using southness & elevation as variables were tested for each phenological index and for each year. The average of delta AIC was summarized (Table 5.3).

Table 5.3 The delta AICs for SAR models of southness and elevation to simulate five phenological indices

Four functions, including single variable, additive variables and multiplied variables were tested under null hypothesis. The higher delta AIC indicates the better capability of the function to explain the variance in phenological index.

Models	SOS		EOS		LOS		POS		PNDVI	
	Δ AIC	(%)	Δ AIC	(%)	Δ AIC	(%)	Δ AIC	(%)	Δ AIC	(%)
Alpine										
~1	0	0.00	0	0.00	0	0.00	0	0.00	0	0.00
~sou	9	0.03	697	2.01	247	0.65	435	1.35	2	0.02
~ele	1984	5.63	91	0.26	863	2.26	608	1.89	2284	27.65
~sou+ele	2016	5.72	742	2.14	1325	3.47	1034	3.22	2379	28.81
~sou*ele	2066	5.86	773	2.23	1338	3.50	1109	3.45	2393	28.97
Tall Tussock										
~1	0	0.00	0	0.00	0	0.00	0	0.00	0	0.00
~sou	78	0.18	508	1.26	169	0.38	426	1.08	7	0.07
~ele	1775	4.18	655	1.62	410	0.92	2080	5.29	2643	24.25
~sou+ele	1849	4.36	1254	3.10	605	1.36	2625	6.68	2676	24.55
~sou*ele	1943	4.58	1373	3.40	773	1.74	2653	6.75	2722	24.98
Low Producing										
~1	0	0.00	0	0.00	0	0.00	0	0.00	0	0.00
~sou	46	0.13	18	0.05	77	0.20	-28	-0.08	10	0.10
~ele	652	1.81	601	1.55	77	0.20	955	2.64	623	5.88
~sou+ele	705	1.95	633	1.63	159	0.41	975	2.70	629	5.94
~sou*ele	719	1.99	656	1.69	169	0.43	993	2.75	650	6.14

Abbreviations: SOS—Start of season, EOS—End of season, LOS—Length of season, POS—Peak of season, P-NDVI—Peak day NDVI, sou—southness, ele—elevation.

Among all the functions, the additive and interaction formula are more adequate than any single variable functions in explaining the changes in the five phenological indices. For specific phenological index in certain grassland type, one single variable function can be sufficient.

For Start of season (SOS), elevation function contributes most of the decrease in AIC, indicating the start of season can be mainly estimated by elevation (Table 5.3). The

additive (~sou+ele) and interaction (~sou*ele) functions have no obvious advantage over the single elevation function (~ele), showing the fact aspect (sou) cannot bring more information to explain the changes in start of season.

For the end of season (EOS) in Alpine grassland, aspect (sou) is a more powerful descriptive variable in SAR model. While in Low Producing grassland, elevation explained more of the changes in end of season. The delta AIC are equal in single southness and elevation functions in Tall Tussock grassland, and the two-variable functions are more adequate to illustrate the end of season. It means that the end of growing season was more correlated with aspect in alpine regions, however it was more likely be affected by elevation in non-alpine areas.

For the length of season (LOS), aspect and elevation are both substantial predictor variables. In three grassland types, the two-variable functions can explain the season length variance much better than single variable functions. In Low Producing grassland, aspect (sou) and elevation (ele) have the same importance, nevertheless the explanation of aspect became weaker in Tall Tussock and Alpine grassland. When comparing to elevation, aspect (sou) has a lower capacity to describe growing season length in alpine habitats than in non-alpine regions.

The two-variable functions can better describe season peak (POS) in Alpine grassland. The single elevation function is efficient enough to explain season peak changes in Tall Tussock grassland. The elevation is the only descriptive variable in Low Producing grassland, as the aspect function (~sou) even performs worse than null function. For the P-NDVI models, elevation is the only adequate explanatory variable in three grassland types, as the single southness functions brings nearly no delta AICs.

I noticed that for all the two-variable functions, the additive function draws analogous delta AIC as interaction function does, indicating the two topographic factors have independent correlations rather than an interaction effect with the timing of growing season.

5.4 Discussion

5.4.1 Growing phenology responses to topography in alpine ecosystems

The results showed the growth timing in New Zealand's alpine ecosystems was highly sensitive to topography, but the mechanism is far from clear. Both aspect and elevation

showed noticeable effects to phenology, but in different ways. Elevation mainly affects the start of season, while aspect mostly modifies the end of season. Lower air temperature at high altitude might be the reason for the delay in start of growing season. More exposure to sunshine and more temperature accumulation would be the rational explanation for the longer season length on north-facing slopes (Zhang *et al.*, 2004, Fontana *et al.*, 2008). However, temperature is not directly affecting the plant phenology, that complex interaction happens between the factors which limit the resources for plant growth(Jolly *et al.*, 2005). Temperature and radiation are proven to be substantial controllers for phenology, nevertheless in high elevation regions there will be more uncertainty in the effect on phenology, due to other dependent factors like water stress (Hwang *et al.*, 2011). The fact that aspect and elevation affect different phenological indices demonstrates that the alpine species are subject to different environmental restrictions at different growth stage.

Due to the diverse mountainous circumstances and species' adaptation, alpine species may not have to migrate uphill and exhaust the habitats as a consequence of contemporary climate change. The topographical heterogeneity can provide wide range of microclimatic conditions on the horizontal direction, which could produce unique ecological niches (Bickford *et al.*, 2011). Microclimate at small-scale might provide "refugia" for montane species to escape from large-scale climate change within a short migration (Opedal *et al.*, 2015). Alpine grassland's plasticity could also lessen the impacts of climate change through adjusting its phenology activities (Frei *et al.*, 2014). Thus, it is more likely to be true that most alpine species could survive under current global climate change due to high heterogeneity in montane habitats.

5.4.2 The differences in topographical effects in alpine and non-alpine ecosystems

The topographical effects on timing of growing season are quite different in alpine and non-alpine regions. The growing phenology in alpine habitats has a higher association with topographical factors, especially when the habitats situate higher than 1,200m elevation. In this study, Alpine grassland represents alpine habitats and Low producing grassland represents non-alpine ecosystems. Tall tussock grassland is a transition type, which includes both alpine and non-alpine components. The distributions of phenological indices in aspect & elevation coordinate show distinct patterns in Alpine and Low producing grassland (Fig. 5-6), and a combined pattern can be seen in Tall tussock type.

Firstly, the growing phenology in alpine habitats is more sensitive to topographical effects than non-alpine regions. The Start of season has larger changes in alpine than in non-alpine regions when elevation rises by the same height. The season end in alpine regions also shows more variations on different aspects. The similar situation can be found in Length of season and P-NDVI. The mountainous terrain, which has higher diversity of topography than the flat lowlands, provides more variance to alpine ecosystems.

Secondly, some phenological indices in non-alpine regions shows opposite response to aspect as in alpine species do. The later season end and season peak in non-alpine species are more likely to occur on the shaded slopes, and the Length of season tends to be shorter on sunny slopes. These responses are reversed in alpine species. The water deficit on the sunny (north-facing) slopes might be the reason for the less growing period of non-alpine species in the low elevations.

5.4.3 Inter-annual variation in the effect of topography on phenology

Notable inter-annual difference of topographical effects on phenology was observed in this study (Figure 5.4 and 5.5). However, there is no trend in these variations of topographical effects on the timing of growing season in both alpine and non-alpine regions. As other studies suggested (Hwang *et al.*, 2011, Zhao *et al.*, 2013), climate factors such as radiation, temperature, humidity, etc. are important factors when explaining the phenology variations in mountainous terrain. In order to quantify how the topographical effects on phenology varies with climate factors, Pearson Correlation Coefficient test was used (Table 5.4). Eight climate factors (Chapter 4, Section 4.2.2) and average of phenology indices in each year were tested with the annual topographical effects (southness effect and elevation effect).

The annual difference of topographical effects on Start of season is correlated with several climate factors and the season start time itself. In Alpine grassland, the aspect effect (southness effect) on Start of season is negatively related to precipitation, which means higher rainfall will make the aspect effect on season start weaker. Rainfall's negative correlation was also found in Tall tussock grassland, but less significant. While a significant negative correlation between aspect effect and average season start time was found in Tall tussock grassland. The earlier growing season starts, the less variance of the Start of season can be seen in different aspect. This negative correlation is even

stronger in Low producing grassland. Radiation positively influences the aspect effect on start of season in Tall tussock and Low producing grassland, indicating higher radiation makes the difference of season start on north- and south-facing slopes even bigger. For the elevation effect on Start of season, there is a weak relation in Alpine grassland, that higher minimum temperature enlarges the degree of delays in season start as elevation grows. Higher rainfall has the same influence in Low producing grassland. In Tall tussock grassland, wind speed and start of season itself have positive correlations with elevation effect, that stronger wind and later season start will enhance the delaying effect on start of season by elevation. In Tall tussock type, higher relative humidity and higher maximum temperature will reduce the delaying effect along elevation.

The inter-annual variance of topographical effects on End of season is mainly consistent with the season end time itself. In all three grassland types, aspect effect on End of season is only negatively correlated to season end itself. This suggests the later the overall season end happens in grassland, the more variance of season end can be observed on different slopes. This negative correlation gets stronger from Alpine, Tall tussock to Low producing grassland. On the other hand, the weak elevation effect on End of season will be even weaker if more precipitation and later overall season end happen in Alpine grassland. The elevation effect on season end has no correlation with any factor investigated in Tall tussock grassland. Earlier overall End of season in Low producing grassland is more likely to be affected by elevation change.

The degree of aspect effect on Length of season is mainly correlated to average season length, while the elevation effect is more corresponding to climate factors. In all three grassland types, the longer of the overall season length, the larger the difference of growing season on sunny and shaded slopes. There is a weak relationship in Tall tussock grassland that high mean sea level pressure can damp the aspect effect on season length. Elevation' effect on Length of season in Alpine grassland does not fluctuate with climate factors and overall season length. Average temperature has a weak positive correlation with the elevation effect on the growing season length in Low producing grassland. In Tall tussock grassland, higher humidity and higher maximum temperature can increase the elevation effect on shortening the season length, while high wind speed will reduce the altitudinal difference in Length of season.

Climate factors influence the aspect effect on Peak of season, but not affect the elevation effect. For Peak of season in Alpine grassland, high humidity may lead to weaker delaying trend of season peak on the north-facing hills. In Tall tussock grassland, precipitation has the same influence. Rainfall's weakening influence to aspect effect in Low producing grassland is more significant. The earlier average season peak in Low producing type can dramatically weaken the aspect effect. In Alpine grassland, the elevation effect on season peak is not correlated to any factors studied here. The elevation effects in Tall tussock and Low producing grassland are affected by average season peak only.

As there is hardly aspect effect on Peak NDVI, climate influences were only found in elevation effect. In Alpine grassland, higher atmospheric pressure can enlarge the P-NDVI difference along elevation, while higher rainfall will reduce this variance. On the other hand, the alpine species with higher P-NDVI is more sensitive to elevation changes. In Tall tussock type, atmospheric pressure has the same influence to elevation effect on P-NDVI, but weaker. Meanwhile, higher humidity and higher minimum temperature can reduce the altitudinal changes in P-NDVI. In Low producing grassland, there is no correlation observed with elevation effect on P-NDVI.

Consequently, the inter-annual difference in topographical effects on phenology shows substantial correlation with climate factors, as well as phenology itself. This means the plant species not only passively adapt to the topographic microclimate, but also actively response to climate change by shifting their phenological behaviours.

Table 5.4 Pearson Correlation Coefficients between climate factors and the topographical effects on phenology

The 16-year changes of quantified topographical effects on growing season phenology (Fig. 5-4 and Fig. 5-5) were analysed with phenological trend and climate data. Grasslands: alp—Alpine grassland, tsk—Tall tussock grassland, lpg—Low producing grassland. Pheno—the value of Index itself. Climate data: ETmp—10cm earth temperature; MSLP—mean sea level pressure; Rad—solar radiation; Rain—rainfall; RH—relative humidity; Tmax, Tmin— maximum and minimum temperatures; Wind—wind speed. (climate data reused from Chapter 4)

Effect	Index	Grassland	Pheno	ETmp	MSLP	Rad	Rain	RH	TMax	Tmin	Wind
Southness effect	Start of season	alp	-0.37	-0.31	0.27	0.41	**-0.53***	-0.19	0.33	-0.27	0.32
		tsk	**-0.57***	-0.28	0.28	**0.44.**	**-0.46.**	-0.33	0.32	-0.17	0.36
		lpg	**-0.73****	-0.06	0.31	**0.57***	-0.2	-0.31	0.04	-0.25	0.31
	End of season	alp	**-0.47.**	-0.05	-0.06	-0.2	-0.16	-0.17	0.02	-0.33	-0.26
		tsk	**-0.7****	-0.15	-0.07	-0.08	-0.33	-0.18	0.18	-0.29	-0.23
		lpg	**-0.98*****	0.13	0.01	-0.08	-0.38	-0.27	0.31	-0.14	-0.37
	Length of season	alp	**-0.69****	0.01	-0.4	-0.19	-0.06	-0.28	-0.26	-0.14	-0.17
		tsk	**-0.72****	0.11	**-0.45.**	-0.13	-0.1	-0.05	-0.03	0.08	-0.3
		lpg	**-0.93*****	0.27	-0.3	-0.15	-0.3	-0.14	0.1	0.01	-0.1
	Peak of season	alp	-0.25	-0.32	-0.18	-0.29	-0.22	**-0.44.**	-0.24	-0.31	-0.05
		tsk	-0.41	-0.25	-0.17	-0.01	**-0.48.**	-0.25	-0.09	-0.11	0.02
		lpg	**-0.93*****	-0.02	0.09	0.21	**-0.53***	-0.34	0.14	-0.26	-0.11
	P-NDVI	alp	0.09	0.17	0.13	-0.25	-0.03	0.34	-0.02	0.29	-0.08
		tsk	0.1	0.26	0.33	-0.02	-0.16	0.15	0.23	0.1	-0.06
		lpg	-0.3	0.22	-0.16	-0.19	-0.37	0.17	0.38	0.08	-0.17

Effect	Index	Grassland	Pheno	ETmp	MSLP	Rad	Rain	RH	TMax	Tmin	Wind
Elevation effect	Start of season	alp	-0.02	0.3	0.11	-0.25	0.09	-0.21	-0.03	**0.46.**	-0.01
		tsk	**0.54***	-0.29	-0.35	0.01	0.27	**-0.62***	**-0.57***	-0.25	**0.46.**
		lpg	-0.02	0.22	-0.36	-0.4	**0.43.**	0.04	-0.26	0.15	-0.05
	End of season	alp	**0.69****	0.36	-0.23	-0.05	**0.5***	-0.15	-0.31	0.25	0.34
		tsk	-0.08	-0.22	0.11	0.31	-0.34	0.26	-0.09	0.28	-0.22
		lpg	**-0.77*****	0.28	0.04	0	-0.19	-0.28	0.19	0.12	-0.21
	Length of season	alp	0.2	0.09	-0.04	0.09	0.4	-0.11	-0.14	-0.37	0.13
		tsk	0.04	0.01	-0.08	-0.09	-0.15	**0.71****	-0.19	**0.58***	**-0.56***
		lpg	-0.31	**0.47.**	0.38	0.14	-0.39	-0.28	0.08	0.08	0.07
	Peak of season	alp	0.25	0.28	-0.15	-0.05	0.01	0.36	-0.03	0.26	0.17
		tsk	**0.49.**	-0.2	-0.04	0.34	-0.12	0.06	0.11	0.28	0.04
		lpg	**-0.78*****	-0.08	0.1	0.19	-0.32	-0.22	0.2	-0.07	-0.01
	P-NDVI	alp	**0.69****	-0.09	**0.71****	0.24	**-0.59***	-0.2	-0.04	-0.1	-0.07
		tsk	-0.31	0.2	**0.49.**	0.38	-0.13	**-0.56***	0.25	**-0.6***	0.32
		lpg	-0.04	0.05	0.09	-0.25	-0.21	0.23	0.39	0.03	-0.1

Significant codes (p<): "***"—0.001, "**"—0.01, "*"—0.05, "."—0.10. The correlation coefficient was bolded if p < 0.10.

5.5 Conclusion

The timing of growing season in New Zealand's natural grasslands has variant correlations with topographical factors (aspect and elevation). The start of growing season was strongly correlated with elevation, showing 7.5, 5.1 and 3.7 days delay /100m-uphill in Alpine, Tall Tussock and Low Producing grassland, respectively. The end of season advanced by 1.7 and 1.3 days /10-degree-south on the slopes in Alpine and Tall Tussock grassland, while delayed by 0.3 days /10-degree-south in Low Producing grassland. In the alpine ecosystems (Alpine grassland and the Tall Tussock grassland above treeline), elevation strongly correlates the start of season, while aspect highly affects the end of season. Consequently, the length of growing season had a strong negative relation with elevation and tended to be longer on the north-facing (sunny) slopes in alpine ecosystems. The season peak delayed as elevation rises and seemed to be earlier on shaded slopes. The higher elevation showed the lower peak NDVI in grassland. These topographical effects are more pronounced at high elevation above 1,300m.

In contrast in the non-alpine regions (Low Producing grassland and the Tall Tussock grassland in low elevations), the end of season responded less to aspect, but more delayed as elevation grows. The start of season showed a weak relationship with elevation and topography has weak effects on the length of season in non-alpine ecosystems. Less responses to topographical changes were also observed in the peak of season and peak day NDVI in non-alpine habitats.

Elevation can explain most of the changes in the timing of growing season in non-alpine ecosystems, while both aspect and elevation are important factors in explaining the changes of growth phenology in alpine ecosystems. Aspect and elevation independently affect the timing of growing season in New Zealand's natural grasslands.

Chapter 6 Conclusions

6.1 Shrub encroachment in natural grasslands

In New Zealand, like in many other parts of the world, large areas of grasslands owe their existence to anthropogenic actions, specifically the clearing of the natural woody vegetation in these areas (McGlone, 2001, McWethy *et al.*, 2009, McWethy *et al.*, 2010). This is particular true for areas below the natural tree line. Therefore, woody shrub encroachment can be seen as a return to a more natural state of these systems. However, in New Zealand, this picture is further complicated by the presence of both native and exotic shrub species with the potential to encroach into grasslands. This study highlights the high level of spatial variability in potential shrub propagule pressure of native and exotic shrub species on the three main types of indigenous grasslands in New Zealand. There is large variation in the spatial distribution of highest propagule pressure areas between different grassland types at local scale (1 km neighbourhood). In any given landscape, high native and high exotic propagule pressure do not coincide spatially at the local scale for any of the grassland types. At the regional scale (5 km neighbourhood), high native and high exotic propagule pressure showed overlapping locations, e.g., grasslands in the like Marlborough region that are under high propagule pressures from both native and exotic shrubs at this scale. The spatial scale of investigation can greatly affect the estimation of grassland areas under risk from native, exotic and combined shrub expansion. In environmental space, high native and high exotic pressure areas occur in very similar climates for Low producing grassland, but not so for Alpine and Tall tussock grassland.

The spatial pattern of high potential shrub propagule pressure is a good indicator of areas which are at risk of shrub invasion. For instance the gorse (*Ulex europeaus*) and broom (*Cytisus scoparius*) expansion was found in low elevation grass habitats (Mark *et al.*, 2013), which coincide with the high exotic pressure areas (Figure 2.4). As propagule pressure, climate preference, species traits, etc. are substantial factors in determining shrub encroachment (Dullinger *et al.*, 2003, Feng *et al.*, 2016, Giorgis *et al.*, 2016), my analysis of climate niche for native and exotic shrubs is an important step to better understand shrub impacts on grasslands. The two processes of native shrub expansion and exotic shrub invasion, which were described in former chapters as different ecological phenomena, do exhibit unlike preferences of climatic niche. Specific management and

strategy are needed when treating either type of woody encroachment into New Zealand's grassland ecosystems (Rose *et al.*, 2004, van Heezik *et al.*, 2014, Lamoureaux *et al.*, 2015).

The information of the spatial distribution and climatic niches of native/exotic shrub propagule pressure in grassland areas is a good indicator for future shrub encroachment prediction. In the study established in a tussock grassland near Arrowtown, South Island, which is anticipated to be under high shrub propagule pressure, I detected 31.60 ha of shrub cover increase in the 2,239 ha study area. During the time period of 2013-2017, the average changing rate of shrub coverage is 0.35% $year^{-1}$. The shrub expansion speed in New Zealand is moderate when comparing to other locations worldwide (O'Connor *et al.*, 2014, Berg *et al.*, 2016b, Stevens *et al.*, 2017). On the other hand, the grassland cover reduced at rate of 0.43% $year^{-1}$. The higher decrease speed of grassland maybe corresponds to the finding from other research (Van Auken, 2009) that the shrub expansion might be the result of grass retreat but not the cause. The proximity of neighboured shrub cover is highly correlated to shrub expansion rate but only above a threshold of c. 40% shrub cover in the neighbourhood of the grassland.

6.2 Phenological shift in grassland ecosystems

Five growing phenology indices in New Zealand's indigenous grasslands were investigated for the time period of 2001-2016. An overall earlier trend of start of season in three grassland types were observed, with 7.2, 6.0 and 8.8 days advanced /decade in Alpine, Tall Tussock and Low Producing grassland, respectively. The end of season advanced by 4.5 days/decade in Alpine grassland, but showed a weak trend in the other two types. The length of growing season extended by 3.2 (Alpine), 5.2 (Tall Tussock) and 7.1 (Low Producing) days/decade in most of area of the three grassland types. An advanced trend of peak of season had 6.3, 3.2 and 6.6 days earlier /decade in the three grasslands. I observed the earlier start of season, less changed end of season and extended growing season in New Zealand's indigenous grasslands, and the identical shifts of growth phenology was also found in other grasslands globally (Ma and Zhou, 2012, Chang *et al.*, 2017, Cui *et al.*, 2017, Leblans *et al.*, 2017). My results indicate the phenological shift in New Zealand's indigenous grasslands is relatively small in the past 16 years at a global scale.

The growth phenological shifts were more sensitive to atmospheric pressure and precipitation than to temperature in New Zealand. Start of season was strongly correlated with atmospheric pressure and precipitation in three grassland types. Higher

precipitation often delayed the end of season and peak of season in Low Producing grassland, but not in Alpine and Tall Tussock grasslands. The length of season was mainly correlated to atmospheric pressure and rainfall. The inconsistency of phenological shifts and climate change in this study indicates the climate factors investigated here are not sufficient to explain all the changes in growth phenology. Studies in other locations worldwide also showed the growth phenology in grassland is sensitive to the same climate factors (Cleland *et al.*, 2006, Xia and Wan, 2012, Cui *et al.*, 2017, Thompson and Paull, 2017). However, more environmental elements need to be taken into account in order to better explain the growth phenological shifts in grassland ecosystems.

6.3 The effect of topography on compositional and phenological shifts

As a considerable portion of New Zealand's grassland situate on high elevation, most of which are recognised as alpine habitats, topographical factors deeply affect the compositional and phenological shifts in these alpine ecosystems.

For compositional change, shrub expansion is mostly observed in low elevation under treeline (< 900 m) and on the north- and northeast- facing slopes. The expansion rate reaches its peak at 600m elevation and slows down as elevation rises. A weak tendency that most shrub expansion occurred on sunny slopes at low elevation was found in this study. A recent study in Otago, New Zealand also showed similar topographical effects on shrub expansion (Ropars *et al.*, 2018).

In phenological shifts, the start of season delayed by 7.5, 5.1 and 3.7 days /100 m elevation increase in Alpine, Tall Tussock and Low Producing grassland, respectively. The end of season advanced by 1.7 and 1.3 days /10-degree-south on the slopes in Alpine and Tall Tussock grassland, while delayed by 0.3 days /10-degree-south in Low Producing grassland. In alpine ecosystems, the start of growing season was driven by elevation, while the end of season was mainly determined by aspect, and this topographical effect is more pronounced at high elevation above 1,300m. The length of growing season is negatively related to elevation and it tends to be longer on the sunny (north-facing) slopes in alpine areas. In contrast, topography plays a less important role in modifying phenology in non-alpine regions. As the topographical heterogeneity can provide wide range of microclimatic conditions in alpine regions (Bickford *et al.*, 2011), the low diversity of topography in non-alpine regions might be the reason for less topographical effects on growth phenology.

6.4 Limitations and outlook

Due to the limitation of this thesis in depth and width, further research in this field is still needed. In shrub encroachment investigation, the potential shrub propagule pressure map produced in this study would only be a prediction. The native and exotic shrub expansions, which are two types of phenomena, would be treated different, and how to separate other drivers of shrub encroachment except climate is still a challenge. Further ground validation will be very helpful to improve its accuracy and to extend its utilization. Secondly, there is only one site investigated with SPOT 6/7 data to monitor the shrub expansion condition. To apply the same method in more locations would obtain more comprehensive situation of shrub encroachment in New Zealand and further develop the detection approach.

The response of growing phenology to environmental change would be more complex than described in this study. Except climate data and topographical factors, more environmental elements, such as snow coverage, fire events, irrigation, grazing management, etc. could also put into account when analysing the phenology trend. MODIS time-series is a long-term and easy-assessable dataset, with which the phenological changes in more types of ecosystems in New Zealand and globally could be compared, in order to better understand the mechanism of phenological shifts.

This thesis studied the compositional and phenological shifts in New Zealand's natural grasslands during the past 16 years. The results show for the first time the rate and spatial distribution of shrub propagule pressure and encroachment New Zealand grasslands. It showed recent shifts of growing phenology in different grassland types in alpine and non-alpine areas, and how climatic and topographical factors can act as drivers of these shifts. This work fills a gap of much needed evidence of recent responses of New Zealand's grassland ecosystems to recent environmental changes.

Acknowledgement

This thesis is sponsored by Miss E. L. Hellaby Indigenous Grasslands Research Trust.

I would like to express my deep appreciation to my dedicated supervisors, Ralf Ohlemüller and Pascal Sirguey. I sincerely thank my primary supervisor, Ralf, for his time spent on the guidance of my research in our meeting every week during three years. I would like to give gratitude to my co-supervisor, Pascal, for sharing the MODIS dataset and the instruction of remote sensing analysis.

I am really grateful to work with the people from University of Otago during my PhD study, who had inspired my research and helped me much beyond study. They are Professor Peter Holland, Professor Tony Binns, Professor Etienne Nel, Administrator Marlene Robertson, Sandra Burgess and my PhD colleagues Miki Nomura, Todd Redpath, Jerram Bateman, Sam McLachlan, etc.

At last and importantly, I should thank for my lovely family. My wife, Fengping, contributed her all to support my PhD study. I cannot finish my work without her understanding and encourage. My children, Justine and Jerry, are my angels in difficult times.

References:

Ali, I., Cawkwell, F., Dwyer, E., Barrett, B. & Green, S. 2016. Satellite remote sensing of grasslands: from observation to management–a review. *Journal of Plant Ecology*.

Allaby, M. 2012. phenology. 3 ed. ed.: Oxford University Press.

Anderson, K. 2009. Advances in Photogrammetry, Remote Sensing and Spatial Information Sciences: 2008 ISPRS Congress Book. *International Journal of Geographical Information Science,* 23**,** 685-686.

Archer, S., Schimel, D. S. & Holland, E. A. 1995. MECHANISMS OF SHRUBLAND EXPANSION - LAND-USE, CLIMATE OR CO-2. *Climatic Change,* 29**,** 91-99.

Ausseil, A.-G. E., Dymond, J. R. & Weeks, E. S. 2011. Provision of natural habitat for biodiversity: quantifying recent trends in New Zealand. *In:* VENORA, O. G. A. G. (ed.) *Biodiversity Loss in a Changing Planet.* InTech-Open Access Publisher.

Barnard, D. M., Barnard, H. R. & Molotch, N. P. 2017. Topoclimate effects on growing season length and montane conifer growth in complex terrain. *Environmental Research Letters,* 12.

Beck, P. S. A., Atzberger, C., Hogda, K. A., Johansen, B. & Skidmore, A. K. 2006. Improved monitoring of vegetation dynamics at very high latitudes: A new method using MODIS NDVI. *Remote Sensing of Environment,* 100**,** 321-334.

Bellingham, P. J. 1998. Shrub succession and invasibility in a New Zealand montane grassland. *Australian Journal of Ecology,* 23**,** 562-573.

Berg, J. A., Meyer, G. A. & Young, E. B. 2016a. Propagule pressure and environmental conditions interact to determine establishment success of an invasive plant species, glossy buckthorn (Frangula alnus), across five different wetland habitat types. *Biological Invasions,* 18**,** 1363-1373.

Berg, M. D., Wilcox, B. P., Angerer, J. P., Rhodes, E. C. & Fox, W. E. 2016b. Deciphering rangeland transformation-complex dynamics obscure interpretations of woody plant encroachment. *Landscape Ecology,* 31**,** 2433-2444.

Betancourt, J. L., Schwartz, M. D., Breshears, D. D., Cayan, D. R., Dettinger, M. D., Inouye, D. W., Post, E. & Reed, B. C. 2005. Implementing a U.S. National Phenology Network. *Eos, Transactions American Geophysical Union,* 86**,** 539-539.

Bickford, C. P., Hunt, J. E. & Heenan, P. B. 2011. Microclimate characteristics of alpine bluff ecosystems of New Zealand's South Island, and implications for plant growth. *New Zealand Journal of Ecology,* 35**,** 273-279.

Blair, J., Nippert, J. & Briggs, J. 2014. *Grassland Ecology*.

Bolton, D. K., Coops, N. C., Hermosilla, T., Wulder, M. A. & white, J. C. 2018. Evidence of vegetation greening at alpine treeline ecotones: three decades of Landsat spectral trends informed by lidar-derived vertical structure. *Environmental Research Letters,* 13.

Bradley, B. A. 2014. Remote detection of invasive plants: a review of spectral, textural and phenological approaches. *Biological Invasions,* 16**,** 1411-1425.

Bradley, B. A. & Mustard, J. F. 2006. Characterizing the landscape dynamics of an invasive plant and risk of invasion using remote sensing. *Ecological Applications,* 16**,** 1132-1147.

Brandt, J. S., Haynes, M. A., Kuemmerle, T., Waller, D. M. & Radeloff, V. C. 2013. Regime shift on the roof of the world: Alpine meadows converting to shrublands in the southern Himalayas. *Biological Conservation,* 158**,** 116-127.

Braunisch, V., Patthey, P. & Arlettaz, R. 2016. Where to Combat Shrub Encroachment in Alpine Timberline Ecosystems: Combining Remotely-Sensed Vegetation Information with Species Habitat Modelling. *Plos One,* 11.

Briggs, J. M., Knapp, A. K., Blair, J. M., Heisler, J. L., Hoch, G. A., Lett, M. S. & McCarron, J. K. 2005. An ecosystem in transition. Causes and consequences of the conversion of mesic grassland to shrubland. *Bioscience,* 55**,** 243-254.

Briggs, J. M., Schaafsma, H. & Trenkov, D. 2007. Woody vegetation expansion in a desert grassland: Prehistoric human impact? *Journal of Arid Environments,* 69**,** 458-472.

Brockerhoff, E. G., Shaw, W. B., Hock, B., Kimberley, M., Paul, T., Quinn, J. & Pawson, S. 2008. Re-examination of recent loss of indigenous cover in New Zealand and the relative contributions of different land uses. *New Zealand Journal of Ecology,* 32**,** 115-126.

Broennimann, O., Fitzpatrick, M. C., Pearman, P. B., Petitpierre, B., Pellissier, L., Yoccoz, N. G., Thuiller, W., Fortin, M. J., Randin, C., Zimmermann, N. E., Graham, C. H. & Guisan, A. 2012. Measuring ecological niche overlap from occurrence and spatial environmental data. *Global Ecology and Biogeography,* 21**,** 481-497.

Buitenwerf, R., Rose, L. & Higgins, S. I. 2015. Three decades of multi-dimensional change in global leaf phenology. *Nature Climate Change,* 5**,** 364-368.

Buitenwerf, R., Sandel, B., Normand, S., Mimet, A. & Svenning, J. C. 2018. Land surface greening suggests vigorous woody regrowth throughout European semi-natural vegetation. *Global Change Biology,* 24**,** 5789-5801.

Caracciolo, D., Istanbulluoglu, E., Noto, L. V. & Collins, S. L. 2016. Mechanisms of shrub encroachment into Northern Chihuahuan Desert grasslands and impacts of climate change investigated using a cellular automata model. *Advances in Water Resources,* 91**,** 46-62.

Chambers, L. E., Altwegg, R., Barbraud, C., Barnard, P., Beaumont, L. J., Crawford, R. J. M., Durant, J. M., Hughes, L., Keatley, M. R., Low, M., Morellato, P. C., Poloczanska, E. S., Ruoppolo, V., Vanstreels, R. E. T., Woehler, E. J. & Wolfaardt, A. C. 2013. Phenological Changes in the Southern Hemisphere. *Plos One,* 8.

Chang, J. F., Ciais, P., Viovy, N., Soussana, J. F., Klumpp, K. & Sultan, B. 2017. Future productivity and phenology changes in European grasslands for different warming levels: implications for grassland management and carbon balance. *Carbon Balance and Management,* 12.

Chazal, J. & Rounsevell, M. D. A. 2009. Land-use and climate change within assessments of biodiversity change: A review. *Global Environmental Change-Human and Policy Dimensions,* 19**,** 306-315.

Chen, I. C., Hill, J. K., Ohlemuller, R., Roy, D. B. & Thomas, C. D. 2011. Rapid Range Shifts of Species Associated with High Levels of Climate Warming. *Science,* 333**,** 1024-1026.

Chen, X. Q., An, S., Inouye, D. W. & Schwartz, M. D. 2015. Temperature and snowfall trigger alpine vegetation green-up on the world's roof. *Global Change Biology,* 21**,** 3635-3646.

Chuine, I. 2010. Why does phenology drive species distribution? *Philosophical Transactions of the Royal Society B-Biological Sciences,* 365**,** 3149-3160.

Cieraad, E., Burrows, L., Monks, A. & Walker, S. 2015. Woody native and exotic species respond differently to New Zealand dryland soil nutrient and moisture gradients. *New Zealand Journal of Ecology,* 39**,** 198-207.

Cleland, E. E., Chiariello, N. R., Loarie, S. R., Mooney, H. A. & Field, C. B. 2006. Diverse responses of phenology to global changes in a grassland ecosystem. *Proceedings of the National Academy of Sciences of the United States of America,* 103**,** 13740-13744.

Cleland, E. E., Chuine, I., Menzel, A., Mooney, H. A. & Schwartz, M. D. 2007. Shifting plant phenology in response to global change. *Trends in Ecology & Evolution,* 22**,** 357-365.

Clinton, N. E., Potter, C., Crabtree, B., Genovese, V., Gross, P. & Gong, P. 2010. Remote Sensing-Based Time-Series Analysis of Cheatgrass (Bromus tectorum L.) Phenology. *Journal of Environmental Quality,* 39**,** 955-963.

Columbus, J., Sirguey, P. & Tenzer, R. 2011. *A free, fully assessed 15-m DEM for New Zealand*.

Colunga-Garcia, M., Haack, R. A., Magarey, R. A. & Margosian, M. L. 2010. Modeling Spatial Establishment Patterns of Exotic Forest Insects in Urban Areas in Relation to Tree Cover and Propagule Pressure. *Journal of Economic Entomology,* 103**,** 108-118.

Cui, T. F., Martz, L. & Guo, X. L. 2017. Grassland Phenology Response to Drought in the Canadian Prairies. *Remote Sensing,* 9.

Day, N. J. & Buckley, H. L. 2013. Twenty-five years of plant community dynamics and invasion in New Zealand tussock grasslands. *Austral Ecology,* 38**,** 688-699.

Dierenbach, J., Badeck, F. W. & Schaber, J. 2013. The plant phenological online database (PPODB): an online database for long-term phenological data. *International Journal of Biometeorology,* 57**,** 805-812.

Ding, M. J., Zhang, Y. L., Sun, X. M., Liu, L. S., Wang, Z. F. & Bai, W. Q. 2013. Spatiotemporal variation in alpine grassland phenology in the Qinghai-Tibetan Plateau from 1999 to 2009. *Chinese Science Bulletin,* 58**,** 396-405.

Dormann, C. F., McPherson, J. M., Araujo, M. B., Bivand, R., Bolliger, J., Carl, G., Davies, R. G., Hirzel, A., Jetz, W., Kissling, W. D., Kuhn, I., Ohlemuller, R., Peres-Neto, P. R., Reineking, B., Schroder, B., Schurr, F. M. & Wilson, R. 2007. Methods to account for spatial autocorrelation in the analysis of species distributional data: a review. *Ecography,* 30**,** 609-628.

Dufour, A., Gadallah, F., Wagner, H. H., Guisan, A. & Buttler, A. 2006. Plant species richness and environmental heterogeneity in a mountain landscape: effects of variability and spatial configuration. *Ecography,* 29**,** 573-584.

Dullinger, S., Dirnbock, T. & Grabherr, G. 2003. Patterns of shrub invasion into high mountain grasslands of the Northern Calcareous Alps, Austria. *Arctic Antarctic and Alpine Research,* 35**,** 434-441.

Dymond, J. R., Shepherd, J. D., Newsome, P. F. & Belliss, S. 2017. Estimating change in areas of indigenous vegetation cover in New Zealand from the New Zealand Land Cover Database (LCDB). *New Zealand Journal of Ecology,* 41**,** 0-0.

Dymond, J. R., Shepherd, J. D., Newsome, P. F., Gapare, N., Burgess, D. W. & Watt, P. 2012. Remote sensing of land-use change for Kyoto Protocol reporting: the New Zealand case. *Environmental Science & Policy,* 16**,** 1-8.

Eldridge, D. J., Bowker, M. A., Maestre, F. T., Roger, E., Reynolds, J. F. & Whitford, W. G. 2011. Impacts of shrub encroachment on ecosystem structure and functioning: towards a global synthesis. *Ecology Letters,* 14**,** 709-722.

Elhorst, J. P. 2014. *Spatial econometrics: from cross-sectional data to spatial panels*, Springer.

Elzinga, J. A., Atlan, A., Biere, A., Gigord, L., Weis, A. E. & Bernasconi, G. 2007. Time after time: flowering phenology and biotic interactions. *Trends in Ecology & Evolution,* 22**,** 432-439.

Espie, P. R. & Barratt, B. I. P. 2006. Biodiversity of indigenous tussock grassland sites in Otago, Canterbury and the central North Island of New Zealand IV. Vegetation and the effect of disturbance by agricultural development and fire. *Journal of the Royal Society of New Zealand,* 36**,** 69-82.

Faulkner, K. T., Robertson, M. P., Rouget, M. & Wilson, J. R. U. 2014. A simple, rapid methodology for developing invasive species watch lists. *Biological Conservation,* 179**,** 25-32.

Feng, Y. H., Maurel, N., Wang, Z. H., Ning, L., Yu, F. H. & van Kleunen, M. 2016. Introduction history, climatic suitability, native range size, species traits and their interactions explain establishment of Chinese woody species in Europe. *Global Ecology and Biogeography,* 25**,** 1356-1366.

Fitter, A. H. & Fitter, R. S. R. 2002. Rapid changes in flowering time in British plants. *Science,* 296**,** 1689-1691.

Fontana, F., Rixen, C., Jonas, T., Aberegg, G. & Wunderle, S. 2008. Alpine grassland phenology as seen in AVHRR, VEGETATION, and MODIS NDVI time series - a comparison with in situ measurements. *Sensors,* 8**,** 2833-2853.

Fortin, M.-J. e. 2005. *Spatial analysis : a guide for ecologists,* New York, Cambridge University Press.

Frei, E. R., Ghazoul, J., Matter, P., Heggli, M. & Pluess, A. R. 2014. Plant population differentiation and climate change: responses of grassland species along an elevational gradient. *Global Change Biology,* 20**,** 441-455.

Froude, V. A. 2011. Wilding conifers in New Zealand: status report. *Prepared for the Ministry of Agriculture and Forestry*.

Ganguly, S., Friedl, M. A., Tan, B., Zhang, X. Y. & Verma, M. 2010. Land surface phenology from MODIS: Characterization of the Collection 5 global land cover dynamics product. *Remote Sensing of Environment,* 114**,** 1805-1816.

Gartzia, M., Alados, C. L. & Perez-Cabello, F. 2014. Assessment of the effects of biophysical and anthropogenic factors on woody plant encroachment in dense and sparse mountain grasslands based on remote sensing data. *Progress in Physical Geography,* 38**,** 201-217.

Geng, L. Y., Ma, M. G. & Wang, H. B. 2016. An Effective Compound Algorithm for Reconstructing MODIS NDVI Time Series Data and Its Validation Based on Ground Measurements. *Ieee*

Journal of Selected Topics in Applied Earth Observations and Remote Sensing, 9**,** 3588-3597.
Giera, N. & Bell, B. 2009. Economic costs of pests to New Zealand. *MAF Biosecurity New Zealand Technical Paper*.
Giorgis, M. A., Cingolani, A. M., Tecco, P. A., Cabido, M., Poca, M. & von Wehrden, H. 2016. Testing alien plant distribution and habitat invasibility in mountain ecosystems: growth form matters. *Biological Invasions,* 18**,** 2017-2028.
Gitelson, A. A., Kaufman, Y. J. & Merzlyak, M. N. 1996. Use of a green channel in remote sensing of global vegetation from EOS-MODIS. *Remote Sensing of Environment,* 58**,** 289-298.
Gitelson, A. A., Kaufman, Y. J., Stark, R. & Rundquist, D. 2002. Novel algorithms for remote estimation of vegetation fraction. *Remote Sensing of Environment,* 80**,** 76-87.
Gomez, C., White, J. C. & Wulder, M. A. 2016. Optical remotely sensed time series data for land cover classification: A review. *Isprs Journal of Photogrammetry and Remote Sensing,* 116**,** 55-72.
Gottfried, M., Pauli, H., Futschik, A., Akhalkatsi, M., Barancok, P., Alonso, J. L. B., Coldea, G., Dick, J., Erschbamer, B., Calzado, M. R. F., Kazakis, G., Krajci, J., Larsson, P., Mallaun, M., Michelsen, O., Moiseev, D., Moiseev, P., Molau, U., Merzouki, A., Nagy, L., Nakhutsrishvili, G., Pedersen, B., Pelino, G., Puscas, M., Rossi, G., Stanisci, A., Theurillat, J. P., Tomaselli, M., Villar, L., Vittoz, P., Vogiatzakis, I. & Grabherr, G. 2012. Continent-wide response of mountain vegetation to climate change. *Nature Climate Change,* 2**,** 111-115.
Grove, P. B., Mark, A. F. & Dickinson, K. J. M. 2002. Vegetation monitoring of recently protected tussock grasslands in the southern South Island, New Zealand. *Journal of the Royal Society of New Zealand,* 32**,** 379-414.
He, Y. 2014. The effect of precipitation on vegetation cover over three landscape units in a protected semi-arid grassland: Temporal dynamics and suitable climatic index. *Journal of Arid Environments,* 109**,** 74-82.
He, Y. F., D'Odorico, P. & De Wekker, S. F. J. 2015. The relative importance of climate change and shrub encroachment on nocturnal warming in the southwestern United States. *International Journal of Climatology,* 35**,** 475-480.
Hession, S. L. & Moore, N. 2011. A spatial regression analysis of the influence of topography on monthly rainfall in East Africa. *International Journal of Climatology,* 31**,** 1440-1456.
Hijmans, R. J., Cameron, S. E., Parra, J. L., Jones, P. G. & Jarvis, A. 2005. Very high resolution interpolated climate surfaces for global land areas. *International journal of climatology,* 25**,** 1965-1978.
Homolová, L., Malenovský, Z., Clevers, J. G. P. W., García-Santos, G. & Schaepman, M. E. 2013. Review of optical- based remote sensing for plant trait mapping. *Ecological complexity,* 15**,** 1-16.
Horning, N., Robinson, J. A., Sterling, E. J., Turner, W. & Spector, S. 2010. Remote sensing for ecology and conservation: a handbook of techniques. *Remote sensing for ecology and conservation: a handbook of techniques. [Techniques in ecology & conservation series.]***,** i-xxvi, 1-465.
Hua, X. & Ohlemüller, R. 2018. Geographic versus environmental space: Patterns of potential native and exotic woody propagule pressure on New Zealand's indigenous grasslands. *New Zealand Geographer*.
Huang, C.-y. & Asner, G. P. 2009. Applications of Remote Sensing to Alien Invasive Plant Studies. *Sensors,* 9**,** 4869-4889.
Hulme, P. E. 2017. Climate change and biological invasions: evidence, expectations, and response options. *Biological Reviews,* 92**,** 1297-1313.
Hwang, T., Song, C. H., Vose, J. M. & Band, L. E. 2011. Topography-mediated controls on local vegetation phenology estimated from MODIS vegetation index. *Landscape Ecology,* 26**,** 541-556.
Ide, R. & Oguma, H. 2010. Use of digital cameras for phenological observations. *Ecological Informatics,* 5**,** 339-347.
Jentsch, A., Kreyling, J., Boettcher-Treschkow, J. & Beierkuhnlein, C. 2009. Beyond gradual warming: extreme weather events alter flower phenology of European grassland and heath species. *Global Change Biology,* 15**,** 837-849.

Jeong, S.-J., Ho, C.-H., Gim, H.-J. & Brown, M. E. 2011. Phenology shifts at start vs. end of growing season in temperate vegetation over the Northern Hemisphere for the period 1982-2008. *Global Change Biology,* 17**,** 2385-2399.
Jolly, W. M., Dobbertin, M., Zimmermann, N. E. & Reichstein, M. 2005. Divergent vegetation growth responses to the 2003 heat wave in the Swiss Alps. *Geophysical Research Letters,* 32.
Jones, M. O., Jones, L. A., Kimball, J. S. & McDonald, K. C. 2011. Satellite passive microwave remote sensing for monitoring global land surface phenology. *Remote Sensing of Environment,* 115**,** 1102-1114.
Jonsson, P. & Eklundh, L. 2002. Seasonality extraction by function fitting to time-series of satellite sensor data. *Ieee Transactions on Geoscience and Remote Sensing,* 40**,** 1824-1832.
Jonsson, P. & Eklundh, L. 2004. TIMESAT - a program for analyzing time-series of satellite sensor data. *Computers & Geosciences,* 30**,** 833-845.
Kidane, Y., Stahlmann, R. & Beierkuhnlein, C. 2012. Vegetation dynamics, and land use and land cover change in the Bale Mountains, Ethiopia. *Environ Monit Assess,* 184**,** 7473-89.
Kissling, W. D. & Carl, G. 2008. Spatial autocorrelation and the selection of simultaneous autoregressive models. *Global Ecology and Biogeography,* 17**,** 59-71.
Knapp, A. K., Briggs, J. M., Collins, S. L., Archer, S. R., Bret-Harte, M. S., Ewers, B. E., Peters, D. P., Young, D. R., Shaver, G. R., Pendall, E. & Cleary, M. B. 2008. Shrub encroachment in North American grasslands: shifts in growth form dominance rapidly alters control of ecosystem carbon inputs. *Global Change Biology,* 14**,** 615-623.
Komac, B., Kefi, S., Nuche, P., Escos, J. & Alados, C. L. 2013. Modeling shrub encroachment in subalpine grasslands under different environmental and management scenarios. *Journal of Environmental Management,* 121**,** 160-169.
Korner, C. & Basler, D. 2010. Phenology Under Global Warming. *Science,* 327**,** 1461-1462.
Lamoureaux, S. L., Basse, B., Bourdot, G. W. & Saville, D. J. 2015. Comparison of management strategies for controlling Nassella trichotoma in modified tussock grasslands in New Zealand: a spatial and economic analysis. *Weed Research,* 55**,** 449-460.
Lawes, R. A. & Wallace, J. F. 2008. Monitoring an invasive perennial at the landscape scale with remote sensing. *Ecological Management & Restoration,* 9**,** 53-59.
LCDB-v4.1. 2015. *Land Cover Database version 4.1* [Online]. LRIS portal: The Land Resource Information Systems Portal and scinfo.org.nz. Available: https://lris.scinfo.org.nz/layer/423-lcdb-v41-land-cover-database-version-41-mainland-new-zealand/ [Accessed 16/06 2017].
Leblans, N. I. W., Sigurdsson, B. D., Vicca, S., Fu, Y. S., Penuelas, J. & Janssens, I. A. 2017. Phenological responses of Icelandic subarctic grasslands to short-term and long-term natural soil warming. *Global Change Biology,* 23**,** 4932-4945.
Lenoir, J., Gegout, J. C., Marquet, P. A., de Ruffray, P. & Brisse, H. 2008. A significant upward shift in plant species optimum elevation during the 20th century. *Science,* 320**,** 1768-1771.
Leong, M. & Roderick, G. K. 2015. Remote sensing captures varying temporal patterns of vegetation between human-altered and natural landscapes. *Peerj,* 3.
Li, G. Y., Jiang, G. H., Bai, J. & Jiang, C. H. 2017. Spatio-temporal variation of alpine grassland spring phenological and its response to environment factors northeastern of Qinghai-Tibetan Plateau during 2000-2016. *Arabian Journal of Geosciences,* 10.
Linkosalo, T., Hakkinen, R., Terhivuo, J., Tuomenvirta, H. & Hari, P. 2009. The time series of flowering and leaf bud burst of boreal trees (1846-2005) support the direct temperature observations of climatic warming. *Agricultural and Forest Meteorology,* 149**,** 453-461.
Llorens, L. & Penuelas, J. 2005. Experimental evidence of future drier and warmer conditions affecting flowering of two co-occurring Mediterranean shrubs. *International Journal of Plant Sciences,* 166**,** 235-245.
Lockwood, J. L., Cassey, P. & Blackburn, T. 2005. The role of propagule pressure in explaining species invasions. *Trends in Ecology & Evolution,* 20**,** 223-228.
Louhaichi, M., Borman, M. M. & Johnson, D. E. 2001. Spatially located platform and aerial photography for documentation of grazing impacts on wheat. *Geocarto International,* 16**,** 65-70.

Ma, T. & Zhou, C. G. 2012. Climate-associated changes in spring plant phenology in China. *International Journal of Biometeorology,* 56**,** 269-275.
Maggini, R., Lehmann, A., Zimmermann, N. E. & Guisan, A. 2006. Improving generalized regression analysis for the spatial prediction of forest communities. *Journal of Biogeography,* 33**,** 1729-1749.
Mander, C. J., Hay, J. R. & Powlesland, R. 1998. *Monitoring and management of kereru (Hemiphaga novaeseelandiae)*.
Mark, A. 1969. Ecology of snow tussocks in the mountain grasslands of New Zealand. *Vegetatio,* 18**,** 289-306.
Mark, A., Barratt, B., Weeks, E. & Dymond, J. 2013. Ecosystem services in New Zealand's indigenous tussock grasslands: conditions and trends. *In:* DYMOND, J. R. (ed.) *Ecosystem services in New Zealand: conditions and trends.* Lincoln, New Zealand: Manaaki Whenua Press, Landcare Research.
Mark, A. & Dawson, M. 2012. Above the treeline: A nature guide to alpine New Zealand. Craig Potton Publishing.
Mark, A. F. & Dickinson, K. J. M. 2003. Temporal responses over 30 years to removal of grazing from a mid-altitude snow tussock grassland reserve, Lammerlaw Ecological Region, New Zealand. *New Zealand Journal of Botany,* 41**,** 655-667.
Mark, A. F. & McLennan, B. 2005. The conservation status of New Zealand's indigenous grasslands. *New Zealand Journal of Botany,* 43**,** 245-270.
Mark, A. F., Michel, P., Dickinson, K. J. M. & McLennan, B. 2009. The conservation (protected area) status of New Zealand's indigenous grasslands: an update. *New Zealand Journal of Botany,* 47**,** 53-60.
Mark, A. F., Wilson, J. B. & Scott, C. 2011. Long-term retirement of New Zealand snow tussock rangeland: effects on canopy structure, hawkweed (Hieracium spp.) invasion and plant diversity. *New Zealand Journal of Botany,* 49**,** 243-262.
McGlone, M. & Walker, S. 2011. Potential effects of climate change on New Zealand's terrestrial biodiversity and policy recommendations for mitigation, adaptation and research. *Science for Conservation (Wellington),* 312**,** 1-78.
McGlone, M., Walker, S., Hay, R. & Christie, J. 2010. Climate change, natural systems and their conservation in New Zealand. *Climate change adaptation in New Zealand: Future scenarios and some sectoral perspectives***,** 82-99.
McGlone, M. S. 2001. The origin of the indigenous grasslands of southeastern South Island in relation to pre-human woody ecosystems. *New Zealand Journal of Ecology,* 25**,** 1-15.
McGlone, M. S., Perry, G. L. W., Houliston, G. J. & Connor, H. E. 2014. Fire, grazing and the evolution of New Zealand grasses. *New Zealand Journal of Ecology,* 38**,** 1-11.
McPhearson, P. T. & Wallace, O. C. 2008. Remote Sensing Applications to Biodiversity Conservation.
McWethy, D. B., Whitlock, C., Wilmshurst, J. M., McGlone, M. S., Fromont, M., Li, X., Dieffenbacher-Krall, A., Hobbs, W. O., Fritz, S. C. & Cook, E. R. 2010. Rapid landscape transformation in South Island, New Zealand, following initial Polynesian settlement. *Proceedings of the National Academy of Sciences of the United States of America,* 107**,** 21343-21348.
McWethy, D. B., Whitlock, C., Wilmshurst, J. M., McGlone, M. S. & Li, X. 2009. Rapid deforestation of South Islands, New Zealands, by early Polynesian fires. *Holocene,* 19**,** 883-897.
Menzel, A., Sparks, T. H., Estrella, N., Koch, E., Aasa, A., Ahas, R., Alm-Kubler, K., Bissolli, P., Braslavska, O., Briede, A., Chmielewski, F. M., Crepinsek, Z., Curnel, Y., Dahl, A., Defila, C., Donnelly, A., Filella, Y., Jatcza, K., Mage, F., Mestre, A., Nordli, O., Penuelas, J., Pirinen, P., Remisova, V., Scheifinger, H., Striz, M., Susnik, A., Van Vliet, A. J. H., Wielgolaski, F. E., Zach, S. & Zust, A. 2006. European phenological response to climate change matches the warming pattern. *Global Change Biology,* 12**,** 1969-1976.
Meurk, C. D., Walker, S., Gibson, R. S. & Espie, P. 2002. Changes in vegetation states in grazed and ungrazed Mackenzie Basin grasslands, New Zealand, 1990-2000. *New Zealand Journal of Ecology,* 26**,** 95-106.
MfE, S. N. 2018. New Zealand's environmental reporting series: our land 2018. *Wellington, Ministry for the Environment*.

Milbau, A., Stout, J. C., Graae, B. J. & Nijs, I. 2009. A hierarchical framework for integrating invasibility experiments incorporating different factors and spatial scales. *Biological Invasions,* 11**,** 941-950.
Miller-Rushing, A. J. & Primack, R. B. 2008. Global warming and flowering times in Thoreau's concord: A community perspective. *Ecology,* 89**,** 332-341.
Mohamed, A. H., Holechek, J. L., Bailey, D. W., Campbell, C. L. & DeMers, M. N. 2011. Mesquite encroachment impact on southern New Mexico rangelands: remote sensing and geographic information systems approach. *Journal of Applied Remote Sensing,* 5.
Morisette, J. T., Richardson, A. D., Knapp, A. K., Fisher, J. I., Graham, E. A., Abatzoglou, J., Wilson, B. E., Breshears, D. D., Henebry, G. M., Hanes, J. M. & Liang, L. 2009. Tracking the rhythm of the seasons in the face of global change: phenological research in the 21st century. *Frontiers in Ecology and the Environment,* 7**,** 253-260.
Moser, L., Fonti, P., Buntgen, U., Esper, J., Luterbacher, J., Franzen, J. & Frank, D. 2010. Timing and duration of European larch growing season along altitudinal gradients in the Swiss Alps. *Tree Physiology,* 30**,** 225-233.
Munyati, C., Shaker, P. & Phasha, M. G. 2011. Using remotely sensed imagery to monitor savanna rangeland deterioration through woody plant proliferation: a case study from communal and biodiversity conservation rangeland sites in Mokopane, South Africa. *Environmental Monitoring and Assessment,* 176**,** 293-311.
Murray, D. 1975. Regional hydrology of the Clutha River. *Journal of Hydrology (New Zealand),* 14**,** 83-98.
Naito, A. T. & Cairns, D. M. 2011. Patterns and processes of global shrub expansion. *Progress in Physical Geography,* 35**,** 423-442.
O'Connor, T. G., Puttick, J. R. & Hoffman, M. T. 2014. Bush encroachment in southern Africa: changes and causes. *African Journal of Range & Forage Science,* 31**,** 67-88.
Ogden, L. E. 2015. Plants Duke It Out in a Warming Arctic. *BioScience,* 65**,** 220-220.
Olsson, A. D., van Leeuwen, W. J. D. & Marsh, S. E. 2011. Feasibility of Invasive Grass Detection in a Desertscrub Community Using Hyperspectral Field Measurements and Landsat TM Imagery. *Remote Sensing,* 3**,** 2283-2304.
Opedal, Ø. H., Armbruster, W. S. & Graae, B. J. 2015. Linking small-scale topography with microclimate, plant species diversity and intra-specific trait variation in an alpine landscape. *Plant Ecology & Diversity,* 8**,** 305-315.
Parmesan, C. 2006. Ecological and evolutionary responses to recent climate change. *Annual Review of Ecology Evolution and Systematics,* 37**,** 637-669.
Parmesan, C. & Yohe, G. 2003. A globally coherent fingerprint of climate change impacts across natural systems. *Nature,* 421**,** 37-42.
Pauchard, A., Kueffer, C., Dietz, H., Daehler, C. C., Alexander, J., Edwards, P. J., Arevalo, J. R., Cavieres, L. A., Guisan, A., Haider, S., Jakobs, G., McDougall, K., Millar, C. I., Naylor, B. J., Parks, C. G., Rew, L. J. & Seipel, T. 2009. Ain't no mountain high enough: plant invasions reaching new elevations. *Frontiers in Ecology and the Environment,* 7**,** 479-486.
Pettorelli, N., Vik, J. O., Mysterud, A., Gaillard, J. M., Tucker, C. J. & Stenseth, N. C. 2005. Using the satellite-derived NDVI to assess ecological responses to environmental change. *Trends in Ecology & Evolution,* 20**,** 503-510.
Redpath, T. A. N., Sirguey, P. & Cullen, N. J. 2018. Repeat mapping of snow depth across an alpine catchment with RPAS photogrammetry. *Cryosphere,* 12**,** 3477-3497.
Reed, B. C., Schwartz, M. D. & Xiao, X. 2009. *Remote Sensing Phenology: Status and the Way Forward*.
Reisinger, A. J., Blair, J. M., Rice, C. W. & Dodds, W. K. 2013. Woody Vegetation Removal Stimulates Riparian and Benthic Denitrification in Tallgrass Prairie. *Ecosystems,* 16**,** 547-560.
Ren, S. L., Yi, S. H., Peichl, M. & Wang, X. Y. 2018. Diverse Responses of Vegetation Phenology to Climate Change in Different Grasslands in Inner Mongolia during 2000-2016. *Remote Sensing,* 10.
Richardson, A. D., Keenan, T. F., Migliavacca, M., Ryu, Y., Sonnentag, O. & Toomey, M. 2013. Climate change, phenology, and phenological control of vegetation feedbacks to the climate system. *Agricultural and Forest Meteorology,* 169**,** 156-173.

Richardson, D. M. & Rejmanek, M. 2011. Trees and shrubs as invasive alien species - a global review. *Diversity and Distributions,* 17**,** 788-809.
Rodder, D. & Engler, J. O. 2011. Quantitative metrics of overlaps in Grinnellian niches: advances and possible drawbacks. *Global Ecology and Biogeography,* 20**,** 915-927.
Rodrigues, A., Marcal, A. R. S. & Cunha, M. 2013. Monitoring Vegetation Dynamics Inferred by Satellite Data Using the PhenoSat Tool. *Ieee Transactions on Geoscience and Remote Sensing,* 51**,** 2096-2104.
Rogers, G. M. & Leathwick, J. R. 1994. NORTH-ISLAND SERAL TUSSOCK GRASSLANDS .2. AUTOGENIC SUCCESSION - CHANGE OF TUSSOCK GRASSLAND TO SHRUBLAND. *New Zealand Journal of Botany,* 32**,** 287-303.
Rogora, M., Frate, L., Carranza, M. L., Freppaz, M., Stanisci, A., Bertani, I., Bottarin, R., Brambilla, A., Canullo, R., Carbognani, M., Cerrato, C., Chelli, S., Cremonese, E., Cutini, M., Di Musciano, M., Erschbamer, B., Godone, D., Iocchi, M., Isabellon, M., Magnani, A., Mazzola, L., Morra di Cella, U., Pauli, H., Petey, M., Petriccione, B., Porro, F., Psenner, R., Rossetti, G., Scotti, A., Sommaruga, R., Tappeiner, U., Theurillat, J. P., Tomaselli, M., Viglietti, D., Viterbi, R., Vittoz, P., Winkler, M. & Matteucci, G. 2018. Assessment of climate change effects on mountain ecosystems through a cross-site analysis in the Alps and Apennines. *Science of The Total Environment,* 624**,** 1429-1442.
Ropars, P., Comeau, E., Lee, W. G. & Boudreau, S. 2018. Biome transition in a changing world: from indigenous grasslands to shrub-dominated communities. *New Zealand Journal of Ecology,* 42**,** 229-239.
Rose, A. B. & Frampton, C. M. 2007. Rapid short-tussock grassland decline with and without grazing, Marlborough, New Zealand. *New Zealand Journal of Ecology,* 31**,** 232-244.
Rose, A. B., Suisted, P. A. & Frampton, C. M. 2004. Recovery, invasion, and decline over 37 years in a Marlborough short-tussock grassland, New Zealand. *New Zealand Journal of Botany,* 42**,** 77-87.
Rouget, M. & Richardson, D. M. 2003. Inferring process from pattern in plant invasions: A semimechanistic model incorporating propagule pressure and environmental factors. *American Naturalist,* 162**,** 713-724.
Rouse Jr, J. W., Haas, R., Schell, J. & Deering, D. 1974. Monitoring vegetation systems in the Great Plains with ERTS.
Saintilan, N. & Rogers, K. 2015. Woody plant encroachment of grasslands: a comparison of terrestrial and wetland settings. *New Phytologist,* 205**,** 1062-1070.
Sala, O. E., Chapin, F. S., Armesto, J. J., Berlow, E., Bloomfield, J., Dirzo, R., Huber-Sanwald, E., Huenneke, L. F., Jackson, R. B., Kinzig, A., Leemans, R., Lodge, D. M., Mooney, H. A., Oesterheld, M., Poff, N. L., Sykes, M. T., Walker, B. H., Walker, M. & Wall, D. H. 2000. Biodiversity - Global biodiversity scenarios for the year 2100. *Science,* 287**,** 1770-1774.
Scherrer, D. & Korner, C. 2010. Infra-red thermometry of alpine landscapes challenges climatic warming projections. *Global Change Biology,* 16**,** 2602-2613.
Schwartz, M. 2013. Phenology An Integrative Environmental Science. *Phenology.* 2nd ed. ed. Dordrecht: Dordrecht : Springer.
Song, C.-Q., You, S.-C., Ke, L.-H., Liu, G.-H. & Zhong, X.-K. 2011. Spatio-temporal variation of vegetation phenology in the Northern Tibetan Plateau as detected by MODIS remote sensing. *Chinese Journal of Plant Ecology,* 35**,** 853-863.
Spasojevic, M. J., Bowman, W. D., Humphries, H. C., Seastedt, T. R. & Suding, K. N. 2013. Changes in alpine vegetation over 21 years: Are patterns across a heterogeneous landscape consistent with predictions? *Ecosphere,* 4.
Srinivasan, M. P. 2012. Exotic shrub invasion in a montane grassland: the role of fire as a potential restoration tool. *Biological Invasions,* 14**,** 1009-1028.
Srivastava, P. K. 2014. Remote sensing applications in environmental research. Cham : Springer.
Stevens, N., Lehmann, C. E. R., Murphy, B. P. & Durigan, G. 2017. Savanna woody encroachment is widespread across three continents. *Global Change Biology,* 23**,** 235-244.
Sun, Z., Wang, Q., Xiao, Q., Batkhishig, O. & Watanabe, M. 2015. Diverse Responses of Remotely Sensed Grassland Phenology to Interannual Climate Variability over Frozen Ground Regions in Mongolia. *Remote Sensing,* 7**,** 360-377.

Tan, B., Morisette, J. T., Wolfe, R. E., Gao, F., Ederer, G. A., Nightingale, J. & Pedelty, J. A. 2011. An Enhanced TIMESAT Algorithm for Estimating Vegetation Phenology Metrics From MODIS Data. *Ieee Journal of Selected Topics in Applied Earth Observations and Remote Sensing,* 4**,** 361-371.

Team, R. C. 2013. R: A language and environment for statistical computing.

Tecco, P. A., Pais-Bosch, A. I., Funes, G., Marcora, P. I., Zeballos, S. R., Cabido, M. & Urcelay, C. 2016. Mountain invasions on the way: are there climatic constraints for the expansion of alien woody species along an elevation gradient in Argentina? *Journal of Plant Ecology,* 9**,** 380-392.

Telwala, Y., Brook, B. W., Manish, K. & Pandit, M. K. 2013. Climate-Induced Elevational Range Shifts and Increase in Plant Species Richness in a Himalayan Biodiversity Epicentre. *Plos One,* 8.

Tennant, C. J., Harpold, A. A., Lohse, K. A., Godsey, S. E., Crosby, B. T., Larsen, L. G., Brooks, P. D., Van Kirk, R. W. & Glenn, N. F. 2017. Regional sensitivities of seasonal snowpack to elevation, aspect, and vegetation cover in western North America. *Water Resources Research,* 53**,** 6908-6926.

Testa, S., Soudani, K., Boschetti, L. & Mondino, E. B. 2018. MODIS-derived EVI, NDVI and WDRVI time series to estimate phenological metrics in French deciduous forests. *International Journal of Applied Earth Observation and Geoinformation,* 64**,** 132-144.

Thomas, S. M. & Moloney, K. A. 2013. Hierarchical factors impacting the distribution of an invasive species: landscape context and propagule pressure. *Landscape Ecology,* 28**,** 81-93.

Thomas, S. M. & Moloney, K. A. 2015. Combining the effects of surrounding land-use and propagule pressure to predict the distribution of an invasive plant. *Biological Invasions,* 17**,** 477-495.

Thompson, J. A. & Paull, D. J. 2017. Assessing spatial and temporal patterns in land surface phenology for the Australian Alps (2000–2014). *Remote Sensing of Environment,* 199**,** 1-13.

Udelhoven, T. 2011. TimeStats: A Software Tool for the Retrieval of Temporal Patterns From Global Satellite Archives. *Ieee Journal of Selected Topics in Applied Earth Observations and Remote Sensing,* 4**,** 310-317.

Van Auken, O. W. 2009. Causes and consequences of woody plant encroachment into western North American grasslands. *Journal of Environmental Management,* 90**,** 2931-2942.

van Heezik, Y. M., Freeman, C., Porter, S. & Dickinson, K. J. M. 2014. Native and exotic woody vegetation communities in domestic gardens in relation to social and environmental factors. *Ecology and Society,* 19.

Visser, M. E. & Both, C. 2005. Shifts in phenology due to global climate change: the need for a yardstick. *Proceedings of the Royal Society B-Biological Sciences,* 272**,** 2561-2569.

Vitasse, Y., Francois, C., Delpierre, N., Dufrene, E., Kremer, A., Chuine, I. & Delzon, S. 2011. Assessing the effects of climate change on the phenology of European temperate trees. *Agricultural and Forest Meteorology,* 151**,** 969-980.

Walker, S. 2000. Post-pastoral changes in composition and guilds in a semi-arid conservation area, Central Otago, New Zealand. *New Zealand Journal of Ecology,* 24**,** 123-137.

Walker, S., King, N., Monks, A., Williams, S., Burrows, L., Cieraad, E., Meurk, C., Overton, J. M., Price, R. & Smale, M. 2009. Secondary woody vegetation patterns in New Zealand's South Island dryland zone. *New Zealand Journal of Botany,* 47**,** 367-393.

Walker, S., Lee, W. G. & Rogers, G. M. 2004. The woody vegetation of Central Otago, New Zealand. *New Zealand Journal of Botany,* 42**,** 589-612.

Wang, K., Franklin, S. E., Guo, X. & Cattet, M. 2010. Remote Sensing of Ecology, Biodiversity and Conservation: A Review from the Perspective of Remote Sensing Specialists. *Sensors (Basel, Switzerland),* 10**,** 9647-9667.

Wardle, P. 1991. *Vegetation of New Zealand,* Cambridge, England, Cambridge University Press.

Wardle, P. 2008. New Zealand forest to alpine transitions in global context. *Arctic Antarctic and Alpine Research,* 40**,** 240-249.

Warren, D. L., Glor, R. E. & Turelli, M. 2008. ENVIRONMENTAL NICHE EQUIVALENCY VERSUS CONSERVATISM: QUANTITATIVE APPROACHES TO NICHE EVOLUTION. *Evolution,* 62**,** 2868-2883.

Weeks, E. S., Ausseil, A.-G. E., Shepherd, J. D. & Dymond, J. R. 2013a. Remote sensing methods to detect land-use/cover changes in New Zealand's 'indigenous' grasslands. *New Zealand Geographer,* 69**,** 1-13.

Weeks, E. S., Waker, S., Dymond, J. R., Shepherd, J. D. & Clarkson, B. D. 2013b. Patterns of past and recent conversion of indigenous grasslands in the South Island, New Zealand. *New Zealand Journal of Ecology,* 37**,** 127-138.

White, M. A., de Beurs, K. M., Didan, K., Inouye, D. W., Richardson, A. D., Jensen, O. P., O'Keefe, J., Zhang, G., Nemani, R. R., van Leeuwen, W. J. D., Brown, J. F., de Wit, A., Schaepman, M., Lin, X., Dettinger, M., Bailey, A. S., Kimball, J., Schwartz, M. D., Baldocchi, D. D., Lee, J. T. & Lauenroth, W. K. 2009. Intercomparison, interpretation, and assessment of spring phenology in North America estimated from remote sensing for 1982-2006. *Global Change Biology,* 15**,** 2335-2359.

Whittington, H. R., Tilman, D., Wragg, P. D. & Powers, J. S. 2015. Phenological responses of prairie plants vary among species and year in a three-year experimental warming study. *Ecosphere,* 6.

Wolkovich, E. M. & Cleland, E. E. 2014. Phenological niches and the future of invaded ecosystems with climate change. *Aob Plants,* 6.

Wolkovich, E. M., Davies, T. J., Schaefer, H., Cleland, E. E., Cook, B. I., Travers, S. E., Willis, C. G. & Davis, C. C. 2013. TEMPERATURE-DEPENDENT SHIFTS IN PHENOLOGY CONTRIBUTE TO THE SUCCESS OF EXOTIC SPECIES WITH CLIMATE CHANGE. *American Journal of Botany,* 100**,** 1407-1421.

Wright, K. W., Vanderbilt, K. L., Inouye, D. W., Bertelsen, C. D. & Crimmins, T. M. 2015. Turnover and reliability of flower communities in extreme environments: Insights from long-term phenology data sets. *Journal of Arid Environments,* 115**,** 27-34.

Wulder, M. A. & Franklin, S. E. 2003. *Remote sensing of forest environments : concepts and case studies,* Boston, Boston : Kluwer Academic Publishers.

Xia, J. Y. & Wan, S. Q. 2012. The Effects of Warming-Shifted Plant Phenology on Ecosystem Carbon Exchange Are Regulated by Precipitation in a Semi-Arid Grassland. *Plos One,* 7.

Xin, Q. C., Broich, M., Zhu, P. & Gong, P. 2015. Modeling grassland spring onset across the Western United States using climate variables and MODIS-derived phenology metrics. *Remote Sensing of Environment,* 161**,** 63-77.

Xu, X. M., Conrad, C. & Doktor, D. 2017. Optimising Phenological Metrics Extraction for Different Crop Types in Germany Using the Moderate Resolution Imaging Spectrometer (MODIS). *Remote Sensing,* 9.

You, J. L., Qin, X. P., Ranjitkar, S., Lougheed, S. C., Wang, M. C., Zhou, W., Ouyang, D. X., Zhou, Y., Xu, J. C., Zhang, W. J., Wang, Y. G., Yang, J. & Song, Z. P. 2018. Response to climate change of montane herbaceous plants in the genus Rhodiola predicted by ecological niche modelling. *Scientific Reports,* 8.

Young, L. M., Norton, D. A. & Lambert, M. T. 2016. One hundred years of vegetation change at Cass, eastern South Island high country. *New Zealand Journal of Ecology,* 40**,** 289-301.

Yu, L. X., Liu, T. X., Bu, K., Yan, F. Q., Yang, J. C., Chang, L. P. & Zhang, S. W. 2017. Monitoring the long term vegetation phenology change in Northeast China from 1982 to 2015. *Scientific Reports,* 7.

Zavaleta, E. S. & Kettley, L. S. 2006. Ecosystem change along a woody invasion chronosequence in a California grassland. *Journal of Arid Environments,* 66**,** 290-306.

Zhang, J. H., Yi, Q. F., Xing, F. W., Tang, C. Y., Wang, L., Ye, W., Ng, II, Chan, T. I., Chen, H. F. & Liu, D. M. 2018. Rapid Shifts of Peak Flowering Phenology in 12 Species under the Effects of Extreme Climate Events in Macao. *Scientific Reports,* 8.

Zhang, X. Y., Friedl, M. A., Schaaf, C. B. & Strahler, A. H. 2004. Climate controls on vegetation phenological patterns in northern mid- and high latitudes inferred from MODIS data. *Global Change Biology,* 10**,** 1133-1145.

Zhang, X. Y., Friedl, M. A., Schaaf, C. B., Strahler, A. H., Hodges, J. C. F., Gao, F., Reed, B. C. & Huete, A. 2003. Monitoring vegetation phenology using MODIS. *Remote Sensing of Environment,* 84**,** 471-475.

Zhao, J. J., Wang, Y. Q., Hashimoto, H., Melton, F. S., Hiatt, S. H., Zhang, H. Y. & Nemani, R. R. 2013. The Variation of Land Surface Phenology From 1982 to 2006 Along the Appalachian Trail. *Ieee Transactions on Geoscience and Remote Sensing,* 51**,** 2087-2095.

Zhou, H. K., Yao, B. Q., Xu, W. X., Ye, X., Fu, J. J., Jin, Y. X. & Zhao, X. Q. 2014. Field evidence for earlier leaf-out dates in alpine grassland on the eastern Tibetan Plateau from 1990 to 2006. *Biology Letters,* 10.

Zhu, L. K. & Meng, J. J. 2015. Determining the relative importance of climatic drivers on spring phenology in grassland ecosystems of semi-arid areas. *International Journal of Biometeorology,* 59**,** 237-248.

Appendices

Appendix I Description of selected classes in LCDB V4.1

Class Name	Definition	Reclassified
Alpine Grass/Herbfield	Typically sparse communities above the actual or theoretical treeline dominated by herbaceous cushion, mat, turf, and rosette plants and lichens. Grasses are a minor or infrequent component, whereas stones, boulders and bare rock are usually conspicuous.	Indigenous grassland
Tall Tussock Grassland	Indigenous snow tussocks in mainly alpine mountain-lands and red tussock in the central North Island and locally in poorly-drained valley floors, terraces and basins of both islands.	Indigenous grassland
Low Producing Grassland	Exotic sward grassland and indigenous short tussock grassland of poor pastoral quality reflecting lower soil fertility and extensive grazing management or non-agricultural use. Browntop, sweet vernal, danthonia, fescue and Yorkshire fog dominate, with indigenous short tussocks (hard tussock, blue tussock and silver tussock) common in the eastern South Island and locally elsewhere.	Indigenous grassland
Manuka and/or Kanuka	Scrub dominated by mānuka and/or kānuka, typically as a successional community in a reversion toward forest. Mānuka has a wider ecological tolerance and distribution than kānuka with the latter somewhat concentrated in the north with particular prominence on the volcanic soils of the central volcanic plateau.	Native shrub
Sub Alpine Shrubland	Highland scrub dominated by indigenous low-growing shrubs including species of *Hebe*, *Dracophyllum*, *Olearia*, and *Cassinia*. Predominantly occurring above the actual or theoretical treeline, this class is also recorded where temperature inversions have created cooler micro-climates at lower elevations e.g. the 'frost flats' of the central North Island.	Native shrub
Matagouri or Grey Scrub	Scrub and shrubland comprising small-leaved, often divaricating shrubs such as matagouri, *Coprosma* spp, *Muehlenbeckia* spp., *Casinnia* spp., and *Parsonsia* spp. These, from a distance, often have a grey appearance.	Native shrub
Gorse and/or Broom	Scrub communities dominated by gorse or Scotch broom generally occurring on sites of low fertility, often with a history of fire, and insufficient grazing pressure to control spread. Left undisturbed, this class can be transitional to Broadleaved Indigenous Hardwoods.	Exotic shrub
Mixed Exotic Shrubland	Communities of introduced shrubs and climbers such as boxthorn, hawthorn, elderberry, blackberry, sweet brier, buddleja, and old man's beard.	Exotic shrub

Appendix II Shrub cover change estimated by GARI and GLI

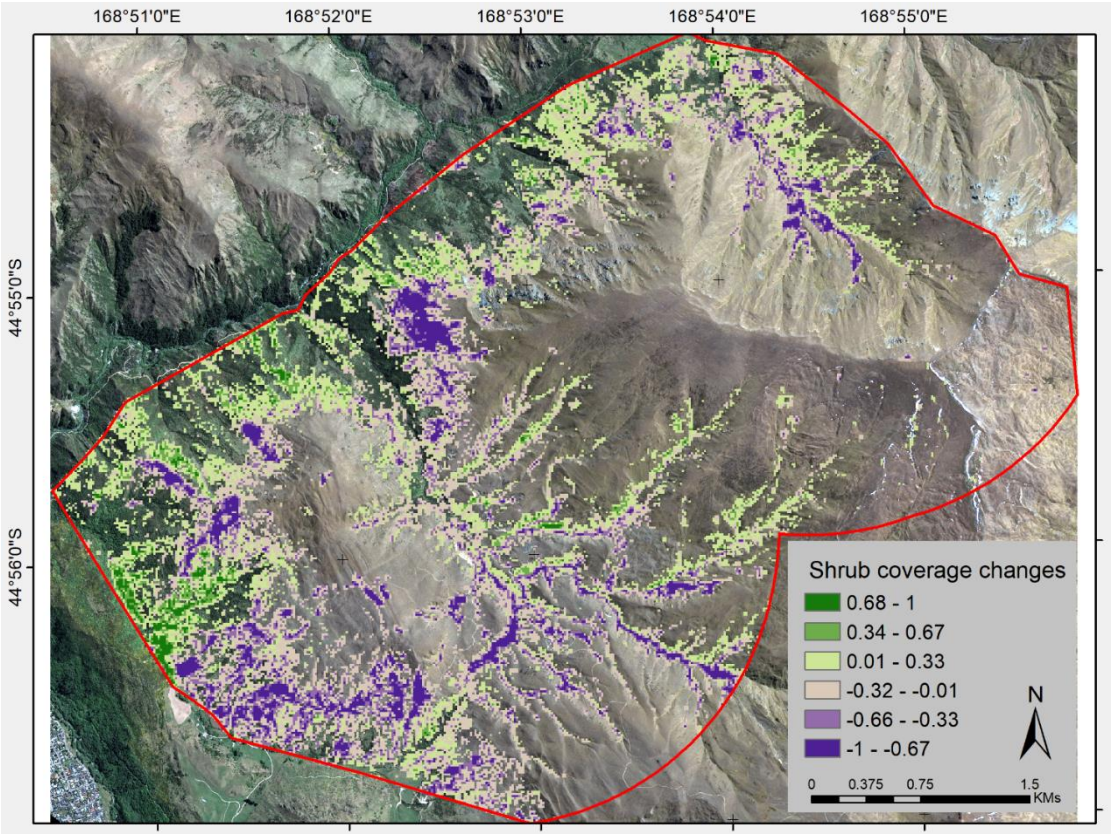

Figure a Shrub coverage change based on GARI classification

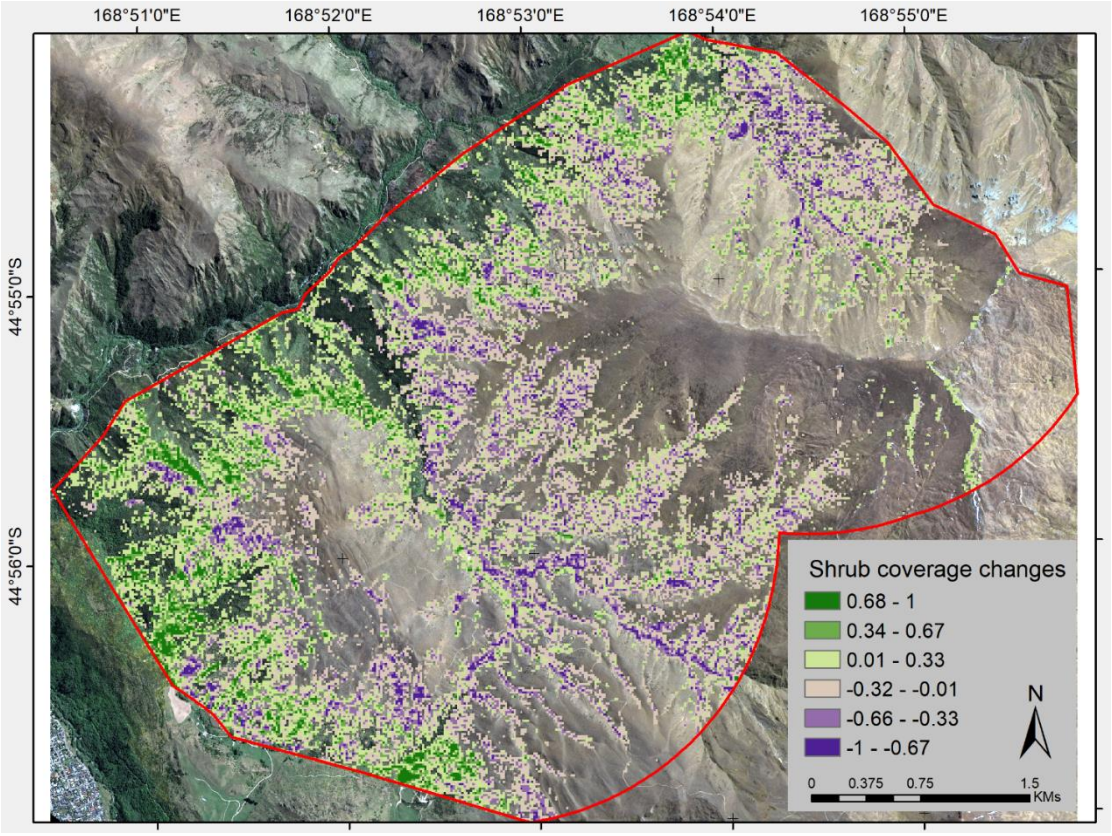

Figure b Shrub coverage change based on GLI classification

Appendix III Photos of invading shrubs in study field

Photo of invading shrubs in study area (a)

Photo of invading shrubs in study area (b)

Photo of invading shrubs in study area (c)

Appendix IV TIMESAT software ".set" file codes

```
Settings file version: 3.3
Alpine_5dayCom_50%      %Job_name (no blanks)
1           %Image /series mode (1/0)
0           %Trend (1/0)
0           %Use quality data (1/0)
D:\software\TIMESAT\timesat33\run\5dayComAlp_16y.txt  %Data file list/name
none  %Mask file list/name
3           %Image file type
0           %Byte order (1/0)
1240 800      %Image dimension (nrow ncol)
1 1240 1 800      %Processing window (start row end row start col end col)
17 73         %No. years and no. points per year
-1 1        %Valid data range (lower upper)
0 0 0      %Quality range 1 and weight
0 0 0      %Quality range 2 and weight
0 0 0      %Quality range 3 and weight
0.0          %Amplitude cutoff value
0           %Debug flag (3/2/1/0)
1 1 0         %Output files (1/0 1/0 1/0)
0           %Use land cover (1/0)
none  %Name of landcover file
1           %Spike method (3/2/1/0)
2.0          %Spike value
3.0          %STL stiffness value (1-10)
1           %No. of landcover classes
**********
1           %Land cover code for class  1
1.0          %Seasonality parameter (0-1)
2           %No. of envelope iterations (3/2/1)
3           %Adaptation strength (1-10)
0 -99999          %Force minimum (1/0) and value
2           %Fitting method (3/2/1)
1           %Weight update method
7           %Window size for Sav-Gol.
0           %Reserved
0           %Reserved
1           %Season start / end method (4/3/2/1)
0.5 0.5       %Season start / end values
```

Appendix V Pearson Correlation Coefficient of climate factors

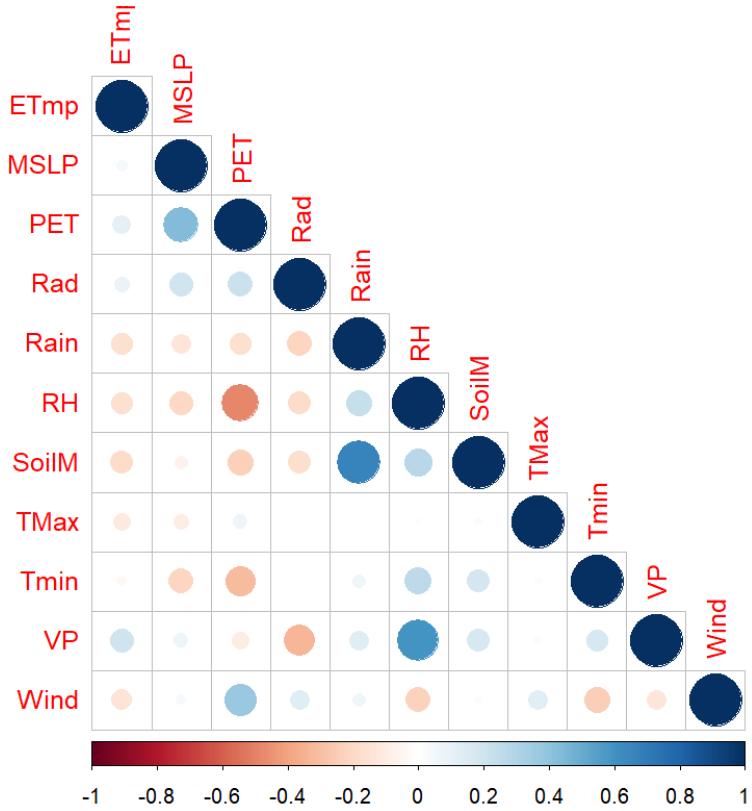

Abbreviations: Earth temperature 10cm at 9am (ETmp), mean sea level pressure (MSLP), potential evapotranspiration (PET), rainfall (Rain), relative humidity (RH), soil moisture (SoilM), , solar radiation (Rad), maximum and minimum temperatures (Tmax, Tmin), vapour pressure (VP) and wind speed (Wind).

Correlation table

	ETmp	MSLP	PET	Rad	Rain	RH	SoilM	TMax	Tmin	VP	Wind
ETmp	1	0.04	0.12	0.08	-0.17	-0.16	-0.19	-0.12	-0.04	0.2	-0.15
MSLP	0.04	1	0.43	0.2	-0.14	-0.21	-0.07	-0.09	-0.22	0.08	0.04
PET	0.12	0.43	1	0.21	-0.17	-0.49	-0.23	0.07	-0.31	-0.11	0.37
Rad	0.08	0.2	0.21	1	-0.21	-0.18	-0.18	0	0.01	-0.33	0.14
Rain	-0.17	-0.14	-0.17	-0.21	1	0.23	0.66	0.01	0.06	0.14	0.06
RH	-0.16	-0.21	-0.49	-0.18	0.23	1	0.27	-0.01	0.26	0.6	-0.22
SoilM	-0.19	-0.07	-0.23	-0.18	0.66	0.27	1	0.02	0.18	0.18	0.02
TMax	-0.12	-0.09	0.07	0	0.01	-0.01	0.02	1	-0.02	0.02	0.13
Tmin	-0.04	-0.22	-0.31	0.01	0.06	0.26	0.18	-0.02	1	0.17	-0.24
VP	0.2	0.08	-0.11	-0.33	0.14	0.6	0.18	0.02	0.17	1	-0.13
Wind	-0.15	0.04	0.37	0.14	0.06	-0.22	0.02	0.13	-0.24	-0.13	1

Note: Pearson Correlation Coefficient ranges from -1 to 1. The value closer to 1 (-1) means the higher positive (negative) correlation between two variables, while the value closer to 0 indicates weaker relationship. Soil moisture (SoilM) shows a strong correlation with rainfall (Rain). Vapour pressure (VP) is strongly related to relative humidity (RH). Potential evapotranspiration (PET) has strong correlations with RH, Wind and MSLP. So I excluded SoilM, VP and PET in analysis in Chapter 4.

Appendix VI SAR regression models

(a) Alpine grassland

index	Year	Index ~ Southness					Index ~ Elevation				
		Coefficients		logLik	Pseudo R^2	type	Coefficients		logLik	Pseudo R^2	type
		intercept	southness				intercept	elevation			
Start of season	2001	162***	-0.0676***	-17721.35	0.557	error	27.4***	0.0843***	-16550.72	0.754	error
	2002	142.2***	-0.0708***	-18790.66	0.326	error	-21.8***	0.1025***	-17395.39	0.666	error
	2003	168.3***	-0.0758***	-17955.9	0.539	error	39.3***	0.0807***	-16835.88	0.737	error
	2004	163.1***	-0.031***	-17009.21	0.629	error	65***	0.0619***	-16386.69	0.728	error
	2005	171.3***	-0.0511***	-17570.68	0.615	error	58***	0.0708***	-16896.34	0.725	error
	2006	129.9***	-0.0415***	-18154.76	0.389	error	-2.7	0.084***	-17171.05	0.627	error
	2007	158.3***	-0.0497***	-18522.64	0.538	error	-0.2	0.1007***	-17217.54	0.76	error
	2008	154.5***	-0.0546***	-17161.49	0.529	error	46.9***	0.0668***	-16303.52	0.694	error
	2009	138.8***	-0.0231**	-17792.54	0.465	error	12.5**	0.0831***	-17080.08	0.626	error
	2010	160***	-0.0291***	-17713.72	0.58	error	25.3**	0.0891***	-16655.99	0.753	error
	2011	139.4***	-0.0087	-16617.55	0.495	error	47.1***	0.0604***	-15730.68	0.676	error
	2012	145.2***	-0.0079	-16804.29	0.519	error	60.5***	0.0554***	-16030.33	0.674	error
	2013	166.1***	-0.0766***	-17397.36	0.49	error	51.2***	0.0727***	-15978.72	0.75	error
	2014	143.1***	-0.0572***	-17842.85	0.503	error	25.8***	0.0737***	-17073.1	0.662	error
	2015	148.7***	-0.0536***	-17337.91	0.523	error	57.4***	0.0576***	-16622.15	0.667	error
	2016	138.3***	-0.021**	-17399.58	0.537	error	38.2***	0.0638***	-16067.89	0.763	error
End of season	2001	325.2***	-0.1192***	-15813.9	0.324	error	295.7***	0.0118***	-16092.79	0.223	error
	2002	331.1***	-0.197***	-17157.62	0.413	error	300***	0.0083***	-17621.12	0.259	error
	2003	343.4***	-0.1879***	-17449.92	0.403	error	312.8***	0.0084***	-17819.29	0.281	error
	2004	333.7***	-0.179***	-17168.14	0.367	error	291.6***	0.0165***	-17476.46	0.261	error
	2005	326.3***	-0.1266***	-16539.89	0.351	error	307.3***	0.0044**	-16761.35	0.275	error
	2006	323.3***	-0.2041***	-17692.8	0.397	error	319.7***	-0.0103***	-18065.35	0.273	error
	2007	335.4***	-0.1785***	-17016.3	0.395	error	305.8***	0.0084***	-17349.05	0.285	error

index	Year	Index ~ Southness					Index ~ Elevation				
		Coefficients		logLik	Pseudo R^2	type	Coefficients		logLik	Pseudo R^2	type
		intercept	southness				intercept	elevation			
	2008	333.3***	-0.1972***	-17420.01	0.38	error	338.7***	-0.0157***	-17811.69	0.245	error
	2009	315***	-0.1075***	-16152.76	0.368	error	303.5***	7.00E-04	-16758.04	0.143	error
	2010	337.5***	-0.1883***	-17255.81	0.305	error	289.3***	0.0193***	-16919.97	0.413	error
	2011	360.4***	-0.292***	-18295.37	0.429	error	298.7***	0.0223***	-18733.89	0.289	error
	2012	324***	-0.147***	-16856.52	0.316	error	316.6***	-0.0042*	-17136.54	0.212	error
	2013	327.2***	-0.1815***	-16827.3	0.398	error	314.3***	-0.0028	-17260.84	0.251	error
	2014	316.4***	-0.148***	-17358.84	0.302	error	292.4***	0.0063**	-17557.14	0.229	error
	2015	318.1***	-0.1621***	-17127.47	0.325	error	318.4***	-0.0101***	-17335.86	0.251	error
	2016	331.1***	-0.1068***	-15138.33	0.343	error	292.9***	0.0182***	-15418.34	0.243	error
Length of season	2001	161.2***	-0.0495***	-18552	0.426	error	271.6***	-0.076***	-17973.72	0.571	error
	2002	189.3***	-0.1455***	-19831.95	0.286	error	328.8***	-0.0997***	-19419.86	0.42	error
	2003	174.9***	-0.132***	-19297.76	0.408	error	277.9***	-0.0765***	-19077.91	0.47	error
	2004	169.3***	-0.1454***	-18677.86	0.468	error	230.3***	-0.0497***	-18680.62	0.467	error
	2005	152.8***	-0.0792***	-18820.88	0.475	error	250.7***	-0.0703***	-18454.92	0.563	error
	2006	193.3***	-0.1906***	-19812.13	0.305	error	437.9***	-0.0974***	-19378.74	0.441	sac
	2007	288.7***	-0.1423***	-19481.56	0.536	sac	306.9***	-0.0924***	-18975.15	0.64	error
	2008	176.8***	-0.1561***	-19058.95	0.365	error	291.2***	-0.0849***	-18758.66	0.454	error
	2009	177.3***	-0.1008***	-18809.04	0.362	error	293.6***	-0.0834***	-18346.41	0.494	error
	2010	174.2***	-0.1543***	-18807.99	0.448	error	271.1***	-0.0733***	-18480.25	0.532	error
	2011	246.7***	-0.3091***	-19125.78	0.5	sac	251.2***	-0.0401***	-19408.53	0.423	error
	2012	178.1***	-0.1461***	-18481.04	0.422	error	258.5***	-0.0613***	-18354.17	0.458	error
	2013	158.8***	-0.1129***	-18808.57	0.368	error	271.8***	-0.0808***	-18285.63	0.514	error
	2014	171.8***	-0.1011***	-19135.89	0.453	error	267.4***	-0.0682***	-18829.31	0.531	error
	2015	169.3***	-0.1225***	-18891.09	0.375	error	269.4***	-0.0728***	-18538.88	0.477	error
	2016	189.4***	-0.1128***	-18045.82	0.505	error	262.7***	-0.0521***	-17751.22	0.573	error
	2001	249.9***	-0.1046***	-15591.21	0.591	error	172.6***	0.0434***	-15618.69	0.585	error

index	Year	Index ~ Southness					Index ~ Elevation				
		Coefficients		logLik	Pseudo R^2	type	Coefficients		logLik	Pseudo R^2	type
		intercept	southness				intercept	elevation			
Peak of season	2002	243.9***	-0.1721***	-16616.92	0.391	error	148.4***	0.0515***	-16403.33	0.453	error
	2003	261.2***	-0.1502***	-16133.16	0.561	error	191.8***	0.0364***	-15944.58	0.601	error
	2004	249.7***	-0.1113***	-15774.22	0.576	error	183.5***	0.0355***	-15722.59	0.587	error
	2005	255.3***	-0.0907***	-15484.77	0.631	error	199.8***	0.0307***	-15203.19	0.68	error
	2006	227.1***	-0.1232***	-16405.21	0.358	error	161.7***	0.0348***	-16333.31	0.381	error
	2007	251.6***	-0.1252***	-16061.2	0.491	error	178.4***	0.0401***	-15363.68	0.642	error
	2008	245***	-0.106***	-15322.22	0.53	error	204.7***	0.02***	-15286.04	0.538	error
	2009	235.9***	-0.1***	-16174.33	0.358	error	171.9***	0.0352***	-15968.12	0.421	error
	2010	255.6***	-0.1323***	-16367.69	0.389	error	171.5***	0.0462***	-16077.95	0.472	error
	2011	249.1***	-0.1568***	-16275.63	0.473	error	175.1***	0.0382***	-16381.13	0.445	error
	2012	234.7***	-0.0732***	-15040.69	0.564	error	192.7***	0.0227***	-14829.95	0.608	error
	2013	250.2***	-0.1394***	-15692.89	0.408	error	191.9***	0.0295***	-15824.6	0.367	error
	2014	230.3***	-0.0792***	-15825.77	0.479	error	169.8***	0.0351***	-15457.39	0.567	error
	2015	234.8***	-0.0965***	-15520.98	0.535	error	201.6***	0.0142***	-16296.37	0.314	error
	2016	239.6***	-0.0791***	-15144.35	0.552	error	175.3***	0.0363***	-15338.75	0.506	error
P-NDVI	2001	0.3***	1.71E-05	4163.93	0.378	error	0.8***	-3e-04***	5326.54	0.653	error
	2002	0.3***	1e-04***	4231.61	0.427	error	0.8***	-3e-04***	5319.29	0.668	error
	2003	0.3***	-1.78E-05	4138.91	0.402	error	0.8***	-3e-04***	5183.99	0.646	error
	2004	0.3***	2.03E-05	3915.04	0.349	error	0.9***	-4e-04***	5100.41	0.641	error
	2005	0.3***	-1.31E-05	3918.36	0.372	error	0.9***	-3e-04***	4982.09	0.632	error
	2006	0.3***	1e-04***	4068.67	0.367	error	0.9***	-3e-04***	5196.62	0.641	error
	2007	0.3***	9.63E-06	4176.64	0.364	error	0.8***	-3e-04***	5205.4	0.621	error
	2008	0.3***	4.69E-05	4114.92	0.372	error	0.9***	-3e-04***	5234.57	0.642	error
	2009	0.3***	4.28E-05	4125.6	0.363	error	0.9***	-4e-04***	5481.41	0.677	error
	2010	0.3***	5.257e-05.	4099.35	0.386	error	0.9***	-3e-04***	5272.54	0.66	error
	2011	0.3***	7.720e-05**	4195.75	0.377	error	0.9***	-3e-04***	5362.69	0.654	error

index	Year	Index ~ Southness					Index ~ Elevation				
		Coefficients		logLik	Pseudo R^2	type	Coefficients		logLik	Pseudo R^2	type
		intercept	southness				intercept	elevation			
	2012	0.3***	7.36E-06	4335.36	0.382	error	0.8***	-3e-04***	5464.77	0.65	error
	2013	0.3***	2.27E-05	4218.21	0.397	error	0.9***	-3e-04***	5315.55	0.652	error
	2014	0.3***	5.298e-05.	4153.51	0.385	error	0.9***	-3e-04***	5286.33	0.652	error
	2015	0.3***	1e-04***	4183.54	0.398	error	0.9***	-3e-04***	5382.85	0.671	error
	2016	0.3***	2.08E-05	4117	0.379	error	0.9***	-3e-04***	5297.92	0.657	error

Significant codes: "***"—0.001, "**"—0.01, "*"—0.05, "."—0.10.

(b)Tall tussock grassland

index	Year	Index ~ Southness					Index ~ Elevation				
		Coefficients		logLik	Pseudo R^2	type	Coefficients		logLik	Pseudo R^2	type
		intercept	southness				intercept	elevation			
Start of season	2001	135.1***	-0.0935***	-21296.64	0.385	error	61.3***	0.0578***	-20302.66	0.597	error
	2002	119***	-0.0896***	-21945.64	0.206	error	65.3***	0.039***	-21697.8	0.285	error
	2003	137.2***	-0.0987***	-21471.39	0.414	error	70.8***	0.0519***	-20634.53	0.59	error
	2004	132.2***	-0.0696***	-21091.95	0.499	error	70.5***	0.0523***	-20229.37	0.653	error
	2005	140.2***	-0.0665***	-21300.49	0.435	error	71.5***	0.0567***	-20142.7	0.655	error
	2006	104.1***	-0.0407***	-21104.49	0.227	error	49.9***	0.0433***	-20527.39	0.396	error
	2007	116.3***	-0.0279***	-21995.54	0.381	error	46.9***	0.0585***	-21283.36	0.543	error
	2008	131.4***	-0.0773***	-21205.87	0.418	error	69.4***	0.0487***	-20479.57	0.573	error
	2009	114.3***	-0.0323***	-20748.9	0.342	error	65.9***	0.0399***	-20204.21	0.479	error
	2010	122.4***	-0.0516***	-21673.31	0.46	error	46.9***	0.064***	-20454.49	0.679	error
	2011	114.9***	-0.0269***	-19934.02	0.478	error	70.3***	0.0381***	-19023.56	0.646	error
	2012	111.2***	0.0246***	-20351.52	0.402	error	60.4***	0.0479***	-19177.91	0.637	error
	2013	137***	-0.1238***	-21505.65	0.411	error	57.8***	0.0626***	-20340.12	0.642	error
	2014	119.5***	-0.0786***	-21038.98	0.368	error	60.7***	0.0456***	-20413.87	0.516	error

index	Year	Index ~ Southness					Index ~ Elevation				
		Coefficients		logLik	Pseudo R^2	type	Coefficients		logLik	Pseudo R^2	type
		intercept	southness				intercept	elevation			
	2015	127.8***	-0.0905***	-21179.44	0.41	error	63.6***	0.0493***	-20480.49	0.562	error
	2016	105.4***	3.56E-05	-20784.91	0.427	error	44.4***	0.0537***	-19659.01	0.645	error
End of season	2001	297.4***	-0.0645***	-19015.77	0.336	error	270.3***	0.0292***	-18382.45	0.493	error
	2002	315.4***	-0.1304***	-19870.37	0.401	error	263.9***	0.0372***	-19596.29	0.467	error
	2003	306.4***	-0.1216***	-20944.71	0.367	error	266.9***	0.0404***	-20122.38	0.554	error
	2004	331.3***	-0.172***	-20056.38	0.321	error	288.4***	0.0234***	-20298.2	0.247	error
	2005	319.6***	-0.1089***	-18486.25	0.346	error	290***	0.0191***	-18545.05	0.329	error
	2006	306.4***	-0.1352***	-21004.5	0.333	error	281.2***	0.018***	-20831.8	0.38	error
	2007	318.9***	-0.1494***	-20222.22	0.352	error	281.6***	0.028***	-19963.99	0.419	error
	2008	332***	-0.1745***	-20240.54	0.344	error	291.6***	0.021***	-20535.81	0.256	error
	2009	310***	-0.0832***	-18279.44	0.217	error	293.4***	0.0095***	-18248.21	0.228	error
	2010	272***	-0.1078***	-20674.9	0.224	error	277.9***	0.0276***	-20147.18	0.38	error
	2011	355.3***	-0.2668***	-21317.66	0.384	error	296.3***	0.0298***	-21757.26	0.257	error
	2012	321.8***	-0.1433***	-19287.68	0.312	error	288.2***	0.0183***	-19536.17	0.236	error
	2013	312.1***	-0.1228***	-19977.52	0.38	error	272.2***	0.0287***	-19928.52	0.393	error
	2014	303.1***	-0.1191***	-20898.24	0.283	error	269.9***	0.0233***	-20500.71	0.395	error
	2015	278.7***	-0.1196***	-20822.77	0.283	error	262.9***	0.0177***	-21044.59	0.212	error
	2016	338.1***	-0.1268***	-17934.42	0.374	error	339.9***	-0.0117***	-18416.97	0.231	error
Length of season	2001	178.7***	0.0179**	-21346.05	0.26	error	217***	-0.0319***	-21115.8	0.329	error
	2002	200***	-0.0393***	-22763.9	0.162	error	201***	-0.004*	-22771.28	0.16	error
	2003	186.5***	-0.0374***	-22243.07	0.24	error	198.3***	-0.0133***	-22229.74	0.244	error
	2004	193.7***	-0.1066***	-22072.08	0.334	error	222.5***	-0.0331***	-22028.6	0.346	error
	2005	180.7***	-0.0554***	-21590.14	0.346	error	221.4***	-0.0403***	-21249.43	0.435	error
	2006	211.4***	-0.0997***	-22872.93	0.253	error	231.2***	-0.0252***	-22850.84	0.26	error
	2007	211.8***	-0.129***	-22769.52	0.336	error	234.9***	-0.0308***	-22753.03	0.34	error
	2008	200.7***	-0.1132***	-22247.04	0.265	error	226.9***	-0.0318***	-22180.14	0.285	error

index	Year	Index ~ Southness					Index ~ Elevation				
		Coefficients		logLik	Pseudo R^2	type	Coefficients		logLik	Pseudo R^2	type
		intercept	southness				intercept	elevation			
Peak of season	2009	198.7***	-0.0595***	-21434.72	0.25	error	228***	-0.0303***	-21268.93	0.301	error
	2010	197.5***	-0.0693***	-22270.48	0.308	error	233.3***	-0.0373***	-22066.94	0.366	error
	2011	238.9***	-0.2462***	-22241.94	0.35	error	232.1***	-0.0139***	-22643.09	0.229	error
	2012	209.9***	-0.1728***	-21591.97	0.322	error	230.6***	-0.0317***	-21609.59	0.316	error
	2013	176.7***	-0.021**	-21898.75	0.219	error	218***	-0.0372***	-21614.35	0.308	error
	2014	191***	-0.0503***	-22335.67	0.272	error	212.5***	-0.0231***	-22296.18	0.284	error
	2015	187.4***	-0.0385***	-22340.33	0.329	error	220***	-0.0354***	-22183.22	0.373	error
	2016	233.6***	-0.1255***	-21717.29	0.46	error	291***	-0.061***	-20947.41	0.611	error
	2001	187.8***	-0.0944***	-19901.87	0.421	error	171.3***	0.042***	-18297.51	0.707	error
	2002	223.9***	-0.1392***	-19614.88	0.418	error	166.9***	0.0395***	-19216.17	0.509	error
	2003	193.2***	-0.1242***	-19891.19	0.539	error	170.4	0.0429***	-18723.14	0.719	sac
	2004	179.5***	-0.1243***	-19310.76	0.468	error	183.5***	0.0346***	-18940.03	0.546	error
	2005	186.9***	-0.1107***	-19478.68	0.456	error	189.7	0.0371***	-18219.64	0.682	sac
	2006	189.5***	-0.0854***	-19248.53	0.365	error	163.7***	0.0317***	-18376.32	0.562	error
	2007	218.8***	-0.1157***	-20008.94	0.426	error	170.8***	0.0423***	-18935.29	0.637	error
	2008	228.3***	-0.1157***	-19356.03	0.451	error	184.3***	0.0331***	-18905.62	0.547	error
	2009	216***	-0.0727***	-18860.72	0.406	error	182.4***	0.0269***	-18095.11	0.571	error
	2010	193.9***	-0.0995***	-20334.78	0.408	error	166.5***	0.0462***	-18768.65	0.696	error
	2011	239***	-0.1893***	-19456.98	0.453	error	182.9***	0.0335***	-19690.67	0.396	error
	2012	215.3***	-0.0716***	-18390.45	0.424	error	176.2***	0.0317***	-17139.9	0.662	error
	2013	186.9***	-0.1198***	-19885.45	0.455	error	173.4***	0.041***	-18804.03	0.656	error
	2014	195.3***	-0.0884***	-19159.6	0.484	error	184.1***	0.03***	-18419.46	0.623	sac
	2015	198.6***	-0.1025***	-19547.13	0.453	error	164.9***	0.0315***	-18939.66	0.578	sac
	2016	228.6***	-0.0972***	-18584.91	0.355	error	189.9***	0.0258***	-18318.8	0.424	error
P-NDVI	2001	0.5***	-1e-04***	5477.63	0.323	error	0.7***	-2e-04***	6960.48	0.64	error
	2002	0.5***	-2.79E-05	5386.87	0.346	error	0.8***	-2e-04***	6805.1	0.642	error

index	Year	Index ~ Southness					Index ~ Elevation				
		Coefficients		logLik	Pseudo R^2	type	Coefficients		logLik	Pseudo R^2	type
		intercept	southness				intercept	elevation			
	2003	0.5***	-9.527e-05***	5447.83	0.316	error	0.7***	-2e-04***	6761.98	0.609	error
	2004	0.5***	-5.680e-05*	5199.51	0.294	error	0.7***	-2e-04***	6544.05	0.601	error
	2005	0.5***	-1e-04***	5329.37	0.317	error	0.8***	-2e-04***	6532.46	0.591	error
	2006	0.5***	4.631e-05*	5477.92	0.321	error	0.7***	-2e-04***	6824.22	0.617	error
	2007	0.5***	-8.868e-05***	5548.08	0.33	error	0.7***	-2e-04***	6807.28	0.608	error
	2008	0.5***	-1.43E-05	5617.78	0.352	error	0.7***	-2e-04***	6546.08	0.563	error
	2009	0.5***	-1e-04***	5225.37	0.306	error	0.8***	-2e-04***	6662	0.623	error
	2010	0.5***	-3.42E-05	5482.38	0.319	error	0.7***	-2e-04***	6696.84	0.594	error
	2011	0.5***	2.76E-06	5579.56	0.333	error	0.7***	-2e-04***	6976.21	0.632	error
	2012	0.5***	-6.173e-05**	5572.5	0.348	error	0.8***	-2e-04***	7043.97	0.652	error
	2013	0.5***	-6.349e-05**	5416.38	0.337	error	0.8***	-2e-04***	6828.82	0.637	error
	2014	0.5***	-5.849e-05*	5374.48	0.32	error	0.8***	-2e-04***	6900.07	0.645	error
	2015	0.5***	-9.29E-06	5496.04	0.316	error	0.7***	-2e-04***	6896	0.623	error
	2016	0.5***	-5.288e-05*	5675.96	0.333	error	0.7***	-2e-04***	6609.28	0.551	error

Significant codes: "***"—0.001, "**"—0.01, "*"—0.05, "."—0.10.

(c)Low producing grassland

index	Year	Index ~ Southness					Index ~ Elevation				
		Coefficients		logLik	Pseudo R^2	type	Coefficients		logLik	Pseudo R^2	type
		intercept	southness				intercept	elevation			
Start of season	2001	108.5***	-0.036***	-18031.1	0.276	error	71.5***	0.0448***	-17498.15	0.443	error
	2002	107.1***	-0.0718***	-17732.8	0.238	error	80.2***	0.0322***	-17668.77	0.261	error
	2003	137.3***	-0.0512***	-18047.27	0.405	error	10.7	0.0467***	-17572.09	0.529	sac
	2004	114.8***	-0.0913***	-18960.04	0.319	error	82.1***	0.0361***	-18852.13	0.354	error
	2005	114.1***	-0.0563***	-18518.07	0.31	error	84.9***	0.0367***	-18392.81	0.351	error

index	Year	Index ~ Southness					Index ~ Elevation				
		Coefficients		logLik	Pseudo R^2	type	Coefficients		logLik	Pseudo R^2	type
		intercept	southness				intercept	elevation			
End of season	2006	94.1***	-0.0339***	-17333.96	0.24	error	64***	0.0351***	-16970.15	0.365	error
	2007	101***	-0.0482***	-18185.07	0.266	error	73.1***	0.0332***	-17977.86	0.337	error
	2008	106.2***	-0.0351***	-17774.57	0.31	error	73.9***	0.0408***	-17428.47	0.418	error
	2009	98.8***	-0.0448***	-17331.72	0.344	error	69.8***	0.0353***	-16978.99	0.449	error
	2010	104.9***	-0.0373***	-17781.11	0.348	error	63.2***	0.0443***	-17108.04	0.532	error
	2011	100.1***	-0.0275***	-17356.76	0.398	error	80.2***	0.0278***	-17138.19	0.459	error
	2012	100.1***	-0.0298***	-16763.62	0.135	error	88.7***	0.0131***	-16732.8	0.148	error
	2013	102.9***	-0.0444***	-18276.03	0.293	error	65.6***	0.0476***	-17861.32	0.424	error
	2014	104.1***	-0.0338***	-18045.23	0.296	error	61.5***	0.0477***	-17549.42	0.449	error
	2015	91.8***	-0.0111	-18926.11	0.336	error	58.7***	0.0493***	-18581.21	0.44	error
	2016	87.4***	0.002	-19075.85	0.298	error	74.4***	0.0204***	-18980.03	0.33	error
	2001	282.1***	0.0575***	-18804.55	0.509	error	244.2***	0.0576***	-18538.63	0.57	error
	2002	340***	0.0416***	-17596.19	0.463	error	261.3***	0.0415***	-16680.93	0.658	error
	2003	274.5***	0.0835***	-19068.76	0.565	error	240.1***	0.0642***	-18748.49	0.629	error
	2004	299.5***	-0.0258**	-19522.06	0.341	error	273.7***	0.0309***	-19395.83	0.381	error
	2005	299.6***	-0.0102.	-17430.57	0.349	error	286.2***	0.0169***	-17349.89	0.375	error
	2006	329***	0.0993***	-20135.52	0.505	error	258.7***	0.0844***	-19485.1	0.641	error
	2007	298.5***	0.0226*	-19242.26	0.464	error	258.1***	0.0565***	-18848.84	0.558	error
	2008	292.3***	0.0046	-19743.13	0.284	error	265.7***	0.0414***	-19556.12	0.348	error
	2009	291.2***	0.0101	-18805.75	0.332	error	276.1***	0.0239***	-18677.18	0.373	error
	2010	274.3***	0.0866***	-20617.9	0.491	error	232.1***	0.0746***	-20278.79	0.57	error
	2011	322.6***	-0.0959***	-18080.09	0.3	error	289***	0.0383***	-17912.75	0.356	error
	2012	295.9***	-0.016.	-19140.29	0.268	error	282***	0.019***	-19120.2	0.276	error
	2013	271.6***	0.0788***	-19341.41	0.478	error	241.8***	0.049***	-19012.57	0.556	error
	2014	307.1***	0.1068***	-20130.83	0.506	error	247***	0.0609***	-19804.16	0.579	error
	2015	288.6***	0.0836***	-20993.07	0.502	error	237.2***	0.068***	-20681.85	0.573	error

index	Year	Index ~ Southness					Index ~ Elevation				
		Coefficients		logLik	Pseudo R^2	type	Coefficients		logLik	Pseudo R^2	type
		intercept	southness				intercept	elevation			
	2016	287.7***	0.0248.	-21299.04	0.42	error	266.4***	0.0321***	-21196.65	0.449	error
Length of season	2001	170.5***	0.1027***	-18783.74	0.25	error	174.4***	0.0075**	-18849.06	0.226	error
	2002	169***	0.1094***	-18211.82	0.271	error	174.1***	0.0086***	-18234.27	0.262	error
	2003	156.5***	0.1366***	-18641.9	0.352	error	161.2***	0.0117***	-18728.8	0.323	error
	2004	187.3***	0.0595***	-19518.32	0.182	error	196.7***	-0.0061*	-19535.31	0.175	error
	2005	183.4***	0.0386***	-18797.78	0.144	error	200.8***	-0.0212***	-18764.54	0.158	error
	2006	189***	0.1282***	-19681.08	0.47	error	153.1***	0.0455***	-19535.45	0.507	error
	2007	184.1***	0.0674***	-19079.62	0.343	error	180.1***	0.0143***	-19080.03	0.343	error
	2008	189***	0.0392***	-19887.62	0.162	error	189.2***	0.005	-19886.37	0.163	error
	2009	193.9***	0.0516***	-19123.03	0.22	error	205.8***	-0.0111***	-19132.58	0.216	error
	2010	174.7***	0.1322***	-20424.99	0.346	error	166.6***	0.0282***	-20335.17	0.375	error
	2011	226.4***	-0.066***	-18496.61	0.182	error	211***	0.0144***	-18511.61	0.176	error
	2012	196.1***	0.0127	-19645.67	0.216	error	194.1***	0.0049	-19645.14	0.216	error
	2013	162.2***	0.1173***	-19433.13	0.267	error	172.1***	0.0011	-19477.77	0.251	error
	2014	165.4***	0.1309***	-20008.13	0.395	error	171.4***	0.0083**	-20044.41	0.384	error
	2015	170.7***	0.0869***	-20737.15	0.367	error	168.4***	0.0135***	-20724.54	0.371	error
	2016	192.4***	0.0332*	-21405.1	0.253	error	186.7***	0.0133**	-21395.94	0.256	error
Peak of season	2001	197***	0.0297***	-18032.71	0.564	error	163.4***	0.0672***	-17522.74	0.661	error
	2002	215.8***	-0.0128*	-16981.26	0.424	error	169.7***	0.0425***	-16192.08	0.61	error
	2003	195.3***	0.0268***	-18052.6	0.577	error	211.4***	0.0653***	-17487.58	0.68	error
	2004	207.7***	-0.0498***	-18696.81	0.379	error	185.2***	0.0277***	-18555.86	0.42	error
	2005	216.1***	-0.0216***	-17241.33	0.453	error	183.9***	0.0372***	-16844.02	0.55	error
	2006	186.8***	0.0346***	-18161.04	0.549	error	183.1***	0.0648***	-17591.92	0.659	error
	2007	3.5**	-0.0022	-18303.08	0.436	lag	165.1***	0.0587***	-17393.55	0.64	error
	2008	197.6***	-4.00E-04	-18051.79	0.391	error	167***	0.0458***	-17600.6	0.512	error
	2009	197.4***	-0.0024	-17457.46	0.505	error	167.6***	0.0428***	-17071.91	0.591	error

index	Year	Index ~ Southness					Index ~ Elevation				
		Coefficients		logLik	Pseudo R^2	type	Coefficients		logLik	Pseudo R^2	type
		intercept	southness				intercept	elevation			
P-NDVI	2010	191.9***	0.036***	-18802.65	0.543	error	144.2***	0.0708***	-18096.01	0.677	error
	2011	212.6***	-0.0688***	-17115.67	0.372	error	181.9***	0.0342***	-16754.46	0.475	error
	2012	197.2***	-0.0206***	-16940.87	0.332	error	180.5***	0.0224***	-16825.95	0.369	error
	2013	191.2***	0.0289***	-18114.66	0.524	error	147.4***	0.0611***	-17499.27	0.649	error
	2014	198***	0.0393***	-18221.9	0.546	error	191.1***	0.0583***	-17800.23	0.631	error
	2015	263.9***	0.0569***	-19413.28	0.491	error	164.8***	0.0681***	-18733.29	0.636	error
	2016	198.2***	0.0303**	-19583.81	0.483	error	159.3***	0.0462***	-19334.98	0.543	error
	2001	0.6***	-4.92E-06	5523.77	0.459	error	0.7***	-2e-04***	5976.21	0.567	error
	2002	0.6***	4.717e-05*	5142.84	0.403	error	0.7***	-1e-04***	5455.37	0.488	error
	2003	0.6***	6.89E-06	5407.39	0.441	error	0.7***	-9.277e-05***	5512.7	0.47	error
	2004	0.6***	9.67E-06	4945.06	0.423	error	0.7***	-2e-04***	5435.17	0.547	error
	2005	0.6***	1.56E-05	5587.53	0.455	error	0.7***	-1e-04***	5860.36	0.524	error
	2006	0.6***	1e-04***	5275.95	0.471	error	0.7***	-7.653e-05***	5379.2	0.497	error
	2007	0.6***	-1.69E-05	5067.41	0.442	error	0.7***	-1e-04***	5206.85	0.479	error
	2008	0.6***	3.35E-05	5408.29	0.516	error	0.6***	-1e-04***	5608.24	0.562	error
	2009	0.6***	-2.13E-05	5281.28	0.422	error	0.7***	-1e-04***	5633.27	0.514	error
	2010	0.6***	1.95E-05	5432.63	0.51	error	0.7***	-1e-04***	5697.08	0.57	error
	2011	0.6***	-1.09E-05	5387.18	0.434	error	0.7***	-1e-04***	5709.83	0.517	error
	2012	0.6***	-1.99E-05	5040.5	0.4	error	0.7***	-1e-04***	5402.62	0.498	error
	2013	0.6***	-3.01E-05	5378.18	0.401	error	0.7***	-1e-04***	5936.64	0.545	error
	2014	0.6***	1.10E-06	5555.36	0.422	error	0.7***	-1e-04***	5812.9	0.491	error
	2015	0.6***	-1.36E-05	5315.15	0.436	error	0.7***	-1e-04***	5687.82	0.531	error
	2016	0.6***	2.48E-05	5173.73	0.492	error	0.7***	-1e-04***	5510.48	0.57	error

Significant codes: “***”—0.001, “**”—0.01, “*”—0.05, “.”—0.10

Appendix VII Publication of Chapter 2

NEW ZEALAND GEOGRAPHER

New Zealand Geographer (2018) doi:10.1111/nzg.12187

Research Article

Geographic versus environmental space: Patterns of potential native and exotic woody propagule pressure on New Zealand's indigenous grasslands

Xiaobin Hua and Ralf Ohlemüller*
Department of Geography, University of Otago, PO Box 56, Dunedin, 9054, New Zealand

Abstract: Indigenous grassland ecosystems worldwide are increasingly subject to shrub encroachment. A key factor determining encroachment patterns is the availability of shrub propagules in the areas surrounding the grasslands. We here provide a multi-scale spatial analysis of the geographic distribution (geographic space) and the climatic conditions (environmental space) of potential native and exotic shrub propagule pressure for New Zealand's main grassland types. We show that alpine grasslands are most at risk from native, and low-producing grasslands are most at risk from exotic shrub propagule pressure. Inferred spatial patterns of potential propagule pressure differ between the local, landscape and regional scale.

Key words: climate change, invasion, land cover, niche.

Introduction

Woody plant encroachment, the increase of woody species into originally grass-dominated ecosystems, is a global phenomenon (Knapp *et al.* 2008; Reisinger *et al.* 2013). In recent decades, grassland and other non-woody ecosystems worldwide have experienced increased invasion by both native and alien plants (Briggs *et al.* 2007; Srinivasan 2012). Evidence suggests that recent anthropogenic climate change has occurred in a direction that favours woody plant growth giving woody species a competitive advantage (Archer *et al.* 1995; Briggs *et al.* 2005; Zavaleta & Kettley 2006). The displacement of grass by woody species can alter ecosystem functions, reduce grassland productivity, decrease the number of native grassland species and lead to degradation of cultural and ecological values of indigenous grasslands (Van Auken 2009; Komac *et al.* 2013; Ogden 2015; Saintilan & Rogers 2015). It is therefore paramount to understand where woody encroachment is most likely to occur in terms of (i) geographic space, that is the geographic/spatial distribution of grassland areas most likely to be invaded and (ii) environmental space, that is the environmental (here: climatic) conditions of these areas.

Propagule pressure is a measure of the number of individuals from one or more species released into a region (Lockwood *et al.* 2005). Two key factors determine the degree to which an indigenous grassland is prone to both native and exotic woody species invasions: environmental suitability for woody species in the grassland area and the proximity of woody species, that is the availability of woody propagules in the neighbourhood of the grasslands. Propagule pressure from surrounding landscapes at different scales is recognised as one of the main driving forces of woody encroachment (Briggs *et al.* 2005; He *et al.* 2015). Its intensity generally decreases with spatial distance and it has been shown to be a predictor of the degree to which an ecosystem is under threat from species invasion (Rouget & Richardson 2003; Colunga-Garcia *et al.* 2010). However, the magnitude of propagule pressure is often difficult to calculate because it is not only sensitive to spatial scales and also deeply related to land cover factors and environmental gradients (Milbau *et al.* 2009). Spatial scales and the size of the neighbourhood chosen for analyses can affect the result when evaluating the intensity of propagule pressure (Thomas & Moloney 2015). Thus, hierarchical approaches across several spatial scales are

Note about authors: Xiaobin Hua is a PhD student working on the application of remote sensing for analyses of spatial processes of landscape change in New Zealand. Ralf Ohlemüller is a Senior Lecturer in Biogeography with a teaching and research focus on spatial and temporal patterns of environmental change.

E-mail: ralf.ohlemuller@otago.ac.nz

Accepted: 01 March 2018

needed to capture different levels of propagule pressure at local, landscape and regional scales (Thomas & Moloney 2013). Such analyses are an effective tool to integrate different factors of invasibility and to infer levels of woody invasion threat at a range of spatial scales (Kidane *et al.* 2012; He 2014; Caracciolo *et al.* 2016). The patterns of shrubby propagule pressure across regions and environmental conditions are a useful measure of the degree to which a community is at risk from invasion from woody species (Pauchard *et al.* 2009; Faulkner *et al.* 2014). We here provide such an analysis for the indigenous grasslands of New Zealand.

New Zealand's non-woody indigenous ecosystems are comprised of two main vegetation types: grasslands below the treeline and alpine grassland/herbfield above treeline. Many of New Zealand's non-forest ecosystems have a high level of biodiversity and offer a wide range of ecosystem services (Wardle 1991; Mark *et al.* 2013). There is currently less than half (44%) of the original, pre-human ca. 82,400 km^2 of indigenous grassland area left (Mark & McLennan 2005). More recently, between 2001 and 2008, 321 km^2 of indigenous grasslands were converted to other non-indigenous land cover (Weeks *et al.* 2013). These indigenous grass-dominated ecosystems are often not free of woody species and would have had significant woody components at least in parts of their range in pre-human times in many cases (Walker *et al.* 2009). Polynesian fires turned large parts of New Zealand's woody ecosystems into open, grass-dominated ecosystems and repeated fires facilitated tussock grasslands to establish and dominate in areas where scrub and forests used to dominate (McGlone 2001; McWethy *et al.* 2010). Long-term monitoring at selected New Zealand sites suggests complex invasion patterns and interactions of native and exotic woody and non-woody species in indigenous grassland areas (Bellingham 1998; Walker 2000; Rose *et al.* 2004; Walker *et al.* 2009). There is currently limited information available on the spatial distribution and relative prevalence of native versus exotic woody shrub species and where they are located in relation to New Zealand's indigenous grasslands; this study fills this gap.

The aim of this paper is to provide a multi-scale spatial analysis of potential propagule pressure from native and exotic shrub species on New Zealand's indigenous grasslands. To this end, we address the following three questions:

1 Which grassland areas have the highest potential woody propagule pressure and where are they located?
2 Do grassland areas with high native and high exotic propagule pressure coincide spatially and do they occur in similar climatic conditions?
3 How does the scale of analysis (local, landscape and regional) change the assessment of the spatial distribution of potential woody propagule pressure on grasslands?

Methods

Land cover data and processing

Our study is based on a spatial analysis of the prevalence of native and exotic shrub ecosystems in the neighbourhood of indigenous grasslands in New Zealand. These analyses use the most recent published land cover data available for New Zealand and are conducted at the grid cell level on a 1 × 1-km grid covering the New Zealand mainland area (including Rakiura–Stewart Island). The units of investigation are grassland grid cells for each of which we quantify the area of woody land cover at three different spatial scales (i.e. neighbourhood sizes). Our principal assumption is that grassland grid cells with a larger area of woody land cover in their neighbourhood are exposed to higher potential woody propagule pressure. We do not include any microtopographical or species trait information that might affect actual dispersal of the propagules.

Our analyses are based on the most recent (2012/2013) New Zealand Land Cover Database (LCDB-v4.1 2015) as land cover dataset. LCDB's information is derived from satellite imagery using manual delineation and automatic detection to improve accuracy (Dymond *et al.* 2017). Even though this dataset has limitations for land cover change detection (Weeks *et al.* 2013; Dymond *et al.* 2017), we consider it as adequate for our propagule pressure analyses at different spatial scales as we are not utilising any between-year change data in our study. The vector-formatted LCDB data were rasterised to 1 km grid resolution using the module 'Polygon to Raster' with the 'cell-centre' assignment option in ArcGIS 10.1.

Three land cover classes were considered as indigenous grasslands: (i) alpine grass/herbfields, (ii) tall tussock grasslands and (iii) low-producing grasslands. The latter land cover class can contain significant parts of exotic elements in parts of its range (Cieraad *et al.* 2015). For native shrub ecosystems, we used the land cover classes: (i) manuka and/or kanuka, (ii) subalpine shrubland and (iii) matagouri or grey scrub. For exotic shrubs, we used the classes: (i) gorse and/or broom and (ii) mixed exotic shrubland. For detailed description of these classes, see Appendix I.

Neighbourhood analysis

We conducted a spatial neighbourhood analysis for each grassland grid cell in order to quantify how many (native and exotic) shrub grid cells are located in the neighbourhood within a distance of 1 km (local), 5 km (landscape) and 25 km (regional). The neighbourhood calculations were conducted using the tool 'focal statistics' in ArcGIS 10.1 with grassland cells set as focal cells and shrub cells

as neighbouring cells. We calculated for each grassland grid cell the proportion of grid cells in its neighbourhood that are shrubland leading to each grassland grid cell having a value between 0 (no shrub grid cell in neighbourhood = no propagule pressure) and 1 (all neighbouring cells are shrub = high propagule pressure). This was done for native and exotic shrubs and for the three neighbourhood sizes. We then ranked all grid cells within each grassland type from highest to lowest propagule pressure resulting in all grassland grid cells with at least one shrub land cover within their neighbourhood being categorised in one of five groups: top 5, 25, 50, 75 and 100%; any grassland grid cell with no shrub grid cell in its neighbourhood was not part of the ranking. We considered the top 25% of grid cells as 'high pressure' and the top 5% as 'very high pressure' hotspots. Finally, we mapped for each grassland grid cell for each neighbourhood size whether the grid cell was part of the high propagule pressure group for native shrubs, exotic shrubs or both.

Climate data and niche overlap analyses

In order to characterise the current climatic conditions in which the grassland and shrubland ecosystems occur, six variables relevant for woody plant growth were selected from the WorldClim dataset (Hijmans *et al.* 2005): mean annual temperature (bio1), temperature seasonality (bio4), minimum temperature of the coldest month (bio6), annual precipitation (bio12), precipitation seasonality (bio15) and precipitation of driest quarter (bio17). These data represent a 1950–2000 average and were used to characterise the climatic conditions (climatic niches) of the different grassland and shrubland ecosystems. We did this through a principle component analysis (PCA) based on these six climate variables, which allowed us to show the position of each ecosystem in a 2-D climate space of the two first PCA axes. Our aim is to quantify if hotspots of native and exotic propagule pressure occur in the same climatic conditions. To do this, we calculated the niche overlap of the native and the exotic hotspot area in climate space for a given grassland type and neighbourhood size using the niche overlap index Schoener's *D*. It is a commonly used ecological metric to quantify the overlap in environmental conditions of two species or populations based on spatial occurrence records (Warren *et al.* 2008). We here adjusted this index to calculate the overlap in climatic conditions between grassland areas of high native and high exotic propagule pressure. The index was calculated using the package 'ecospat' in the statistical software package R platform (version 3.3.3, 2017-03-06) (Broennimann *et al.* 2012). Schoener's *D* ranges from 0 to 1 (Rodder & Engler 2011) and in our study indicates that for any given grassland type, native and exotic high-propagule pressure grassland areas occur in different ($D = 0$) or in similar ($D = 1$) climates.

Results

Spatial patterns of woody propagule pressure

The three indigenous grassland types investigated here cover a total of 15.5% of the New Zealand land area with alpine grass/herbfield having the smallest (0.8%) and tall tussock grassland having the largest extent (8.7%; Table 1). The majority of indigenous grassland cover is located in the South Island (Fig. 1). The spatial distribution of native and exotic shrublands affects the degree to which these grasslands are exposed to propagule pressure from woody species.

At the local scale (1 km neighbourhood), all grassland types are mostly exposed to native rather than exotic propagule pressure (Table 1, Fig. 2): more than one-third of the area of each of the three grassland types has at least some native shrubland within a 1-km neighbourhood (Table 1). In contrast, only 0.5% of alpine grasslands, 2.4% of tussock grasslands and 11.2% of low-producing grasslands have at least some exotic shrubland nearby. The largest spatial overlap of areas under native and areas under exotic pressure at this local level is for low-producing grasslands with 3.3% of grid cells being located in areas where at least some native and exotic shrubland is within 1 km (Table 1).

At the landscape scale (5 km neighbourhood), almost all grid cells of all grassland types have at least some native shrubland in their neighbourhood: alpine: 97.4% of grid cells, tussock: 88.2% and low-producing grasslands: 89.5%. As with the local neighbourhood, these values are much smaller for exotic shrubland with 9, 22.6 and 55.2% for the three grassland types. At this spatial scale, however, one fifth (tussock) and half (low producing) of the grid cells are exposed to native and exotic shrub species propagule pressure in their neighbourhood (Table 1). These native and exotic spatial locations are mostly located on the eastern foothills of the Southern Alps in the northern half of the South Island (Fig. 2).

At the regional scale (25 km neighbourhood), basically all grassland areas have at least some native shrublands within their neighbourhood (>99.9% of grassland cells, Table 1) while more than 73, 86 and 99% of alpine, tussock and low-producing grassland areas have at least some exotic shrubland in the neighbourhood. Looking at the top 25% quartile of grid cells with the highest proportions of neighbouring shrub cover, alpine and low-producing grasslands have over 6% of their area under combined pressure of native and exotic species (Table 1). Most of these areas are located in the northern half of the South Island (Fig. 2).

Climatic patterns of woody propagule pressure

The three grassland types investigated here occupy distinct climatic niche space (Fig. 3), which is a reflection of their geographic distribution (Fig. 1). As expected, alpine grass/herbfields occupy cooler and moderately

Table 1 The spatial distribution of potential native and exotic woody propagule pressure in the three grassland types at three spatial scales.

Grassland type	Pressure intensity (top %)	Propagule pressure sources	Local (1 km)		Landscape (5 km)		Regional (25 km)	
			Areas (pixels)	Percent	Areas (pixels)	Percent	Areas (pixels)	Percent
Alpine grass/Herbfield, 0.85% of NZ	Top 5%	Native	108	4.8	121	5.4	113	5.0
		Exotic	12	0.5	19	0.8	82	3.6
		Both	1	<0.1	5	0.2	7	0.3
	Top 25%	Native	367	16.3	592	26.3	564	25.1
		Exotic	12	0.5	114	5.1	414	18.4
		Both	1	<0.1	52	2.3	147	6.5
	All	Native	952	42.3	2189	97.4	2248	100.0
		Exotic	12	0.5	202	9.0	1632	72.6
		Both	6	0.3	193	8.6	1632	72.6
Tall tussock grassland, 8.71% of NZ	Top 5%	Native	539	2.3	1126	4.8	1188	5.0
		Exotic	31	0.1	278	1.2	1042	4.4
		Both	0	<0.1%	0	<0.1	12	0.1
	Top 25%	Native	3410	14.5	5530	23.5	5900	25.1
		Exotic	556	2.4	1796	7.6	5286	22.4
		Both	47	0.2	233	1.0	795	3.4
	All	Native	8245	35.0	20770	88.2	23551	100.0
		Exotic	556	2.4	5311	22.6	20372	86.5
		Both	137	0.6	4534	19.3	20372	86.5
Low-producing grassland, 5.99% of NZ	Top 5%	Native	422	2.6	720	4.5	813	5.0
		Exotic	107	0.67	466	2.9	803	5.0
		Both	1	<0.1	2	<0.1	48	0.3
	Top 25%	Native	2221	13.8	3654	22.7	4022	25.0
		Exotic	1805	11.2	2975	18.5	3986	24.8
		Both	215	1.3	623	3.9	1105	6.9
	All	Native	5315	33.0	14391	89.5	16072	100.0
		Exotic	1805	11.2	8878	55.2	15944	99.1
		Both	536	3.3	7987	49.7	15932	99.1

Percentages indicate the percent area of grassland that is classified as having very high (top 5%), high (top 25%) and any (all) woody propagule pressure. 'Top 5%' indicates the 5% of grassland grid cells with the highest proportion of woody land cover in their neighbourhood; 'all' indicates all grassland grid cells with at least one shrub grid cell within their neighbourhood. For alpine grasslands, 108 pixels are under high 'native' shrubby propagule pressure at the threshold of top 5%, and 4.8% is the proportion of the 108 pixels in all 2,248 pixels in that land cover class. NZ, New Zealand.

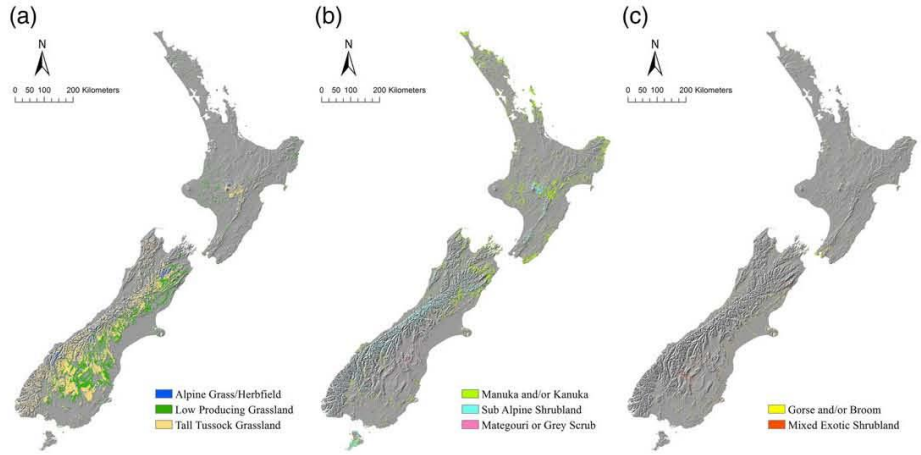

Figure 1 Grass- and shrubland land cover classes from LCDB 4.1 used in this study. (a) Indigenous grasslands: alpine grass/herbfield, low-producing grassland and tall tussock grassland. (b) Native shrublands: manuka and/or kanuka, subalpine shrubland and matagouri or grey scrub. (c) Exotic shrubland: gorse and/or broom, mixed exotic shrubland.

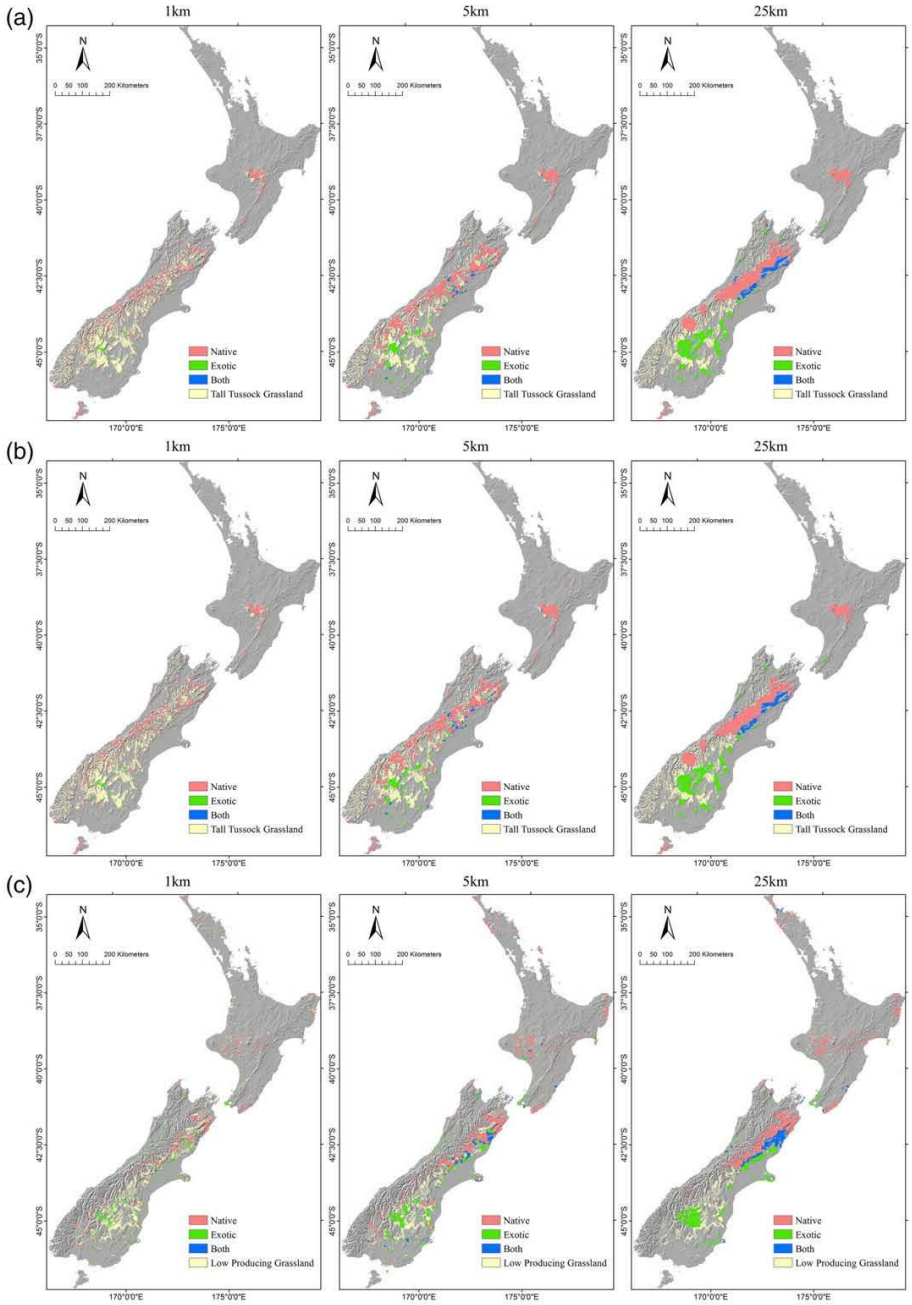

Figure 2 Spatial distribution of grassland areas with high (top 25%) shrub propagule pressure for the three main types of indigenous grasslands: (a) alpine grass/herbfield, (b) tall tussock grassland and (c) low-producing grassland at three different neighbourhood sizes (1, 5 and 25 km). Red/Green: Top quartile of grassland grid cells with the highest proportion of native/exotic shrub grid cells in neighbourhood. Blue: Grassland grid cells which are part of the top quartile for both native and exotic shrubland cover in their neighbourhood. Yellow: Grassland grid cells which are not part of the top 25% quartile.

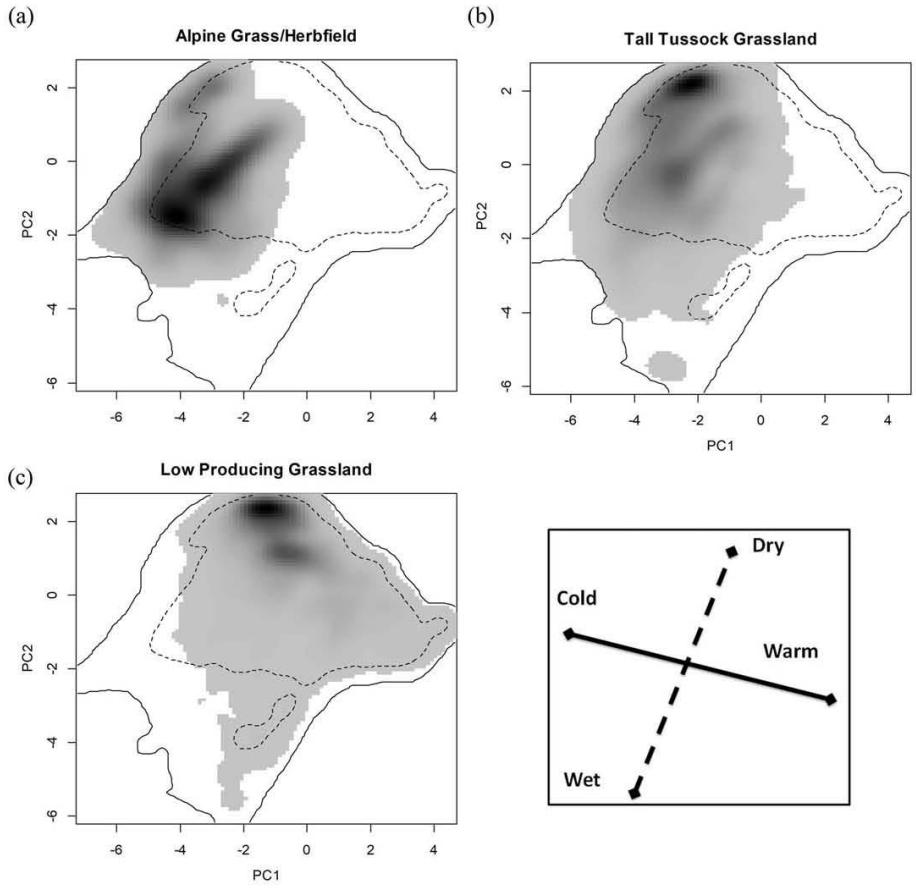

Figure 3 Climate conditions of the three indigenous grassland types (a–c) investigated in this study. Grey areas show the space occupied by each grassland type in 2-D climate space made up of the first two axes of a principal component analysis (PCA) of six climate variables (see Methods section). PCA axis 1 represents a cold to warm gradient, axis 2 a wet to dry gradient (see inset). The solid outline illustrates the overall climate space available in New Zealand, and the dotted line is the 50% quantile region. Darker grey tones indicate more grid cells in that part of the climate space.

wet parts of the climate space available in New Zealand (Fig. 3a). Tall tussock grasslands occur in drier and cooler areas (Fig. 3b) while low-producing grasslands are found in warmer and very dry areas (Fig. 3c). Climatic preferences between any of the grassland and any of the shrubland types are most similar for low-producing grasslands and native matagouri/grey scrub ($D = 0.72$; Table 2). Of all grassland types, low-producing grasslands have the highest and alpine grasslands the lowest similarity in climatic conditions with exotic shrublands (Table 2).

The degree to which a grassland area is exposed to combined native and exotic shrub propagule pressure depends on the level of propagule pressure and the neighbourhood size applied (Table 1). When considering all grassland grid cells with at least one native and one exotic grid cell in the neighbourhood, climatic niche overlap between grassland areas under native pressure and grassland areas under exotic pressure was lowest for alpine and tall tussock grassland ($D = 0.11$, 0.28), and highest for low-producing grasslands ($D = 0.63$) at the local scale (Table 3). This indicates that in the immediate surroundings of grassland areas native and exotic shrublands occupy much more similar climates in the vicinity of low-producing grasslands than they do in the vicinity of alpine grasslands. This pattern holds for higher propagule pressure intensities, for example when only considering the top 5% of grassland grid cells with the largest areas of native and exotic shrubland in the neighbourhood (Table 2). At larger spatial scales (landscape and regional), overlap between native and exotic climate niches increases but the relative order of grassland types remains: for alpine grasslands, areas with high combined native and exotic shrub pressure occur in

Table 2 Climatic niche overlap (Schoener's *D*) between the three grassland and five shrubland types.

	Alpine grass/Herbfield	Tall tussock grassland	Low-producing grassland
Native shrubland			
Manuka and/or kanuka	0.03	0.07	0.27
Subalpine shrubland	0.33	0.47	0.16
Matagouri or grey scrub	0.12	0.28	0.72
Exotic shrubland			
Gorse and/or broom	0.01	0.04	0.27
Mixed exotic shrubland	0.08	0.18	0.37

Values range from 0 to 1 with higher values indicating more similar climatic conditions within which the two ecosystems occur.

more different climate conditions than for tussock grasslands and low-producing grasslands. Overall, these niche overlap values (Schoener's *D* values) indicate that native and exotic shrubby propagules have less specific climate preferences near low-producing grassland than near the other two grasslands.

Discussion

Quantifying shrub propagule pressure in indigenous grassland types

Our results suggest that alpine grass/herbfields are the grassland type most exposed to native shrub propagule pressure while low-producing grasslands are most exposed to exotic propagule pressure (Table 1). This is, at the most general level, a reflection of the spatial distribution of these grassland types in relation to native and exotic shrublands (Fig. 1). The changes from grassland to shrubland land cover recorded in LCDB dataset since 1996 (LCDB-v4.1 2015) should constitute a good reference to test our results. According to the 'change pivot table' included in the LCDB v4.1 files, there were no conversions from alpine grass/herbfields to shrublands during any of the LCDB assessment periods 1996–2001, 2001–2008 and 2008–2012. For tall tussock grasslands, 1,274, 464 and 52 ha have changed to shrubland during these three periods. However, the major change in tussock grassland was associated with the conversions to pasture and forestry: 9,011, 5,309 and 1,911 ha of tussock grassland changed to exotic forest during the three periods (LCDB-4.1, 2015) with the decreasing trend possibly indicating a change in awareness and appreciation of New Zealand's native grassland ecosystems (Mark & McLennan 2005; Mark *et al.* 2009). Most change from tall tussock grassland to other land cover types detectable with the LCDB land cover methodology was due to agricultural activities rather than invasion of (native or exotic) species. Local on-the-ground or high-resolution airborne multi-year surveys are needed to reliably detect shrub species invasions into grasslands.

Grasslands classified as low-producing grasslands are the most anthropogenically modified grassland types that are also in closest proximity to agricultural activity (Walker *et al.* 2009; Cieraad *et al.* 2015). For alpine grass/herbfields, there were no recent changes to

Table 3 Climate niche overlap (Schoener's *D*) between grassland areas affected by native and exotic woody propagule pressure at different levels of pressure intensity.

Grassland type	Pressure intensity (top %)	Local (1 km)	Landscape (5 km)	Regional (25 km)
Alpine grass/Herbfield	Top 5%	0.06	0.68	0.01
	Top 25%	0.07	0.13	0.09
	Top 50%	0.11	0.22	0.25
	Top 75%	0.11	0.46	0.54
	All	0.11	0.55	0.88
Tall tussock grassland	Top 5%	0.02	0.03	0.01
	Top 25%	0.22	0.25	0.09
	Top 50%	0.28	0.35	0.29
	Top 75%	0.28	0.54	0.57
	All	0.28	0.60	0.92
Low-producing grassland	Top 5%	0.42	0.27	0.07
	Top 25%	0.51	0.37	0.27
	Top 50%	0.63	0.63	0.49
	Top 75%	0.63	0.77	0.74
	All	0.63	0.83	0.98

'Top 5%' indicates the 5% of grassland grid cells with the highest proportion of shrubland cover in their neighbourhood; 'all' indicates all grassland grid cells with at least one shrub grid cell within a given neighbourhood size. Local, landscape and regional scales indicate three neighbourhood sizes within which the area of woody land cover was quantified (see Methods section).

shrubland detected in LCDB v4.1, but our results show that they are under high-propagule pressure from native shrubs (Table 1). Montane and alpine regions, where climate conditions are harsh to most species, are not 'immune' to woody invasion as long as the woody species can reach them (Tecco *et al.* 2016). Our analysis is based only on spatial patterns of certain land cover types. Even though there might be large areas of shrubland near an area of grassland, the shrub propagules might not be able to reach the grassland area because of topography, wind direction etc. and this will be particularly relevant in alpine environments.

There are uncertainties and accuracy issues associated with the LCDB dataset in specific indigenous grassland areas (Brockerhoff *et al.* 2008) and small changes may not be recorded correctly (Dymond *et al.* 2017). Some transitions from grasslands to shrublands might have happened but they were not obvious enough to be captured by the remote sensing methodology applied in the current LCDB datasets.

Spatial coincidence of high native and exotic propagule pressure

Of the three grassland types, low-producing grassland had the highest propensity to be located in areas where high native and exotic propagule pressure coincide (Table 1). At the landscape and the regional scale, 50% (99%) of low-producing grasslands have at least some native and exotic shrublands in their neighbourhood. Alpine grass/herbfield is the least likely to be located in areas with high pressure from natives and exotics with only 9 and 73% of its area being located in areas that have at least some shrubland in the neighbourhood at the landscape and regional scale (Table 1). Woody native shrubs such as manuka (*Leptospermum scoparium*), kanuka (*Kunzea* spp.), monoao (*Dracophyllum subulatum*), inaka (*Dracophyllum longifolium*) are a typical and natural feature in New Zealand's native grasslands as for instance in red tussock (*Chionochloa rubra ssp. rubra*) communities in the Rangipo and Mangaohane areas in central North Island (Rogers & Leathwick 1994). In a study (Bellingham 1998) near Porters Pass, South Island, native and exotic shrub invasions into alpine grassland were already observed over 20 years ago; the native shrub, matagouri (*Discaria toumatou*), was often observed in habitats where tussock species decreased. The exotic Scotch broom (*Cytisus scoparius*) was seldom seen among the gaps between tussock and matagouri communities but the exotic shrub was predicted to surpass the biomass of matagouri (Bellingham 1998). Several exotic shrub invasions into indigenous grasslands have been observed and documented; for example, Scotch heather (*Calluna vulgaris*) has invaded the North Island's volcanic plateau, Spanish heath (*Erica lusitanica*) has spread into tall tussock grasslands in Otago and gorse (*Ulex europaeus*) and broom (*Cytisus scoparius*) into low altitude grassland habitats (Mark *et al.* 2013). The latter areas coincide with our high exotic pressure areas in the South Island (Fig. 2).

In more recent years, expansion of several native woody species continue to be observed in tussock-dominated areas at high elevation (species from the genera *Brachyglottis*, *Coprosma* and *Dracophyllum*), with manuka and kanuka being more prominent in lower altitude grassland sites (Ausseil *et al.* 2011). Our results indicate that even at the local scale (i.e. 1 km distance around a grassland grid cell) there are usually both native and exotic shrublands present near grassland areas and the proportion of grassland grid cells for which this is the case increases with neighbourhood size (Table 1). The spatial distribution of grassland areas that are under high native and exotic pressure is spatially more scattered at the local scale than at the regional scale (Fig. 2). A general pattern emerges at larger spatial scales: alpine and eastern foothill areas in the upper South Island seem to be the areas most prone to both native and exotic propagule pressure acting on any grassland area (Fig. 2).

Climatic conditions favouring high native and exotic propagule pressure

Local climatic factors can affect the establishment and dispersal of the expanding shrubs based on species' traits, but the dominant drivers in woody encroachment are often propagule pressure and human activities (Briggs *et al.* 2005). Global climate change and increase of CO_2 in the atmosphere should favour woody shrub growth (Saintilan & Rogers 2015) but the degree to which this happens will depend on the system and species in question (Van Auken 2009). Woody plant encroachment is also likely to alter interactions between species and climate, CO_2 enrichment, fire disturbance and grazing management (Naito & Cairns 2011). Often, climatic preference and introduction history of an invasive species can explain a large proportion of the variation in the spatial distribution of alien species (Feng *et al.* 2016), and the traits and growth form of a species can play substantial roles in the invasion process (Giorgis *et al.* 2016). However, given the importance of propagule pressure in determining shrub encroachment rates into grasslands (Dullinger *et al.* 2003), we therefore see our analysis as a first but important step towards a better understanding of New Zealand wide threats to grasslands. We show where (Fig. 2) and in which climate conditions (Appendix II) the highest potential for high-propagule pressure from native and exotic (and both combined) species exists. At the local scale, low-producing grasslands with high-propagule pressure (top25%) occur in areas with climatic conditions suited for native and exotic woody species (high niche overlap, $D = 0.51$, Table 3, Appendix II). For alpine grasslands in contrast, niche overlap at the local scale is low ($D = 0.07$) indicating that alpine grassland areas with

native and exotic shrubs in their immediate neighbourhood occur in climatically dissimilar conditions. This might have implications for management strategies for native versus exotic shrub invasions into alpine grasslands under changing climate conditions. Understanding which shrub species will actually invade a grassland ecosystem at what rate and in which regions of New Zealand requires more local understanding of the environment and the species involved.

Conclusions

Our study highlights the high degree of spatial variability in shrubby propagule pressure among the three main types of indigenous grasslands in New Zealand. In particular at the local scale, that is in the immediate neighbourhood of grassland areas, there is large variation in the spatial distribution of highest propagule pressure areas between grassland types. In geographic space, high native and high exotic propagule pressure does not coincide spatially at the local scale for any of the grassland types. However, in environmental space, high native and high exotic pressure areas occur in very similar climates for low-producing grasslands but not so for alpine and tussock grasslands. The spatial scale of investigation greatly affects where grassland areas with highest potential risk from native, exotic and combined shrub invasion are considered to be (Fig. 2). In the central South island, tall tussock grasslands have only small areas of exotic shrubland in their immediate neighbourhood but considerably larger areas at the landscape and regional scale. It is therefore important to understand species-specific dispersal processes and local landscape topography for more accurate predictions of actual shrub invasion risk. Using this information on the spatial distribution and the climatic conditions of native versus exotic shrub propagule pressure in grassland areas is a first step towards a predictive model of potential future shrub encroachment patterns and rates in New Zealand's grasslands ecosystems.

References

Archer S, Schimel DS, Holland EA (1995). Mechanisms of SHRUBLAND expansion – Land-use, climate or CO-2. *Climatic Change* **29**, 91–9.

Ausseil A-GE, Dymond JR, Weeks ES (2011). Provision of natural habitat for biodiversity: Quantifying recent trends in New Zealand. In: Venora OGaG, ed. *Biodiversity Loss in a Changing Planet*, InTech-Open Access Publisher, pp. 978–953.

Bellingham PJ (1998). Shrub succession and invasibility in a New Zealand montane grassland. *Australian Journal of Ecology* **23**, 562–73.

Briggs JM, Knapp AK, Blair JM, Heisler JL, Hoch GA, Lett MS, McCarron JK (2005). An ecosystem in transition. Causes and consequences of the conversion of mesic grassland to shrubland. *Bioscience* **55**, 243–54.

Briggs JM, Schaafsma H, Trenkov D (2007). Woody vegetation expansion in a desert grassland: Prehistoric human impact? *Journal of Arid Environments* **69**, 458–72.

Brockerhoff EG, Shaw WB, Hock B, Kimberley M, Paul T, Quinn J, Pawson S (2008). Re-examination of recent loss of indigenous cover in New Zealand and the relative contributions of different land uses. *New Zealand Journal of Ecology* **32**, 115–26.

Broennimann O, Fitzpatrick MC, Pearman PB, Petitpierre B, Pellissier L, Yoccoz NG, Thuiller W, Fortin MJ, Randin C, Zimmermann NE, Graham CH, Guisan A (2012). Measuring ecological niche overlap from occurrence and spatial environmental data. *Global Ecology and Biogeography* **21**, 481–97.

Caracciolo D, Istanbulluoglu E, Noto LV, Collins SL (2016). Mechanisms of shrub encroachment into Northern Chihuahuan Desert grasslands and impacts of climate change investigated using a cellular automata model. *Advances in Water Resources* **91**, 46–62.

Cieraad E, Walker S, Price R, Barringer J (2015). An updated assessment of indigenous cover remaining and legal protection in New Zealand's land environments. *New Zealand Journal of Ecology* **39**, 309–15.

Colunga-Garcia M, Haack RA, Magarey RA, Margosian ML (2010). Modeling spatial establishment patterns of exotic forest insects in urban areas in relation to tree cover and propagule pressure. *Journal of Economic Entomology* **103**, 108–18.

Dullinger S, Dirnbock T, Grabherr G (2003). Patterns of shrub invasion into high mountain grasslands of the Northern Calcareous Alps, Austria. *Arctic Antarctic and Alpine Research* **35**, 434–41.

Dymond JR, Shepherd JD, Newsome PF, Belliss S (2017). Estimating change in areas of indigenous vegetation cover in New Zealand from the New Zealand Land Cover Database (LCDB). *New Zealand Journal of Ecology* **41**, 0–0.

Faulkner KT, Robertson MP, Rouget M, Wilson JRU (2014). A simple, rapid methodology for developing invasive species watch lists. *Biological Conservation* **179**, 25–32.

Feng YH, Maurel N, Wang ZH, Ning L, Yu FH, van Kleunen M (2016). Introduction history, climatic suitability, native range size, species traits and their interactions explain establishment of Chinese woody species in Europe. *Global Ecology and Biogeography* **25**, 1356–66.

Giorgis MA, Cingolani AM, Tecco PA, Cabido M, Poca M, von Wehrden H (2016). Testing alien plant distribution and habitat invasibility in mountain ecosystems: Growth form matters. *Biological Invasions* **18**, 2017–28.

He Y (2014). The effect of precipitation on vegetation cover over three landscape units in a protected semi-arid grassland: Temporal dynamics and suitable climatic index. *Journal of Arid Environments* **109**, 74–82.

He YF, D'Odorico P, De Wekker SFJ (2015). The relative importance of climate change and shrub encroachment on nocturnal warming in the southwestern United States. *International Journal of Climatology* **35**, 475–80.

Hijmans RJ, Cameron SE, Parra JL, Jones PG, Jarvis A (2005). Very high resolution interpolated climate surfaces for global land areas. *International Journal of Climatology* **25**, 1965–78.

Kidane Y, Stahlmann R, Beierkuhnlein C (2012). Vegetation dynamics, and land use and land cover change in the Bale Mountains, Ethiopia. *Environmental Monitoring and Assessment* **184**, 7473–89.

Knapp AK, Briggs JM, Collins SL, Archer SR, Bret-Harte MS, Ewers BE, Peters DP, Young DR, Shaver GR, Pendall E, Cleary MB (2008). Shrub encroachment in North American grasslands: Shifts in growth form dominance rapidly alters control of ecosystem carbon inputs. *Global Change Biology* **14**, 615–23.

Komac B, Kefi S, Nuche P, Escos J, Alados CL (2013). Modeling shrub encroachment in subalpine grasslands under different environmental and management scenarios. *Journal of Environmental Management* **121**, 160–9.

LCDB-v4.1 (2015) *Land Cover Database Version 4.1*. [Cited 16 Jun 2017]. Available from URL: https://lris.scinfo.org.nz/layer/423-lcdb-v41-land-cover-database-version-41-mainland-new-zealand/

Lockwood JL, Cassey P, Blackburn T (2005). The role of propagule pressure in explaining species invasions. *Trends in Ecology & Evolution* **20**, 223–8.

Mark AF, McLennan B (2005). The conservation status of New Zealand's indigenous grasslands. *New Zealand Journal of Botany* **43**, 245–70.

Mark AF, Michel P, Dickinson KJM, McLennan B (2009). The conservation (protected area) status of New Zealand's indigenous grasslands: An update. *New Zealand Journal of Botany* **47**, 53–60.

Mark A, Barratt B, Weeks E, Dymond J (2013). Ecosystem services in New Zealand's indigenous tussock grasslands: Conditions and trends. In: Dymond JR, ed. *Ecosystem services in New Zealand: conditions and trends*, Lincoln, New Zealand: Manaaki Whenua Press, Landcare Research, pp. 1–33.

McGlone MS (2001). The origin of the indigenous grasslands of southeastern South Island in relation to pre-human woody ecosystems. *New Zealand Journal of Ecology* **25**, 1–15.

McWethy DB, Whitlock C, Wilmshurst JM, McGlone MS, Fromont M, Li X, Dieffenbacher-Krall A, Hobbs WO, Fritz SC, Cook ER (2010). Rapid landscape transformation in South Island, New Zealand, following initial Polynesian settlement. *Proceedings of the National Academy of Sciences of the United States of America* **107**, 21343–8.

Milbau A, Stout JC, Graae BJ, Nijs I (2009). A hierarchical framework for integrating invasibility experiments incorporating different factors and spatial scales. *Biological Invasions* **11**, 941–50.

Naito AT, Cairns DM (2011). Patterns and processes of global shrub expansion. *Progress in Physical Geography* **35**, 423–42.

Ogden LE (2015). Plants duke it out in a warming Arctic. *Bioscience* **65**, 220–0.

Pauchard A, Kueffer C, Dietz H, Daehler CC, Alexander J, Edwards PJ, Arevalo JR, Cavieres LA, Guisan A, Haider S, Jakobs G, McDougall K, Millar CI, Naylor BJ, Parks CG, Rew LJ, Seipel T (2009). Ain't no mountain high enough: Plant invasions reaching new elevations. *Frontiers in Ecology and the Environment* **7**, 479–86.

Reisinger AJ, Blair JM, Rice CW, Dodds WK (2013). Woody vegetation removal stimulates riparian and benthic denitrification in tallgrass prairie. *Ecosystems* **16**, 547–60.

Rodder D, Engler JO (2011). Quantitative metrics of overlaps in Grinnellian niches: Advances and possible drawbacks. *Global Ecology and Biogeography* **20**, 915–27.

Rogers GM, Leathwick JR (1994). North-island seral tussock grasslands: 2. Autogenic succession: Change of tussock grassland to shrubland. *New Zealand Journal of Botany* **32**, 287–303.

Rose AB, Suisted PA, Frampton CM (2004). Recovery, invasion, and decline over 37 years in a Marlborough short-tussock grassland, New Zealand. *New Zealand Journal of Botany* **42**, 77–87.

Rouget M, Richardson DM (2003). Inferring process from pattern in plant invasions: A semimechanistic model incorporating propagule pressure and environmental factors. *American Naturalist* **162**, 713–24.

Saintilan N, Rogers K (2015). Woody plant encroachment of grasslands: A comparison of terrestrial and wetland settings. *New Phytologist* **205**, 1062–70.

Srinivasan MP (2012). Exotic shrub invasion in a montane grassland: The role of fire as a potential restoration tool. *Biological Invasions* **14**, 1009–28.

Tecco PA, Pais-Bosch AI, Funes G, Marcora PI, Zeballos SR, Cabido M, Urcelay C (2016). Mountain invasions on the way: Are there climatic constraints for the expansion of alien woody species along an elevation gradient in Argentina? *Journal of Plant Ecology* **9**, 380–92.

Thomas SM, Moloney KA (2013). Hierarchical factors impacting the distribution of an invasive species: Landscape context and propagule pressure. *Landscape Ecology* **28**, 81–93.

Thomas SM, Moloney KA (2015). Combining the effects of surrounding land-use and propagule pressure to predict the distribution of an invasive plant. *Biological Invasions* **17**, 477–95.

Van Auken OW (2009). Causes and consequences of woody plant encroachment into western north American grasslands. *Journal of Environmental Management* **90**, 2931–42.

Walker S (2000). Post-pastoral changes in composition and guilds in a semi-arid conservation area, Central Otago, New Zealand. *New Zealand Journal of Ecology* **24**, 123–37.

Walker S, King N, Monks A, Williams S, Burrows L, Cieraad E, Meurk C, Overton JM, Price R, Smale M (2009). Secondary woody vegetation patterns in New Zealand's south island dryland zone. *New Zealand Journal of Botany* **47**, 367–93.

Wardle P (1991). *Vegetation of New Zealand*. Cambridge, England: Cambridge University Press.

Warren DL, Glor RE, Turelli M (2008). Environmental niche equivalency versus conservatism: Quantitative approaches to niche evolution. *Evolution* **62**, 2868–83.

Weeks ES, Waker S, Dymond JR, Shepherd JD, Clarkson BD (2013). Patterns of past and recent conversion of indigenous grasslands in the South Island, New Zealand. *New Zealand Journal of Ecology* **37**, 127–38.

Zavaleta ES, Kettley LS (2006). Ecosystem change along a woody invasion chronosequence in a California grassland. *Journal of Arid Environments* **66**, 290–306.

APPENDIX I

Table Appendix 1 Description of selected classes in LCDB v4.1 (from LCDB-4.1, 2015).

Class name	Definition	Reclassified
Alpine grass/Herbfield	Typically sparse communities above the actual or theoretical treeline dominated by herbaceous cushion, mat, turf and rosette plants and lichens. Grasses are a minor or infrequent component, whereas stones, boulders and bare rock are usually conspicuous.	Indigenous grassland
Tall tussock grassland	Indigenous snow tussocks in mainly alpine mountain-lands and red tussock in the central North Island and locally in poorly-drained valley floors, terraces and basins of both islands.	Indigenous grassland
Low-producing grassland	Exotic sward grassland and indigenous short tussock grassland of poor pastoral quality reflecting lower soil fertility and extensive grazing management or non-agricultural use. Browntop, sweet vernal, danthonia, fescue and Yorkshire fog dominate, with indigenous short tussocks (hard tussock, blue tussock and silver tussock) common in the eastern South Island and locally elsewhere.	Indigenous grassland
Manuka and/or kanuka	Scrub dominated by mānuka and/or kānuka, typically as a successional community in a reversion towards forest. Mānuka has a wider ecological tolerance and distribution than kānuka with the latter somewhat concentrated in the north with particular prominence on the volcanic soils of the central volcanic plateau.	Native shrub
Subalpine shrubland	Highland scrub dominated by indigenous low-growing shrubs including species of *Hebe*, *Dracophyllum*, *Olearia* and *Cassinia*. Predominantly occurring above the actual or theoretical treeline, this class is also recorded where temperature inversions have created cooler micro-climates at lower elevations, for example the 'frost flats' of the central North Island.	Native shrub
Matagouri or grey scrub	Scrub and shrubland comprising small-leaved, often divaricating shrubs such as matagouri, *Coprosma* spp, *Muehlenbeckia* spp., *Casinnia* spp. and *Parsonsia* spp. These, from a distance, often have a grey appearance.	Native shrub
Gorse and/or Broom	Scrub communities dominated by gorse or Scotch broom generally occurring on sites of low fertility, often with a history of fire, and insufficient grazing pressure to control spread. Left undisturbed, this class can be transitional to Broadleaved Indigenous Hardwoods.	Exotic shrub
Mixed exotic shrubland	Communities of introduced shrubs and climbers such as boxthorn, hawthorn, elderberry, blackberry, sweet brier, buddleja and old man's beard.	Exotic shrub

APPENDIX II

Graphical representation of climate niche overlap (Schoener's D) between climatic conditions of grassland areas affected by native (red) and exotic (green) shrub propagule pressure at two levels of pressure intensity: 'top 25%' indicates the area with the 25% of grassland grid cells with the highest proportion of shrubland in their neighbourhood; 'all' indicates all grassland grid cells with at least one shrub grid cell within their neighbourhood. 1 km (local), 5 km (landscape) and 25 km (regional) indicate three neighbourhood sizes (see Methods section). Blue areas indicate climatic conditions in which the grassland type occurs and is subject to high exotic *and* native propagule pressure. The x- and y-axes are the first two axes of a principal component analysis of six climate variables – areas close together in the diagram have similar climate conditions. Line indicates overall climate conditions available in New Zealand.

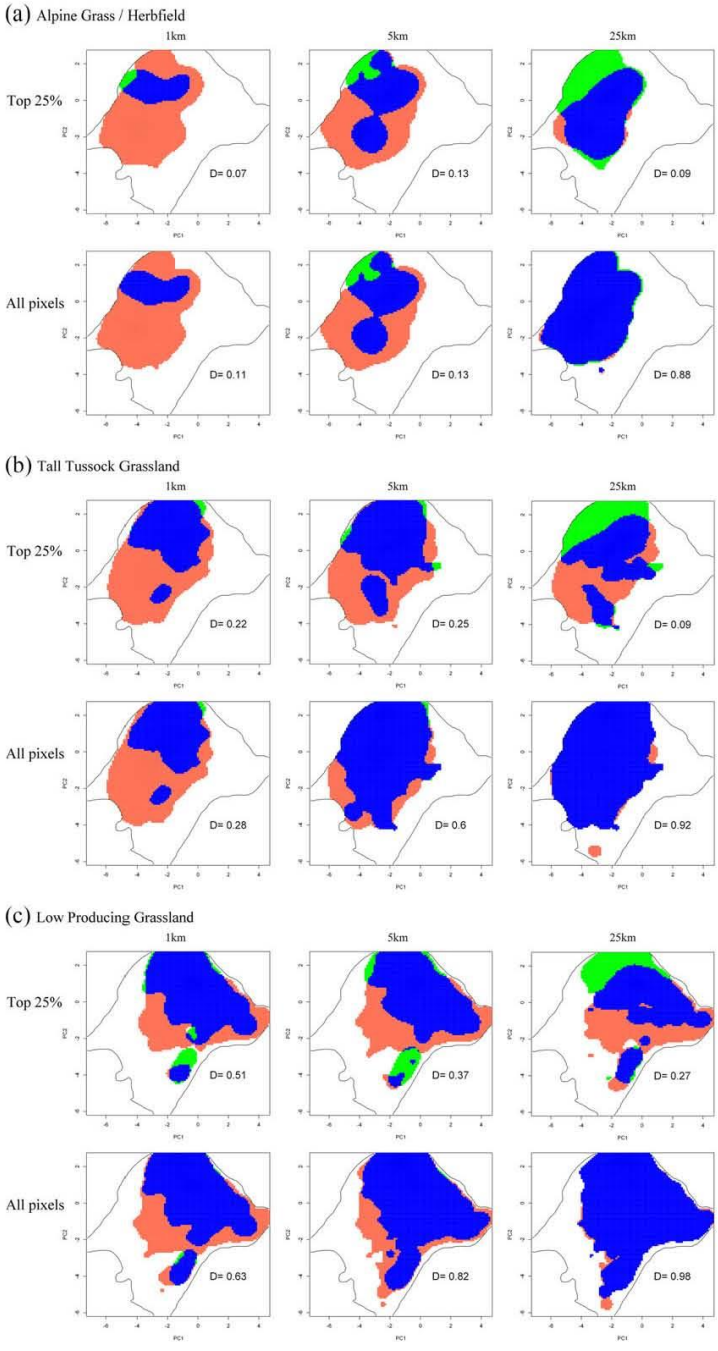

Appendix VIII R codes applied in chapters

Chapter 2

Niche overlap calculation:

```
# load packages
library(sp)
library(raster)
library(gtools)
library(ecospat)
library(devEMF)


#### Propagule Pressure niche overlap ####

## Load climate data

# obtain climate raster file paths
list.bioclim <- mixedsort(list.files(paste(getwd(),"/bioclimNZTM",
sep = ""),pattern="NZTM.asc$",full.names=TRUE))
list.bioclim

# extract six selected climate factors
bioclim <- stack(list.bioclim[c(1,4,6,12,15,17)])
names(bioclim) <- c("bio1","bio4","bio6","bio12","bio15","bio17")
bioclim

# convert climate raster to point values
bioval <- rasterToPoints(bioclim)
clim <- na.exclude(data.frame(bioval))
head(clim)



# Load raster of potential propagule pressure data

list.pp <-
mixedsort(list.files(paste(getwd(),"/Neighborhood/NZ_Top%maps", sep =
""),pattern=".tif$",full.names=TRUE))
list.pp


## Niche overlap calculation of Alpine Grass type for example


t <- 1  # count of loops
n <- c("Alp_1k_25%",
       "Alp_5k_25%",
       "Alp_25k_25%") # names of output plots
m <- c("1 KM","5 KM","25 KM") # names of scales

for (i in c(2,7,12))  {

# extract high native shrub pressured Alpine Grass points
nat <- raster(list.pp[i+15])
val <- rasterToPoints(nat)
val[,3][val[,3]==0] <- NA
```

```
val <- na.exclude(data.frame(val))
nat <- val[,c(1,2)]
nat[,"sp"] <- c("Nat-P")

# extract high exotic shrub pressured Alpine Grass points
exo <- raster(list.pp[i])
val <- rasterToPoints(exo)
val[,3][val[,3]==0] <- NA
val <- na.exclude(data.frame(val))
exo <- val[,c(1,2)]
exo[,"sp"] <- c("Exo-P")

# combine high native and exotic shrub pressured Alpine grass points
in the same table
asp <- rbind(nat,exo)
asp$sp <- as.factor(asp$sp)


# sample climatic values for all Alpine Grass occurrences
occ.asp <-
na.exclude(ecospat.sample.envar(dfsp=asp,colspxy=1:2,colspkept=1:3,
dfvar=clim,colvarxy=1:2,colvar="all",resolution=1000))


# PCA processing

data1 <- rbind(occ.asp[,c(4:9)],clim[,c(3:8)])
w<-c(rep(0,nrow(occ.asp)),rep(1,nrow(clim)))
pca.asp <-dudi.pca(data1, row.w = w, center = T, scale = T, scannf =
F, nf = 2)

row.nat<-which(occ.asp[,3] == "Nat-P") # rows of native shrub
pressured points
row.exo<-which(occ.asp[,3] == "Exo-P") # rows of exotic shrub
pressured points

scores.clim<- pca.asp$li[(nrow(occ.asp)+1):nrow(data1),] # PCA scores
of the climate niche of New Zealand
scores.nat<- pca.asp$li[row.nat,]  # PCA scores of native shrub
pressured points
scores.exo<- pca.asp$li[row.exo,]  # PCA scores of exotic shrub
pressured points

R <- 100
za<- ecospat.grid.clim.dyn(scores.clim,scores.clim,scores.nat,R)
zb<- ecospat.grid.clim.dyn(scores.clim,scores.clim,scores.exo,R)

# Niche overlap (Schoener's D) calculation
D.asp <- ecospat.niche.overlap (za, zb, cor=TRUE)

# export plots for all scales
n1 <- n[t]
n2 <- m[t]
emf(file=paste(getwd(),"/Niche/NZ_result_new/",n1,".emf",sep=""))
ecospat.plot.niche.dyn(za,zb,quant=1.0,interest=1,title=n2,name.axis1
="PC1",name.axis2="PC2",
colinter="blue",colz1="coral1",colz2="green",colZ2="black")
text(2,-4,paste("D=",round(as.numeric(D.asp[1]),2)),cex = 2.0)
t <- t+1
}
```

Chapter 3

Shrub & Grass classification for vegetation index image:

```
# load packages
library(overlapping)
library(sp)
library(sf)
library(raster)
library(gtools)


#### build a classification function ####

Classify_ab <- function(d1,d2,ras,sig=0.01) {

  ## comparison of signal densities of two land cover types

  des1 <- density(d1)
  des2 <- density(d2)

  f1 <- approxfun(des1)
  f2 <- approxfun(des2)

  dts <- list(Shrub=d1,Tussock=d2)
  d.ov <- overlap(dts)

  # get quantiles at 0.01 significance
  qt1 <- quantile(des1,probs=c(sig,1-sig))
  qt2 <- quantile(des2,probs=c(sig,1-sig))

  # find the intersect point
  for (i in length(d.ov$xpoints[[1]])) {
    if (d.ov$xpoints[[1]][i]<mean(des1$x) &
d.ov$xpoints[[1]][i]>mean(des2$x)) {
      intct <- d.ov$xpoints[[1]][i]
    }
  }

  rs <- ras
  rs[] <- 0
  rs[which(ras[]>=intct & ras[]<=qt1[2])] <- 1
  rs[which(ras[]>=qt2[1] & ras[]<=intct)] <- 2

  return(rs)

}



#### Classification using NDVI raster ####

# load data
index <- "NDVI"
i1 <- paste0("D:/SPOT-
test/Queenstown_a/QUAC/Queenstown_2013_PMS_QUAC_ref_",index,".dat")
i2 <- paste0("D:/SPOT-
test/Queenstown_a/QUAC/Queenstown_2017_PMS_QUAC_ref_",index,".dat")

ind2013 <- raster(i1)
ind2017 <- raster(i2)
```

```
# load shrub & grass training samples

shrub <- readOGR("D:/SPOT-test/Queenstown_a/SHP/NewTraining",layer =
"Shrub_Train_p")
grass <- readOGR("D:/SPOT-test/Queenstown_a/SHP",layer =
"Queenstown_TTussock_sample")

sample.shrub <- as.data.frame(shrub)[,2:3]
sample.grass <- as.data.frame(grass)[,3:4]


# get signal density overlap in the scene of 2013
ind2013.shrub <- extract(ind2013,sample.shrub)
ind2013.grass <- extract(ind2013,sample.grass)
d1 <- list(Shrub=ind2013.shrub,
           Grass=ind2013.grass)
overlap.d1 <- overlap(d1)

# get signal density overlap in the scene of 2017
ind2017.shrub <- extract(ind2017,sample.shrub)
ind2017.grass <- extract(ind2017,sample.grass)
d2 <- list(Shrub=ind2017.shrub,
           Grass=ind2017.grass)
overlap.d2 <- overlap(d2)

# plot signal density overlap
png(filename = paste0("E:/R work/SPOT
analysis/Queenstown_2019/Separation/ModifiedSample/SG_separation_",index,".
png"),
    width = 1000, height = 500,res=150)

p1 <- final.plot(d1,overlap.d1$OV)+ggtitle(paste0("2013.01.21 ",index))
p2 <- final.plot(d2,overlap.d2$OV)+ggtitle(paste0("2017.11.18 ",index))

grid.arrange(p1,p2, nrow = 1)

dev.off()



# image classification

# result for the scene of 2013
rs1 <- Classify_ab(d1=ind2013.shrub,d2=ind2013.grass,ras = ind2013,sig =
0.01)
writeRaster(rs1,filename = paste0("D:/SPOT-
test/Queenstown_a/Raster/ModifiedSample/Classification_AB_2013_",index,".ti
f"),overwrite=TRUE)

# result for the scene of 2017
rs2 <- Classify_ab(d1=ind2017.shrub,d2=ind2017.grass,ras = ind2017,sig =
0.01)
writeRaster(rs2,filename = paste0("D:/SPOT-
test/Queenstown_a/Raster/ModifiedSample/Classification_AB_2017_",index,".ti
f"),overwrite=TRUE)


#### accuracy analysis(confusion matrix) ####

# load classification results
index <- "NDVI"
```

```
ras1 <- paste0("D:/SPOT-
test/Queenstown_a/Raster/ModifiedSample/Classification_AB_2013_",index,".ti
f")
ras2 <- paste0("D:/SPOT-
test/Queenstown_a/Raster/ModifiedSample/Classification_AB_2017_",index,".ti
f")

class1 <- raster(ras1)
class2 <- raster(ras2)

# load reference points
ref.SS <- readOGR("D:/SPOT-test/Queenstown_a/SHP/NewTraining",layer =
"Shrub_Valid_p")
ref.GG <- readOGR("D:/SPOT-test/Queenstown_a/SHP",layer =
"Queenstown_TTussock_verify")
ref.GS <- readOGR("D:/SPOT-test/Queenstown_a/SHP/NewTraining",layer =
"G_to_S_verify")
ref.SG <- readOGR("D:/SPOT-test/Queenstown_a/SHP/NewTraining",layer =
"S_to_G_verify")


# compare result of 2013 and reference
ref1.ss <- extract(class1,ref.SS)
ref1.gg <- extract(class1,ref.GG)
ref1.gs <- extract(class1,ref.GS)
ref1.sg <- extract(class1,ref.SG)


# compare result of 2017 and reference
ref2.ss <- extract(class2,ref.SS)
ref2.gg <- extract(class2,ref.GG)
ref2.gs <- extract(class2,ref.GS)
ref2.sg <- extract(class2,ref.SG)

## build confusion matrix
emat <- matrix(NA,nrow = 6,ncol = 5)

colnames(emat) <- c("SS.ref","GG.ref","GS.ref","SG.ref","Total")
rownames(emat) <- c("SS","GG","GS","SG","OT","Sum")

emat["SS","SS.ref"] <- length(which(ref1.ss==1 & ref2.ss==1))
emat["GG","SS.ref"] <- length(which(ref1.ss==2 & ref2.ss==2))
emat["GS","SS.ref"] <- length(which(ref1.ss==2 & ref2.ss==1))
emat["SG","SS.ref"] <- length(which(ref1.ss==1 & ref2.ss==2))
emat["OT","SS.ref"] <- length(which(ref1.ss==3 | ref2.ss==3))

emat["SS","GG.ref"] <- length(which(ref1.gg==1 & ref2.gg==1))
emat["GG","GG.ref"] <- length(which(ref1.gg==2 & ref2.gg==2))
emat["GS","GG.ref"] <- length(which(ref1.gg==2 & ref2.gg==1))
emat["SG","GG.ref"] <- length(which(ref1.gg==1 & ref2.gg==2))
emat["OT","GG.ref"] <- length(which(ref1.gg==3 | ref2.gg==3))

emat["SS","GS.ref"] <- length(which(ref1.gs==1 & ref2.gs==1))
emat["GG","GS.ref"] <- length(which(ref1.gs==2 & ref2.gs==2))
emat["GS","GS.ref"] <- length(which(ref1.gs==2 & ref2.gs==1))
emat["SG","GS.ref"] <- length(which(ref1.gs==1 & ref2.gs==2))
emat["OT","GS.ref"] <- length(which(ref1.gs==3 | ref2.gs==3))

emat["SS","SG.ref"] <- length(which(ref1.sg==1 & ref2.sg==1))
emat["GG","SG.ref"] <- length(which(ref1.sg==2 & ref2.sg==2))
emat["GS","SG.ref"] <- length(which(ref1.sg==2 & ref2.sg==1))
emat["SG","SG.ref"] <- length(which(ref1.sg==1 & ref2.sg==2))
```

```
emat["OT","SG.ref"] <- length(which(ref1.sg==3 | ref2.sg==3))

emat[,"Total"] <- rowSums(emat,na.rm = TRUE)
emat["Sum",] <- colSums(emat,na.rm = TRUE)
emat

write.table(emat,file = paste0("D:/SPOT-
test/Queenstown_a/accuracy/ModifiedSample_eMatrix_",index,".txt"))
```

Chapter 4

Pearson Correlation Coefficient (PCC) calculation between phenology and climate:

```
# load packages
library(sp)
library(sf)
library(raster)


#### PCC calculation based on VCSN pixels ####

#load climate factors table list
list.cp <- mixedsort(list.files(path="E:/R
work/MODIS_NDVI/MODISrst/Climate_LM/SeasonSpecific",
pattern=".txt",full.names = TRUE,recursive=FALSE))

#load phenological indices table list
list.phe <- mixedsort(list.files(path = "E:/R
work/MODIS_NDVI/MODISrst/Climate_LM/Climate_Agent_pheno",
pattern = ".txt$",full.names = TRUE,recursive = FALSE))

# select eight climate factors in database by numbers
cls <- c(1,2,4,5,6,8,9,11)

# calculate PCC for each pair of phenological indices and climate factors
for (g in 1:3) { # loop of each grassland type
  for (p in 1:5) { # loop of each phenological index

    # load phenology table
    m <- (p-1)*3+switch(g,1,3,2)
    df.p <- data.frame(read.table(list.phe[m]))
    # load climate table
    df.c <- list()
    for (cc in cls) {
      n <- (cc-1)*5+p
      df.c[[which(cls[]==cc)]] <- data.frame(read.table(list.cp[n]))
    }

    # build tables to contain results
    tb.cor <- matrix(0,nrow = nrow(df.p),ncol = length(cls)+1)
    colnames(tb.cor) <- c("Agent",climate1[cls])
    tb.p <- tb.cor
    tb.lm <- tb.cor

    # loops for each row of dataframe
    for (i in 1:nrow(df.p)) {

      df <- t(df.p[i,col.y])
      colnames(df) <- d.var <- paste0(pheno[p],"_",grass[g])
      ag <- df.p[i,'Agent']
      tb.cor[i,'Agent'] <- tb.p[i,'Agent'] <- tb.lm[i,'Agent'] <- ag

      for (cc in cls) {
        tb <- df.c[[which(cls[]==cc)]]
        tb1 <- t(tb[which(tb[,'Agent']==ag),col.y])
        colnames(tb1) <- i.var <- climate1[cc]

        dt <- cbind(df,tb1)
        cort <- cor.test(dt[,d.var],dt[,i.var],method = "pearson")
        cov <- cov(dt[,d.var],dt[,i.var],method = "pearson")
```

```
        fm <- as.formula(paste(d.var,i.var,sep = "~"))
        md <- lm(fm,data = data.frame(dt))

        tb.cor[i,climate1[cc]] <- cort$estimate
        tb.p[i,climate1[cc]] <- cort$p.value
        tb.lm[i,climate1[cc]] <- md$coefficients[2]
      }

    } # dataframe rows loops end

# save results as tables
    write.table(tb.cor,file = paste0("E:/R
work/MODIS_NDVI/MODISrst/Climate_LM/Climate_correlation/",

"Correlation_",pheno[p],"_",grass[g],"_est.txt"))
    write.table(tb.p,file = paste0("E:/R
work/MODIS_NDVI/MODISrst/Climate_LM/Climate_correlation/",

"Correlation_",pheno[p],"_",grass[g],"_p.txt"))
    write.table(tb.lm,file = paste0("E:/R
work/MODIS_NDVI/MODISrst/Climate_LM/Climate_correlation/",

"Correlation_",pheno[p],"_",grass[g],"_lm.txt"))

  }# phenological indices loops end
} # grassland types loops end
```

Chapter 5

SAR models fitting:

```
# load packages
library(sp)
library(sf)
library(raster)
library(spdep)


## load background data

alp.tm <- read.table("E:/R work/MODIS_NDVI/MODISrst/Alpine/Base_alp.txt")
tsk.tm <- read.table("E:/R work/MODIS_NDVI/MODISrst/Tussock/Base_tsk.txt")
lpg.tm <- read.table("E:/R work/MODIS_NDVI/MODISrst/LowPro/Base_lpg.txt")
list.base <- list(alp.tm,tsk.tm,lpg.tm)

## load phenology results and error points ##

pho.alp <- "E:/R work/MODIS_NDVI/MODISrst/Alpine/Pheno_0.5/standardized"
pho.tsk <- "E:/R work/MODIS_NDVI/MODISrst/Tussock/Pheno_0.5/standardized"
pho.lpg <- "E:/R work/MODIS_NDVI/MODISrst/LowPro/Pheno_0.5/standardized"
pth.p <- c(pho.alp,pho.tsk,pho.lpg)

alp.er <- "E:/R work/MODIS_NDVI/MODISrst/Alpine/errPs_alp.txt"
tsk.er <- "E:/R work/MODIS_NDVI/MODISrst/Tussock/errPs_ttk.txt"
lpg.er <- "E:/R work/MODIS_NDVI/MODISrst/LowPro/errPs_lpg.txt"
pth.er <- c(alp.er,tsk.er,lpg.er)

alp.grid <- raster("E:/R work/MODIS_NDVI/MODISrst/Alpine/AlpAllTime.tif")
tsk.grid <- raster("E:/R
work/MODIS_NDVI/MODISrst/Tussock/TussockAllTime.tif")
lpg.grid <- raster("E:/R work/MODIS_NDVI/MODISrst/LowPro/LowPAllTime.tif")
grass.st <- stack(alp.grid,tsk.grid,lpg.grid)

# var setting

grass <- c("alp","tsk","lpg")
col.y <- paste0("X",c(2001:2016))
pheno <- c("End","Length","P.NDVI","Peak","Start")


## resample the Tussock grassland and Low producing grassland dataset
r0 <- raster("E:/R work/MODIS_NDVI/NDVI_samples/empty.tif")

tsk.code <- rasterize(tsk.tm[,1:2],r0,field=tsk.tm[,'order'])
tskr <- raster("E:/R
work/MODIS_NDVI/MODISrst/Raster/TussockAllTime_Resample1.5k.tif")
tskr.code <- resample(tsk.code,tskr,method="ngb")
tsk.rs <- rasterToPoints(tskr.code)


lpg.code <- rasterize(lpg.tm[,1:2],r0,field=lpg.tm[,'order'])
lpgr <- raster("E:/R
work/MODIS_NDVI/MODISrst/Raster/LowPAllTime_Resample5p.tif")
lpgr.code <- resample(lpg.code,lpgr,method="ngb")
lpg.rs <- rasterToPoints(lpgr.code)

tskc <- tsk.rs[,3]
lpgc <- lpg.rs[,3]
```

```
#### Semi-Variogram test ####

grass.n <- c("Alpine","Tussock","Low Producing")

## calculate distances (diameters) of spatial autocorrelation ##

tb.dist <- matrix(0,nrow = 75,ncol = 16)
colnames(tb.dist) <- col.y
rownames(tb.dist) <- paste0(rep(grass,each=25),"_",
                            rep(rep(pheno[c(5,1,2,4,3)],each=5),3),"_",
                            rep(1:5,15))

for (g in 1:3) {
  list.pheno <- list.files(path = pth.p[g],
                           pattern = ".txt$",full.names = TRUE,recursive =
FALSE)
  p.sys <- scan(pth.er[g])
  base1 <- list.base[[g]]

  for (p in c(5,1,2,4,3)) {

    tb2 <- read.table(list.pheno[p])
    tb1 <- cbind(base1,tb2[,col.y])

    # data clean
    data1 <- data.frame(tb1[-p.sys,])
    if (g==1) { # for Alpine grass type, exclude the pixel under 900m
      row <- which(data1[,'ele']<900)
      data1 <- data1[-row,]
    }

    # dataset resample
    if (g==1) {df1 <- data1}
    if (g==2) {# resampling the huge dataset of Tussock grassland
      row1 <- which(match(data1[,'order'],tskc)>0)
      df1 <- data1[row1,]
    }
    if (g==3) {# resampling the huge dataset of Low producing grassland
      row1 <- which(match(data1[,'order'],lpgc)>0)
      df1 <- data1[row1,]
    }

    # build grid
    grid1 <-
SpatialPointsDataFrame(df1[,1:2],df1[,3:ncol(df1)],proj4string=crs(r0),matc
h.ID=TRUE)

    # loops of five formulas
    for (n in 1:5) {


      for (y in 1:16) { # loops of 16 years

        fm <- switch (n,
                      as.formula(paste(col.y[y],1,sep = "~")),
                      as.formula(paste(col.y[y],"nor",sep = "~")),
                      as.formula(paste(col.y[y],"ele",sep = "~")),
                      as.formula(paste(col.y[y],
                                       paste(c("nor","ele"), collapse =
"+"),
                                       sep = "~")),
```

```
                      as.formula(paste(col.y[y],
                                       paste(c("nor","ele"), collapse =
"*"),
                                       sep = "~"))
        )

        v = variogram(fm ,data = grid1,width=1000,cutoff = 50000) # set
50km as max distance of spatial autocorrelation
        v.fit = fit.variogram(v, vgm(c("Exp","Sph","Gau","Mat")),fit.kappa
= TRUE)

        if (v.fit$range[2]>20000||v.fit$range[2]<1000) { # re-fit if
extreme value occurs
          v.fit = fit.variogram(v, vgm(c("Exp","Sph","Gau")))
        }

        rn <- (g-1)*25+(switch(p,2,3,5,4,1)-1)*5+n
        tb.dist[rn,col.y[y]] <- v.fit$range[2]

      }# year loops end
    } # formula loops end
  }# phenology loops end
}# grassland type loops end

write.table(tb.dist,file = "E:/R
work/MODIS_NDVI/MODISrst/summary/Semivariogram_distances.txt")




#### build spatial weight matrices #####

tb.dist <- read.table("E:/R
work/MODIS_NDVI/MODISrst/summary/Semivariogram_distances.txt")
fname <- c("1","nor","ele","add","int")

## save nb(neighbourhood) objects

for (g in 1:3) {
  list.pheno <- list.files(path = pth.p[g],
                           pattern = ".txt$",full.names = TRUE,recursive =
FALSE)
  p.sys <- scan(pth.er[g])
  base1 <- list.base[[g]]

  for (p in c(5,1,2,4,3)) {

    tb2 <- read.table(list.pheno[p])
    tb1 <- cbind(base1,tb2[,col.y])

    # data clean
    data1 <- data.frame(tb1[-p.sys,])
    if (g==1) { # for alpine, exclude the pixel under 900m
      row <- which(data1[,'ele']<900)
      data1 <- data1[-row,]
    }

    # big dataset resample
    if (g==1) {df1 <- data1}
    if (g==2) {
      row1 <- which(match(data1[,'order'],tskc)>0)
      df1 <- data1[row1,]
```

```
    }
    if (g==3) {
      row1 <- which(match(data1[,'order'],lpgc)>0)
      df1 <- data1[row1,]
    }

    # build grid
    grid1 <-
SpatialPointsDataFrame(df1[,1:2],df1[,3:ncol(df1)],proj4string=crs(r0),matc
h.ID=TRUE)

    # formulas loops
    for (n in 1:5) {

      for (y in 1:16) {# 16 years loops

        rn <- (g-1)*25+(switch(p,2,3,5,4,1)-1)*5+n
        d <- tb.dist[rn,col.y[y]]
        nb <- dnearneigh(grid1,0,d)
        write.nb.gal(nb,file =
                       paste0("E:/R
work/MODIS_NDVI/MODISrst/SAR_models_mxt/nbs/nb_",
                              col.y[y],"_",fname[n],"_",pheno[p],"_",
                              grass[g],".gal"))

      }# year loops end
    } # formula loops end
  }# phenology loops end
}# grassland type loops end



#### LM tests of spatial autocorrelation ####

# load spatial weight matrices
list.nb <- mixedsort(list.files(path = "E:/R
work/MODIS_NDVI/MODISrst/SAR_models_mxt/nbs",
pattern = ".gal",full.names = TRUE,recursive = FALSE))

nb.name <- mixedsort(list.files(path = "E:/R
work/MODIS_NDVI/MODISrst/SAR_models_mxt/nbs",
pattern = ".gal",full.names = FALSE,recursive = FALSE))

nbs <- file_path_sans_ext(nb.name)

fname <- c("1","nor","ele","add","int")

## LM tests and model selection ##

for (g in 1:3) {
  list.pheno <- list.files(path = pth.p[g],
                           pattern = ".txt$",full.names = TRUE,recursive =
FALSE)
  p.sys <- scan(pth.er[g])
  base1 <- list.base[[g]]

  for (p in c(5,1,2,4,3)) {

    tb2 <- read.table(list.pheno[p])
    tb1 <- cbind(base1,tb2[,col.y])

    # data clean
    data1 <- data.frame(tb1[-p.sys,])
```

```
    if (g==1) { # for alpine, exclude the pixel under 900m
      row <- which(data1[,'ele']<900)
      data1 <- data1[-row,]
    }

    # dataset resample
    if (g==1) {df1 <- data1}
    if (g==2) {
      row1 <- which(match(data1[,'order'],tskc)>0)
      df1 <- data1[row1,]
    }
    if (g==3) {
      row1 <- which(match(data1[,'order'],lpgc)>0)
      df1 <- data1[row1,]
    }

    # formulas loops
    for (n in 1:5) {

      # For 16 years
      for (y in 1:16) {

        fm <- switch (n,
                      as.formula(paste(col.y[y],1,sep = "~")),
                      as.formula(paste(col.y[y],"nor",sep = "~")),
                      as.formula(paste(col.y[y],"ele",sep = "~")),
                      as.formula(paste(col.y[y],
                                       paste(c("nor","ele"), collapse =
"+"),
                                       sep = "~")),
                      as.formula(paste(col.y[y],
                                       paste(c("nor","ele"), collapse =
"*"),
                                       sep = "~"))
        )

        fun.lm <- lm(fm,data = df1)
        # load nb

        model.n <- paste0(col.y[y],"_",fname[n],"_",
                          pheno[p],"_",grass[g])

        m <- which(nbs[]==paste0("nb_",model.n))
        nb <- read.gal(list.nb[m])
        nb.list <- nb2listw(nb,style="W",zero.policy=TRUE)

        lmTs <- lm.LMtests(fun.lm,nb.list,zero.policy = TRUE,test = "all")

        saveRDS(lmTs, file=paste0("E:/R
work/MODIS_NDVI/MODISrst/SAR_models_mxt/LM_Tests/LMt_",
                                  model.n,".rds"))
      }# year loops end
    } # formula loops end
  }# phenology loops end
}# grassland type loops end



#### model selection based on LM test results ####

list.LM <- mixedsort(list.files(path = "E:/R
work/MODIS_NDVI/MODISrst/SAR_models_mxt/LM_Tests",
pattern = ".rds",full.names = TRUE,recursive = FALSE))
```

```
LM.name <- mixedsort(list.files(path = "E:/R
work/MODIS_NDVI/MODISrst/SAR_models_mxt/LM_Tests",
pattern = ".rds",full.names = FALSE,recursive = FALSE))

LMs <- file_path_sans_ext(LM.name)
fname <- c("1","nor","ele","add","int")

## build a table for summary
tb.LM <- matrix(0,nrow = 1200,ncol = 10)
colnames(tb.LM) <- c("Model","LMerr","LMerr_p","LMlag","LMlag_p",
                     "RLMerr","RLMerr_p","RLMlag","RLMlag_p","Selected")
tb.LM[,'Model'] <- paste0(rep(col.y,75),"_",
                          rep(rep(fname,each=16),15),"_",
                          rep(rep(pheno[c(5,1,2,4,3)],each=80),3),"_",
                          rep(grass,each=400))

for (i in 1:length(list.LM)) {
  lmTs <- readRDS(list.LM[i])

  m <- which(paste0("LMt_",tb.LM[,'Model'])==LMs[i])

  tb.LM[m,"LMerr"] <- lmTs$LMerr$statistic
  tb.LM[m,"LMerr_p"] <- lmTs$LMerr$p.value
  tb.LM[m,"LMlag"] <- lmTs$LMlag$statistic
  tb.LM[m,"LMlag_p"] <- lmTs$LMlag$p.value
  tb.LM[m,"RLMerr"] <- lmTs$RLMerr$statistic
  tb.LM[m,"RLMerr_p"] <- lmTs$RLMerr$p.value
  tb.LM[m,"RLMlag"] <- lmTs$RLMlag$statistic
  tb.LM[m,"RLMlag_p"] <- lmTs$RLMlag$p.value

  # model selection
  err <- lmTs$LMerr$p.value<0.05
  lag <- lmTs$LMlag$p.value<0.05
  Rerr <- lmTs$RLMerr$p.value<0.05
  Rlag <- lmTs$RLMlag$p.value<0.05

  # 0:OLS, 1:SAR,2:SEM,3:SAC

  if (err & lag) {

    if (Rerr & Rlag) {
      selection <- 3 # "SAC"
    }else {
      if (Rerr) {selection <- 2}
      if (Rlag) {selection <- 1}
    }

  }else {

    if (err) {
      selection <- 2
    }else if (lag) {
      selection <- 1
    }else {
      selection <- 0}
  }

  tb.LM[m,'Selected'] <- selection

}
```

```
write.table(tb.LM,file = "E:/R
work/MODIS_NDVI/MODISrst/summary/LMtest_Model.txt")
tb.LM <- read.table("E:/R
work/MODIS_NDVI/MODISrst/summary/LMtest_Model.txt")


## SAR/SEM/OLS regression


fun.ols <- lm(fm,data = df1)

fun.sar <- lagsarlm(fm,data=df1,listw=nb.list,type = "lag",
                    zero.policy = TRUE,method = "Matrix")
fun.sem <- errorsarlm(fm,data=df1,listw=nb.list,
                      zero.policy = TRUE,method = "Matrix")
fun.sac <- sacsarlm(fm,data=df1,listw=nb.list,
                    zero.policy = TRUE,method = "Matrix")

# use similar loops to go through all grassland types, all years and all
phenological indices
```